UNIVERSITY OF SOUTHAMPTON

Faculty of Environmental and Life Sciences
School of Ocean and Earth Science

Macroecological study of otolith-derived field metabolic rates of marine fishes

by

Sarah Rose Alewijnse

MSci

ORCiD: 0000-0002-3479-2443

A thesis for the degree of
Doctor of Philosophy

July 2022

University of Southampton

Abstract

Faculty of Environmental and Life Sciences
School of Ocean and Earth Science

Doctor of Philosophy

Macroecological study of otolith-derived field metabolic rates of marine fishes

by Sarah Rose Alewijnse

Metabolic rate - the energy expenditure of an organism over time - is considered by some ecologists to be the driver of all other ecological processes. Several theories seek to describe how metabolic rates vary at a macroecological scale, particularly with respect to individual body mass and temperature. Body size and temperature scaling of metabolic rate (and linked biological and ecological processes) underpin many ecological models, particularly models predicting regional to global scale responses of organisms to climate change. The relationship between body size, temperature and metabolic rate is therefore of primary concern to ecologists. Some theories propose universal scaling exponents to describe the relationships between metabolic rate and body mass or temperature, while other theories suggest that scaling exponents are context-dependent. Field metabolic rate - the full, time-averaged costs of an organism living in the wild - is relatively understudied compared to metabolic rates measured in laboratory settings. Despite their great importance to humans, the field metabolic rates of teleost fishes are especially understudied, due to a lack of methods appropriate for determining metabolic rate in aquatic animals.

Here, I used a proxy derived from stable isotope analysis of otolith aragonite (C_{resp} values) to estimate the field metabolic rates of 114 species of marine teleost fishes. I investigated the effects of two ecological traits - species' thermal realm and depth of occurrence - on field metabolic rates, after accounting for body mass and temperature. In the full dataset, field metabolic rate scaled with body mass with an exponent of 0.90 and with temperature with an Arrhenius activation energy of 0.26. Importantly, the scaling of field metabolic rate with temperature varied with thermal tolerance range; scaling was steeper in stenothermic groups compared to eurythermic groups. Both thermal realm and depth of occurrence had significant effects on field metabolic rates. The mean field metabolic rate of polar species was elevated compared to temperate species, suggesting partial metabolic cold adaptation. Deeper-dwelling species, operating at similarly cold temperatures, did not show high field metabolic rates, likely due to increasing food and light limitations with increasing depths.

My results emphasise the importance of studying metabolic rates across a range of taxa. Current marine ecosystem models, which use scaling exponents derived from terrestrial animals, are likely overestimating the effects of climate change on body mass, while underestimating the ability of marine animals to mitigate the effects of rising temperatures on their metabolic rates, and the costs of that mitigation. Studying field metabolic rates in fish specifically enables more appropriate model parameterisation, and the C_{resp} method is a useful tool to aid in this endeavour.

Contents

List of Figures

List of Tables

List of Additional Material

Data generated for this thesis are deposited at https://doi.org/10.5258/SOTON/D2292

Declaration of Authorship

I declare that this thesis and the work presented in it is my own and has been generated by me as the result of my own original research.

I confirm that:

1. This work was done wholly or mainly while in candidature for a research degree at this University;
2. Where any part of this thesis has previously been submitted for a degree or any other qualification at this University or any other institution, this has been clearly stated;
3. Where I have consulted the published work of others, this is always clearly attributed;
4. Where I have quoted from the work of others, the source is always given. With the exception of such quotations, this thesis is entirely my own work;
5. I have acknowledged all main sources of help;
6. Where the thesis is based on work done by myself jointly with others, I have made clear exactly what was done by others and what I have contributed myself;
7. Parts of this work have been published as:
   S. R. Alewijnse, G. Stowasser, R. A. Saunders, A. Belcher, O. A. Crimmen, N. Cooper, and C. N. Trueman. Otolith-derived field metabolic rates of myctophids (Family Myctophidae) from the Scotia Sea (Southern Ocean). *Marine Ecology Progress Series*, 675:113–131, 2021

Signed:..... Date:.....

Acknowledgements

This thesis was funded by the Natural Environment Research Council (grant number NE/L002531/1). Additional funding was provided by the National Environmental Isotope Facility (grant number EK307-08/18). Additional thanks to Prof. Melanie Leng, Hilary Sloane and Carol Arrowsmith at the British Geological Survey for hosting me, and making me feel so welcome. Special thanks in particular to Hilary for running the isotope samples, and for providing refreshment after our marathon trip to Nottingham and back! Thanks also to Bastian Hambach and Megan Wilding for running isotope samples at the Stable Isotope Mass Spectrometry Laboratory at Southampton.

A huge thank you to my two main supervisors, Dr Clive Trueman and Dr Natalie Cooper. You both have been amazingly supportive and patient on my journey from newly-minted Masters student to fully fledged researcher. None of this would have been possible without your expertise and mentorship, and I will be forever grateful. A second huge thank you to my co-supervisor Ollie Crimmen, for always having time to share your expertise with me. Thank you also for your infectious enthusiasm for fish, and your wonderful kindness.

Such a large-scale project would not have been possible without the wonderful generosity of so many otolith donors. Thank you to Dr Ewan Hunter and Dr Valerio Visconti at Cefas; Kate Chadwick at the Ascension Islands Government; Dr Yoni Belmaker and Dr Alex Slavenko at Tel-Aviv University; Dr Pierre Cresson and Solène Telliez at IFREMER; Prof. Beatriz Morales-Nin and Sílvia Pérez at IMEDEA, and Dr Julie Vecchio at the University of South Florida. Further thanks to Dr James Kennedy at MFRI for donating otoliths, and also for a helpful discussion on lumpfish ecology. Thank you also to Dr Gabriele Stowasser, Dr Ryan Saunders and Dr Anna Belcher at the British Antartic Survey for donating lanternfish samples, and for co-authoring the first paper of my PhD. Your support and technical knowledge are greatly appreciated.

I must extend thanks to Dan Doran and Matt Beverley-Smith at the University of Southampton, for their help in preparing otoliths, and for the multiple cups of tea! Thank you also to Dr Andrew Jackson for your help with statistics, and Prof. Tom Ezard for being my panel chair. Thank you also to my examiners, Dr Shaun Killen and Dr Phil Fenberg, for an interesting and enjoyable viva, and for suggesting corrections to improve this thesis.

Thank you to my office mates Juliet Wilson, Abbie Mabey, Yuan-Tian “Olivia” Chou and Joe Jones, for your endless support and for always being there for me when I ended up on the beanbag of doom! Thank you to Juliet and Abbie for your friendship

and support as we navigated the world of PhD research. Thank you to Joe for helping me prepare otoliths and for your company, especially in the latter stages of the PhD. Thank you to Olivia, not only for your friendship, but for donating me some otoliths you collected in your time at NSYSU. Thank you also to "The Science Ladies", Sarah Lu, Jess Stead and Natasha Easton, for your wonderful friendship and support, especially as Covid and isolation started to bite. Special thanks to Sarah and Jess for helping to proofread my thesis.

Thank you to my friends Beth Sims and Jago Staplehurst, for your unwavering friendship, your boundless emotional support and for your help in proofreading. Additional thanks to Mir Walker Browning and Caitlin Doyle for helping to proofread. Thank you to the SUMIE lab alumni, especially Dr Ming-Tsung Chung for collecting many of the otoliths which I used for this project, and for your help and kindness when we met in Taiwan. Thank you also to Dr Katie St. John Glew and Dr Matt Cobain for supporting me as a new PhD student, especially for emphasising the importance of a work life balance.

Thank you to my family: to my sister Rebecca Alewijnse, my aunt Lucy Buckland and my granddad Bill Buckland. Thank you for supporting me, despite not always knowing what it was that I was up to!

It may seem frivolous to thank one's pet, but my late cat Marmite provided great company and support, especially when Covid meant I had to work from home. PhD life has been less cheerful without her.

Finally, my unending thanks to my wife, Alex Fforde. In practical terms, thank you for your help with maths and coding, and for picking up the slack when I started working feverishly in the final few months. More importantly, thank you for loving me and for always reminding me that my worth as a person isn't solely tied to my career. As you do in all things, you've made my PhD experience brighter and more joyous in every possible way.

This thesis is dedicated to the memory of my parents,
Rik & Amanda Alewijnse

To Mum and Dad,
I am forever grateful for your love and support.
None of this would have been possible without you.
I hope somewhere, somehow, you are proud of me.
I love you both, always.

Chapter 1

Introduction

Metabolic rate is the rate at which an organism converts energy and nutrients into power, biomass and waste products (Brown et al., 2004). The key process of an organism's metabolism is the generation of adenosine triphosphate (ATP), via glycolysis and the tricarboxylic acid cycle (Clarke and Fraser, 2004). Although directly measured in watts (the unit of power) or joules (the unit of energy) via direct calorimetry, metabolic rate is most often approximated by oxygen consumption rates, with the two terms often used interchangeably (Chabot et al., 2016; Nelson, 2016; Treberg et al., 2016). There are different measures of metabolic rate, depending upon the activity level of the organism when its oxygen consumption is measured (Fry and Hart, 1948, section 1.1).

The metabolic theory of ecology proposes that metabolic rate underlies most other biological rates, ranging from the ontogenetic growth rate of an individual, to population density, to global patterns in species diversity (Brown et al., 2004). Many ecosystem models draw on metabolic theory for their construction and parameterisation (section 1.3.1). Understanding the broad-scale patterns of metabolic rates across vertebrates can enable more accurate modelling of the impacts of climate change on ecosystems and the role species play biogeochemical cycling (section 1.3).

1.1 Measures of metabolic rate

Standard metabolic rate (SMR), arguably the most common measure of metabolic rate in ectotherms, aims to measure the minimum metabolic rate necessary to maintain homeostasis (Fry and Hart, 1948; Treberg et al., 2016). SMR is similar to the measure of basal metabolic rates in endotherms, although basal metabolic rate includes the cost of internal temperature regulation (Hulbert and Else, 2004). In ectotherms, SMR is usually studied via respirometry, measuring the oxygen consumption of a

non-moving, unstressed, post-absorptive animal at a standard temperature within the species' natural range (Chabot et al., 2016). While SMR may appear the most straightforward measure of metabolic rate to replicate across different studies, a myriad of factors must be considered, including but not limited to: the reproductive condition of the animal, setting appropriate fasting and acclimation periods, and ensuring the animal is unmoving (Chabot et al., 2016). Furthermore, the ecological relevance of SMR is debated, as SMR does not include several metabolic costs which are essential for an individual's long-term survival, such as food acquisition and predator evasion, or the fitness components of growth and reproduction (Chabot et al., 2016; Treberg et al., 2016). It is therefore likely that ectotherms only exist at SMR in the carefully controlled conditions of a laboratory, and unlikely that a wild ectotherm would ever persist at SMR for any length of time (Chabot et al., 2016).

Maximum metabolic rate (MMR) aims to measure the maximum aerobic capacity of an animal (Fry and Hart, 1948; Farrell, 2016; Norin and Clark, 2016; Treberg et al., 2016). Like SMR, MMR is also measured using respirometry, either during or just after exercise, using either a swim tunnel for continuously swimming species, or a manual chase for burst swimming species (Norin and Clark, 2016). MMR is more difficult to standardise than SMR: the same fish may have a different MMR depending on the exercise protocol (Farrell, 2016) and as with SMR, the ecological relevance of MMR is debated (Norin and Clark, 2016). The intervals over which MMR is calculated can have a significant effect on the resulting oxygen consumption when using the chase protocol (Prinzing et al., 2021), indicating that the maximal aerobic capacity measured by MMR may not be sustainable for an individual of a burst swimming species over longer periods of time (Peterson et al., 1990). As with SMR, individuals may spend little to no time at their MMR in the wild (Norin and Clark, 2016). Finally, manual chase protocols often involve exposing the fish to air to ensure maximum stress (Norin and Clark, 2016), despite air exposure being something unlikely to happen to a wild fish on a regular basis.

Laboratory measures of metabolic rates have given important information about the nature of metabolic rates across a wide range of taxa, and have formed the basis of many macroecological (large-scale) patterns and theories of metabolic rate (section 1.2). However, it would be ideal to also have knowledge of metabolic rates of animals living in the wild. Field metabolic rate (FMR) is the total, time-averaged metabolic rate of an unconstrained animal, living in and interacting with its natural ecosystem (Nagy, 1987; Nagy et al., 1999; Treberg et al., 2016). As well as the costs of maintenance measured by SMR, FMR also measures costs essential for long-term survival, such as movement and specific dynamic action (the costs of digesting and assimilating food), and the fitness components of growth and reproduction (Figure 1.1, Treberg et al., 2016).

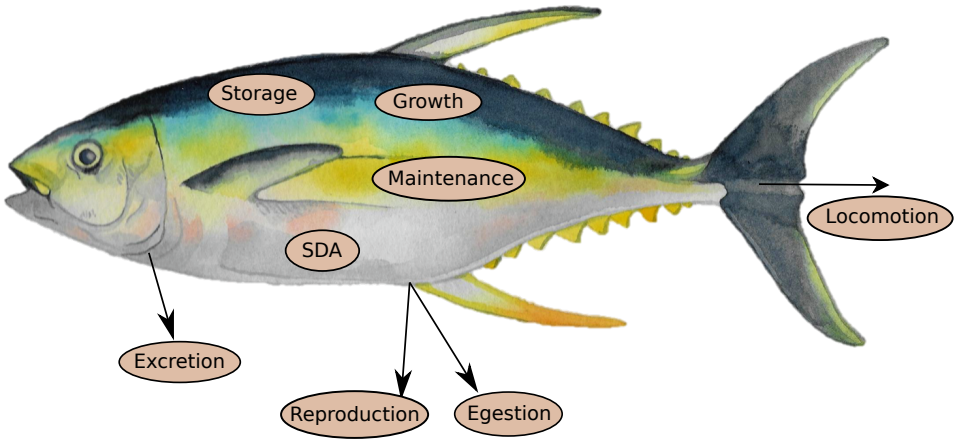

FIGURE 1.1: Conceptual diagram of the components of field metabolic rate - the energetic costs of a fish living in the wild - illustrated by *Thunnus albacares* (yellowfin tuna). SDA = specific dynamic action. Egestion is the removal of undigested food, while excretion is the removal of metabolic waste products. Diagram adapted from Treberg et al. (2016).

Despite its ecological relevance, the logistical and financial expenses associated with measuring FMR means it is relatively understudied, even within the most well studied groups. For example, a recent large-scale study of FMR in humans caused controversy by finding that, despite popular belief, mass-independent FMR in humans does not change between the ages of 20 to 60 years (Pontzer et al., 2021), highlighting how little we understand FMR. In terrestrial animals, FMR is most commonly measured using the doubly-labelled water method, which involves using isotopically-labelled water ($^2H_2^{18}O$) to estimate carbon dioxide production (Lifson et al., 1955). As well as the expense of the labelled water itself, measuring FMR in this way requires capturing and recapturing the animal, which while relatively straightforward for philopatric animals (or humans), becomes increasingly difficult for migratory animals (Treberg et al., 2016). Furthermore, because the doubly-labelled water method involves water elimination, it cannot be used in animals with high water turnover rates, which prevents its use in aquatic ectotherms (Treberg et al., 2016). The lack of a standardised method for determining FMR in ectotherms currently limits our understanding of FMR evolution and diversity across vertebrates as a whole.

Less commonly, measures of metabolic rate can be described as resting or routine metabolic rates (both abbreviated to RMR), both of which are measured via respirometry. The difference between resting and standard metabolic rates are often unclear, routine metabolic rate includes the cost of "routine" voluntary movement, and can also include specific dynamic action (Treberg et al., 2016). Although RMR, like FMR, includes the cost of movement, the two measures are very different and should not be conflated, particularly when describing *in situ* RMR measures. As RMR is measured via respirometry, the animal is confined and not interacting with its natural

environment, contrary to the conditions required for measuring FMR. Furthermore, the time periods over which oxygen consumption is measured are typically far shorter for RMR measures (12-24 hours) compared to FMR (integrated over several days, months or years, Chapter 2, Treberg et al., 2016).

Finally, while not a measure of metabolic rate in itself, aerobic scope is an important metric used to describe the possible range of metabolic rates at which a fish can operate (Fry and Hart, 1948; Peterson et al., 1990; Farrell, 2016; Pörtner et al., 2017). For well fed animals in normoxia, SMR and MMR act as functional aerobic limits within which the actual metabolic rate can vary (Fry and Hart, 1948; Brett and Glass, 1973). The difference between standard and maximum metabolic rate is termed absolute aerobic scope, while the ratio of standard to maximum metabolic rate is termed the factorial aerobic scope (Clark et al., 2013; Farrell, 2016). Aerobic scope is the basis for frameworks concerning how aquatic animals are affected by climate change, including oxygen- and capacity-limited thermal tolerance (OCLTT, Pörtner et al., 2017) and metabolic index (Deutsch et al., 2015, 2020).

1.2 Macroecological patterns of metabolic rate

Given the vastness and diversity of the natural world, it is helpful to investigate the broad-scale patterns underlying ecological processes. Macroecology - ecology at large scales - is the description and explanation of broad-scale processes and patterns within ecology (Brown, 1996; Costa and Sinervo, 2004). In this section, I introduce some of the key macroecological theories of metabolic rate, which are important in the understanding and rationale of the overall thesis.

1.2.1 Body mass

Since the experiments of Rubner (1883) it has been known that metabolic rate scales with body mass according to the allometric equation:

$$Y = aM^b \tag{1.1}$$

where Y is the metabolic rate, M is the body mass (in grams), b is the scaling exponent, and a is the normalisation constant (Rubner, 1883; Kleiber, 1932, 1947; West et al., 1997; Brown et al., 2004). Specifically, metabolic rate scales with negative allometry, or with a scaling exponent (b) of less than one (Figure 1.2A). In contrast to allometry, in isometry a property scales in direct proportion to body mass (b = 1). Properties can also scale with positive allometry (hypermetry) where $b > 1$ (Figure 1.2A). The

negative allometry of metabolic rate means that although larger animals have greater absolute metabolic rates, smaller animals have greater metabolic rates per unit of body mass (Figure 1.2B).

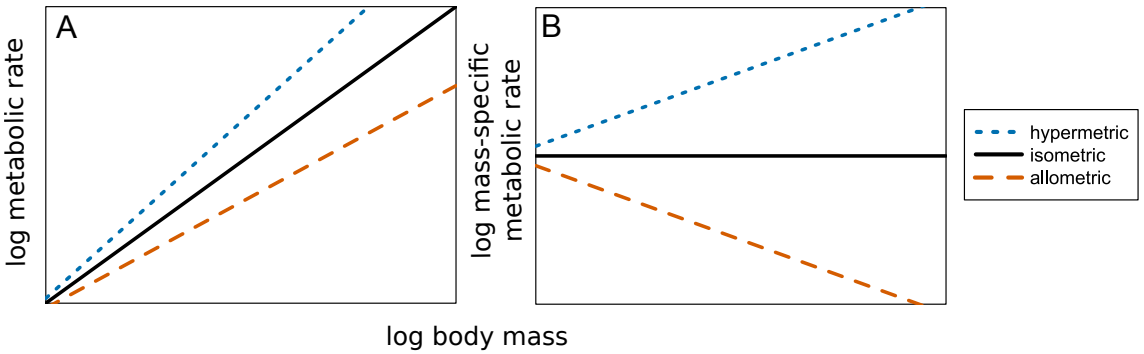

FIGURE 1.2: Schematic of relationships between absolute (A) and mass-specific (B) metabolic rate and body mass on a log-log scale. Black line = isometry ($b = 1$), red line = allometry ($b < 1$), blue line = hyperometry ($b > 1$).

By measuring the metabolic rates of differently sized domestic dogs (*Canis familiaris*), Rubner (1883) determined that metabolic rate scaled with a b of 0.67, or $\frac{2}{3}$, which is the surface-area to volume ratio of a sphere. Kleiber (1932, 1947) took a more macroecological approach by compiling metabolic rates of different species, with a range in body mass from 150 g (ring dove, *Streptopelia capicola*) to 680 kg (steer, *Bos taurus*). Using their multispecies dataset, Kleiber (1932, 1947) found the best-fit value for b to be 0.75 ($\frac{3}{4}$), rather than 0.67 (Kleiber, 1932, 1947). Later, West et al. (1997) proposed a mechanistic explanation for the 0.75 value of b: that 0.75 is the surface-area to volume ratio of the fractal distribution networks, which are present in animals and plants in systems such as blood vessels and the water vascular system, respectively. The 0.75 value of b, and the underlying fractal-network theory, became the metabolic theory of ecology (MTE). According to strict MTE, b is always 0.75, and any variation around this universal value is statistical noise (Brown et al., 2004). The metabolic theory of ecology is used to parameterise many ecosystem models, however, it is not without controversy, both in terms of the theoretical underpinnings (Kozłowski and Konarzewski, 2004) and empirical evidence.

Despite the proposal of strict MTE that b is universally 0.75, many studies have found b to be variable, including among life stages (Giguère et al., 1988; Killen et al., 2007), hierarchical levels (Norin and Gamperl, 2018) and activity levels (Brett and Glass, 1973; White et al., 2007; Glazier, 2009; Killen et al., 2010; Norin and Malte, 2012). One of the most explored causes of differences in b at a macroecological scale is thermoregulatory strategy, specifically the difference in b between endotherms and ectotherms. When considering best fit values of b, ectotherms tend to have greater values of b compared to endotherms. For example, the best fit value of b_{BMR} (determined by ordinary least-squares regression) in endotherms ranged from 0.64 in

birds to 0.68 in mammals, compared to b_{SMR} ranging from 0.76 in reptiles to 0.88 in fish and amphibians (White et al., 2006). Similar trends were seen in b_{FMR}, which ranged in endotherms from 0.68 in birds to 0.73 in mammals, compared to a greater b_{FMR} of 0.89 in reptiles (Nagy et al., 1999).

The heterogeneity seen in b, which arguably challenges strict MTE, is interpreted differently by different ecologists. For instance, despite finding a value of b for resting metabolic rate in endotherms (b_{RMR} = 0.74) lower than that for ectotherms (b_{RMR} = 0.80), Gillooly et al. (2017) found that the scaling exponents between the two thermoregulatory strategies are statistically indistinguishable at the 95% confidence level. The focus on statistical significance in deviations (or lack thereof) in b, either among groups or from 0.75, is part of why the body mass scaling of metabolic rate remains controversial despite decades of research (del Rio, 2008). There is a distinct difference between statistical and biological significance: just as statistically significant difference may have little significance at the biological scale, a difference in value which is statistically non-significant may be very different on the biological scale (Glazier, 2021). The difference between statistical and biological significance is especially important when considering scaling exponents, where even small differences in values may result in very different predictions (Lefevre et al., 2017, 2018). Therefore, some have argued that even though the average value of b may converge on 0.75, there is still significant variation around this average value which does not support strict MTE (Bokma, 2004; Isaac and Carbone, 2010). When parameterising models, rather than focusing on statistical significance an information theoretic approach - which seeks the best fit model with the least number of parameters - may be more appropriate (White et al., 2012b).

An alternative to MTE which allows for variation in b is the metabolic level boundaries hypothesis (MLBH, Glazier, 2005, 2009, 2010). According to MLBH, the value of b varies between the boundaries of 0.67 and 1.00. The allometric lower bound (b = 0.67) is set by the surface area to volume ratio of a sphere, whereas the isometric upper bound is set by the mass to volume ratio ($b = 1$, Glazier, 2005, 2010). Where b falls between the allometric and isometric boundaries is determined by the metabolic level. Metabolic level is similar to a in equation 1.1 in that it deals with metabolic elevation (Glazier, 2010), however, metabolic level is more correctly approximated by the metabolic rate at the midpoint of the relationship with body mass (i.e. a when body mass values are mean-centred, Killen et al., 2010, 2016). The relationship between b and metabolic level depends upon what is limiting to metabolic rate scaling with body mass: if resource supply is limiting to metabolic rate then b will be closer to 0.67, whereas if volume is limiting b will be closer to 1 (Glazier, 2010). Considering SMR, athletic animals will have a high maintenance demand, and so will be more limited by nutrient and oxygen supply, so their b will be closer to 0.67, while more sluggish animals will have a value of b closer to 1 (Glazier, 2005, 2009, 2010; Killen

et al., 2010, 2016). The difference in b_{SMR} between athletic and sluggish animals has been proposed as the mechanism behind the typically lower b_{BMR} of endotherms compared to b_{SMR} of ectotherms (Glazier, 2010). In contrast, according to MLBH b_{MMR} is closer to isometry in athletic species, as their MMRs are more limited by muscle power, whereas for sluggish species, their b_{MMR} is more limited by nutrient and oxygen supply, and scales towards 0.67 (Glazier, 2005, 2010). One limitation of MLBH, particularly with regards to this thesis, is that much of its support comes from intraspecific studies (Glazier, 2009; Isaac and Carbone, 2010; Killen et al., 2010). Furthermore, it is thought that b_{FMR} should relate to metabolic level similarly to b_{SMR} under MLBH (Glazier, 2010), which has not been tested at a large scale.

1.2.2 Temperature

After body mass, temperature is a key driver of metabolic rate due to its effects on enzyme-catalysed reaction kinetics. The effect of temperature on enzyme-catalysed reactions can be described using an Arrhenius equation:

$$Y \propto e^{\frac{-E}{kT}} \tag{1.2}$$

where Y is the rate of reaction (e.g. metabolic rate), E is the activation energy, k is the Boltzmann constant, and T is the absolute temperature in kelvin (Gillooly et al., 2001; Brown et al., 2004). Under the universal temperature dependence hypothesis, which forms part of the metabolic theory of ecology, E has an average value of between 0.6 and 0.7 eV, which is the average activation energy of respiration (Gillooly et al., 2001; Brown et al., 2004). When combining MTE with universal temperature dependence, the full equation becomes (Brown et al., 2004):

$$Y = aM^{0.75}e^{\frac{-0.65}{kT}} \tag{1.3}$$

While Arrhenius relationships may describe enzyme thermodynamics, such relationships may not scale up when considering the temperature effects on the metabolic rates of a whole organism (Clarke, 2004; Clarke and Fraser, 2004) Instead, the effect of temperature on metabolic rate may vary depending upon the range of temperatures over which an organism is adapted (Clarke, 2004; Clarke and Fraser, 2004). Additionally, in the wild organisms may be able to compensate for temperature effects on their SMR by reducing other components of their FMR (Richards, 2010; Norin and Clark, 2017; Jutfelt et al., 2021).

Importantly, the Arrhenius equation only describes the relationship between metabolic rate and temperature over a physiologically relevant, non-stressful temperature range

(Gillooly et al., 2001; Knies and Kingsolver, 2010). Therefore, the Arrhenius relationship would not be appropriate for describing the temperature scaling of an organism in hypoxia (Rubalcaba et al., 2020), without adequate food, (Nunes et al., 2021), or where enzyme activity is not at 100% (Knies and Kingsolver, 2010).

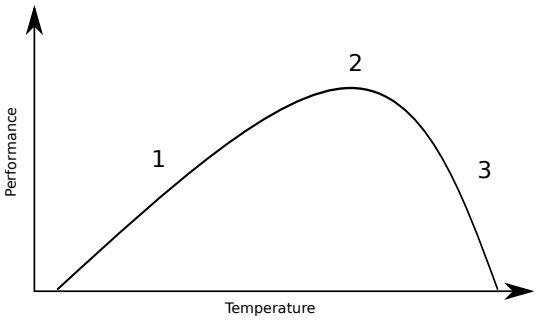

FIGURE 1.3: Schematic of an idealised thermal performance curve. 1 = the rising phase, which can be described by an Arrhenius equation, 2 = the plateau, 3 = the drop phase, proposed to be caused either by enzyme denaturation, or a mismatch between aerobic supply and demand (Pörtner et al., 2017). Adapted from Schulte (2015).

Over a full temperature range, the relationship between the biological performance of ectotherms and temperature can be described using a thermal performance curve, with three phases (Figure 1.3, Schulte, 2015). During the first phase, the reactions of metabolism are enzyme limited, and thus are described by reaction kinetics (equation 5.1, Gillooly et al., 2001; Clarke and Fraser, 2004). A plateau occurs in the second phase, when the organism is at its optimum temperature, followed by a steep drop traditionally attributed to denaturation of enzymes at high temperatures (Schulte, 2015), or more recently to a mismatch between aerobic supply and demand (Pörtner et al., 2017).

1.2.3 Ecological correlates of metabolic rate

Body mass and temperature describe much of the variation in metabolic rate among organisms, however, a large amount of variation in metabolic rate remains unexplained after accounting for these factors. For example, when normalised to a common body mass and temperature, the resting metabolic rates of teleost fishes can vary 38-fold (Killen et al., 2016). Furthermore, the premise that ecological factors influence the scaling of metabolic rate with body mass is fundamental to the metabolic level boundaries hypothesis (Glazier, 2005, 2009, 2010), and runs counter to the strict metabolic theory of ecology (West et al., 1997; Brown et al., 2004).

In fish, a number of ecological factors correlate with metabolic rate, many of which are summarised in Table 1.1. For the purposes of this thesis, I am particularly interested in three of these factors: taxonomic group, thermal realm and depth of occurrence. The importance of these ecological correlates will be expanded in their respective chapters, so here I give a brief summary of previous findings.

TABLE 1.1: Ecological correlates of metabolic rate at a macroecological scale (i.e. greater than community). A check mark indicates that the study investigated the ecological factor **and** found it had a significant correlation with metabolic rate in fish. n = number of fish species studied.

Study	n	Ecological correlate of metabolic rate				
		Taxonomic group	Thermal realm	Depth	Activity level	Habitat
Scholander et al. (1953)	11		✓			
Gordon (1972)	39				✓	✓
Koslow (1996)	11					
Clarke and Johnston (1999)	69	✓				
Drazen and Seibel (2007)	55			✓		✓
Glazier (2009)	19				✓	
Killen et al. (2010)	82				✓	✓
White et al. (2012a)	49		✓	✓		
Drazen et al. (2015)	61			✓		✓
Ikeda (2016)	90			✓		
Killen et al. (2016)	92				✓	✓
Uyeda et al. (2017)	82	✓				

While taxonomic group is not an ecological factor *per se*, metabolic rate does show variation at different taxonomic levels (Clarke and Johnston, 1999). For example, the mass- and temperature- normalised metabolic rate of Gadiformes (cods) was 4.8x higher than that of Anguilliformes (eels, Clarke and Johnston, 1999). Futhermore, when studying relationships at a macroecological scale, it is important to consider species-relateness as a confounding factor. Phylogenetic non-independence is the concept that related species are not truly indepedent data points, as they have a shared evolutionary history that must be accounted for in statistical modelling (Harvey and Pagel, 1991). Along with all enabling more robust statistical testing, accounting for shared evolutionary history allows investigation into the evolution of metabolic rate (Uyeda et al., 2017), and can provide insight into potential ecological drivers, when combined with knowledge of different taxonomic groups (Chapter 4).

The thermal realm and range to which is a species or group is adapted is thought to be a key driver of variation in the relationship between metabolic rate and temperature (Clarke, 2004; Clarke and Fraser, 2004, Chapter 5). Groups adapted to large temperature ranges (eurytherms) are thought to have evolved metabolic enzymes which can function well across large temperature ranges, and therefore have a low temperature sensitivity of metabolic rate compared to species adapted to a narrow range of temperatures (stenotherms, Scholander et al., 1953; Wohlschlag, 1960; Clarke and Fraser, 2004; Pörtner et al., 2005; Schulte, 2015). The effect of thermal realm on metabolic rate is also important in testing the controversial theory of metabolic cold adaptation. Metabolic cold adaptation proposes that cold-adapted (typically polar)

organisms have higher metabolic rates compared to warmer-adapted organisms when those metabolic rates are normalised to the same low temperature (Ege and Krogh, 1914; Scholander et al., 1953; Wohlschlag, 1960).

Finally, ecologists have often noted that metabolic rates of marine animals decline with increasing depth of occurrence, independently of body mass and temperature effects (Drazen and Seibel, 2007; Seibel and Drazen, 2007; Drazen et al., 2015; Ikeda, 2016, Chapter 6). While this depth-dependent decline in metabolic rate has been found across marine taxa, the drivers of this pattern remain unclear (Drazen and Seibel, 2007; Seibel and Drazen, 2007; Drazen et al., 2015; Ikeda, 2016; Gerringer et al., 2017; Brown et al., 2018).

1.3 The importance of understanding metabolic rate in fish

At present, the understanding of variation in metabolic rate across taxa is primarily derived from measures of standard metabolic rate (e.g. Uyeda et al., 2017). Few studies investigate how field metabolic rates vary at a macroecological scale, and those that do typically do not included aquatic ectotherms (Nagy, 1987; Nagy et al., 1999), due to a lack of suitable methods (Treberg et al., 2016). Teleost fish occupy a unique and important position within the vertebrates. In terms of species, they are the most diverse of the vertebrate taxa, encompassing 36,128 valid species as of March 2022 (Fricke et al., 2022). Fish include the most numerous vertebrates on the planet, the Gonostomatidae (bristlemouths, Moyle and Cech, 2004), and play important roles in biogeochemical cycling (Saba et al., 2021, section 1.3.2). Many species of fish are of great importance to humans, both for economic and food security reasons. As of 2018, an estimated 59.51 million people are employed in fisheries or aquaculture (FAO, 2020), and fish remain the last animal group to be wild harvested on a global industrial scale. Good management of fish, as both a natural resources and an important component of ecosystems, is vital to the continued prosperity of humanity. In this section I explain how understanding metabolic rate in fish enable us to improve ecosystem models and evaluate the role of fish in biogeochemical cycling, and emphasise the importance of considering field metabolic rates in these applications.

1.3.1 Ecosystem models

Ecosystem models are prominent in the field of marine ecology, as they can be used both to set catch limits for species of commercial interest (Christensen and Walters, 2004), and predict the impacts of stressors such as climate change on marine ecosystems (Tittensor et al., 2018). For example, the dynamic bioclimatic envelope model predicted a reduction in the average maximum body size for fish assemblages

between 14 and 24% from 2000 to 2050, due gill growth (and thus oxygen supply) being unable to keep pace with the increasing metabolic demands caused by higher temperatures (Cheung et al., 2013).

Most regional to global scale marine ecosystem models either directly incorporate metabolic theory (e.g. the macroecological model Jennings and Collingridge, 2015) or use metabolic theory to derive other ecological parameters (Table 1.2). For example, the BOATS model derives the temperature dependence of growth and mortality from metabolic theory (Carozza et al., 2019). Most marine ecosystem models use a single body mass scaling exponent (b) based on surface area-volume relationships (Table 1.2). One exception is the general ecosystem model, which uses three values of b, allowing for variation in b with thermoregulatory strategy and activity level (Harfoot et al., 2014). Similarly to body mass, the effects of temperature are largely incorporated into marine ecosystem models using a single value of E which ranges between 0.6 and 0.7 (Table 1.2), following the universal temperature dependence hypothesis (Gillooly et al., 2001, 2006).

In addition to parameterising body mass and temperature effects within marine ecosystem models, metabolic rate can also be used to estimate food and oxygen consumption rates, either by using mass and temperature scaling relationships (Rall et al., 2012) or by enabling empirical estimations (Nagy, 1987; Nagy et al., 1999). As metabolic rate is a measure (or proxy) of energy requirements, when combined with the caloric density of the diet, the mass of food the animal requires can be estimated (Nagy, 1987; Nagy et al., 1999). While food consumption rates are essential components of the widely-used Ecopath with Ecosim models (Christensen et al., 2005), oxygen consumption rates are also important in investigating the synergistic effects of temperature change and oxygen depletion on species distribution (Deutsch et al., 2015, 2020).

1.3.2 Biogeochemical cycling

Along with their interest to fisheries, fish also play an important role in biogeochemical cycling, in particular the active transport of carbon (Davison et al., 2013; Trueman et al., 2014; St John et al., 2016; Anderson et al., 2018; Saba et al., 2021). The oceans are estimated to have taken up approximately 25-30% of all anthropogenic carbon outputs, thereby preventing those carbon emissions from contributing to atmospheric warming (Gruber et al., 2019; Watson et al., 2020). Fish and other marine biota play a key role in transporting carbon from the surface, where it readily fluxes in and out of the atmosphere, to the deep-sea where the it becomes effectively sequestered (Hidaka et al., 2001; Davison et al., 2013; Anderson et al., 2018).

TABLE 1.2: Global- to regional-scale marine ecosystem models, and their use of metabolic (or metabolically) derived scaling exponents. b = body mass scaling exponent. E = Arrhenius activation energy (or equivalent derived from Q_{10} value). Model type from (Tittensor et al., 2018). Ecto = ectotherm, Endo = endotherm, SMR = standard metabolic rate, FMR = field metabolic rate.

Model		**Model type**	b	E
Name	Reference(s)			
Dynamic bioclimatic envelope model	Cheung et al. (2013)	Species distribution	0.70	0.62
Dynamic pelagic-benthic model	Blanchard et al. (2012)	Size-spectrum	Predators: 0.82 Prey: 0.75	0.63
Macroecological model	Jennings and Collingridge (2015)	Size-spectrum	0.75	0.67
Bioeconomic marine tropic size-spectrum model	Carozza et al. (2016, 2019)	Size-spectrum	0.68	Growth: 0.21 to 0.43 Mortality: 0.34 to 0.64
Atlantis	Audzijonyte et al. (2019)	Composite	0.70	User determined, usually set to 0.65
General ecosystem model	Harfoot et al. (2014)	Composite	Ecto FMR: 0.88 Endo FMR: 0.70 SMR: 0.69	0.69

Species that undertake diel vertical migrations move from depth during the day to near-surface water at night, to feed under the cover of darkness (Gjøsæter and Kawaguchi, 1980). Before daybreak these fish return to the deeper waters (Gjøsæter and Kawaguchi, 1980), carrying with them carbon originating from the surface. The fish then release this carbon through respiration, excretion and mortality (Hidaka et al., 2001; Davison et al., 2013; Anderson et al., 2018). If carbon is released below the thermocline (typically 200 - 1000 m) the released carbon is effectively sequestered (Saba et al., 2021). Non-migratory fish also play a crucial role in carbon flux, as their fast-sinking faecal pellets and carcasses transport carbon to the deep ocean (Davison et al., 2013; Bianchi et al., 2021; Saba et al., 2021).

Combined with estimates of biomass, metabolic rate can be used to estimate species' contribution to fish-mediated carbon flux (Belcher et al., 2019, 2020; Saba et al., 2021). These estimates are crucial to ensuring sustainable fisheries as when fish are captured, either for consumption by humans or for aquaculture for feedstock (St John et al., 2016), their biomass carbon is released back into the atmosphere (Bianchi et al., 2021). Understanding the role fish play in biogeochemical cycling is a key part of considering sustainable fisheries, beyond simply ensuring self-sustaining biomass.

1.3.3 Field metabolic rates

Current macroecological models of metabolic rate have enabled ecosystem models to have excellent first insights into the roles of fish in biochemical cycling (Anderson et al., 2018; Belcher et al., 2019), and the potential impacts of anthropogenic stressors such as climate change on fish and their wider ecosystems (Tittensor et al., 2018). However, understanding macroecological patterns of *field* metabolic rates in fishes would enable new insights on metabolic theories, and potentially enable more appropriate parameterisation of marine ecosystem models (Treberg et al., 2016).

For models considering consumption rates, FMR is important as a wild fish must consume enough nutrients and oxygen to sustain all of its metabolic activities, not just basal costs (Treberg et al., 2016). Understanding and incorporating the costs of key life history events, such as spawning and migration (Smoliński et al., 2021), is crucial to estimating the biomass required to support a fish population. There have been several attempts to overcome the limitations of SMR-derived food-consumption estimates, including using energy budgets (Drazen, 2002), adding activity multipliers to SMR, and estimating FMR using morphometric measures (Palomares and Pauly, 1989; Sambilay Jr., 1990). Despite these advances and recommendations, the majority of ecosystem-based models use measures based on laboratory studies, which may not reflect field conditions (Hansen et al., 1993; Treberg et al., 2016).

For models which consider the scaling of metabolic rate with body mass and temperature, if these scaling relationships are different in the field, they may be over- or underestimating the effects of body mass and temperature on the metabolic rates of wild fishes. Understanding the macroecological patterns of fish metabolic rates in the field will enable better understanding of FMR across a wider range of vertebrates, and more appropriate parameterisation of ecosystem models.

1.4 Methodology

To improve ecosystem and biogeochemical models, and to predict the impact of climate change on fish, it is crucial to explore the applicability of macroecological patterns in wild, free-living individuals. The typical method for measuring metabolic rates in the field (FMR) is the doubly-labelled water method (Lifson et al., 1955). Unfortunately, this method cannot be applied to fish due to their high water-turnover rate (Butler et al., 2004; Treberg et al., 2016). The lack of a suitable method has led to a paucity of research investigating FMR in fishes, particularly at a macroecological scale.

Given FMR must be measured on a free-living animal (Treberg et al., 2016), respirometry cannot be used for this type of metabolic rate. Instead, proxy methods must be used, although it should be noted that oxygen consumption itself is a proxy-measure of metabolic rate (Nelson, 2016; Treberg et al., 2016). In this thesis I used the otolith-stable isotope (C_{resp}) method (Chapter 2, section 2.4), however, for completeness I also describe other methods of measuring fish FMR below.

1.4.1 Otolith-stable isotope (C_{resp}) method

The C_{resp} method estimates the proportion of metabolic carbon in a fish's blood by analysing the stable isotopic composition of the otolith carbon ($\delta^{13}C$ values, Chung et al., 2019a,b; Trueman et al., 2016). Otoliths are paired calcium carbonate (aragonite) structures that grow in the inner ear of fishes, and are used by the fish for hearing and balance (Campana, 1999). Carbonate in the otolith forms from carbonate in the endolymph, the fluid surrounding the otolith, which itself comes from the fish's blood. Blood carbonate in fishes originates from two isotopically-distinct sources: dissolved inorganic carbon (DIC) in the ambient water, which is ingested through the gills and gut, and metabolic carbon from the respiration of food (Schwarcz et al., 1998; Tohse and Mugiya, 2008; Trueman et al., 2016; Chung et al., 2019a,b). Metabolic carbon typically has lower $\delta^{13}C$ values than DIC, therefore if a fish is operating at a higher metabolic rate, more metabolic carbon will be produced, shifting the $\delta^{13}C$ value of the otolith to a lower value, closer to that of the metabolic carbon (Trueman et al., 2016; Chung et al., 2019a,b). This phenomenon had previously been explored by regressing

published $\delta^{13}C$ values from otoliths against caudal aspect ratio (a morphometric proxy for activity level, Sherwood and Rose, 2003). Across a wide range of species, $\delta^{13}C$ values of otoliths had a negative correlation with the caudal aspect ratio, suggesting that activity, and therefore FMR, was linked to $\delta^{13}C$ values of otoliths (Sherwood and Rose, 2003).

The approach of using $\delta^{13}C$ values of otoliths was refined by estimating proportion of metabolic carbon in the fish's blood, termed the C_{resp} value, can be estimated via a mass-balance equation (Chapter 2):

$$\delta^{13}C_{oto} = C_{resp} \times \delta^{13}C_{diet} + (1 - C_{resp}) \times \delta^{13}C_{DIC} + \epsilon_{total} \tag{1.4}$$

where $\delta^{13}C_{oto}$ is the $\delta^{13}C$ value of the otolith, $\delta^{13}C_{diet}$ is the $\delta^{13}C$ value of the fish's diet, $\delta^{13}C_{DIC}$ is the $\delta^{13}C$ value of the DIC within the ambient water, and ϵ_{total} is the net isotopic fractionation (the change in $\delta^{13}C$ value from the fish's blood, to endolymph, to aragonite in the otolith, Trueman et al., 2016; Chung et al., 2019a,b). C_{resp} values have been positively correlated with oxygen consumption in Atlantic cod (*Gadus morhua*, Chung et al., 2019b) and Australasian snapper (*Chrysophrys auratus*, Martino et al., 2020).

It is important to note, however, that to calibrate C_{resp} values (or any other proxy measure) to metabolic rate in the strict sense, direct calorimetry should be used, as oxygen consumption itself is a proxy for metabolic rate (Treberg et al., 2016). Furthermore, the relationship between oxygen consumption and strict metabolic rate varies depending upon the fuel oxidised during respiration (Frayn, 1983). While direct calorimetry is possible for small (< 1 g) aquatic animals (van Ginneken and van den Thillart, 2009), it is difficult due to the high heat capacity of water (Chabot et al., 2016; Treberg et al., 2016).

Studies using $\delta^{13}C_{oto}$ and C_{resp} values to investigate metabolic rate have primarily focused on single-species studies, with some studies of small communities of fishes. Many studies have investigated life-history profiles of FMR alongside intristic or extrinsic factors (Schwarcz et al., 1998; Gerdeaux and Dufour, 2015; Lin et al., 2012; Trueman et al., 2013; Shephard et al., 2007; Shiao et al., 2017). Temperature is one extrinsic factor which consistently arises as affecting $\delta^{13}C_{oto}$ values, often correlating with other factors such as depth (Lin et al., 2012; Shiao et al., 2017; Shephard et al., 2007; Trueman et al., 2013), latitude (Sinnatamby et al., 2015) and season (Wurster et al., 2005).

The C_{resp} method has been applied to *G. morhua* multiple times, due to its socio-economic importance, large otoliths and available calibration curve (Chung et al., 2019a). Results have shown differences between *G. morhua* ecotypes in terms of C_{resp} values and thermal sensitivity. For example, *G. morhua* from the Barents Sea had

higher mean C_{resp} values compared to *G. morhua* inhabiting Icelandic shelf seas (C_{resp} values of 0.295 and 0.275 respectively, which was attributed to the energetic costs of annual spawning migrations undertaken by the Barents Sea population (Smoliński et al., 2021). The ability to derive C_{resp} values from archival otoliths enables long-term studies, and circumvents many of the ethical and husbandry considerations which are present when capturing and experimenting on live fish (Sloman et al., 2019). The ability to derive C_{resp} values from samples of non-living animals, requiring no special storage conditions, enables efficient study of a large number and variety of species. Unlike tagging approaches, there is no requirement to recapture a free-ranging fish (Treberg et al., 2016), something which is particularly challenging for wide-ranging pelagic species (Watanabe and Goldbogen, 2021). The C_{resp} method also enables estimates of FMR to be obtained for species which are otherwise hard to reach, such as those in the deep-sea, or those which do not survive will in captivity, such as lanternfish (family: Myctophidae, Belcher et al., 2019; Torres and Somero, 1988, Chapter 3). Another advantage of the C_{resp} method is the ability to derive temperature from the same sample as is used for C_{resp} values (Chapter 2, section 2.5). Oxygen stable isotope ($\delta^{18}O$) values from otoliths are widely used to estimate the experienced temperature of ectothermic fishes (Thorrold et al., 1997; Høie et al., 2004), or the brain temperature of mesothermic fishes (Radtke et al., 1987).

While the C_{resp} method is useful in estimating fish FMR, it is not without limitations. Firstly, while C_{resp} values have been calibrated to oxygen consumption for juveniles of two species (*G. morhua* and *C. auratus*), these two species are relatively similar in that they are both relatively large, benthopelagic species (Chung et al., 2019a; Martino et al., 2020). The calibration relationship between C_{resp} values and oxygen consumption determined from these two species may not be the most appropriate across the diversity of fishes (Treberg et al., 2016). One aim of this thesis is to gain an understanding of the differences in C_{resp} values across a wide range of fishes, which may go some way to exploring how C_{resp} values relate to oxygen consumption. Secondly, C_{resp} values can only be estimated with some degree of accuracy when the $\delta^{13}C$ values of the DIC in the ambient water ($\delta^{13}C_{DIC}$) and of the diet ($\delta^{13}C_{diet}$) are known or can be estimated. For marine fishes, $\delta^{13}C_{DIC}$ values can be estimated using isoscapes (Tagliabue and Bopp, 2008), or via measures of apparent oxygen use (Smoliński et al., 2021, section 2.4.1). Conversely, the greater variability of $\delta^{13}C_{DIC}$ values in areas of high freshwater input (Bade et al., 2004), largely restricts the use of the C_{resp} method to fully marine species, unless $\delta^{13}C_{DIC}$ values are measured from ambient water (Chung et al., 2019a). Finally, the C_{resp} method is only applicable to teleost fish; although there is some work determining the applicability of the C_{resp} method to other taxa (e.g. cephalopods, Chung et al., 2021a), this method excludes a large amount of vertebrate and invertebrate diversity. Although not an issue when focusing on teleost fishes, the need for biogeneic carbonates precludes the C_{resp} method from broader use in macroecological studies.

Although this thesis focuses on using the C_{resp} method of determining FMR, for completeness I also describe three additional proxy measures of FMR in fish: (1) electron transport system activity, (2) heart and ventilation rate, and (3) accelerometry.

1.4.2 Electron transport system activity (ETS)

Electron transport system activity (ETS) measures the respiratory potential of a tissue via specific enzyme activities (Belcher et al., 2020; Treberg et al., 2016; Cammen et al., 1990; Ikeda, 1989). These enzymes can be involved in aerobic respiration, such as citrate synthase, or anaerobic respiration, such as lactate dehydrogenase (Drazen et al., 2015; Gerringer et al., 2017). Similarly to the C_{resp} method, ETS is advantageous in that it does not require the capture and maintenance of a live individual (as with respirometry), or the recapture of a free-living individual (as with tagging). That being said, ETS is slightly more logistically challenging than the C_{resp} method, as it requires tissue from a recently deceased individual, or tissue which has been stored at -80°C (Drazen et al., 2015).

Like the C_{resp} method, ETS is a proxy of oxygen consumption, and is converted into whole-organism oxygen consumption (μl O_2 hr^{-1}) using a ratio (R:ETS Belcher et al., 2020), which ranges from 0.98 to 2.25 in fishes (Ikeda, 1989). However, the relationships between oxygen consumption and aerobic enzyme activities, such as citrate synthase and cytochrome C oxidase, are inconsistent in fishes (Treberg et al., 2016). A key difference between the ETS and C_{resp} methods is the amount of time incorporated within a sample. Whereas C_{resp} values can incorporate time over the life history of a fish, or a specific time period of months to years (Appendix E, Trueman et al., 2016; Chung et al., 2019a,b), ETS measures metabolic rate across the hours before the fish was captured (Gómez et al., 1996; Hernández-León et al., 2019).

There remains some uncertainty as to what kind of metabolic rate ETS acts as a proxy for (section 1.1, as this often goes unspecified. Given that ETS measures the maximum respiratory potential of a tissue, which is variable over short timescales Ikeda, 1989; Cammen et al., 1990, it is likely that ETS approximates a measure between field and maximum metabolic rate.

1.4.3 Heart and ventilation rates

The use of heart rate as a proxy for oxygen consumption is based on Fick's principle of cardiac output:

$$V_{O_2} = f_H V_S (Ca_{O_2} - Cv_{O_2}) \tag{1.5}$$

where V_{O_2} is oxygen consumption, f_H is the heart rate, V_S is the stroke volume, and Ca_{O_2} and Cv_{O_2} are the oxygen contents of arterial and venous blood, respectively (Fick, 1870). From this principle, assuming the stroke volume and difference in oxygen content between arterial and venous blood remain the same, an increase in heart rate will confer an increase in oxygen consumption (Watanabe and Goldbogen, 2021).

Heart rate measures can be a useful proxy for FMR, as it incorporates both the cost of movement and specific dynamic action (Treberg et al., 2016; Watanabe and Goldbogen, 2021). On larger fish ($>$ 1kg body mass), biologgers can be implanted which can record heart rate over a long period (Butler et al., 2004; Metcalfe et al., 2016). Unfortunately, as with any technique involving tagging or surgical implantation, the size of the biologger prevents the use of this method on smaller fish (Treberg et al., 2016). The size restriction limits the usefulness of this method when wanting to capture a broad range of fish body masses, such as in ontogenetic or macroecological studies.

Similar to heart rate, ventilation rate has also been used as a proxy for oxygen consumption (Castejón-Silvo et al., 2021). Ventilation can be useful for smaller fish, as it is measured by observation rather than burdening the animal with a tag or biologger. However, measuring via visual observation opens the method to observer error, and increases the logistical difficulties of such studies, particularly in the field where the presence of a diver observing the animal is likely to cause stress. Factors such as stress can violate the two assumptions inherent in Fick's principle: that the oxygen differential and stroke (or ventilation) volume remain the same (Watanabe and Goldbogen, 2021). Additionally, correlations between oxygen consumption and heart or ventilation rates are species-specific; more so than for C_{resp} values or ETS activities (Butler et al., 2004; Metcalfe et al., 2016; Castejón-Silvo et al., 2021). A final logistical consideration is the expense of retrieving the biologgers, and the cost of lost biologgers (Treberg et al., 2016). The variation in correlation between oxygen consumption and ventilation or heart rates, combined with the logistical difficulties, makes these methods more suitable for intraspecific studies of field metabolic rates.

1.4.4 Accelerometry

A final approach to estimating FMR in fishes is the use of accelerometry tags, which measure the locomotory component of metabolism (Metcalfe et al., 2016; Treberg et al., 2016). The key advantage of accelerometry tags is that they can be combined with other types of data-storage tags, enabling FMR estimates to be compared with fine-scale environmental and behavioural data (Metcalfe et al., 2016; Treberg et al., 2016). Accelerometry has been applied to estimating the FMRs of marine animals including sawfish (*Pristis pristis*, Lear et al., 2020) and yellowtail kingfish (*Seriola lalandi*, Brodie et al., 2016). In the latter study, the ability to incorporate the locomotory

aspect of metabolic rate significantly improved estimates of consumption rates for *S. lalandi*, a commercially important carnivorous species (Brodie et al., 2016).

The key drawback of accelerometry is the same as for other tagging or biologging approaches: the need for a tag limits this method to relatively large species and individuals (Bridger and Booth, 2003; Cooke et al., 2004; Metcalfe et al., 2016; Treberg et al., 2016). Furthermore, given that accelerometry measures only the locomotory component of metabolism, this method is less suitable for sedentary species (Watanabe and Goldbogen, 2021). Even when applied to active species, the relationship between the accelerometry and oxygen consumption may be altered if the animal is employing energy-saving techniques such as gliding, or adjusting their buoyancy (Watanabe and Goldbogen, 2021). The use of tailbeat frequency measurements can help to determine whether the movement recorded is active or passive, but requires further machinery and a further burden to the animal (Watanabe and Goldbogen, 2021). Finally, as with all proxy measures, this method requires calibration to oxygen consumption or direct energy expenditure, something which is likely to vary among and within species (Treberg et al., 2016).

1.5 Thesis aim, objectives and structure

1.5.1 Thesis aim and objectives

While laboratory and assay-based methods have allowed ecologists to determine macroecological patterns of metabolic rate in fishes, questions remain as to whether these patterns apply in the context of free-living wild fish. Thus, the core aim of my thesis is to test whether key macroecological theories apply to otolith-derived estimates of field metabolic rates, which I will achieve via the following objectives:

1. To create a large interspecific dataset of C_{resp} values, covering as broad a range as possible of taxonomic and function groups of marine teleost fishes.
2. To complete a case-study investigating the driving factors influencing field metabolic rates within a biogeochemically important group of marine teleosts.
3. To determine the interspecific scaling patterns of C_{resp} values within marine teleost fishes, and to examine the influence of shared evolutionary history on field metabolic rates.
4. To determine what effect thermal realm and range has on species' C_{resp} values, after accounting for differences in body mass and experienced temperatures.
5. To explore whether deep-sea fish species have lower field metabolic rates compared to shallower-living fishes.

1.5.2 Thesis structure

My thesis tests whether key macroecolgical patterns of metabolic rates apply when using otolith-derived field metabolic rates. Each chapter draws upon a large interspecific dataset of C_{resp} values and estimates of experienced temperatures, the creation of which is detailed in Chapter 2. Chapter 3 focuses on a region- and taxon-specific case-study, while chapters 4 - 6 each explore a different macroecological patterns of field metabolic rate. Finally, Chapter 7 synthesises information across the thesis, drawing conclusions about field metabolic rate, the use of the C_{resp} method, and its application to macroecological questions.

- **Chapter 2:** Methods
  - Details the creation of the main dataset. This chapter covers:
    - the otolith acquisition process
    - the stable isotope analysis of the otolith samples
    - the statistical processes used to estimate C_{resp} values and experienced temperatures
    - the compilation of the species' ecological dataset
    - the phylogeny inference
  - This chapter also provides a summary of the dataset coverage across taxonomic and functional groups.
- **Chapter 3:** Otolith-derived field metabolic rates of myctophids from the Scotia Sea
  - Explores the scaling of C_{resp} values with body mass and temperature within a biogeochemically important group of fishes: the myctophids (lanternfish) from the Scotia Sea in the Southern Ocean.
  - This chapter has been published in the Marine Ecology Progress Series (Alewijnse et al., 2021).
- **Chapter 4:** Body mass and temperature scaling of C_{resp} values
  - Determines where C_{resp}-derived field oxygen consumption estimates fall between species' standard and maximum oxygen consumption rates.
  - Determines the best-fit scaling exponents of estimated field oxygen consumption with body mass and temperature.
  - Examines the effect of shared evolutionary history on field metabolic rates.
- **Chapter 5:** Do cold fish run hot? The effect of species thermal realm on otolith-derived field metabolic rates
  - Test the hypothesis of "metabolic cold adaptation" by determining whether C_{resp} values differ due to species thermal realm, after accounting for differences in body mass and temperature.
  - Test whether species thermal adaptation range affects the scaling of C_{resp} values with temperature.
- **Chapter 6:** Depth
  - Determine whether C_{resp} values decrease with depth in marine teleosts, after accounting for differences in body mass, temperature and habitat.

Chapter 2

Methods

2.1 Introduction

The analyses in Chapters 4, 5 and 6 required a large dataset of C_{resp} values and experienced temperatures, from a broad range of species. Therefore, I compiled data on $\delta^{13}C$ and $\delta^{18}O$ values from otoliths - both my own original data and data from the literature - which I converted into C_{resp} values and experienced temperatures.

This chapter details the creation of the main dataset, how I assigned traits to species and individuals, and how I quality checked the dataset. To my knowledge, the main dataset is the largest and most comprehensive interspecific compilation of otolith stable isotope data currently available. The main dataset is comprised of data from otoliths sampled by myself, other members of the Southampton University Marine Isotope Ecology Laboratory (SUMIE) and data from the literature (section 2.2.2). I used the main dataset as the basis for analyses in all subsequent chapters, with the data subsetted according to specific questions or analyses; this is described in detail in each chapter.

2.2 Otolith acquisition

FIGURE 2.1: A sagittal otolith from a *Pollachius pollachius* (pollock) from the collections at the Natural History Museum, London. The label for this individual did not include body size, catch location or year of capture, and so was excluded from my analyses.

I identified target taxa based on the availability of otoliths for destructive sampling, and attempted to obtain as broad a representation as possible across taxonomic and functional groups (section 2.7), within the constraints of the inclusion criteria (Figures 2.1 and 2.2).

2.2.1 Inclusion criteria

As body mass is a key driver of metabolic rate (West et al., 1997; Brown et al., 2004), a measure of body size was required for all analyses. Wet weight (g) was preferable, however, where this was not available I estimated weight from body length using the equation:

$$W = aL^b \tag{2.1}$$

where W is wet weight (g) and L is a measure of body length (usually but not always total length in cm, section 2.6). a and b are species-specific parameters describing the relationship between length and body mass. I preferentially sought species-specific values for a and b where possible, however, where these were not available I used closely related species parameters, or parameters for the genus of the species in question. Appendix B gives a full list of length-weight parameters used, and their sources.

An approximate catch location was required to estimate $\delta^{13}C$ values of dissolved inorganic carbon in the seawater (DIC, section 2.4.1). $\delta^{13}C_{DIC}$ varies spatially in the oceans, due to the fractionation which occurs during photosynthesis and air-sea gas exchange (Gruber et al., 1999). However, $\delta^{13}C_{DIC}$ is less variable and more predictable in marine compared to fresh waters ($\delta^{13}C_{DIC}$ maximum range 0 to 2.9 ‰ in marine vs. -31.3 to -2.1 ‰ in lakes; Bade et al., 2004; Tagliabue and Bopp, 2008), which is why this this thesis focused on marine teleosts. The relatively low variability of marine $\delta^{13}C_{DIC}$

also meant that precise catch location was not necessary; within one degree of latitude and longitude was acceptable precision. Where only landing port was available, I set the catch location offshore of the port using Google Maps (Google, 2021).

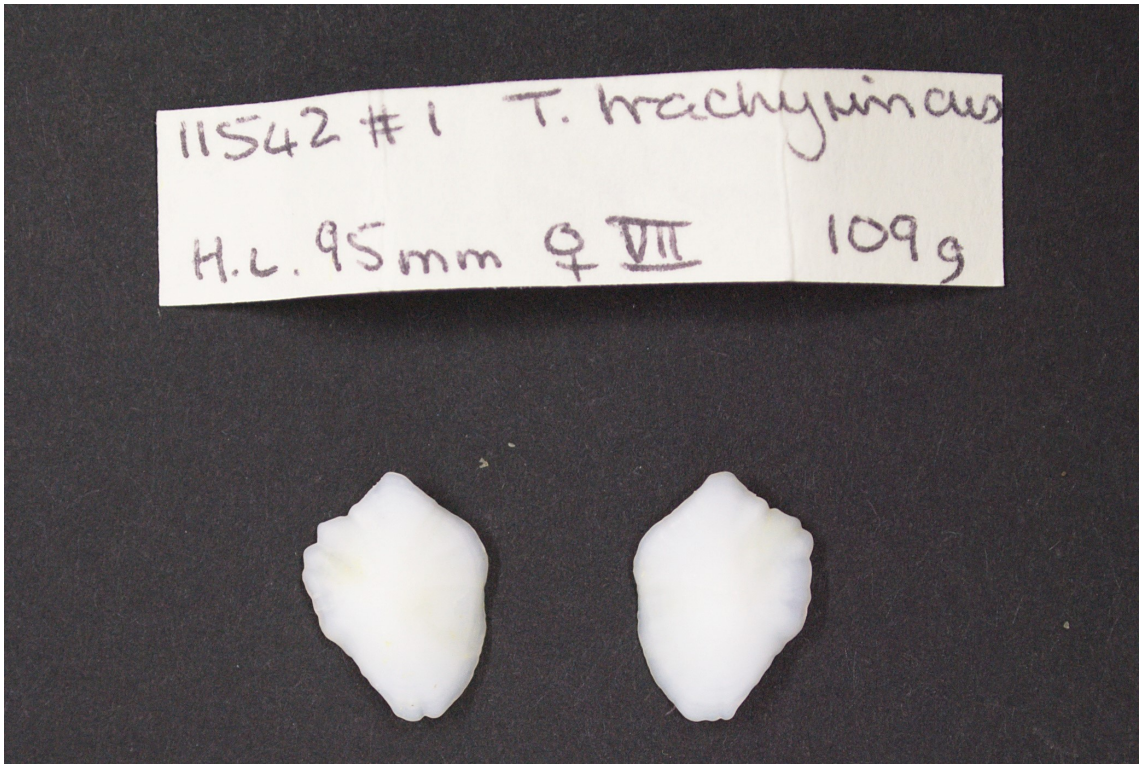

FIGURE 2.2: Sagittal otoliths from an individual *Trachyrincus scabrus* (roughsnout grenadier) from the collections at the Natural History Museum, London. This photograph illustrates the ideal accompanying label, which includes species, body mass and station number (from which catch location and year can be obtained).

Year of capture was necessary to adjust for the Suess effect, which is the decrease in $\delta^{13}C_{DIC}$ over time since the industrial revolution (~1860) due to anthropogenic carbon emissions, which have relatively low $\delta^{13}C$ values (Gruber et al., 1999; Tagliabue and Bopp, 2008). The extent to which the Suess effect is present at a particular location depends upon the exchange of carbon between the ocean and the atmosphere (Gruber et al., 1999; Tagliabue and Bopp, 2008; Eide et al., 2017). In general, the oceanic Suess effect is strongest in areas of high atmospheric exchange, such as subtropical gyres, whereas the Suess effect is weakest at areas of upwelling, such as the Benguela and Peru upwelling regions (Tagliabue and Bopp, 2008; Eide et al., 2017). Furthermore, the magnitude of the Suess effect has changed over time as anthropogenic carbon emissions have increased (Tagliabue and Bopp, 2008; Schöne et al., 2011). For fish captured between 1939 and 1970, I used a rate of -0.07‰ decade^{-1}. Post-1970, I set the Suess effect correction according to location; this ranged between -0.22 and -0.08 ‰ decade^{-1} (section 2.4.1).

2.2.2 Contributing otolith collections

The majority of the samples in this dataset were from the otolith collection at the Southampton University Marine Isotope Ecology Laboratory (SUMIE) and the Discovery Collections at the Natural History Museum London (NHM, Table 2.1). The Discovery Collection otoliths were un-catalogued specimens (though a catalogue was created as part of this project) and as such do not yet have accession numbers. The SUMIE dataset also includes data from the Coldfish project (NERC, 2021), and data analysed by SUMIE alumnus Dr Ming-Tsung Chung as part of his PhD research (Chung, 2015). The resulting otolith collection totalled 88 species. Table 2.1 summarises the collections which contributed to the otolith stable isotope dataset, and the gaps they fill.

TABLE 2.1: Summary of contributing collections to the otolith isotope dataset, including the major gaps filled by each collection in terms of temperature, size and habitat. SUMIE = Southampton University Marine Isotope Ecology, NHM = Natural History Museum London, BAS = British Antarctic Survey, IFREMER = Institut Français de Recherche pour l'Exploitation de la Mer, NSYSY = 國立中山大學 (National Sun Yat-sen University) , MFRI = Marine and Freshwater Institute Iceland, IMEDEA = Institut Mediterrani d'Estudis Avançats, USF = University of South Florida.

Institution	Location(s)	Gaps filled	Number	
			Species	Otoliths
SUMIE	North-East Atlantic	Deep-sea	27	588
	Croatia, Mediterranean Sea	Medium-sized, pelagic	2	
	Barents Sea	Polar species	6	
NHM	Global	Deep-sea, benthopelagic	16	130
Cefas	United Kingdom, North-East Atlantic	Temperate, benthic and benthopelagic, shelf-sea	9	44
	Tristan da Cunha, South-Central Atlantic	Small-to-medium sized, temperate, benthopelagic	3	30
BAS	Scotia Sea, Southern Ocean	Small-to-medium sized, polar, pelagic	7	110
Ascension Islands Government	Ascension Island, Central Atlantic	Tropical and subtropical, pelagic	6	54
Tel-Aviv University	Israel, Mediterranean	Small-to-medium sized, subtropical, benthopelagic	5	25
IFREMER	Gulf of Lions, Mediterranean	Small, subtropical, pelagic	2	10
NSYSU	Taiwan, Central-West Pacific	Small-to-medium sized, tropical, benthopelagic	2	10
MFRI	Iceland, North-Central Atlantic	Lumpfish (*Cyclopterus lumpus*) - a large, benthopelagic, temperate species	1	5

IMEDEA	Mallorca, Mediterranean	Dolphinfish (*Coryphanea hippurus*) - a large, pelagic, subtropical species	1	5
USF	Florida, Gulf of Mexico	Red grouper (*Epinephelus morio*) - a large, benthopelagic, subtropical species	1	5

2.2.3 Literature otolith isotope data

Using data from the literature to fill gaps in my dataset was essential, particularly due to Covid-19 restrictions. Previous studies have largely examined otolith stable isotopes to explore the location of fishes throughout their life histories, for example by using $\delta^{13}C$ and $\delta^{18}O$ as proxies for temperature (e.g. Shiao et al., 2017; Kawazu et al., 2020). I used the data of SUMIE alumna Diana Shores (unpublished thesis) as a starting point, cross-referencing the data from the papers cited and excluding unusable data (see below).

I used Google Scholar and Web of Knowledge to search for otolith isotope data, using the search term `"otolith" AND "stable isotope"`. As of March 2021, the search term yields 5120 results on Google Scholar and 347 results on Web of Knowledge. I also kept search alerts for both of these databases to ensure my dataset was up to date. From the search results, papers were filtered by the following criteria:

1. The paper must concern marine teleosts, or contain measured $\delta^{13}C_{DIC}$ values of the ambient water for non-marine teleosts. The teleosts must also have been free-living in the wild.
2. The paper must give some measure of body size, either wet weight (g) or length (cm or mm).
3. The paper must give at least $\delta^{13}C$ of the otolith, ideally also $\delta^{18}O$, in either a table or graph.
    - Where data was present in graphs, but not in the paper, I used the R package `digitize` to extract the data (Poisot et al., 2011).
4. The paper must give a catch location within at least one degree of latitude and longitude, or a landing port.
5. The paper must sample either the outer surface or the whole otolith. I excluded papers sampling only the otolith core (i.e. the larval stage).

After filtering the results, the literature yielded 352 data points, representing 35 species across 28 papers (Table 2.2). Sometimes $\delta^{13}C$, $\delta^{18}O$ or metadata were only available as mean values; this was the case for 230 of the recovered data points. To account for this, in all models using literature data (Chapters 4, 5 & 6) the number of of individuals per data point (`n`) was incorporated as a random factor in the models.

TABLE 2.2: All species present within the final dataset. n = number of individuals per species. Literature sources are provided where applicable.

Order	Family	Species	n	Literature source (if applicable)
Acanthuriformes	Acanthuridae	*Acanthurus triostegus*	4	Dufour et al. (1998)
		Chaetodon ulietensis	4	Dufour et al. (1998)
Alepocephaliformes	Alepocephalidae	*Alepocephalus agassizii*	6	
		Alepocephalus bairdii	3	
		Rouleina attrita	7	
		Xenodermichthys copei	5	
Anguilliformes	Congridae	*Conger conger*	4	Correia et al. (2011)
	Synaphobranchidae	*Synaphobranchus kaupii*	5	
Argentiniformes	Argentinidae	*Argentina silus*	4	
Ateleopodiformes	Ateleopodidae	*Ateleopus japonicus*	6	Shiao et al. (2017)
		Ijimaia dofleini	2	Shiao et al. (2017)
Aulopiformes	Bathysauridae	*Bathysaurus ferox*	7	
	Ipnopidae	*Bathypterois dubius*	5	
	Synodontidae	*Saurida lessepsianus*	5	
		Saurida undosquamis	5	
Beloniformes	Exocoetidae	*Exocoetus volitans*	10	
Beryciformes	Berycidae	*Beryx splendens*	10	

	Trachichthyidae	*Hoplostethus atlanticus*	6	
		Hoplostethus mediterraneus mediterraneus	10	
Carangiformes	Carangidae	*Seriola dumerili*	7	
		Trachurus trachurus	5	
	Coryphaenidae	*Coryphaena hippurus*	5	
Clupeiformes	Clupeidae	*Sprattus sprattus*	5	
	Engraulidae	*Engraulis encrasicolus*	5	
Gadiformes	Gadidae	*Boreogadus saida*	59	
		Gadus morhua	97	Gao et al. (2001) (n = 10) Weidman and Millner (2000) (n = 10)
		Melanogrammus aeglefinus	62	
		Merlangius merlangus	5	
		Micromesistius poutassou	28	
		Pollachius virens	5	
	Lotidae	*Molva dypterygia*	14	
	Macrouridae	*Bathygadus nipponicus*	8	Lin et al. (2012)
		Cetonurus globiceps	10	
		Coelorinchus caelorhincus	18	
		Coelorinchus fasciatus	10	

		Coryphaenoides acrolepis	8	Lin et al. (2012)
		Coryphaenoides armatus	10	
		Coryphaenoides guentheri	5	
		Coryphaenoides marginatus	8	Lin et al. (2012)
		Coryphaenoides mediterraneus	12	
		Coryphaenoides paramarshalli	5	
		Coryphaenoides profundicolus	10	
		Coryphaenoides rupestris	11	
		Hymenocephalus lethonemus	4	Lin et al. (2012)
		Malacocephalus laevis	7	
		Nezumia aequalis	5	
		Nezumia duodecim	10	
		Squalogadus modificatus	10	
		Trachyrincus murrayi	9	
		Trachyrincus scabrus	10	
	Merlucciidae	*Merluccius merluccius*	22	Hidalgo et al. (2008) (n = 12)
	Moridae	*Antimora rostrata*	16	
		Lepidion eques	19	
		Mora moro	14	

	Phycidae	*Phycis blennoides*	15	
Gobiiformes	Gobiidae	*Gobius bucchichi*	2	Mirasole et al. (2017)
Holocentriformes	Holocentriae	*Holocentrus adscensionis*	9	
Incertae sedis in Eupercaria	Emmelichthyidae	*Plagiogeneion rubiginosum*	5	Horn et al. (2012)
	Lutjanidae	*Lutjanus fulviflamma*	4	Kimirei et al. (2013)
		Lutjanus sebae	20	Stephenson et al. (2001)
		Pristipomoides filamentosus	1	Radtke et al. (1987)
		Pristipomoides multidens	15	Newman et al. (2000)
Istiophoriformes	Istiophoridae	*Kajikia albida*	2	Wells et al. (2010)
		Makaira nigricans	3	Wells et al. (2010)
Labriformes	Labridae	*Coris julis*	2	Mirasole et al. (2017)
Myctophiformes	Myctophidae	*Electrona antarctica*	19	
		Electrona carlsbergi	10	
		Gymnoscopelus braueri	20	
		Gymnoscopelus nicholsi	12	
		Krefftichthys anderssoni	20	
		Protomyctophum bolini	20	
	Neoscopelidae	*Neoscopelus microchir*	10	
Notacanthiformes	Halosauridae	*Halosauropsis macrochir*	5	

Ophidiiformes	Bythitidae	*Cataetyx laticeps*	8	
Pempheriformes	Acropomatidae	*Doederleinia berycoides*	5	
	Epigonidae	*Epigonus telescopus*	10	
Perciformes	Channichthyidae	*Champsocephalus gunnari*	9	
	Cottidae	*Artediellus atlanticus*	22	
		Triglops nybelini	20	
	Cyclopteridae	*Cyclopterus lumpus*	5	
	Nototheniidae	*Dissostichus eleginoides*	43	Ashford and Jones (2007)
	Sebastidae	*Helicolenus dactylopterus*	8	
		Helicolenus mouchezi	10	
		Sebastes mentella	44	
		Epinephelus adscensionis	10	
		Epinephelus morio	5	
		Epinephelus multinotatus	14	Stephenson et al. (2001)
		Hyporthodus nigritus	4	Sanchez et al. (2020)
	Zoarcidae	*Lycodes gracilis*	13	
Pleuronectiformes	Pleuronectidae	*Glyptocephalus cynoglossus*	5	
		Hippoglossoides platessoides	22	
		Limanda limanda	4	

		Microstomus kitt	5	
	Scophthalmidae	*Lepidorhombus whiffiagonis*	5	
		Scophthalmus maximus	5	
	Soleidae	*Solea solea*	5	
Salmoniformes	Salmonidae	*Salmo salar*	7	Hanson et al. (2013)
Scombriformes	Arripidae	*Arripis georgianus*	5	Ayvazian et al. (2004)
	Scombridae	*Acanthocybium solandri*	9	
		Scomber colias	11	Correia et al. (2021) (n = 6)
		Scomber scombrus	32	Moura et al. (2020) (n = 6)
		Thunnus albacares	9	
		Thunnus maccoyii	11	Shiao et al. (2009)
		Thunnus orientalis	69	Kawazu et al. (2020)
	Trichiuridae	*Aphanopus carbo*	8	
Spariformes	Lethrinidae	*Lethrinus harak*	3	Kimirei et al. (2013)
		Lethrinus lentjan	4	Kimirei et al. (2013)
	Sparidae	*Chrysophrys auratus*	6	Bastow et al. (2002)
		Diplodus vulgaris	2	Mirasole et al. (2017)
		Oblada melanura	10	
		Pagellus erythrinus	5	

		Pagrus caeruleostictus	5
Syngnathiformes	Mullidae	*Mullus barbatus barbatus*	5
		Upeneus moluccensis	5
Total		**114**	**1327**

2.3 Stable isotope analysis

2.3.1 Otolith preparation

I cleaned all otoliths before milling by soaking them in tap water for approximately one minute, and then using a mounted needle and forceps to carefully remove any debris stuck to the surface. Once the otolith was cleaned I blotted it on blue roll or Kimwipe and left it to air dry completely.

In all cases I aimed to obtain powder from the outermost portion of the otolith, where possible. The outermost portion represents the most recent life history of the fish (Campana, 1999), so it is the point for which we have the most accurate catch location and body size data.

I affixed large otoliths to a glass slide using Blu Tack and used a Dremel 4000 rotary tool with a flexible shaft extension, tipped with an 0.8mm or 1.6mm engraver, depending on the otolith size (Dremel bits 108 and 106, respectively). I used the lowest drill speed possible to carefully mill the outer edge, as far away from the core as possible. For small otoliths, I used a Wild Heerbrugg M3C stereomicroscope to assist milling (Figure 2.3). Where growth rings were visible, I milled the portion of the other surface where the bands were widest, to ensure that the amount of time incorporated in the powdered sample was minimal. Whether the proximal or distal surface was sampled depended upon the shape of the otolith, which itself varied among the species sampled. For more fragile otoliths it was often necessary to position them curved-side down on a mound of Blu Tack, strengthening them similar to a veneer. I aimed to mill the minimum amount necessary to gather enough otolith powder for stable isotope analyses. From the otoliths sectioned, the amount of fish life history incorporated into each sample ranged from 0.5 to 6.0 years,

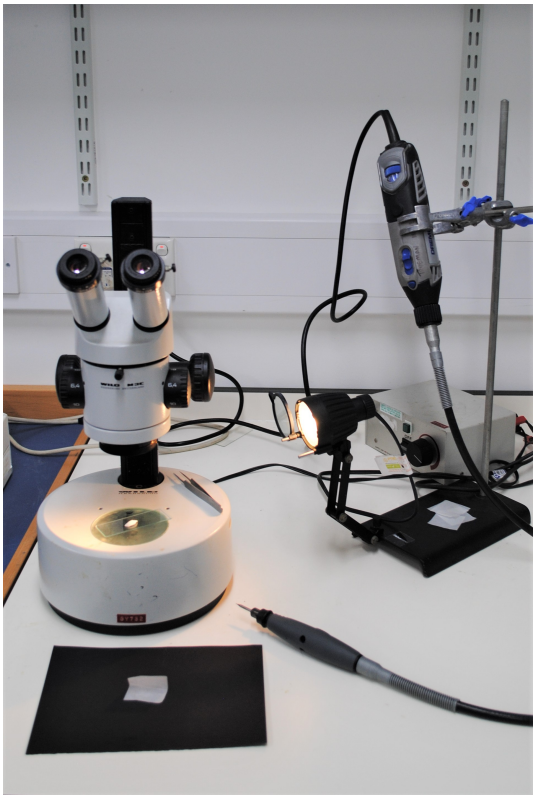

FIGURE 2.3: The setup for milling otoliths using a Dremel 4000 rotary tool with a flexible shaft extension, including weighing paper used to store otolith powder. Also shown is a Wild Heerbrugg M3C stereomicroscope and reflected light, used to aid milling of the smallest otoliths.

with a mean as 2.3 years (Appendix E). I tipped the resulting powder into a weighing paper packet and stored this upright until weighing. Although 50 μg was the amount required for each sample, in practice I took more than this to account for powder lost between transfer from the paper packet and vials, in the weighing process and for powder lost in transport, particularly for samples analysed at NEIF. Between each otolith, I cleaned the drill bit and glass slide using compressed air and Kimwipes.

FIGURE 2.4: The three methods used for mounting otoliths for milling. Top left is a *Pollachius virens* (saithe) otolith mounted onto a glass slide with Blu Tack. Top right is an *Epinephelus adscensionis* (rock hind grouper) otolith mounted onto a resin backing plate and affixed with resin. Bottom is a *Halosauropsis macrochir* (abyssal halosaur) otolith mounted onto a glass slide using Loctite superglue.

I prepared small or very fragile otoliths in one of three ways (Figure 2.4): I mounted most of these otoliths using Streurs EpoFix resin, and milled the outer portion using an ESI New Wave Micromill (Figure 2.5). As with the Dremel, I milled as far away from the core as possible and preferentially where growth bands were thickest (if visible). I plotted the milling points as discrete spots, and then took a surface profile of the otolith. The milling bits used were all flat edged and had cut widths of 900-1000 μm. I set the drill speed to 5250 rpm (15% of maximum) and the depth per pass to 200 μm.

FIGURE 2.5: Top left shows the otolith milling setup, using an ESI New Wave Micromill. Top right shows how mounted otoliths were affixed to the Micromill stage, using masking tape. The drill bit mounted is flat edged with a cut width of 900 μm.

I collected otolith powder using two scalpel blades and tapped this into weigh-paper packets for long-term storage. As with the Dremel, I cleaned the drill bit and plate with compressed air and Kimwipe between each otolith. Despite using discrete points to mill each otolith the Micromill experienced some drift, which resulted in some otoliths being milled closer to the centre of their lateral surface (between the outer edge and the core), rather than the outer surface (Figure 2.6).

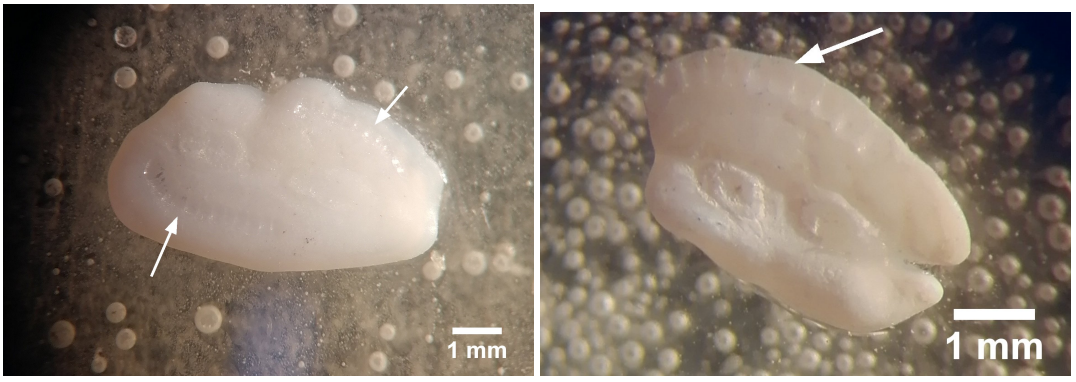

FIGURE 2.6: Photos illustrating Micromill drift. Top left shows a milled *Coryphaenoides mediterraneus* otolith where drift has occurred, resulting in milling across the midpoint between the outer edge and centre of the otolith. Top right shows the ideal micromilling pattern along the outer edge, on an otolith from *C. paramarshalli*. Arrows point to the milling tracks.

I used the micromill to sample the majority of small otoliths, however, the Covid-19 pandemic and moving of labs necessitated using a different method for later milling. This involved me mounting the otoliths on a glass slide with Loctite super glue, and very carefully using a Dremel to mill the outer edge using the procedure described for larger otoliths. Finally, I crushed those otoliths which were too small to mill ($<$ 1mm diameter) using a mortar and pestle, incorporating the whole otolith into the final sample.

2.3.2 Stable isotope analysis

Due to funding requirements, two separate facilities were used to analyse the otolith material. The first was the Stable Isotope Ratio Mass Spectrometry (SIRMS) laboratory at the University of Southampton. This facility used a Kiel IV Carbonate device coupled with MAT253 isotope ratio mass spectrometer. The second was the National Environmental Isotope Facility (NEIF) at the British Geological Society in Keyworth, Nottingham. This facility used an IsoPrime dual inlet mass spectrometer plus Multiprep device. Both facilities ran the international standards NBS18 (carbonatite) and NBS19 (limestone) to ensure precision and check for any instrumental drift. The in-house standard GS1 (Carrara marble) used at SIRMS was also run at NEIF to test for any difference between the two facilities. I report all values of $\delta^{13}C$ and $\delta^{18}O$ relative to Vienna Pee Dee Belemnite:

$$\delta = \frac{R_{sample} - R_{standard}}{R_{standard}} \times 1000 \tag{2.2}$$

where R is the ratio of either ^{13}C:^{12}C for $\delta^{13}C$ or ^{18}O:^{16}O for $\delta^{18}O$ (Fry, 2006).

Although there were differences in GS1 stable isotope ratios between the two facilities, these differences were minimal, with a difference in means of 0.02‰ for $\delta^{13}C$ and 0.03‰ for $\delta^{18}O$. Standard deviations for $\delta^{13}C$ and $\delta^{18}O$ values of GS1 across both facilities were 0.03‰ and 0.04‰ respectively, therefore these differences between facilities is consistent with measurement error.

2.4 Estimating C_{resp} values

The proportion of respiratory carbon in the fish's blood, as derived from otolith isotope data (C_{resp}, our proxy for field metabolic rate), was estimated according to the following mass balance equation (Trueman et al., 2016; Chung et al., 2019b,a; Martino et al., 2020):

$$\delta^{13}C_{oto} = C_{resp} \times \delta^{13}C_{diet} + (1 - C_{resp}) \times \delta^{13}C_{DIC} + \epsilon_{total} \quad (2.3)$$

where $\delta^{13}C_{oto}$ is the $\delta^{13}C$ of the otolith, $\delta^{13}C_{diet}$ is the $\delta^{13}C$ of the fish's diet, $\delta^{13}C_{DIC}$ is the $\delta^{13}C$ of the DIC within the ambient water, and ϵ_{total} is the net isotopic fractionation (the change in $\delta^{13}C$ value from the fish's blood, to endolymph, to aragonite in the otolith, Trueman et al., 2016; Chung et al., 2019a,b; Martino et al., 2020). I estimated C_{resp} using the `MixSIAR` package (Stock et al., 2018). `MixSIAR` is a Bayesian mixing model framework originally developed to analyse biotracer data, and is most commonly used to estimate proportions of diet sources using stable isotope or fatty acid analyses (Stock et al., 2018). `MixSIAR` estimates the proportions of sources' (in our case $\delta^{13}C_{DIC}$ and $\delta^{13}C_{diet}$) contributions to a mixture (in our case $\delta^{13}C_{oto}$). I ran each model for 100,000 iterations, with a burnin of 50,000, thinning parameter of 50, and three chains. I checked for model convergence and reliability using the Gelman-Rubin and Geweke's diagnostics, effective sample size and visual inspection of the traceplots (Plummer et al., 2006).

I describe the procedure for measuring $\delta^{13}C_{oto}$ values in section 2.3. In the following sections I will outline the procedures for estimating the other C_{resp} equation components. I estimated $\delta^{13}C_{DIC}$ and $\delta^{13}C_{diet}$ values using a Bayesian framework using the `rjags` package (Plummer, 2019). Each model was run for 100,000 iterations, with a warmup of 50,000, three chains, and a thinning parameter of 50. As with C_{resp} value estimations, I checked for model convergence and reliability using the Gelman-Rubin and Geweke's diagnostics, effective sample size and visual inspection of the traceplots (Plummer et al., 2006).

2.4.1 Dissolved inorganic carbon

I estimated $\delta^{13}C_{DIC}$ values by combining isoscape estimates and estimates derived from apparent oxygen utilisation (AOU; Smoliński et al., 2021) in a Bayesian framework. First, I set the annual average distribution of $\delta^{13}C_{DIC}$ values in the ocean's surface waters from the PISCES-A model (Tagliabue and Bopp, 2008), according to catch location. I used these values, along with a standard deviation of 0.202 as informative priors for the estimation of $\delta^{13}C_{DIC}$ values from AOU:

$$AOU = \frac{\delta^{13}C_{DIC} - a}{b} \tag{2.4}$$

where a = 1.300 ($\pm$ 0.404) and b = -0.006 ($\pm$ 0.003), which were set according to a linear regression of AOU against $\delta^{13}C_{DIC}$ values from the Global Ocean Data Analysis Project (GLODAP) database (Olsen et al., 2016). I removed data points where $\delta^{13}C_{DIC}$ $<$ -2.00‰. AOU was set based on catch location, year and depth. I used a fuzzy-join procedure (Robinson, 2020) to match AOU from GLODAP (Olsen et al., 2016) to catch location, allowing a margin of 1 degree for latitude and longitude, 10 years for year and 100 m for depth.

I adjusted $\delta^{13}C_{DIC}$ values for the Suess effect, which was set to -0.07‰ decade^{-1} for fishes caught up to 1970. For fishes caught after 1970, the Suess effect was set according to location based on the PISCES-A model of surface water Suess effect (Tagliabue and Bopp, 2008). These values ranged from -0.22 to -0.08 ‰ decade^{-1}. Section 2.2.1 gives a full explanation of the Suess effect.

2.4.2 Diet

I estimated $\delta^{13}C_{diet}$ values using $\delta^{13}C$ values of muscle ($\delta^{13}C_{musc}$), as this reflects the $\delta^{13}C_{diet}$, plus a trophic enrichment factor (TEF; DeNiro and Epstein, 1978):

$$\delta^{13}C_{diet} = \delta^{13}C_{musc} - TEF \tag{2.5}$$

I set the TEF according to McCutchan Jr. et al. (2003) for Chapters 4 and 5, using 1.10 ($\pm$ 0.35) for untreated muscle, and 1.80 ($\pm$ 0.29) for lipid-corrected or lipid-extracted muscle. Note that in Chapter 3, I set the TEF to 0.80 ($\pm$ 1.10) according to DeNiro and Epstein (1978).

Wherever possible, I used muscle isotope data collected from the same individuals or group as the otolith isotope data. In the case of the myctophids (Chapter 3), I collected this data to an individual level. Many otoliths from the SUMIE collections had corresponding $\delta^{13}C_{musc}$ values available within Chung (2015) at the group level. *Merluccius merluccius* (European hake) also had corresponding $\delta^{13}C_{musc}$ values at the group level, which were collected by SUMIE lab member Juliet Wilson.

Where corresponding $\delta^{13}C_{musc}$ values were unavailable, I used $\delta^{13}C_{musc}$ data from the literature to determine $\delta^{13}C_{diet}$ values. I chose studies that were as close as possible in location and year to their corresponding otoliths, and where there were multiple such studies I took an average of $\delta^{13}C_{musc}$ values, weighted by the number of individuals. Where there was a difference in year of capture between my $\delta^{13}C_{oto}$ data and $\delta^{13}C_{musc}$

values from the literature, I corrected the $\delta^{13}C_{musc}$ values for the Suess effect (section 2.4.1). I gave priority to studies that did not lipid-correct or lipid-extract the muscle before stable isotope analyses, as $\delta^{13}C_{diet}$ values should reflect all respired carbon, including the lipid fraction. Appendix D lists the $\delta^{13}C_{musc}$ values used for each species.

2.4.3 ϵ-term

The ϵ-term, also referred to ϵ_{total}, is the net isotopic fractionation factor. Fractionation is a change in relative isotopic abundances during a reaction (e.g. photosynthesis, Fry, 2006) or when crossing boundaries (e.g. carbon moving from the blood to endolymph, Solomon et al., 2006). ϵ_{total} specifically is the summed change in $\delta^{13}C$ values across all transformations from blood to endolymph, and endolymph to otolith (Solomon et al., 2006; Trueman et al., 2016). Overall, the value of the ϵ-term, and how it may vary across species or physiological states, is relatively poorly researched but unlikely to be large (Trueman et al., 2016; Chung et al., 2019b). Various values for ϵ_{total} have been proposed based upon experimental studies and mass-balance models, ranging from -1.8 ($\pm$ 1.8) in rainbow trout (*Onchyrhynchus mykiss*; Solomon et al., 2006), to 2.7 in freshwater drum (*Aplodinotus grunniens*; Wurster and Patterson, 2003). Importantly, while Solomon et al. (2006) found relatively large fractionation factors of components of ϵ_{total} (e.g. an $\epsilon_{blood-endolymph}$ of 13.2), these component ϵ-terms were balanced overall.

Given the lack of research into the ϵ-term, particularly across different species and functional groups, I conducted a sensitivity test. To speed up computing, I carried out this sensitivity test on a random subsample of 100 individuals from the main dataset, setting the mean ϵ-term $\pm$ standard deviation (SD) to either 0.0 $\pm$ 0.0, 0.0 $\pm$ 1.0, -1.8 $\pm$ 0.0, or 1.8 $\pm$ 0.0, based on the results of Solomon et al. (2006). Aside from the change in the ϵ-term, I ran the `MixSIAR` models as described in section 2.4.

The results showed very little change in C_{resp} values when adding uncertainty (Figure 2.7, SD = 1.0). When the mean of the ϵ-term was set to -1.8, the distribution of resulting C_{resp} values began to compress towards 0. As C_{resp} values are proportions, they are by nature bound between 0 and 1, almost always occurring within the lower half of that distribution (0.0 - 0.5; Trueman et al., 2016; Chung et al., 2019a,b). When the ϵ-term was set to + 1.8, the resulting C_{resp} values increased compared to the standard setting. For example, when the ϵ-term was set to 1.8 the minimum C_{resp} value was 0.13, compared to a C_{resp} value of 0.06 in same individual (*Coryphaenodies armatus*, abyssal grenadier) when the ϵ-term was set to 0 (standard setting). Given the results of this sensitivity test, and the recommendations of Solomon et al. (2006) and Chung et al. (2019a), I set the ϵ-term to 0, and assumed it was invariant across species.

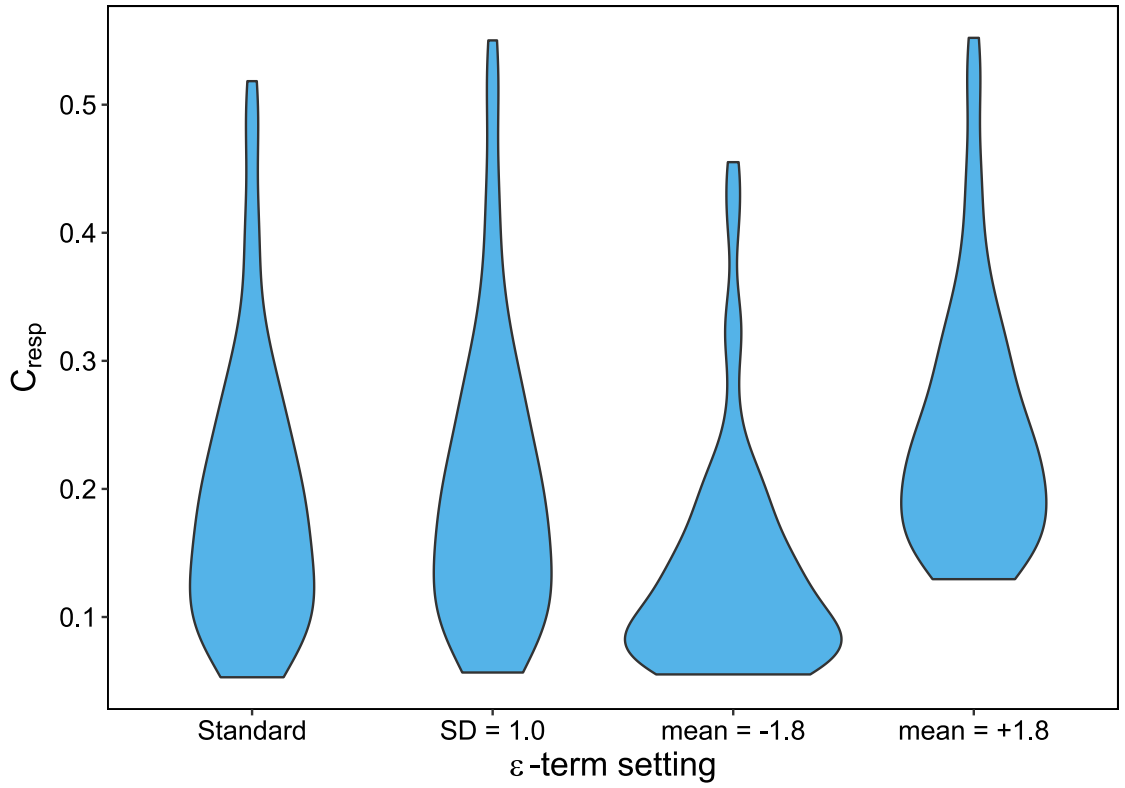

FIGURE 2.7: Distribution of C_{resp} values of a random sample of 100 individuals, taken from the main dataset. C_{resp} values were estimated from the same individuals with variable ϵ-terms using MixSIAR (Stock et al., 2018). Standard ϵ-term: mean = 0.0, SD = 0.0.

2.5 Otolith-derived experienced temperature

Otolith oxygen-isotope thermometry is commonly used to estimate the ambient temperature experienced by fish. Otolith aragonite forms in equilibrium with endolymph, with respect to oxygen isotopes. The equilibrium fractionation of oxygen during aragonite precipitation has a linear relationship with temperature (Kalish, 1991; Thorrold et al., 1997; Høie et al., 2004):

$$\delta^{18}O_{oto} - \delta^{18}O_{SW} = a + b \times T \tag{2.6}$$

where $\delta^{18}O_{oto}$ is the $\delta^{18}O$ value of the otolith, $\delta^{18}O_{SW}$ is the $\delta^{18}O$ value of the ambient seawater, and a and b are parameters that describe the linear relationship between $\delta^{18}O$ and the fluid from which the otolith aragonite was deposited (Kalish, 1991; Thorrold et al., 1997; Høie et al., 2004). In fully ectothermic fishes the estimated temperature reflects the ambient water temperature. However, in mesothermic fishes such as some tunas, otolith-derived experienced temperature represents the elevated temperature of the fish's core, rather than the temperature of the surrounding waters (Radtke et al., 1987). I set parameters a and b according to Høie et al. (2004) so that a = 3.90 ($\pm$ 0.24) and b = -0.200 ($\pm$ 0.019). Here I used a single set of parameters, as the variations in slopes and intercepts of equation 2.6 across species are minor (Kalish, 1991; Thorrold et al., 1997; Høie et al., 2004; Sakamoto et al., 2017).

Where possible, I estimated $\delta^{18}O_{SW}$ from CTD measurements of salinity (S, PSU) taken concurrently to fish capture. I used the linear equation from LeGrande and Schmidt (2006) to estimate $\delta^{18}O_{SW}$ values:

$$\delta 18O_{SW} = aS + b \tag{2.7}$$

where a and b are parameters set according to LeGrande and Schmidt (2006) based on catch location. Where CTD measures of salinity were not available, I set $\delta^{18}O_{SW}$ using an isoscape based on catch location and depth (Schmidt et al., 1999).

2.6 Body mass

Where possible, I took body mass data from measured wet weight (g) for each individual. Where only length information was available, I calculated weight (W) from length (L) using the following equation:

$$W = aL^b \tag{2.8}$$

where a and b are parameters which describe the relationship between weight and length. These parameters are species specific, and were acquired from FishBase (Froese and Pauly, 2021), or from the literature (Appendix B). Often it was necessary to convert between length types (Figure 2.8), so in these cases I used either morphometrics from FishBase (Froese and Pauly, 2021), or measured morphometrics using ImageJ 1.52a (Schneider et al., 2018). A list of source images used for these morphometrics can be found in Appendix C.

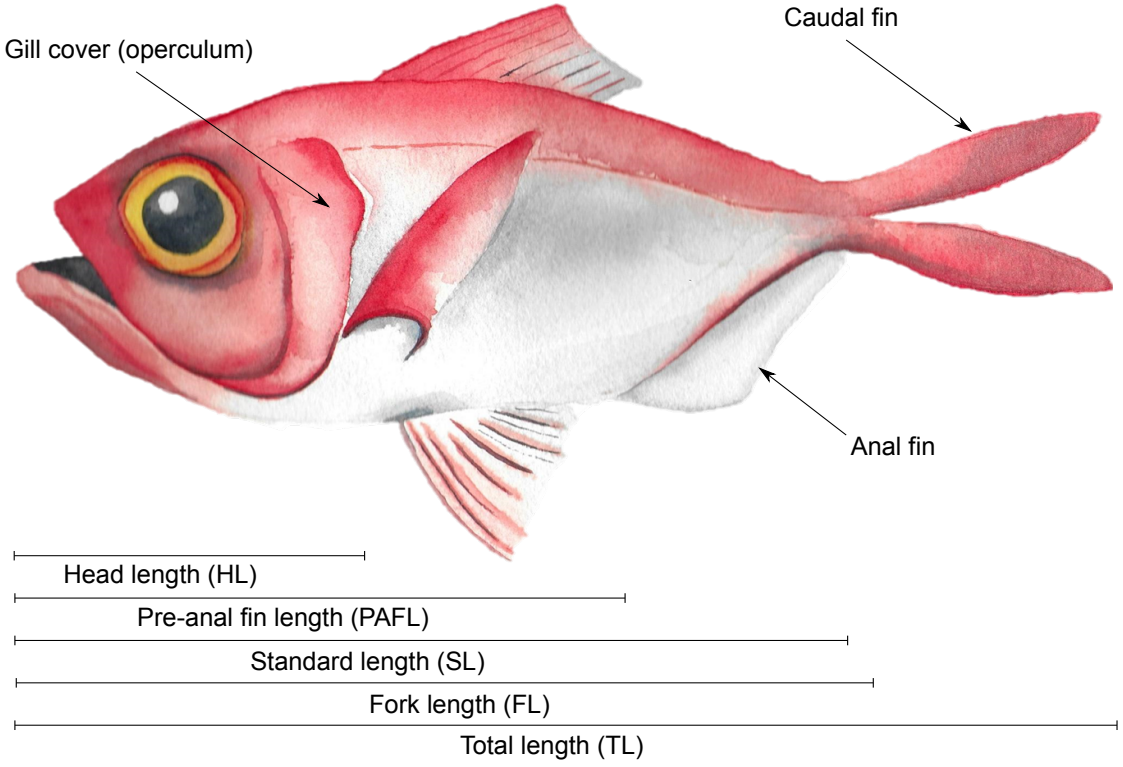

FIGURE 2.8: Annotated diagram of a spelndid alfonsino *Beryx splendens* showing fish length measurement types. Based on Linley (2013).

The body mass of individuals in the dataset covers almost the complete range of teleost fishes, and spans six orders of magnitude. The smallest fish was an individual of *Kreffichthys anderssoni* weighing 0.5 g. The largest fish was an individual of *Thunnus orientalis* (Pacific bluefin tuna) weighing 295 kg. Overall, the dataset has a normal

distribution of $\log_{10}$ transformed body mass (Figure 2.9), and the wide range enables thorough testing of C_{resp} scaling with body mass (Chapter 4).

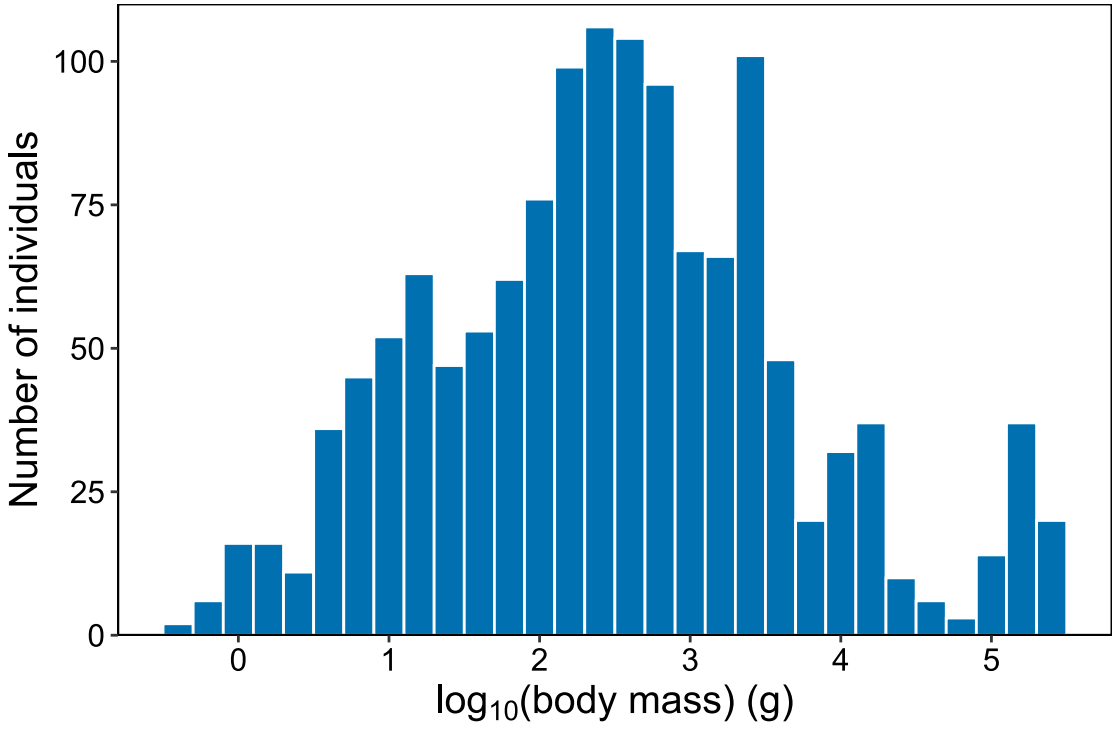

FIGURE 2.9: Histogram of $\log_{10}$ transformed body mass, (g wet weight) for individual fish in the main dataset.

2.7 Species ecological information and phylogeny

I compiled species ecological information using FishBase (Froese and Pauly, 2021), and cross-referenced these with identification guides and scientific articles listed in Appendix A. Where information conflicted across sources, I took the consensus view and discussed these with with my supervisor and Senior Curator of Fishes at the NHM, Oliver Crimmen.

While depth of occurrence, thermal realm and habitat are the only ecological correlates analysed directly in this thesis, I discuss other correlates such as body shape and migration to illustrate the coverage of the main dataset.

2.7.1 Phylogeny inference

I used the phylogeny from Rabosky et al. (2018) as the basis for inferring the phylogeny which was subsequently used for all phylogenetic comparative analyses. I accessed the Rabosky et al. (2018) phylogeny through the R package `fishtree` (Chang et al., 2019).

Of the 117 species in my dataset, 12 were missing from the Rabosky et al. (2018) phylogeny. Of these missing species, four came from monophyletic genera with no other representatives in my dataset. For these missing monophyletic species I substituted a member of the same genus within the base phylogeny for the species within my data. I added five species to the phylogeny using the `bind.tip` function in the `phytools` package, using an arbitrary branch length of 0.5 units. I determined the positions of these species using literature information, which is detailed in Appendix F. Unfortunately, there was no phylogenetic information for three species (*Spectrunculus grandis, Coelorinchus labiatus* and *Lycodes gracialis*), so these were dropped from the tree and omitted from phylogenetic comparative analyses.

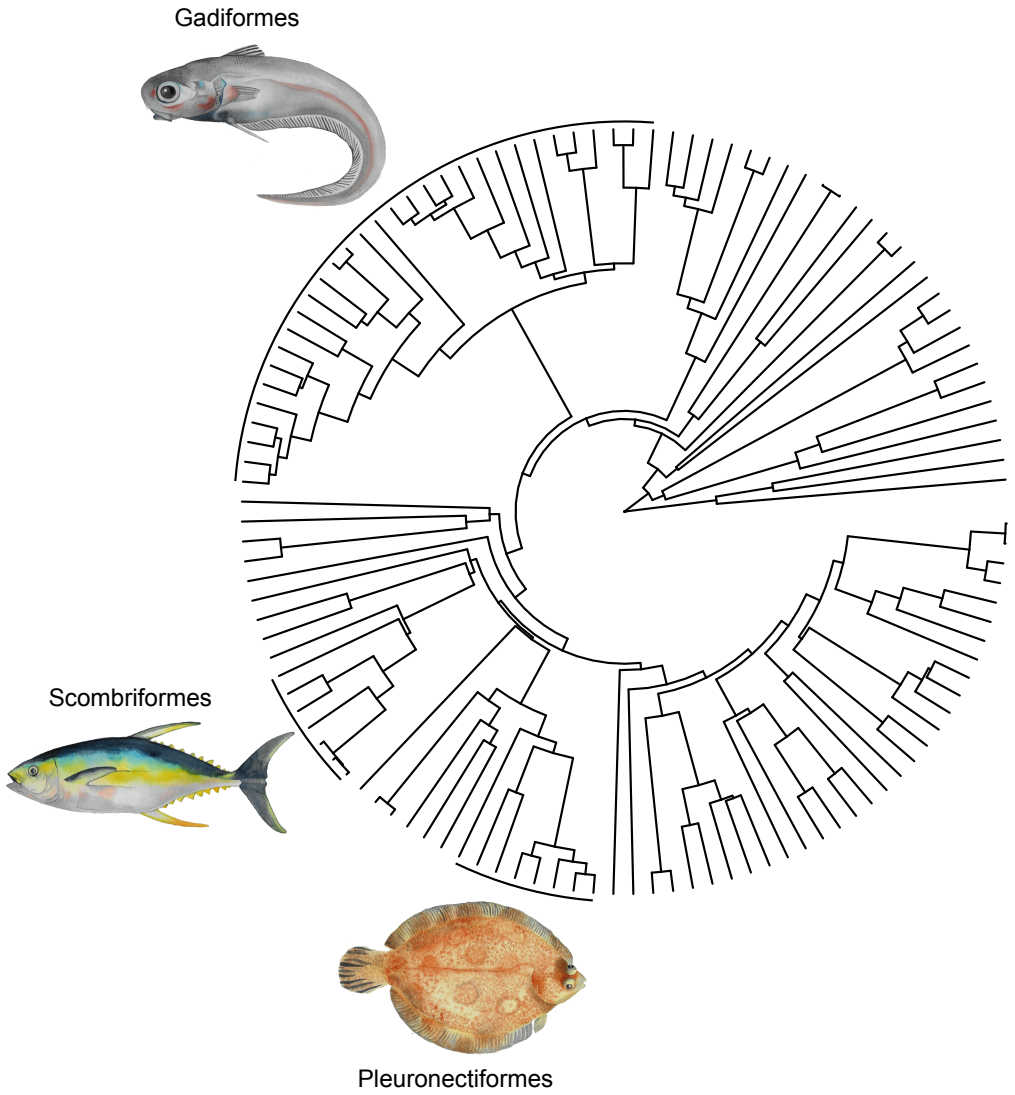

FIGURE 2.10: The final trimmed and edited phylogenetic tree. Key taxonomic orders are highlighted by representative species: Gadiformes by *Coryphanoides rupestris* (roundnose grenadier), Scombriformes by *Thunnus albacares* (yellowfin tuna) and Pleuronectiformes by *Microstomus kitt* (lemon sole). Original phylogenetic tree from Rabosky et al. (2018), accessed through Chang et al. (2019).

The final dataset consisted of 114 species made up of 1327 data points, representing 26 orders and 50 families of marine fishes. Although limited compared to the total diversity of fishes (Rabosky et al., 2018), these species comprise a representative sample of teleost taxonomic and functional groups (Figure 2.11).

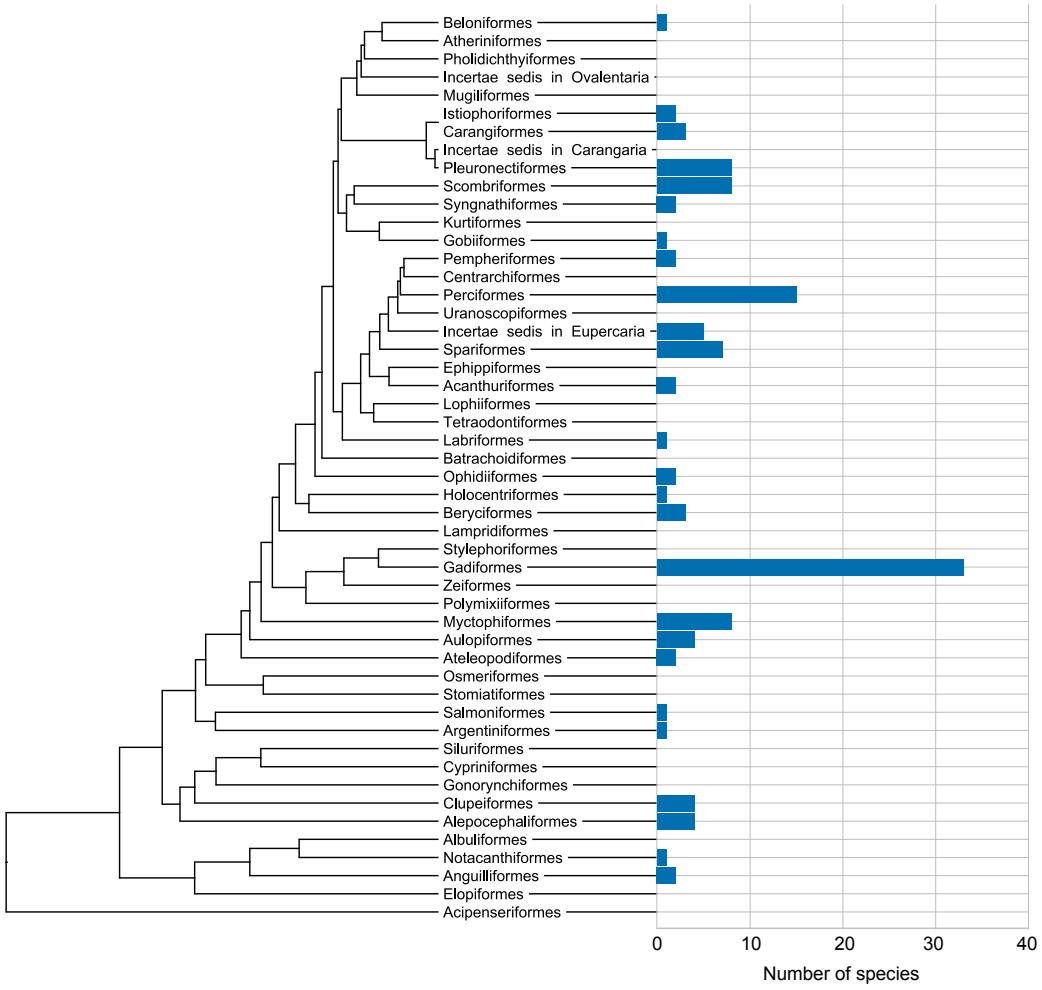

FIGURE 2.11: Number of species in this study by taxonomic order across the teleost tree of life. Strictly freshwater orders have been removed for clarity. Phylogenetic tree from Rabosky et al. (2018), accessed through Chang et al. (2019).

2.7.2 Spatial coverage

The resulting dataset had good spatial coverage, including samples from each of the world's oceans as well as the Mediterranean Sea and the Gulf of Mexico (Figure 2.12). My own data, along with data the Coldfish project (NERC, 2021) and Chung (2015), gave good coverage of the Atlantic and Mediterranean. Literature data broadened coverage, especially in the northern Pacific and eastern Indian oceans (Figure 2.12).

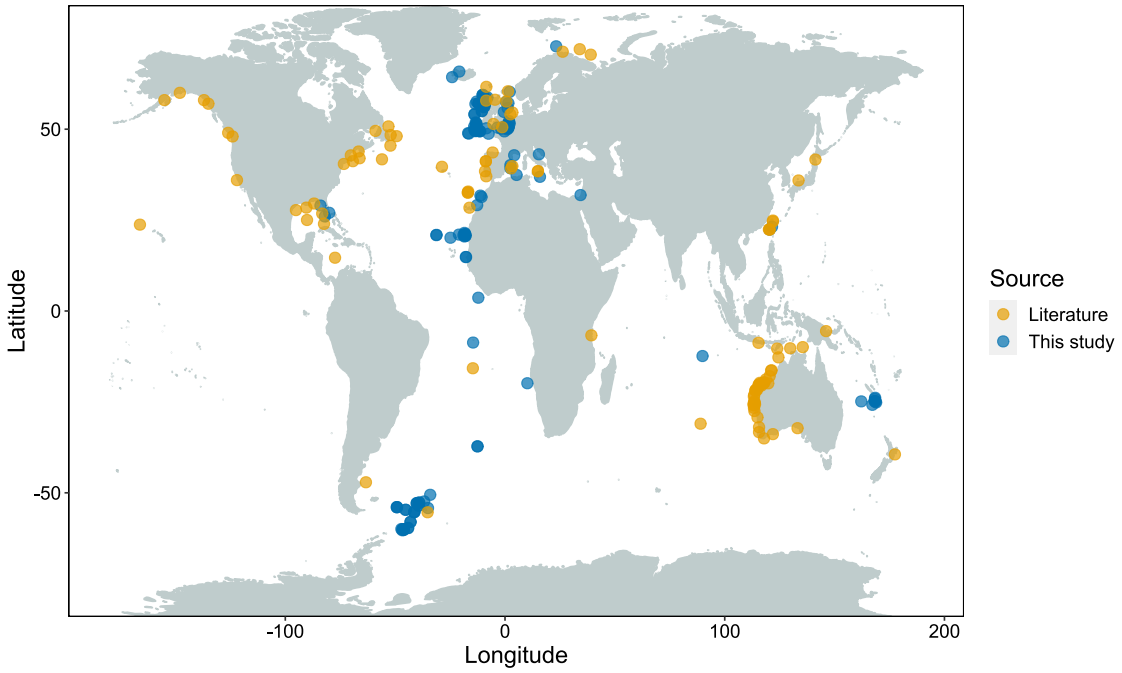

FIGURE 2.12: Map of sample locations, from this study (dark blue) and from the literature (yellow).

2.7.3 Depth of occurrence

I set depth ranges as minimum and maximum depths of occurrence. I preferentially chose common depth range over absolute depth range, as this avoided outliers.

Depth of occurrence ranged from 0 to 4865 m (Figure 2.13), with the deepest living species being *Coryphaenoides profundicolus* (deepwater grenadier). This dataset had a good distribution across the depth ranges, particularly with respect to maximum depth of occurrence (Figure 2.13). Minimum depth ranges tended to be clustered around 0 m, although some species had deeper minimum depth ranges.

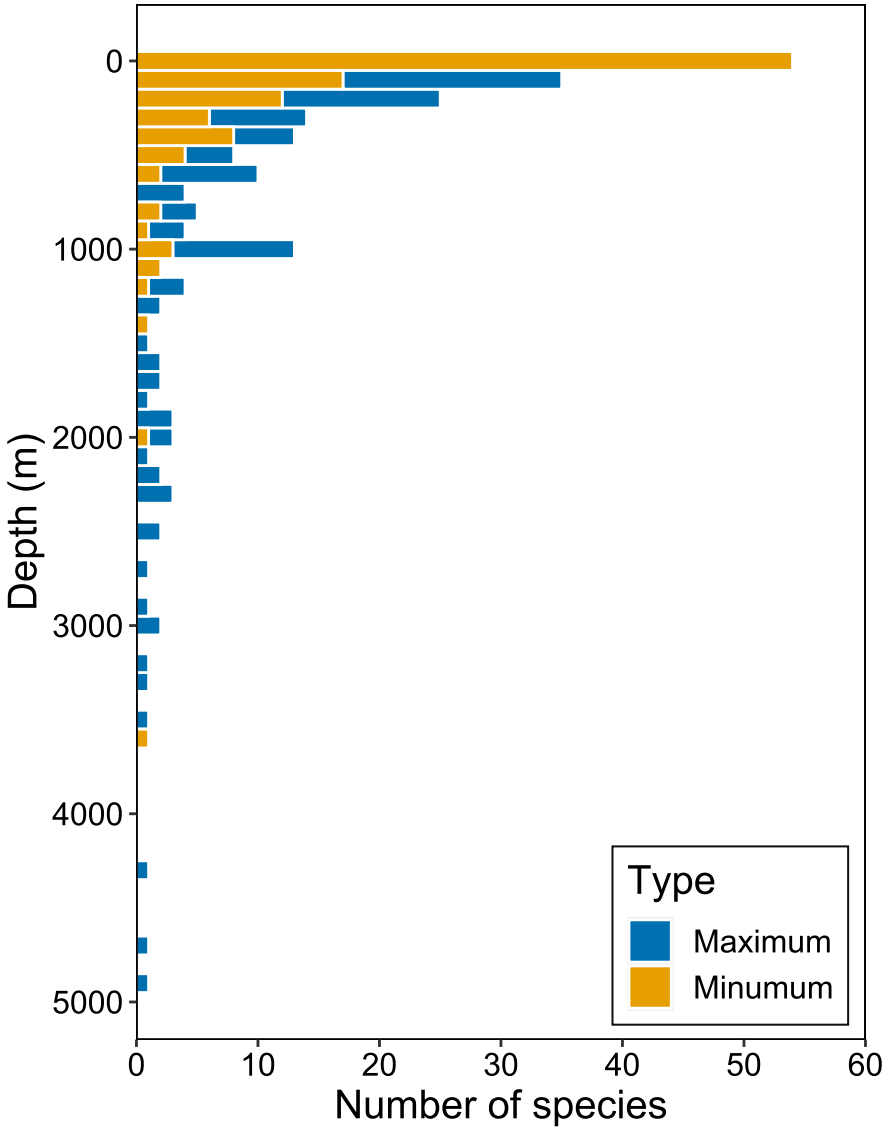

FIGURE 2.13: Number of species in the dataset coloured by minimum (yellow) and maximum (blue) depth of occurrence.

2.7.4 Thermal realm

I categorised species' thermal realm as either tropical, subtropical, temperate, polar or deep-sea. Species with a minimum depth of occurrence >200 m were categorised as deep-sea, as these environments are characterised by consistently low temperatures. Using minimum depth of occurrence means that vertically migrating species were not classified as deep-sea if their regular depth distribution included depths < 200 m.

All other species were assigned a thermal realm using occurrences from the Ocean Biodiversity Information System (OBIS; IOC-UNESCO, 2021), which was accessed via the `robis` package (Provoost and Bosch, 2020). I first filtered OBIS occurrence records by year. Where all individuals of a species were collected in the same year, I selected all occurrences within 5 years either side of that year (10 years in total). Where all individuals were collected within the same decade, I selected all OBIS data within the decade which best encompassed the sampling years. Where there were disparate collection dates within a species, I selected the minimum length of time which encompassed the collection dates. I then filtered data according to depth, selecting occurrences which fit within minimum and maximum depth of occurrences. From these filtered occurrences, I assigned thermal realm using the mean latitude according to Figure 2.14.

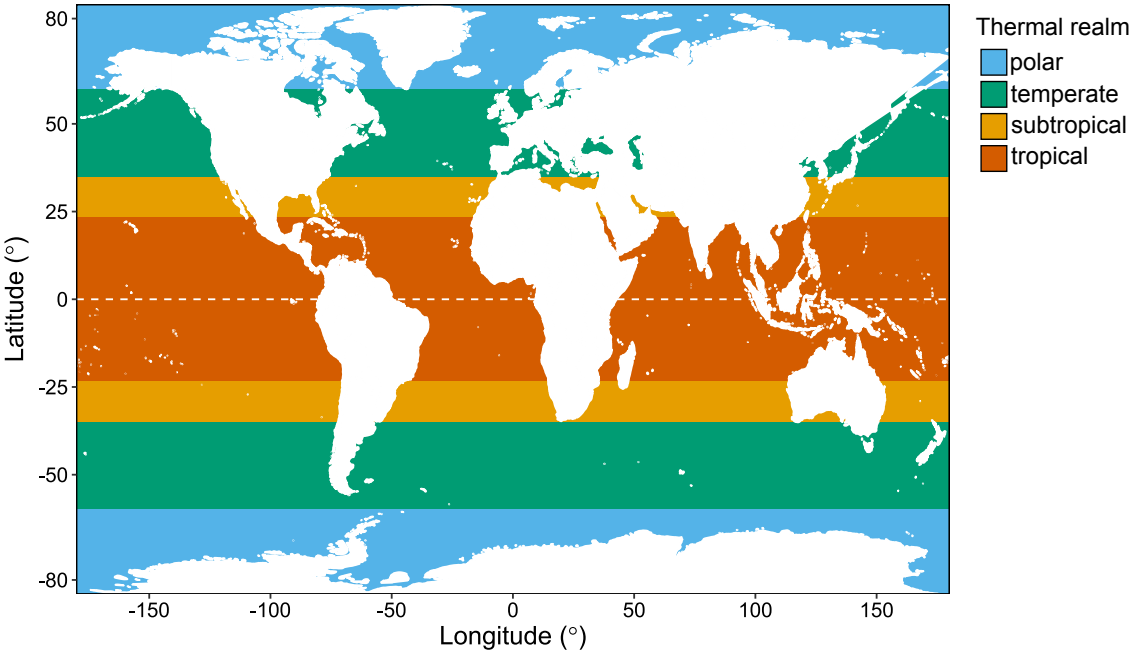

FIGURE 2.14: Approximate thermal realm boundaries for non-deep-sea species, based on (Costello et al., 2017). Blue = polar (set according to the approximate boundary of the Southern Ocean), green = temperate, yellow = subtropical, orange = tropical (set at the tropics of Cancer and Capricorn). The dashed white line indicates the equator (0 ° latitude).

I checked the output of each result and amended if necessary, based on the sources used to gather the ecological information. For example, this method assigns polar cod (*Boreogadus saida*) as temperate, whereas I have categorised this species as polar. I had some difficulty in definitively categorising species according to thermal realm, which is further discussed in chapters 5 and 7.

Given the location of most of the contributing collections (Table 2.1) it is unsurprising that deep-sea and temperate species are the most numerous, however there is also reasonable representation of tropical and subtropical species (Figure 2.15). Polar species are the least well represented in the main dataset, however, due to the latitudinal diversity gradient (Hillebrand, 2004), polar species are arguably better represented than tropical species.

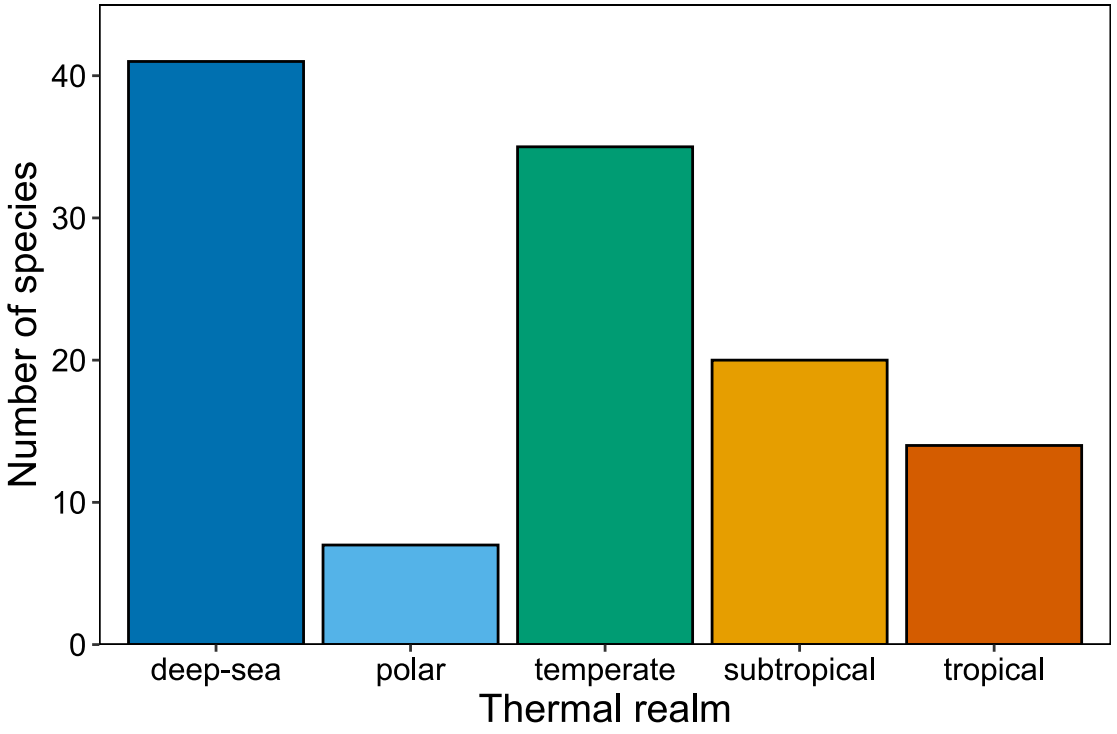

FIGURE 2.15: Number of species in the dataset, sorted by thermal realm.

Along with thermal realm, I also used the filtered OBIS records to get the means (Figure 2.16) and ranges (Figure 2.17) of temperature of occurrence. Although there is some variability, species classified as polar, subtropical or tropical tended to have smaller ranges in temperature of occurrence compared to temperate species.

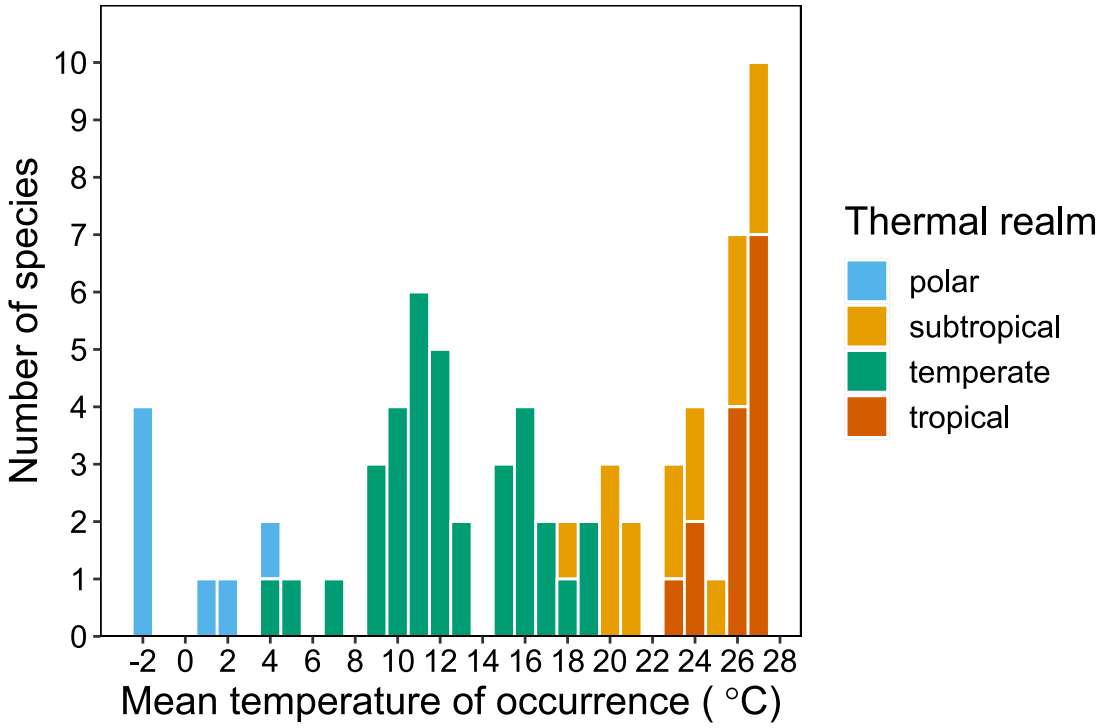

FIGURE 2.16: Mean temperatures of occurrence (°C) for species in the dataset, coloured by thermal realm.

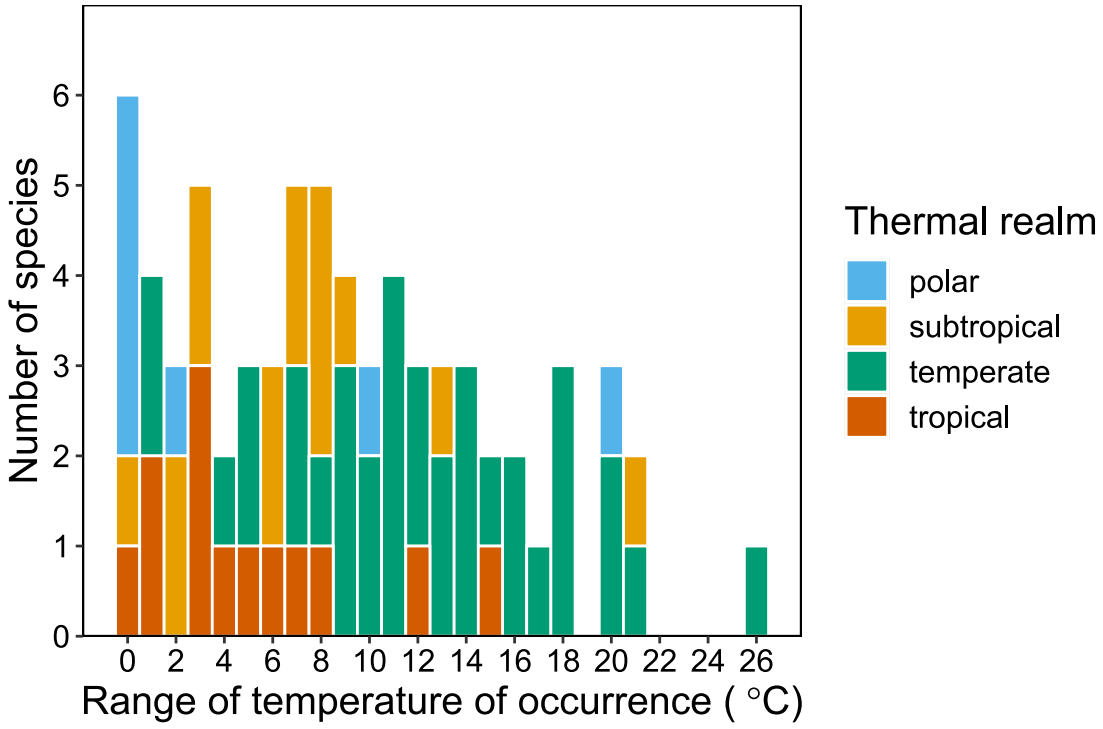

FIGURE 2.17: Range of temperatures of occurrence (°C) for species in the dataset, coloured by thermal realm.

2.7.5 Habitat

I categorised species as being either pelagic, benthic, benthopelagic, or (tropical) reef-associated, based on the typical habitat for adult fish of the species in question (Moyle and Cech, 2004; FAO, 2021):

- **Pelagic**: living in the water column with little-to-no reliance on the seafloor.
- **Benthic**: living in near-constant contact with the seafloor. Usually negatively buoyant.
- **Benthopelagic**: living near the seafloor but without near-constant contact. Usually neutrally buoyant.
- **Reef-associated**: living and feeding on coral reefs.

For this category, I based my categorisations on the movement (or lack thereof) and position of the species in its environment.

Benthopelagic species dominate the dataset (Figure 2.18), likely because this habitat definition is the most broad, and reflects the abundance of Gadiformes in the dataset. There is reasonable representation among benthic and pelagic species, with reef-associated species being the least well represented in the main dataset; all data for reef-associated species came from the literature rather than my own measured $\delta^{13}C_{oto}$ values.

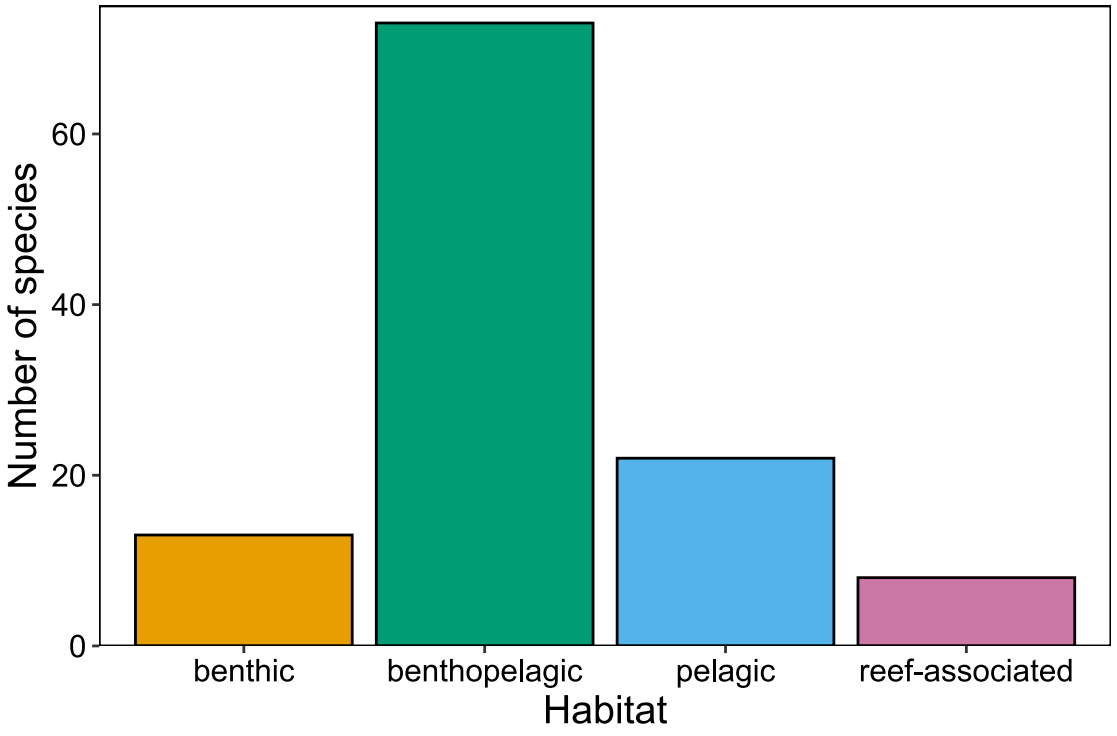

FIGURE 2.18: Number of species in the dataset sorted by habitat.

2.7.6 Body shape

I based the body shape categories on those from FishBase (Froese and Pauly, 2021), using body depth as a percentage of total length (%BD) to quantitatively define each body shape:

$$\%BD = \frac{BD}{TL} \times 100 \tag{2.9}$$

where BD is the body depth, and TL is the total length. These measures were either taken from FishBase (Froese and Pauly, 2021), or I measured them myself from representative photographs using ImageJ 1.52a (Schneider et al., 2018, Appendix C). Body depth is measured at the broadest part of the body, excluding fins. For the flatfishes (order: Pleuronectiformes), body depth was replaced by body width, and again measured at the broadest point and excluding the fins. Total length is the length from the tip of the nose to the tip of the caudal fin (Figure 2.8). Table 2.3 gives the definitions and examples of each body shape.

TABLE 2.3: Body shape categories assigned according to % body depth.

Body shape	% Body depth	Example species
Eel-like	< 11	*Synaphobranchus kaupii*
Elongate	11 - 19.5	*Coryphaenoides rupestris*
Fusiform/normal	19.5 - 28	*Thunnus albacares*
Short/deep	28	*Microstomus kitt*

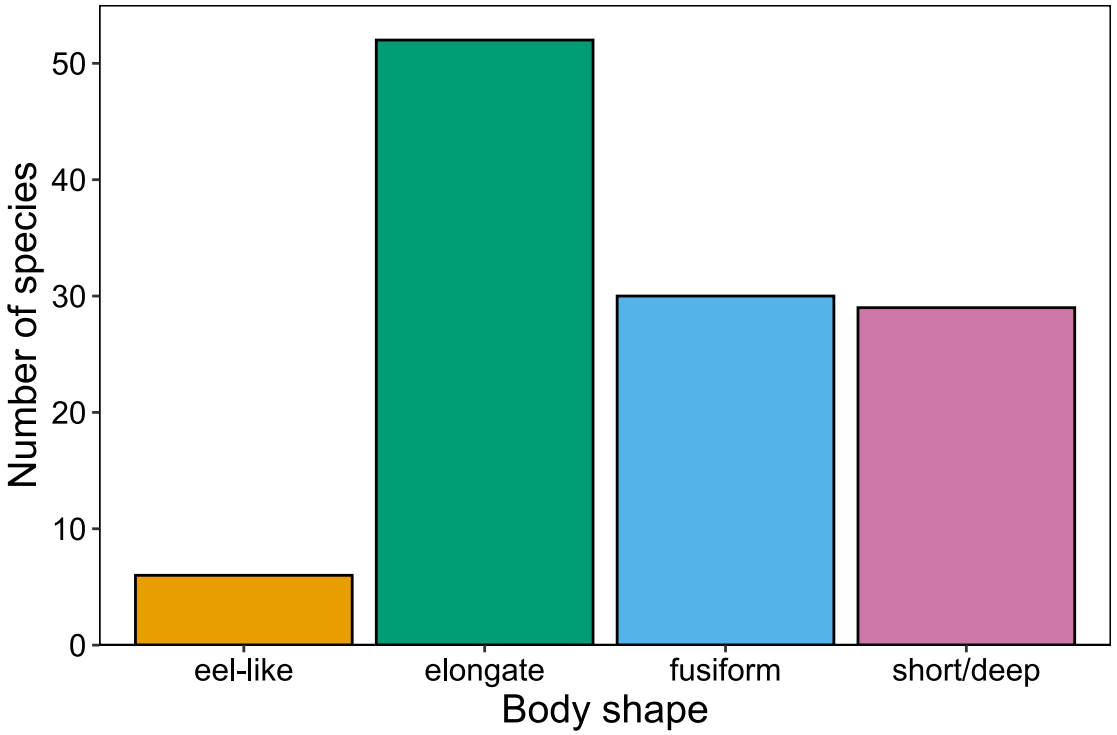

FIGURE 2.19: Number of species in the dataset sorted by body shape.

Elongate species are the most numerous in the main dataset (Figure 2.19), largely due to the high numbers of Macrouridae (grenadiers) which typify this body shape. Fusiform and short/deep body shapes are also well represented, while species with an eel-like body shape are the least numerous.

2.7.7 Schooling and Shoaling

Schooling and shoaling describe social behaviours where fish swim together. Shoaling is the broad term describing fish swimming together in group, but this can be loose and uncoordinated (Moyle and Cech, 2004). Schooling is a specific type of shoaling where fish swim together in a synchronised and polarised manner (Shaw, 1978; Pitcher and Parrish, 1986). I categorised species as shoaling if they were described using terms such as "gregarious", whereas the term "schooling" had to be mentioned specifically for a species to be categorised as such.

FIGURE 2.20: Number of species in the dataset sorted by schooling or shoaling behaviour.

Unfortunately, data on schooling and shoaling behaviour tends to be sparse, particularly if the species in question is not part of a commercial fishery. Consequently, I could classify less than half of the species in my dataset according to schooling or shoaling behaviour (Figure 2.20).

2.7.8 Migration

Migration was divided into vertical and horizontal types. For vertical migration, I categorised species as non-migratory, potential migrators or diel vertical migrators. Diel vertical migration is the movement of animals from deep waters during the day to near surface waters at night, before returning to deep waters during the day (Gjøsæter and Kawaguchi, 1980). Diel vertical migration enables species to consume prey which is more abundant at the surface, while using the cover of darkness to avoid predators which rely on vision to hunt (Gjøsæter and Kawaguchi, 1980). I defined potential migrators as species where there was inconclusive evidence for diel vertical migration, or where the species only performed diel vertical migration for part of the year. For example, the lanternfish *Electrona carlsbergi* likely only undertakes diel vertical migration during the summer (Kozlov et al., 1991), so I categorised this species as a potential migrator.

For horizontal migration, I categorised species as non-migrators, potential migrators or migrators. I considered migrators to be species which travel from one place to another on an at least annual basis (Moyle and Cech, 2004). Reasons for migration can include for spawning or foraging purposes. This definition is inherently subjective as there is no set distance a species has to travel regularly for it to be considered migratory. As with habitat, I only considered whether or not a species migrates in its adult stages.

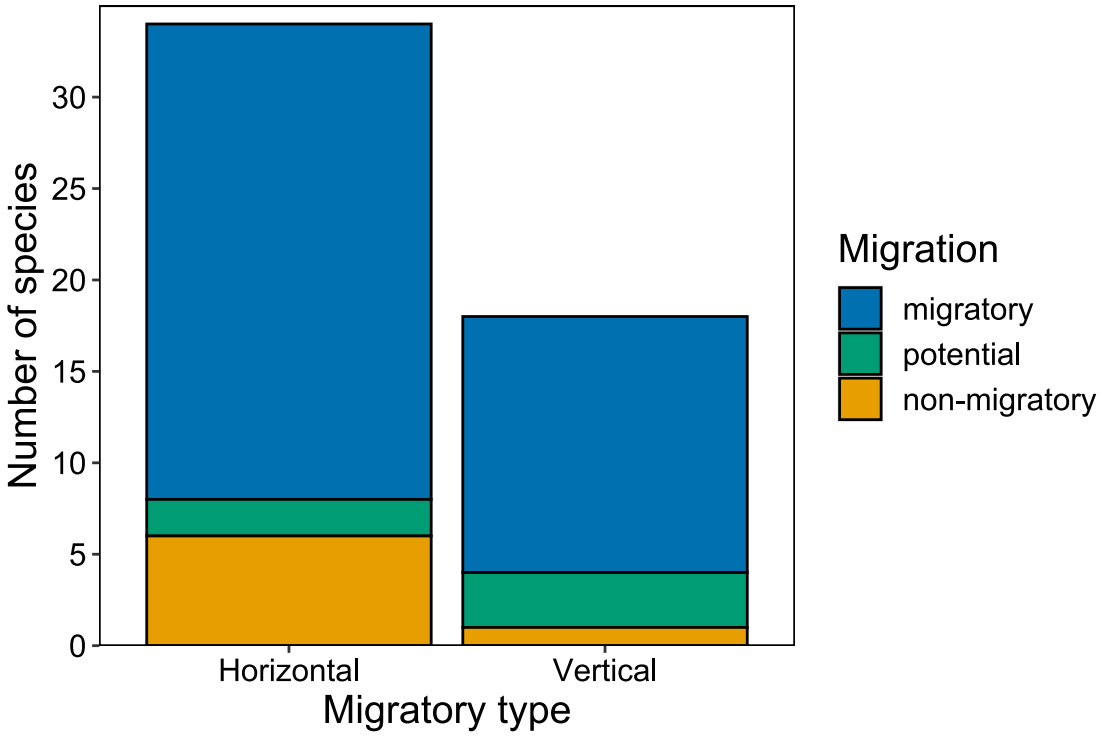

FIGURE 2.21: Number of species in the dataset sorted by migratory behaviour.

Similarly to schooling and shoaling behaviour (section 2.7.7), there is little reliable information on migratory behaviour for most of the species in my dataset (Figure 2.21). Of those species which could be classified according to migratory type, most were migrators, with few species classified as non-migratory.

2.8 Model sensitivity testing

I ran three sensitivity tests alongside the main models for each of the chapters which used the main dataset (4, 5 and 6). These sensitivity tests are referred to in those chapters as the "standard sensitivity tests". Where I ran sensitivity tests specific to a particular chapter, these are detailed within that chapter.

Crushed whole otolith samples (Section 2.3.1) incorporate material from the whole life history of the fish (Campana, 1999). As mass-specific metabolic rates, and therefore C_{resp} values, decrease from larval to juvenile to adult life stages (Chung et al., 2019b), using a whole otolith sample may have increased the C_{resp} value from that sample, relative to a sample taken from the outer edge (i.e. the most recent adult portion). To test for the effect of sample type, I ran each model without whole otolith samples and compared these to the main models.

Literature values of $\delta^{13}C_{oto}$ (Section 2.2.3) were invaluable in filling gaps within my dataset, however, the precise materials and methods for measuring $\delta^{13}C_{oto}$ values varied across studies. I accounted for variation among studies by incorporating a random effect of otolith source (study, or for my data, the institution providing the otoliths), and by running models after removing data from the literature.

Finally, I ran all models with very different priors, to test for the effect of the regularising priors on the model outcomes. Testing the effect of priors is not specific to my dataset, but is general good practice when using Bayesian methods (Depaoli et al., 2020).

Chapter 3

Otolith-derived field metabolic rates of myctophids from the Scotia Sea

This chapter is a reproduction of Alewijnse et al. (2021) published in *Marine Ecology Progress Series*.

https://doi.org/10.3354/meps13827

Sarah R. Alewijnse, Gabriele Stowasser, Ryan A. Saunders, Anna Belcher, Oliver A. Crimmen, Natalie Cooper, Clive N. Trueman

Author contributions: I collected the data, performed the data analyses and wrote the manuscript. All authors contributed to data interpretation and made critical revisions to the manuscript.

3.1 Abstract

Myctophids (family Myctophidae, commonly known as the lanternfishes) are critical components of open ocean food webs and an important part of the ocean biological carbon pump, as many species actively transport carbon to the deep ocean through their diel vertical migrations. Estimating the magnitude of myctophids' contribution to the biological carbon pump requires knowledge of their metabolic rate. Unfortunately, data on myctophid metabolic rates are sparse, as they rarely survive being captured and placed in a respirometer. Because of this, many studies estimate myctophid metabolic rates indirectly from body mass and temperature scaling relationships, often extrapolating regressions from global datasets to regional scales. To test the validity of these estimates, we employ a newly-developed proxy for mass-specific field metabolic rate (C_{resp}: the proportion of metabolically derived carbon in the otolith) based on the stable carbon isotope composition ($\delta^{13}C$) of otolith aragonite. We recovered estimates of C_{resp} for individuals of six species of myctophids from the Scotia Sea; giving a range in C_{resp} values from 0.123 to 0.248. We find that ecological and physiological differences among species are better predictors of variation in C_{resp} values than body mass and temperature. We compared our results to estimates of metabolic rates derived from scaling relationships and from measurements of electron transport system activity (ETS). When considering myctophids as a whole, we find estimates of oxygen consumption from different methods are broadly similar, however, there are considerable discrepancies at the species level. Our study highlights the usefulness of metabolic proxies where respirometry is currently unavailable, and provides valuable information on field metabolic rates of myctophids.

3.2 Introduction

Fishes living in the mesopelagic zone (∼150 - 1000 m depth) are central to many ecosystems. They link primary consumers such as copepods to higher trophic level predators such as marine mammals, birds, and commercially important fishes (Trueman et al., 2014; Anderson et al., 2018; Saunders et al., 2018). Additionally, mesopelagic fishes make an active contribution to the oceanic biological carbon pump (Davison et al., 2013; Trueman et al., 2014; St John et al., 2016; Anderson et al., 2018). Many species undertake diel vertical migrations, moving from depth to near-surface waters at night to feed on zooplankton under cover of darkness, before returning to deep waters before daybreak (Gjøsæter and Kawaguchi, 1980). By predating on surface-dwelling zooplankton, mesopelagic fishes ingest surface carbon and export it to depth through respiration, excretion and mortality, where it is effectively sequestered (Hidaka et al., 2001; Davison et al., 2013; Anderson et al., 2018). Non-migratory mesopelagic fishes also contribute to the biological carbon pump by consuming migrating zooplankton when those zooplankton enter the mesopelagic zone (Davison et al., 2013).

Myctophids (family Myctophidae) are among the most abundant mesopelagic fishes in the global oceans (Gjøsæter and Kawaguchi, 1980; Catul et al., 2011). Currently there is no commercial fishery for myctophids, however, there is increasing interest in harvesting them, driven by a requirement for fishmeal to sustain the global increase in aquaculture production (Catul et al., 2011; St John et al., 2016; FAO, 2018). As with all mesopelagic fish, myctophids are understudied compared to species which are currently more commercially relevant. If harvesting myctophids is to be sustainable, we must be able to estimate their biomass, understand their role in the food web, and estimate their contribution to the biological carbon pump (St John et al., 2016). Quantifying myctophids' metabolic rates can aid in filling these three knowledge gaps by enabling more robust energy and carbon budgets to be produced (Anderson et al., 2018).

By knowing metabolic rates, we can calculate energy budgets and estimate feeding rates (Ikeda, 1996), which are essential components of ecosystem models (Christensen and Walters, 2004). Ecosystem models can in turn be used to assess biomass (Anderson et al., 2018), an essential piece of information for informing sustainable fishing practices. Metabolic rates are commonly described in terms of oxygen consumption rates measured using respirometry. Respirometry is problematic for myctophids, as they are delicate fish and often do not survive capture from mesopelagic depths (Torres et al., 1979; Torres and Somero, 1988; Catul et al., 2011). Additionally, respirometry experiments typically determine standard or resting metabolic rates, however, in ecological studies estimates of time averaged field metabolic rates may be more relevant (Treberg et al., 2016; Trueman et al., 2016; Chung

et al., 2019a,b). As with standard metabolic rate, field metabolic rate includes energy expended on basal costs, but also incorporates the thermic effect of food (also called specific dynamic action), as well as energy expended for growth, reproduction, excretion and movement (Treberg et al., 2016; Chung et al., 2019a,b). However, field metabolic rates are challenging to measure, especially for aquatic organisms.

The activity of enzymes associated with electron transfer during respiration (ETS) within animal tissues provides an indirect proxy for the respiratory potential of tissues which can be calibrated to convert into units of field oxygen consumption rate (Ikeda, 1989; Cammen et al., 1990; Ariza et al., 2015). Measurements of ETS activity can be performed on samples of fish tissue, which avoids the issue of needing to catch fit specimens for respirometry (Torres and Somero, 1988; Ikeda, 1989; Ariza et al., 2015; Belcher et al., 2020), however, ETS is sensitive to the temperature at which the assays are carried out (Cammen et al., 1990). Additionally, there are currently no direct calibrations between ETS and whole organism oxygen consumption available for myctophids, and measures of metabolic rates for myctophids remain sparse (Belcher et al., 2019).

Metabolic rate for myctophids can also be estimated assuming scaling relationships between metabolic rate and body mass and temperature (Hidaka et al., 2001; Hudson et al., 2014; Belcher et al., 2019). This allometric approach was used to estimate the metabolic rates of myctophids from the Scotia Sea (Belcher et al., 2019); a highly productive area in the Atlantic sector of the Southern Ocean where myctophids are the dominant fishes in the upper mesopelagic (Collins et al., 2008, 2012). The resulting equation used wet mass (W, g) and temperature (T, °C) to estimate mass-specific metabolic rates (MR_W, μl O_2 mg WM^{-1} h^{-1}):

$$ln(MR_W) = a + b_W \times ln(W) + b_T \times T \tag{3.1}$$

Where a is the intercept and b_W and b_T are slopes relating to body mass and temperature, respectively (Belcher et al., 2019). However, this equation was parameterised based on a dataset of global myctophid metabolic rates (Torres et al., 1979; Donnelly and Torres, 1988; Torres and Somero, 1988; Ikeda, 1989; Ariza et al., 2015), which may not be applicable at regional scales (Belcher et al., 2020).

Here we address some of the issues raised above by we applying the C_{resp} proxy to myctophids from the Scotia Sea. We use C_{resp} values to compare relative field metabolic rates between six species of myctophids common in the Scotia Sea: *Electrona antarctica*, *Electrona carlsbergi*, *Gymnoscopelus braueri*, *Gymnoscopelus nicholsi*, *Protomyctophum bolini*, and *Krefftichthys anderssoni* (Piatkowski et al., 1994; Collins et al., 2008, 2012). We summarize key ecological information available in the literature for each species in Table 3.1.

In this study, we investigate whether C_{resp} values exhibit linear scaling with body mass and temperature, both inter- and intra-specifically. Additionally, we compare estimates of mass-specific oxygen consumption generated using allometric scaling (equation 3.1) to values derived from C_{resp} values, and to values derived from ETS (Belcher et al., 2020). Finally, we investigate whether estimates from equation 3.1 for individuals covary with C_{resp} values, as this should be the case if both accurately reflect field metabolic rates.

TABLE 3.1: Literature-derived ecological information for six species of myctophids examined in this study. LN = *Electrona antarctica*, GYR = *Gymnoscopelus braueri*, KRA = *Krefftichthys anderssoni*, ELC = *Electrona carlsbergi* and GYN = *Gymnoscopelus nicholsi*. Partial migrants are species in which part of the population migrates to the lower epipelagic at night ($\sim$ 200 m) while a proportion remains at the daytime depth. Near surface migrants are species which regularly migrate into mesopelagic zone of the upper 200 m, but rarely reach the upper 50 m (Watanabe et al., 1999; Catul et al., 2011). Values for % mass for primary prey groups are from Saunders et al. (2015a). Values for % NA of highly-unsaturated fatty acids (HUFAs) are from Stowasser et al. (2009). References: (1) Andriashev (1965); (2) Collins et al. (2008); (3) Collins et al. (2012); (4) Connan et al. (2010); (5) Duhamel et al. (2000);(6) Duhamel et al. (2014);(7) Gon and Heemstra (1990); (8) Hulley (1981); (9) Kozlov et al. (1991);(10) Lea et al. (2002); (11) Linkowski (1985); (12) Lourenço et al. (2017); (13) Lubimova et al. (1987);(14) McGinnis (1982); (15) Oven et al. (1990); (16) Phleger et al. (1999); (17) Piatkowski et al. (1994); (18) Pusch et al. (2004); (19) Reinhardt and Van Vleet (1986); (20) Ruck et al. (2014); (21) Saunders et al. (2014); (22) Saunders et al. (2015a); (23) Saunders et al. (2015b);(24) Saunders et al. (2015c); (25) Saunders et al. (2017); (26) Saunders et al. (2018); (27) Saunders et al. (2019); (28) Shreeve et al. (2009); (29) Stowasser et al. (2009).

	ELN	**ELC**	**GYR**	**GYN**	**KRA**	**PRM**	**Sources**
Maximum standard length (mm)	115	93	162	165	74	66	2, 7, 12, 21, 23, 24, 28
Estimated standard length at maturity (mm)	74	83	114	114	54	51	7, 8, 12, 15, 21, 23, 24

Depth range (m)	0 - 1000	0 - 400	0 - 1000	0 - 700	0 - 1000	0 - 700	2, 3, 5, 7, 12, 17, 21, 22, 23, 24, 26, 27, 28
Core depth range (m)	0 - 1000	0 - 400	0 - 700	0 - 400	200 - 1000	200 - 400	2, 3, 21, 22, 23, 24, 26, 28
Habitat	Mesopelagic	Mesopelagic	Mesopelagic	Mesopelagic and benthopelagic	Mesopelagic	Mesopelagic	7, 8, 11, 12, 21, 23, 24
Diel vertical migration type	Partial-migrant	Near-surface migrant (summer only)	Partial-migrant	Near-surface migrant (mesopelagic) and non-migrant (benthopelagic)	Near-surface migrant	Near-surface migrant	2, 5, 9, 12, 17, 18, 21, 23, 24
Thermal realm	Antarctic	Sub-Antarctic	Broadly Antarctic	Broadly Antarctic	Broadly Antarctic	Broadly Antarctic	6, 7, 8

Upper limiting temperature (C)	3	5	5 - 6	9	2 - 5.6	6 - 7	1, 3, 6, 7, 8
Spawns in the Scotia Sea?	Yes	No	No	No	Yes	No	7, 8, 12, 14, 15, 25
Primary lipid class	Wax ester	Triglycerides	Wax esters	Triglycerides	Wax esters	Triglycerides	4, 10, 16, 19, 20, 29
Mean normalised area percentages (% NA) of HUFAs in tissue	13.6	22.8	8.9	27.1	12.6	28.4	29

Primary prey classes groups	Euphausiids Amphipods	Copepods Euphausiids	Euphausiids Amphipods Copepods	Euphausiids Copepods	Copepods Euphausiids	Copepods Euphausiids	12, 13, 21, 22, 23, 24, 26, 28, 29

3.3 Methods

3.3.1 Samples

We obtained otoliths and muscle samples from fish collected during four cruises of the RRS *James Clark Ross* in the Scotia Sea during the austral summer (JR38, December 1998 - January 1999; JR177, December 2007 - February 2008; JR15004, January - February 2016; JR16003 December 2016 - January 2017). Fish were collected using 8 and 25 m^2 rectangular midwater trawl nets (RMT8 and RMT25) and were stored frozen at -20 °C. Fish were defrosted, weighed, and standard length was measured before removing the otoliths and a sample of muscle. Muscle was refrozen and stored at -20 °C until freeze drying. We analysed individuals from six species of myctophids: *Electrona antarctica* (n = 19, sampling depth = 15 - 1000 m), *Electrona carlsbergi* (n = 17, sampling depth = 5 - 205 m), *Gymnoscopelus braueri* (n = 20, sampling depth = 15 - 1000 m), *Gymnoscopelus nicholsi* (n = 12, sampling depth = 0 - 720 m), *Krefftichthys anderssoni* (n = 20, sampling depth = 80 - 995 m) and *Protomyctophum bolini* (n = 20, sampling depth = 195 - 405 m). For a summary of metadata for myctophids examined in this study, see Table 3.2.

Due to a labelling error, one *E. antarctica* and *seven E. carlsbergi* individuals did not have corresponding body masses; therefore we omitted data from these individuals during body mass analyses.

Details of the otolith stable isotope analyses are available in Chapter 2.3. As we had muscle samples from the same individuals as the otolith samples, we used muscle $\delta^{13}C$ to estimate diet $\delta^{13}C$. We freeze dried muscle tissue using a Heto PowerDry LL3000 freeze dryer for 24 - 48 hours, then crushed the tissue to a powder using a mortar and pestle. Stable isotope compositions of carbon in muscle tissue were analysed using a Vario Isotope select elemental analyser, coupled with an Isoprime 100 isotope ratio mass spectrometer. Replicates of the international standards USGS 40 and USGS 41, and the in-house standards acetanilide, glutamic acid and fish muscle were run for quality control and calibration. Standard deviations of quality controls averaged across runs were 0.14 ‰ for $\delta^{13}C$ of fish muscle.

We set $\delta^{13}C_{diet}$ using muscle $\delta^{13}C$ from the corresponding individual, minus a trophic enrichment factor for carbon (0.8 ‰ $\pm$ 1.1, DeNiro and Epstein, 1978), which is the increase in $\delta^{13}C$ of an animal's body relative to its diet (DeNiro and Epstein, 1978). We did not lipid extract or correct the $\delta^{13}C$ from muscle, as $\delta^{13}C_{diet}$ aims to capture the $\delta^{13}C$ of all respired carbon, including that from lipids.

TABLE 3.2: Summary table of metadata for myctophids examined in this study. ELN = *Electrona antarctica*, GYR = *Gymnoscopelus braueri*, KRA = *Krefftichthys anderssoni*, ELC = *Electrona carlsbergi* and GYN = *Gymnoscopelus nicholsi*. Myctophids were captured using either rectangular midwater trawl 25 m^2 (RMT25) or 8 m^2 (RMT8) nets. Diet was estimated using individual uncorrected muscle $\delta^{13}C$ and adjusted assuming a trophic enrichment factor of 1 ‰ (DeNiro and Epstein, 1978). Age estimates were obtained from rearranged length-at-age equations from Linkowski (1985, 1987); Saunders et al. (2020, 2021), (Supplementary Information 5). Unfortunately, no length-at-age parameters are available for *Protomyctophum bolini*. For information on how time incorporated in otolith samples was estimated see Appendix E.

	ELN	**ELC**	**GYR**	**GYN**	**KRA**	**PRM**
n	19	17	20	12	20	20
Year of capture	2008 2016	1998 2008	2008 2016	2008 2016	2008 2016	2008 2016
Gear type	RMT25 RMT8	RMT25 RMT8	RMT25	RMT25	RMT25	RMT25
Net depth range (m)	15 - 1000	5 - 205	15 - 1000	0 - 720	80 - 995	195 - 405
Mean standard length (mm)	72	75	107	139	47	45
Mean wet mass (g)	5.6	6.1	10.4	29.2	1.3	1.4
Mean estimated diet $\delta^{13}C$ (‰)	-28.01	-25.22	-27.79	-26.95	-27.96	-25.78
Mean estimated age (years)	5.1	2.1	5.9	5.0	1.2	Unavailable
Estimated time incorporated into otolith isotope samples (years)	2.0	1.0	3.5	2.5	1.5	2.0
Otolith sampling method	Micromill	Micromill	Micromill	Dremel	Crushed	Micromill Crushed

3.3.2 Comparison to previous study

To enable comparison to previous studies (Belcher et al., 2019, 2020), we used equation 3.1 to estimate mass-specific oxygen consumption based on body mass and temperature scaling. We set the parameters according to Belcher et al. (2019), so that a = -1.315 ($\pm$ 0.468), b_W = -0.267 ($\pm$ 0.052), and b_T = 0.848 ($\pm$ 0.011). These parameters were generated from a compilation of published myctophid metabolic rate data (Belcher et al., 2019).

To further enable us to compare our otolith-derived field metabolic rates to those estimated from equation 3.1, and to ETS-derived estimates of oxygen consumption rates (Belcher et al., 2020), we converted mean C_{resp} values for each species to oxygen consumption (mg O_2 kg^{-1} h^{-1}) according to the following equation:

$$C_{resp} = C(1 - e^{-kO}) \tag{3.2}$$

The relationship between C_{resp} values and oxygen consumption (O) is an exponential decay curve where k is the decay constant and C is the upper bound of the percentage of metabolically derived carbon in the blood (C_{resp}; Trueman et al., 2016; Chung et al., 2019b). We set k and C using experimentally derived values for *Chrysophrys auratus*, so that k = 0.0040 and C = 0.2746 (Martino et al., 2020). We chose these values over those from *Gadus morhua* (Chung et al., 2019b) as *C. auratus* had higher C_{resp} values which better matched those in our study. Values of oxygen consumption rates from equation 3.1 and ETS were converted from μl O_2 kg^{-1} h^{-1} to mg O_2 kg^{-1} h^{-1} assuming an oxygen density of 1.4 kg m^{-3} (2 °C, 100 kPa).

3.3.3 Statistical analyses

We carried out all statistical analyses in R version 4.0.5 (R Core Team, 2021b). Scripts for data analysis and visualisation are available at github.com/sarah-alewijnse/myctophid-ears. We fitted Hamiltonian Monte Carlo (HMC) models in RStan version 2.21.2 (Team, 2020) using the rethinking package version 2.01 (McElreath, 2020). We ran a single chain of 10,000 iterations, 5,000 warmup and a thinning parameter of one for each model, and checked models for mixing and convergence using traceplots, number of effective samples and the Gelman-Rubin diagnostic. We z-scored all predictors before adding them to the model. Therefore a is the expected value of the dependent variable (C_{resp} values) at the mean values of the predictors, and b indicates the change in the dependent variable per standard deviation of the predictor.

To examine the effect of body mass and temperature on estimates of field metabolic rate, we modelled C_{resp} values (proportion of respiratory carbon in the fish's blood, from equation 2.3) as a linear function of log body mass (ln(W), g) and temperature (T, °C). We included species in the model as a random factor ($a\_Var_{Species}$), both to address pseudoreplication, and to assess differences in C_{resp} values among species while accounting for body mass and temperature variation:

$$C_{resp} = a + b_W \times ln(W) + b_T \times T + a\_Var_{Species} \tag{3.3}$$

Here b_W and b_T are the effects of body mass and temperature on C_{resp} values, respectively. The intercept a is the expected C_{resp} value at the mean body mass and temperature, and $a\_Var_{Species}$ is the change in a for each species.

For each species, we ran same model, without the $a\_Var_{Species}$ term to test for intraspecific effects of body mass and temperature on C_{resp} values:

$$C_{resp} = a + b_W \times ln(W) + b_T \times T \tag{3.4}$$

We modelled C_{resp} values as a linear function of estimated mass-specific metabolic rate from equation 3.1 (MR_W) using the following model:

$$C_{resp} = a + b \times MR_W \tag{3.5}$$

Here the intercept a is the expected C_{resp} value at the mean mass-specific metabolic rate. We considered results to be statistically significant when the 95% highest density posterior intervals (HDPIs) for parameters did not overlap with zero.

3.4 Results

3.4.1 Interspecific C_{resp}

Individual C_{resp} values (our mass-specific proxy for field metabolic rate) ranged from 0.123 to 0.248. The model of C_{resp} with body mass, temperature and species (equation 3.3) showed that species was the only variable that had a significant influence on C_{resp} values (Figure 3.1).

Among the six species of myctophids (Figure 3.2), *Electrona antarctica* had the highest species mean C_{resp} value (C_{resp} = 0.213 $\pm$ 0.015). *Gymnoscopelus braueri* (C_{resp} = 0.201 $\pm$ 0.016) and *Krefftichthys anderssoni* (C_{resp} = 0.191 $\pm$ 0.016) showed the next highest species mean C_{resp} values. *Electrona carlsbergi* (C_{resp} = 0.174 $\pm$ 0.016) and *Protomyctophum bolini* (C_{resp} = 0.169 $\pm$ 0.016) had slightly lower mean C_{resp} values, but this difference was not significant. *Gymnoscopelus nicholsi* had a significantly lower mean C_{resp} than all other species (C_{resp} = 0.150 $\pm$ 0.018; Figures 3.1 & 3.2).

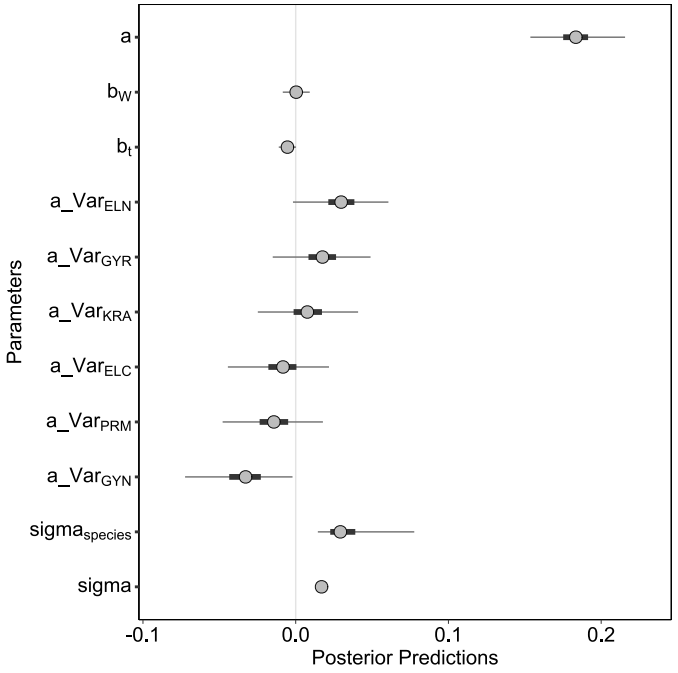

FIGURE 3.1: Posterior predictions for equation 3.3 ($C_{resp} = a + b_W \times W + b_T \times T + a_{VarSpecies}$). a is the intercept; b_W and b_T are the effects of body mass and temperature respectively (slopes). a_{Var} represents the variable intercept for each species: ELN = *Electrona antarctica*, GYR = *Gymnoscopelus braueri*, KRA = *Krefftichthys anderssoni*, ELC = *E. carlsbergi*, PRM = *Protomyctophum bolini* and GYN = *G. nicholsi*. *sigma* is overall residual error, and $sigma_{species}$ is residual error of the species variable intercept. Circles are the mean of the posterior predictions. Thick lines show the 50% highest density posterior intervals, and thin lines show the 95% highest density posterior intervals. Results are considered statistically significant if the 95% highest density posterior intervals do not overlap with zero.

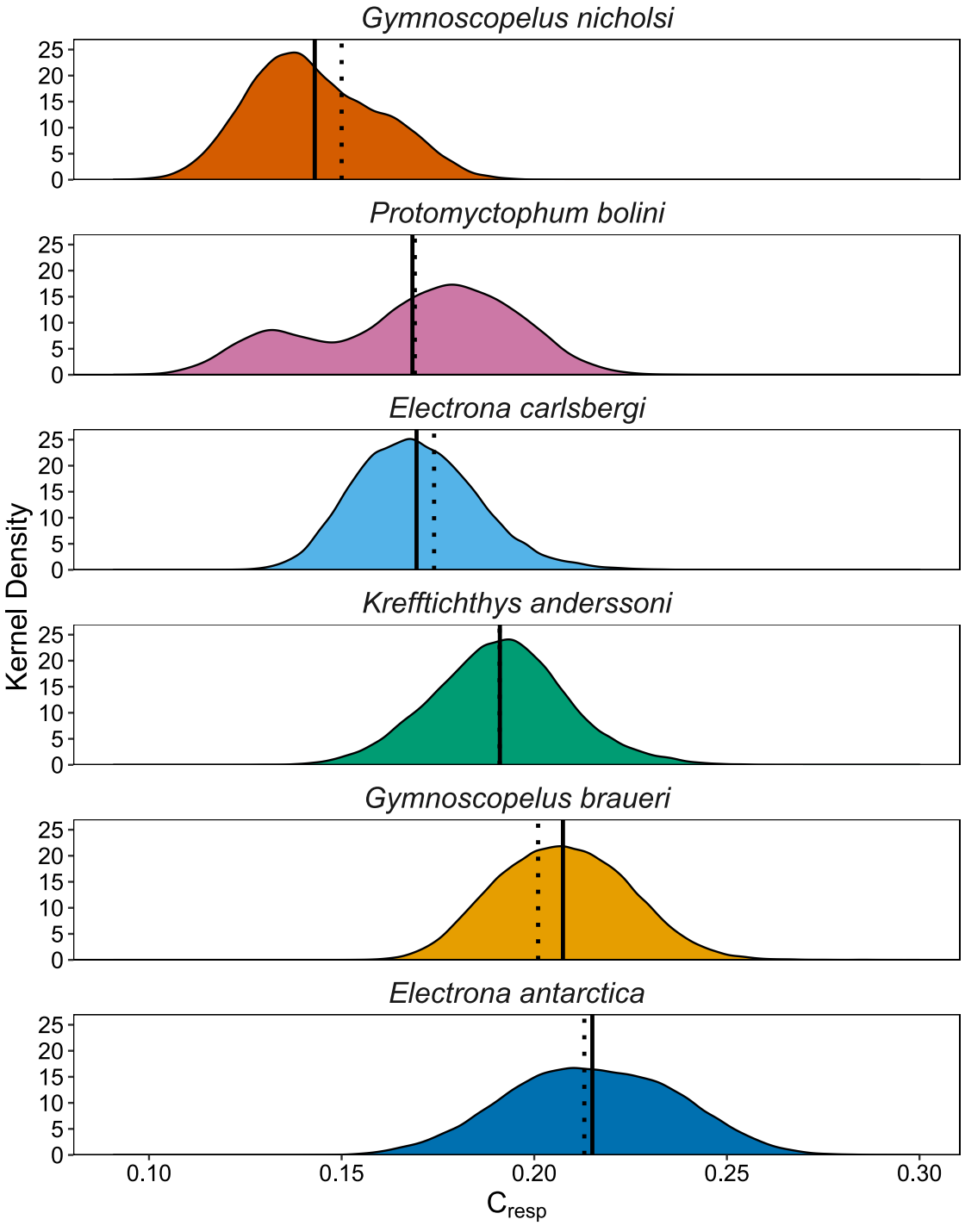

FIGURE 3.2: Kernel density of posterior predictions of C_{resp} values for each individual, grouped by species. Solid lines show the mean C_{resp} value for each species. Dotted lines show species expected values of C_{resp} at mean body mass and temperature (intercept), according to equation 3.3 ($C_{resp} = a + b_W \times W + b_T \times T + a_{VarSpecies}$).

The body masses of the myctophids ranged from 0.5 to 38.7g wet weight. There was no significant effect of natural log body mass on C_{resp} values (Figure 3.3) when modelling all species together (equation 3.3), as indicated by the constant for body mass, b_W, overlapping with zero (Figure 3.1).

Individual mean otolith-derived experienced temperatures ranged from -0.30 to 2.89°C. Despite an apparent decrease in C_{resp} values with temperature (Figure 3.4), there was no significant effect of temperature on C_{resp} values when modelling with species and body mass (Figure 3.1; equation 3.3). We also investigated the effect of life stage on C_{resp} values, but found no significant correlation (Appendix I).

FIGURE 3.3: Mean C_{resp} values against mean natural log body mass (g) for each individual of six myctophid species

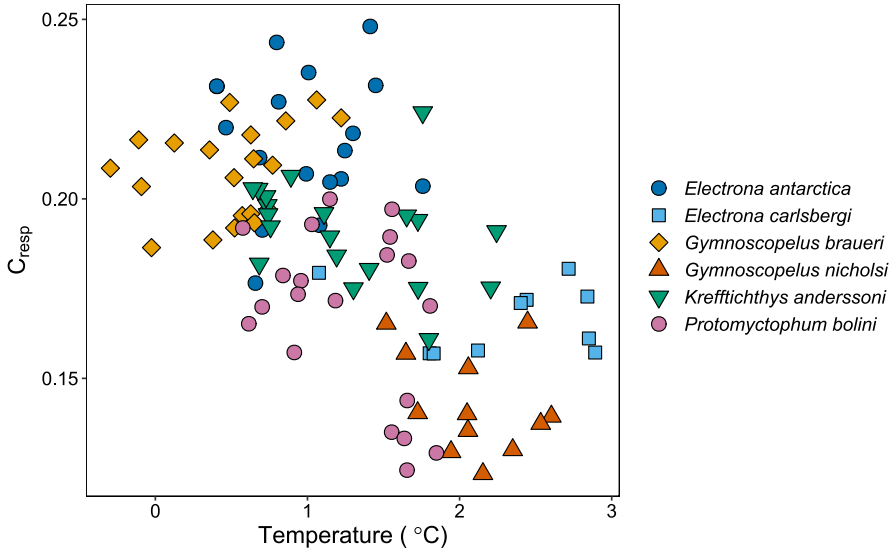

FIGURE 3.4: Mean C_resp values against mean otolith-derived experienced temperature (°C) for each individual of six myctophid species.

3.4.2 Intraspecific C_{resp}

For *G. braueri*, C_{resp} values decreased with increasing body mass (b_W = 0.008 $\pm$ 0.004, Figures 3.5 & 3.6a). There were no significant effects of body mass (Figures 3.5 & 3.6a) or temperature (Figures 3.5 & 3.6b) on C_{resp} values within the other five species. There was no significant effect of year of capture on C_{resp} values within species, aside from *P. bolini* (Appendix I).

The double peak in the distribution of C_{resp} values of *P. bolini* (Figure 3.2) was caused by individuals sampled further south (n = 12, latitude -54.680 to -55.290, cruise JR16003) having higher C_{resp} values (b_{Lat} = -0.014 $\pm$ 0.005) than those sampled further north (n = 8, latitude -52.720 to -52.900, cruise JR177). This pattern is specific to *P. bolini* and was not seen when comparing latitude of capture among species (Appendix I).

Within *G. nicholsi*, we found that individuals captured from the shelf breaks around the South Orkney Islands had a lower C_{resp} values (mean = 0.138 $\pm$ 0.008) than those caught elsewhere (mean = 0.152 $\pm$ 0.009), however, this difference was not significant (Appendix I).

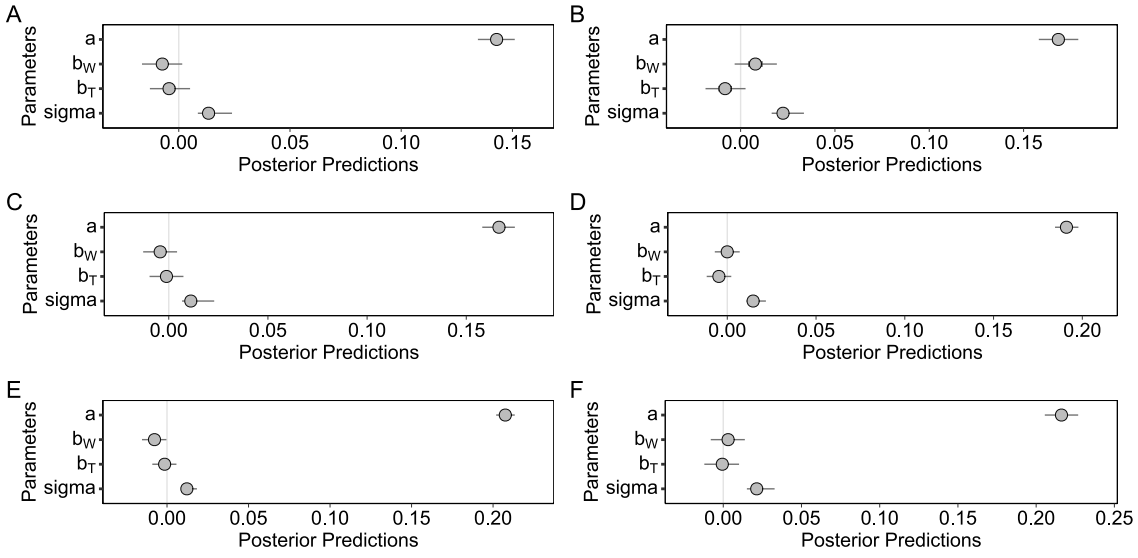

FIGURE 3.5: Posterior predictions for equation 3.4 ($C_{resp} = a + b_W \times W + b_T \times T$) within species (A = *Gymnoscopelus nicholsi*, B = *Protomyctophum bolini*, C = *Electrona carlsbergi*, D = *Krefftichthys anderssoni*, E = *Gymnoscopelus braueri*, F = *Electrona antarctica*). *a* is the intercept, b_W and b_T are effects of body mass and temperature respectively (slopes), and *sigma* is residual error. Circles are the mean of the posterior predictions. Thin lines show the 95% highest density posterior intervals. Results are considered statistically significant if the 95% highest density posterior intervals do not overlap with zero.

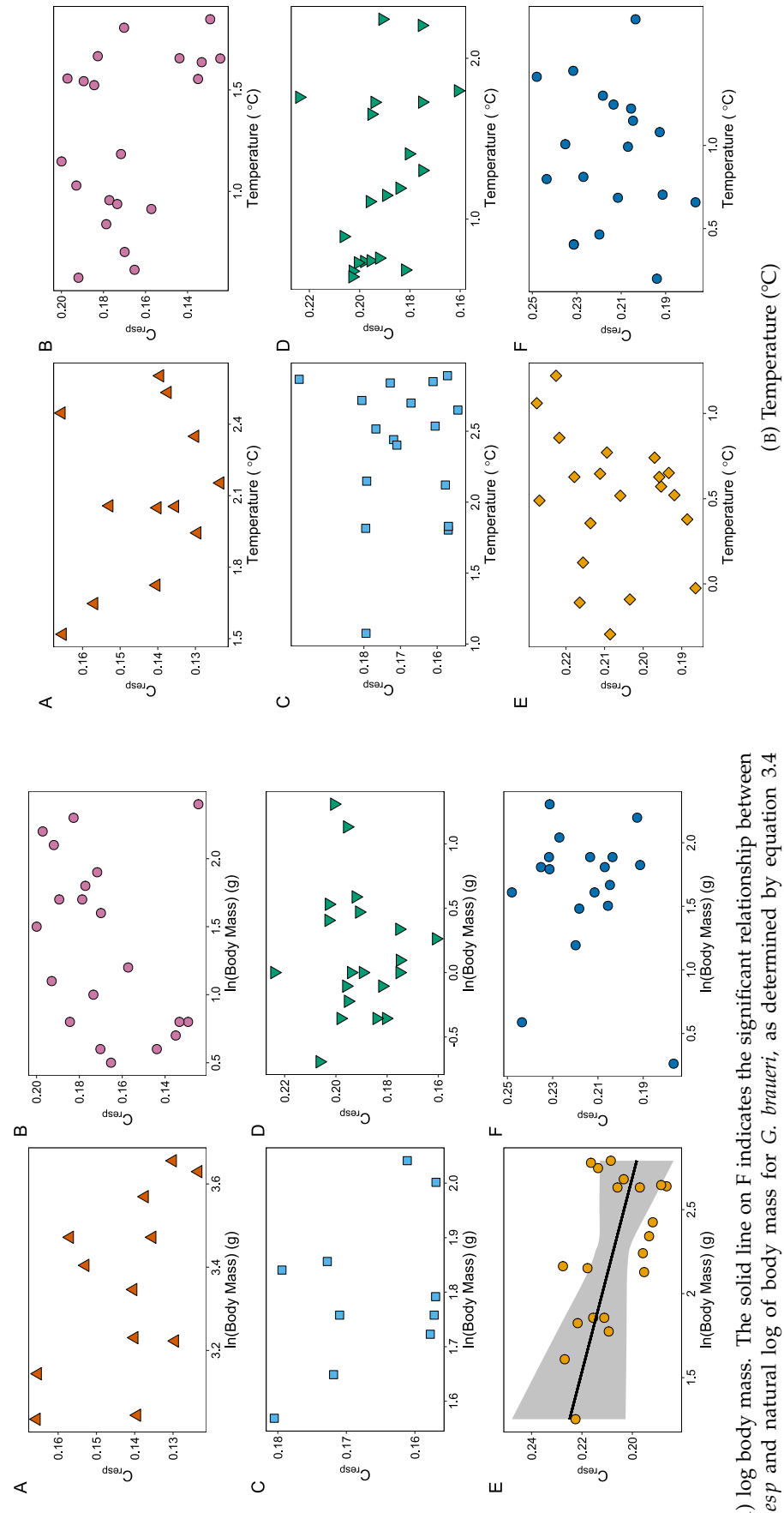

(A) log body mass. The solid line on F indicates the significant relationship between C_resp and natural log of body mass for *G. braueri*, as determined by equation 3.4 ($C_{resp} = a + b_W \times W + b_T \times T$), with 95% confidence intervals shaded in grey.

(B) Temperature (°C)

FIGURE 3.6: Mean C_{resp} values against mean natural log body mass (A) and mean otolith-derived experienced temperature (B) for each individual of six myctophid species. A = *Gymnoscopelus nicholsi*, B = *Protomyctophum bolini*, C = *Electrona carlsbergi*, D = *Krefftichthys anderssoni*, E = *Gymnoscopelus braueri*, F = *Electrona antarctica*.

3.4.3 Comparison of C_{resp} values with allometrically-derived oxygen consumption

We found no significant correlation between estimates of mass-specific oxygen consumption rate derived from allometric scaling (equation 3.1) and C_{resp} values (Figures 3.7 & 3.8).

Estimates of oxygen consumption rates for individuals derived from allometric relationships had larger posterior intervals than C_{resp} values, due to the uncertainty associated with calculating temperature from otolith $\delta^{18}O$ values and the propagation of this uncertainty in our models.

Species mean oxygen consumption rate estimates from allometric scaling predicted species means within a similar range (184.37 – 407.59 mg kg^{-1} h^{-1}) to those derived from C_{resp} values and converted to oxygen consumption based on equation 4.5 (197.55 – 373.66 mg kg^{-1} h^{-1}), however, each method resulted in differences when comparing oxygen consumption rates among species (Table 3.3). Both C_{resp} values and allometric scaling approaches identified *G. nicholsi* as having the lowest mean oxygen consumption rate, with a difference of only 13.18 mg kg^{-1} h^{-1} (6.67 % of otolith-derived oxygen consumption rate) between the two methods (Table 3.3; Figures 3.7 & 3.8). Differences between the two methods were greater for other species, with *P. bolini* having the greatest difference; allometrically-derived oxygen consumption rate was 162.87 mg kg^{-1} h^{-1} greater than otolith-derived oxygen consumption rate (68.17 % of otolith-derived oxygen consumption rate; Table 3.3; Figures 3.7 & 3.8).

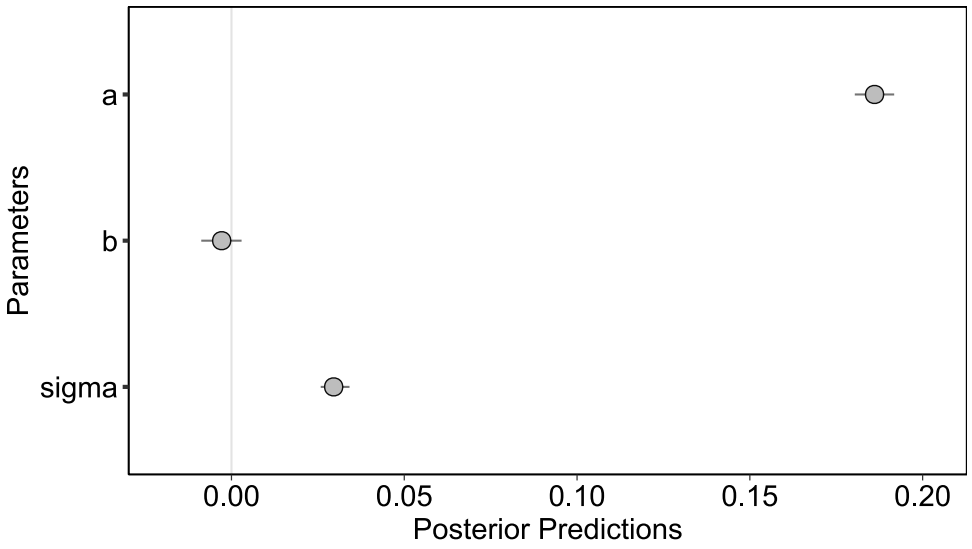

FIGURE 3.7: Posteriors predictions for equation 3.5 ($C_{resp} = a + b \times M_{RW}$) comparing otolith derived C_{resp} values with allometrically estimated mass-specific metabolic rate (M_{RW}). a is the intercept, b is the slope and *sigma* is residual error. Circles indicate the mean of the posterior predictions. Thin lines show 95% highest density posterior intervals. Results are considered statistically significant if the 95% highest density posterior intervals do not overlap with zero.

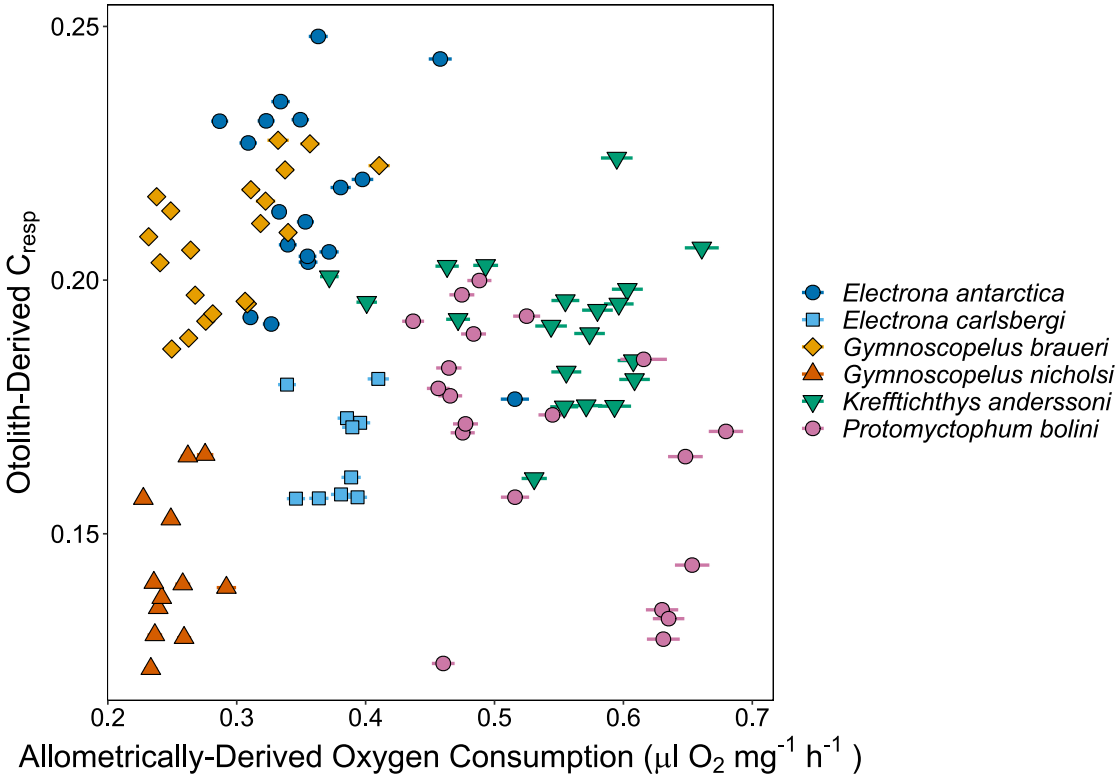

FIGURE 3.8: Mean otolith-derived C_{resp} values against mean allometrically-derived mass-specific oxygen consumption (μl O_2 mg^{-1} h^{-1}, estimated using equation 3.2 after Belcher et al. (2019)) for each individual of six myctophid species. Horizontal bars show the standard error of oxygen consumption estimates.

TABLE 3.3: Estimates of mean oxygen consumption (mg O_2 kg^{-1} h^{-1}) for species of myctophids, as determined by otolith derived metabolic rates from our study (C_{resp} values, 3.2) and converted to oxygen consumption, estimates derived from body mass and temperature scaling relationships (equation 1 from Belcher et al., 2019), and from electron transport system (ETS) measurements Belcher et al. (2020).

Species	**Otolith derived (our study)**		**Derived from scaling relationships (equation from Belcher et al. 2019)**		**Measured from ETS (Belcher et al. 2020)**	
	Oxygen consumption (mg O2 kg^{-1} h^{-1})	C_{resp} values	Oxygen consumption (mg O2 kg^{-1} h^{-1})	C_{resp} values	Oxygen Consumption (mg O2 kg^{-1} h^{-1})	C_{resp} values
Electrona antarctica	373.66 (257.43 – 583.88)	0.213 (0.177 – 0.248)	266.56 (211.45 – 372.00)	0.180 (0.157 – 0.213)	190.29 (102.26 – 422.28)	0.140 (0.092 – 0.224)
Gymnoscopelus braueri	329.17 (283.97 – 441.07)	0.201 (0.186 – 0.228)	217.34 (172.42 – 301.70)	0.159 (0.137 – 0.192)		
Krefftichthys anderssoni	297.32 (220.45 – 423.19)	0.191 (0.161 – 0.224)	407.59 (280.19 – 492.94)	0.221 (0.185 – 0.236)	672.88 (376.66 – 1023.11)	0.249 (0.214 – 0.270)
Electrona carlsbergi	253.54 (206.44 – 317.94)	0.175 (0.154 – 0.198)	283.02 (253.69 – 310.00)	0.186 (0.175 – 0.195)		
Protomyctophum bolini	238.91 (150.90 – 325.52)	0.169 (0.124 – 0.200)	401.78 (325.12 – 510.12)	0.220 (0.200 – 0.239)		
Gymnoscopelus nicholsi	197.55 (149.16 – 230.98)	0.150 (0.123 – 0.166)	184.37 (170.43 – 210.58)	0.143 (0.136 – 0.156)		
Gymnoscopelus spp.					158.19 (20.59 – 940.80)	0.107 (0.022 – 0.268)

3.5 Discussion

3.5.1 Lack of influence of temperature and body mass on C_{resp} values

Despite being primary drivers of standard (basal) metabolic rate (Gillooly et al., 2001; Brown et al., 2004) and field metabolic rate among myctophids globally (Belcher et al., 2019), we found neither body mass nor temperature had significant relationships with C_{resp} values, our proxy for mass-specific field metabolic rate in Scotia Sea myctophids. In our interspecific analysis, species was the most useful variable in modelling C_{resp} values. Within species, temperature had no relationship with C_{resp} values, and body mass had a significant relationship with C_{resp} values only in *Gymnoscopelus braueri*. These results are unexpected according to the metabolic theory of ecology, but can be explained by considering differences in methodologies, and issues with applying allometric scaling to relatively limited body mass and temperature ranges.

Standard and maximum metabolic rate must increase with increasing temperature at least until optimal temperatures are exceeded (Gillooly et al., 2001; Brown et al., 2004), a pattern that is evident in the global myctophid dataset used to parameterise equation 1 (Belcher et al., 2019). However, this dataset had a much larger temperature range than that experienced by myctophids in our study (0.5 to 27.0°C in Belcher et al. (2019), compared to -1.9 to 3.0°C in this study). Furthermore, most of the metabolic rates from the compilation were from temperatures greater than 5°C (Belcher et al., 2019, 2020). In contrast, the Scotia Sea is a cold (<5 °C) relatively isothermal environment (Venables et al., 2012), which is reflected in the small range of temperatures experienced by myctophids in our study. It is therefore likely that equation 3.1 is not appropriate for determining field metabolic rate in our dataset, as it includes data from a larger range of temperatures than are encountered in the cold Scotia Sea.

Metabolic theory also predicts a decrease in mass-specific metabolic rate with increasing body mass (Kleiber, 1947; Brown et al., 2004), however, we found no significant interspecific scaling relationship between body mass and C_{resp} values. Intraspecifically, the relationship between body mass and metabolic rate was inconsistent: all species aside from *G. braueri* showed no significant relationship between C_{resp} values and body mass. A study of electron transport system (ETS) derived metabolic rate found limited metabolic rate-body mass scaling in Scotia Sea myctophids as a whole (Belcher et al., 2020). This was primarily driven by a lack of scaling with body mass in *Gymnoscopelus* spp., similar to the lack of scaling seen in *Gymnoscopelus nicholsi* in our study. Belcher et al. (2020) attributed this lack of intraspecific scaling in *Gymnoscopelus* spp. to sampling a small range in body mass of their sample populations for this genus. In contrast, we did see scaling of C_{resp} within *G. braueri*, despite our sample of this species having a slightly smaller range in body

size (3.5 - 16.3 g) than that of Belcher et al. (2020)'s *Gymnoscopelus* spp. (1.9 - 16.9 g). Inter- and intra-specifically, our sampling covered a wide range of body masses, though had a slightly smaller range compared to other studies. For example, the global myctophid dataset ranged from 0.026 to 40 g (Belcher et al., 2019), while ours covered 0.5 to 38.7 g. However, we found large variability in C_{resp} values among myctophids of similar body masses, both inter- and intraspecifically, something also evident through ETS (Belcher et al., 2020). Additionally, we found similar C_{resp} values among species with vastly different body masses, such as *Protomyctophum bolini* and *G. nicholsi*.

Field metabolic rates include the energetic costs of movement, feeding and digestion and reproduction superimposed over the energetic costs of maintenance (Treberg et al., 2016). For the myctophids studied here, we infer that energy demands associated with movement and reproduction do not covary with temperature and body mass, and are large enough to obscure body mass and temperature effects on respiration. This is particularly relevant to the relatively small ranges in body size and temperature encountered among adult Scotia Sea myctophids.

3.5.2 Ecological and physiological drivers of species differences in C_{resp} values

Interspecifically, species identity was the most useful variable for modelling C_{resp} values equation 3.3, regardless of differences in body mass or temperature. We argue that this is due to differences in ecology and physiology among species, which may include differences in habitat, depth range and diel vertical migration, reproduction, and lipids, which are discussed below.

3.5.2.1 Differences in habitat

G. nicholsi had significantly lower species mean C_{resp} values than other species, which we attribute to a difference in habitat. While most species in our study are pelagic (Table 3.1), *G. nicholsi* becomes benthopelagic (living nearer to the seafloor) on reaching adulthood, at around 3 to 5 years of age (Linkowski, 1985). Benthopelagic lifestyles are typically associated with less movement and lower metabolic rates than pelagic lifestyles (Killen et al., 2010, 2016), which may explain the lower species mean C_{resp} values observed in *G. nicholsi* compared to other myctophid species analysed in this study. As with other species, *G. nicholsi* individuals in our study were caught using midwater trawls (Table 3.2), but their size (124 - 154 mm standard length) indicates they are adults of ages estimated at 3.5 to 6.9 years (Table 3.2; Saunders et al., 2015b), meaning they are of the age where a benthopelagic lifestyle may occur (Linkowski, 1985; Appendices E & I). Additionally, several individuals (those captured in 2016; Table 3.2) were caught around the shelf-break area of the South Orkney Islands, an area where adult benthopelagic *G. nicholsi* are known to congregate (Duhamel et al., 2014). These individuals had lower C_{resp} values (mean = 0.138 ± 0.008) than those caught in open water (mean = 0.152 ± 0.009), though this was not a significant difference (Appendix I). It is therefore possible that at least a portion of the *G. nicholsi* individuals in our study were benthopelagic (i.e. those caught around the South Orkney Islands in 2016), contributing to their lower species mean C_{resp} value compared to other species.

3.5.2.2 Depth range and diel vertical migration

Species of myctophids undertake diel vertical migrations to different extents, being either full, partial, or near-surface migrants, or non-migrants (Watanabe et al., 1999; Catul et al., 2011). The species studied here are either partial migrants - meaning a proportion of the populations performs diel vertical migrations to the upper 200 m while a proportion remains at depth - or near surface migrants - meaning individuals regularly migrate to the upper 200 m but rarely the upper 50 m (Watanabe et al., 1999; Duhamel et al., 2000).

The two species with the highest mean C_{resp} values, *Electrona antarctica* and *G. braueri*, have relatively broad core depth ranges (0 - 1000 m and 0 - 700 m respectively), and are partial migrants (Table 3.1; Piatkowski et al., 1994; Collins et al., 2008; Saunders et al., 2014, 2015b). *Krefftichthys anderssoni*, which had the third-highest species mean C_{resp} value, also has a relatively broad core depth range (200 - 1000 m) and is a near-surface migrant (Table 1; Piatkowski et al., 1994; Lourenço et al., 2017; Saunders et al., 2018), lending support to the idea that the extent of diel vertical migration impacts C_{resp} values. However, this pattern is complicated by the inclusion of larval and juvenile

material in our otolith samples for *K. anderssoni*, which will have increased C_{resp} values for this species compared to the other species studied here (Chung et al., 2019a).

In contrast, species with lower mean C_{resp} values have narrower depth ranges; *E. carlsbergi* and *P. bolini* are largely confined to the upper 400 m and therefore undertake shorter diel vertical migrations relative to species with higher mean C_{resp} values (Table 3.1; Kozlov et al., 1991; Pusch et al., 2004; Collins et al., 2008, 2012; Saunders et al., 2014, 2015c). Furthermore *E. carlsbergi* is thought to have seasonal variation in its diel vertical migration, only doing so in the summer (Table 3.1; Kozlov et al., 1991; Collins et al., 2008, 2012; Saunders et al., 2014). As discussed above (section 3.5.2.1) it is likely that a proportion of the *G. nicholsi* examined in this study were benthopelagic, and therefore non-migrators (Linkowski, 1985). *G. nicholsi* individuals living in the mesopelagic do perform diel vertical migration (Duhamel et al., 2000; Pusch et al., 2004; Saunders et al., 2015b), but their core depth range is restricted to above 400 m (Table 3.1; Collins et al., 2008; Saunders et al., 2015b, 2018).

Given that vertical migration is an active undertaking for myctophids (Barham, 1966; Kaartvedt et al., 2008), differences in the extent of vertical migrations may partially explain the variation among species means seen in C_{resp} values. Scotia Sea myctophids' diets are dominated by species found in the upper 200 - 400 m (Saunders et al., 2015a, 2018), therefore individuals living below those depths would have to migrate upwards to feed. Species with deeper core depth distributions (*E. antarctica, G. braueri* and *K. anderssoni*) are likely expending more energy to reach shallower waters than those with shallower depth distributions (*E. carlsbergi, P. bolini* and *G. nicholsi*), which may account for the higher mean C_{resp} seen in the former group. As well as energy expenditure, species with more active lifestyles may experience a higher metabolic rate due to the metabolic costs of an increased capacity for movement (Killen et al., 2016; Belcher et al., 2020). Determining whether increased energy expenditure or maintenance costs (or both) contribute to the higher mean C_{resp} values seen in migratory species is beyond the scope of our study.

3.5.2.3 Reproduction within the Scotia Sea

The species with the highest mean C_{resp} value, *E. antarctica*, is one of the few myctophid species that successfully spawns and recruits in the Scotia Sea (Table 3.1; Hulley, 1981; McGinnis, 1982; Gon and Heemstra, 1990; Oven et al., 1990; Saunders et al., 2017). Eleven out of the nineteen *E. antarctica* individuals in our study were above the species' length at 50% maturity (Table 3.1 & 3.2; 74 mm SL; Hulley, 1981; Gon and Heemstra, 1990; Oven et al., 1990; Saunders et al., 2014, therefore it is possible that the metabolic costs associated with reproduction, a component of field metabolic rates (Treberg et al., 2016), may explain the higher species mean C_{resp} values for *E. antarctica*.

K. anderssoni is also known to spawn and recruit in the Scotia Sea in waters around the South Georgian shelf Hulley (1981); Gon and Heemstra (1990); Oven et al. (1990); Belchier and Lawson (2013); Saunders et al. (2017)). Most *K. anderssoni* in our samples were relatively small, with only three out of twenty individuals being above length at 50% maturity (Table 3.1 & 3.2; 54 mm SL; Hulley, 1981; Gon and Heemstra, 1990; Oven et al., 1990; Lourenço et al., 2017). Therefore these *K. anderssoni* individuals may not yet have begun expending energy towards reproduction, which may explain why this species has a lower mean C_{resp} value than *E. antarctica*, despite this species also spawning within the Scotia Sea.

3.5.2.4 Lipids and C_{resp} values

Differences in how myctophid species store lipids (Table 3.1) may contribute to interspecific differences in C_{resp} values. In the species showing higher mean C_{resp} values (*E. antarctica, G. braueri* and *K. anderssoni*) the lipids of their tissue consist primarily of wax esters (Table 3.1; Reinhardt and Van Vleet, 1986; Phleger et al., 1999; Lea et al., 2002; Stowasser et al., 2009; Connan et al., 2010). In contrast, triglycerides dominate the tissue lipid composition in species with lower C_{resp} values (E. *carlsbergi, P. bolini* and *G. nicholsi*; Table 3.1; Reinhardt and Van Vleet, 1986; Phleger et al., 1999; Lea et al., 2002; Stowasser et al., 2009; Connan et al., 2010). Triglycerides retain their fluidity at lower temperatures, and are hydrolysed more quickly than wax esters, making triglycerides a more efficient source of energy (Sargent et al., 1977; Phleger et al., 1999; Connan et al., 2010), and potentially reducing metabolic costs for the species with triglyceride-rich lipid stores.

As well as having high levels of triglycerides in their tissues, species which had low mean C_{resp} values (*E. carlsbergi, P. bolini* and *G. nicholsi*) also show high levels of highly-unsaturated fatty acids (HUFAs; fatty acids with 20 or more carbon atoms and three or more double bonds; Bell and Tocher, 2009) in their tissues. HUFAs cannot be synthesised by fish and must be obtained from dietary sources (Bell Tocher, 2009); in this case these species all prey largely on copepods (Table 3.1; Phleger et al., 1999; Lea et al., 2002; Stowasser et al., 2009; Connan et al., 2010; Saunders et al., 2015a). The relationship between diets high in HUFAs and metabolic rates is not consistent among studies: higher levels of HUFAs in fish diets have been shown to reduce minimum, resting or maximum metabolic rates (McKenzie, 2001; Chatelier et al., 2006; Vagner et al., 2015) whereas some experiments showed no effect of HUFAs on metabolic rate (Silva-Brito et al., 2019; Vagner et al., 2019), and one showed a greater active metabolic rate for fish on a higher HUFA diet (Vagner et al., 2014). All of the aforementioned studies examined the effect of HUFAs in the diet within a species, so it is not clear how this would translate to interspecific effects particularly in wild fishes. Further

investigation is required to definitively link high HUFA diets with reduced field metabolic rates across species.

3.5.3 Methodological comparisons and considerations

Metabolic rates of fishes are typically estimated via respirometry, however, respirometry approaches are difficult in migrating mesopelagic species such as myctophids, and also can only estimate resting (standard) or maximum metabolic rates. Thus alternative proxies are useful for measuring metabolic rates in mesopelagic species, particularly field metabolic rates. Our study used otolith-derived estimates of field metabolic rate (C_{resp} values), and our species means for C_{resp} values are within the range measured by the same method in other non-myctophid species (C_{resp} values 0.10 - 0.28, Chung et al., 2019a; Martino et al., 2020). However, this is a relatively new technique, so comparisons with allometrically-derived oxygen consumptions (equation 3.1) and ETS, another proxy for field metabolic rate, are warranted.

The similar ranges between otolith-derived oxygen consumption rates and those from allometric scaling lend confidence to the use of C_{resp} values as a proxy for oxygen consumption in the field. Equation 3.1 estimates oxygen consumption rates based on body mass and temperature. Given the small temperature range in this study, equation 3.1 produces oxygen consumption estimates that are ranked in the same order as body mass, with the smallest species (*K. anderssoni*) having the highest allometrically-derived oxygen consumption rate, and the largest species (*G. nicholsi*) having the lowest allometrically-derived oxygen consumption rate. Contrary to this, body mass was not a significant predictor of our otolith-derived C_{resp} values, although all methods had *G. nicholsi* (or *Gymnoscopelus* spp.) as having the lowest field metabolic rate.

C_{resp} values derived from otolith stable isotopes offers a useful proxy for investigating field metabolic rates in fishes, however, its key limitation is the same as that for ETS; the lack of myctophid-specific calibration between the proxy and oxygen consumption (Belcher et al., 2019, 2020). In our study, we use experimentally derived calibration coefficients to convert between C_{resp} values and mass-specific oxygen consumption rates, however, these coefficients are not specific to the species we measure here. The values of the upper bound (C) and decay constant (k) from equation 3.2 vary between the two species for which calibrations have been made (Chung et al., 2019b; Martino et al., 2020). Additionally, there may be a mass-specific component to the calibration, which may partly explain the lack of body-mass scaling seen in our data.

Comparing results between ETS (Belcher et al., 2020) and C_{resp} values (Table 3.3), *K. anderssoni* had the highest oxygen consumption rate as determined by ETS, but not when oxygen consumption rates were inferred from C_{resp} derived values. This is

despite our sampling employing whole otoliths for the small *K. anderssoni*, which should result in a higher C_{resp} values than milled otoliths due to the incorporation of otolith material deposited during larval and juvenile life stages when mass-specific metabolic rate is high (Chung et al., 2019b). Discrepancies between ETS- and C_{resp}-derived oxygen consumption rates may be due to intraspecific variability, which is large in both methods. Future research should measure ETS and C_{resp} values on the same individuals to determine whether the two proxies for field metabolic rate covary. Additionally, ETS and otolith based approaches measure respiration on different timescales. ETS activity should be stable over the sampling process, likely reflecting the field metabolic rate in the hours prior to sampling (Gómez et al., 1996; Hernández-León et al., 2019). However, otolith based measurements integrate over much longer timescales of weeks to years, depending on how much otolith material is incorporated into a sample (Trueman et al., 2016; Chung et al., 2019a,b, 2021b). Therefore short term changes in individual respiration rates may partly explain why ETS derived and otolith derived rates do not covary (Figures 3.7, 3.8). Despite these methodological differences, the ranges of our C_{resp}-derived oxygen consumption rates and allometrically derived oxygen consumption rates are similar (Table 3.3), giving us confidence in C_{resp} as a metabolic proxy.

More accurately determining and parameterising ecological determinants of field metabolic rates would require a larger dataset than is available in this study. Future work could look to incorporate such factors into models estimating field metabolic rates; for example Ikeda (2016) estimated fish and cephalopod metabolic rate as a function of depth as well as body mass and temperature. Incorporating species-level effects appears to be essential to accurately estimate myctophid field metabolic rates, and may be required in order to determine their contribution to carbon flux as accurately as possible (St John et al., 2016; Belcher et al., 2019).

3.6 Conclusion

Our research highlights that field metabolic rates of myctophids in the Scotia Sea vary beyond generic scaling relationships with body mass and temperature. Instead, species identity was the most important driver of variation in C_{resp} values, probably due to differences among species in habitat, migratory behaviour and diet. Realised field metabolic rates, and therefore the role of myctophids, and likely other mesopelagic fishes, in active ocean carbon flux, may not be adequately described through these allometric scaling relationships. Estimating metabolic rates based on allometric scaling is especially problematic when scaling exponents are derived from global datasets and applied to multiple species with similar body masses and environmental temperatures.

Given the small number of species in our study, and the inherent complexity of their ecology, it is difficult to definitively say which factors have driven differences in C_{resp} values among species, and to what extent each factor has played a role. More work is needed across a wider range of teleost species to investigate how ecological differences affect field metabolic rates, and whether these differences are more or less useful than body-mass and temperature in explaining field metabolic rate variation in different contexts. F actors which should be considered include habitat (pelagic vs. benthopelagic) and the extent of migration and, potentially, the proportion of HUFAs in the diet. The use of proxies for oxygen consumption, such as C_{resp} values and ETS, are especially important in understanding metabolic rate variation in species where respirometry is not currently feasible, such as myctophids.

Chapter 4

Body mass and temperature scaling of otolith-derived field metabolic rates

4.1 Abstract

Some ecologists have proposed that metabolic rate - the rate at which an organism converts energy and nutrients into power, biomass and waste products - underpins all other ecological processes. Metabolic rate has long been known to scale with body mass and temperature. Under the metabolic theory of ecology, metabolic rate scales allometrically with an exponent of 0.75 across organisms. Similarly, the universal temperature dependence hypothesis proposes that the effect of temperature on metabolic rate can be described using an Arrhenius equation, with an average activation energy of 0.65. Despite widespread controversy, these universal scaling exponents are used in models to predict the impacts of climate change on ecosystems at regional and global scales.

While laboratory studies have enabled the development of metabolic ecology, few studies have investigated the applicability of universal scaling relationships to organisms living in the wild. Furthermore, despite their importance as a food resource, no studies have yet investigated the metabolic scaling relationships of wild marine teleost fishes.

In this study, I use otolith-derived field metabolic rates to explore the scaling of fish metabolic rates in the wild. I find that fish field metabolic rate scales with body mass with an exponent of 0.90, and with temperature with an activation energy of 0.26. This study joins others in demonstrating that the body mass scaling exponent for fishes is significantly greater than is proposed by the metabolic theory of ecology, and that the

metabolic level boundaries hypothesis may offer a more appropriate framework for explaining metabolic rate across different taxa. The use of low body mass scaling exponents in marine ecosystem models is likely overestimating the effects of body mass on mass-specific ecological rates. Similarly, the low temperature sensitivity of fish field metabolic rates highlights the ability of wild-living organisms to behaviourally compensate for thermodynamic effects on their metabolic rates.

This study emphasises the importance of studying field metabolic rates across all taxa, particularly those groups which are thus far understudied. Otolith-derived field metabolic rates offer a powerful tool with which to investigate metabolic rates across wild marine fish.

4.2 Introduction

Metabolic rate - the rate at which an organism converts energy and nutrients into power, biomass and waste products - is thought to underpin all other ecological rates, including growth, survival and abundance (Brown et al., 2004). Given the importance of metabolic rate, scientists have long been interested in what determines an organism's metabolic rate and how these determinants operate at different biological scales.

4.2.1 Body mass

The scaling of metabolic rates with body mass can be described by the equation:

$$Y = aM^b \tag{4.1}$$

where Y is the metabolic rate, M is the body mass (in grams), b is the scaling exponent, and a is the normalisation constant (West et al., 1997; Brown et al., 2004).

It has long been known that metabolic rate scales with negative allometry (Rubner, 1883), less than directly proportional to body mass ($b < 1$), as opposed to isometrically, where rates scale in direct proportion with body mass ($b = 1$), or with positive allometry, where rates increase faster than body size ($b > 1$). Macroecological studies determined that b tended towards an average value of 0.75 ($\frac{3}{4}$, Kleiber, 1932, 1947), as opposed to the original scaling exponent of 0.67 ($\frac{2}{3}$, Rubner, 1883). West et al. (1997) proposed that the driver of the 0.75 value of b is the fractal nature of delivery systems, such as blood vessels and water vascular systems. 0.75 power scaling and the fractal network theory became the basis for the metabolic theory of ecology (MTE, West et al., 1997; Brown et al., 2004). According to strict MTE, the value of b is constant at 0.75, which is equivalent to -0.25 for mass-specific metabolic rates (West et al., 1997; Brown et al., 2004).

Despite its ubiquity, MTE has been controversial since its proposal, both in terms of its theoretical underpinnings (e.g. Kozłowski and Konarzewski, 2004) and empirical evidence. Many studies have found systematic variations in the value of b among life stages (Giguère et al., 1988; Killen et al., 2007), hierarchical levels (Norin and Gamperl, 2018), activity levels (Brett and Glass, 1973; White et al., 2007; Glazier, 2009; Killen et al., 2010; Norin and Malte, 2012) and taxonomic groups (White et al., 2006, 2007; Capellini et al., 2010; White et al., 2012b; Uyeda et al., 2017). Most macroecological studies of metabolic rates in vertebrates have tended to use data on endotherms (i.e. birds and mammals), which typically result in values of b tending towards 0.75 or 0.67. In contrast, ectotherms typically have a higher value of b (White et al., 2006;

Glazier, 2010; White et al., 2012b). For example, studies of standard metabolic rates (SMR, the metabolic rate of an unmoving, post-absorptive ectotherm at a specific temperature) in fish have given b values of approximately 0.80 to 0.90 (equivalent to -0.10 to -0.20 for mass-specific metabolic rates, Winberg, 1956; Clarke and Johnston, 1999; White et al., 2006; Killen et al., 2016). The heterogeneity found in the value of b across vertebrates raises the question: is a single average value of b (i.e. 0.75) sufficient for broad applications?

Much of the controversy around whether a single value of 0.75 is appropriate across all vertebrates has arisen from different statistical approaches. In particular, there is a difference between statistical hypothesis testing, which may support or reject a universal value of b based on statistical overlap (or lack thereof) with 0.75 (Dodds et al., 2001; Savage et al., 2004), and an information theoretical approach which seeks to select the best fit model with the least number of parameters (Isaac and Carbone, 2010; White et al., 2012b).

An alternative theoretical framework to MTE is the metabolic level boundaries hypothesis (MLBH, Glazier, 2005, 2009, 2010, 2015). MLBH proposes that b, rather than being a universal value is context dependent, and varies between the boundaries of 0.67 and 1.00. The allometric lower bound of 0.67 is set by surface area-volume constraints of fractal supply networks, while the isometric upper bound of 1.00 is set by mass-volume constraints such as muscle power. The specific value of b for a group or species depends upon the metabolic level - the mass-specific metabolic rate at the midpoint of an organism's body mass (Glazier, 2005, 2010; Killen et al., 2010). Metabolic level is similar to a in equation 4.1 in that it deals with the elevation of metabolic rate (Glazier, 2005).

An important concept within MLBH is that the value of b, and its relationship to metabolic level, changes with activity level (Glazier, 2009, 2010). For SMR, b decreases with increasing metabolic level, so that organisms or groups with higher maintenance demands (e.g. athletic tunas) will have metabolic rates which scale with b_{SMR} closer to 0.75. In contrast, organisms or groups with low metabolic levels at SMR (e.g. sluggish carp) will have b_{SMR} close to 1.00 (Glazier, 2009, 2010; Killen et al., 2016). For maximum metabolic rates (MMR), b increases with increased metabolic level, as more active species are constrained by muscle output (a mass-volume constraint), b_{MMR} is closer to 1.00, while sluggish species are constrained by supply networks b_{MMR} is closer to 0.75 (Glazier, 2009, 2010)). The difference in the relationship between metabolic level and b at different activity levels is proposed as an explanation for why across vertebrates b_{MMR} is typically higher than b_{SMR} (Glazier, 2009).

4.2.2 Temperature

After body mass, temperature is a key driver of metabolic rates, due to its effects on enzyme-catalysed reaction kinetics. The effect of temperature on enzyme-catalysed reactions can be described using an Arrhenius equation:

$$Y \propto e^{\frac{-E}{kT}} \tag{4.2}$$

where Y is the rate of reaction (in our case metabolic rate), E is the activation energy, k is the Boltzmann constant, and T is the absolute temperature in kelvin (Gillooly et al., 2001; Brown et al., 2004).

According to the universal temperature dependence hypothesis (UTD), E has an average value of between 0.60 and 0.70 eV (often reported as 0.65 eV), which is the average activation energy when combining the reactions which comprise respiration (Gillooly et al., 2001). However, UTD is based on enzyme thermodynamics, therefore it is unclear how the value of 0.65 eV might scale up to whole-organism metabolic rates.

When combining MTE with UTD, the full equation becomes (Brown et al., 2004):

$$Y = aM^{0.75}e^{\frac{-0.65}{kT}} \tag{4.3}$$

4.2.3 Field metabolic rate scaling

Field metabolic rate (FMR) is the time-averaged metabolic rate of a free-living animal. FMR includes the metabolic costs incurred by different experienced temperatures, specific dynamic action (the increase in metabolic rate due to digestion and assimilation of food), foraging, predator evasion and reproduction (Treberg et al., 2016; Trueman et al., 2016). The extent to which metabolic frameworks such as MTE, UTD and MLBH apply to FMR has not been fully ascertained, as the established method for measuring FMR (doubly-labelled water, Lifson et al., 1955) is expensive and logistically challenging (Treberg et al., 2016). Furthermore, the doubly-labelled water method cannot be applied to organisms with a high water turnover rate, such as fish (Treberg et al., 2016).

Across studies which have estimated b_{FMR} in terrestrial organisms, there is variation as to whether b_{FMR} is higher than (Nagy, 1987), lower than (Koteja, 1991; Nagy, 1987), or the same as b_{SMR} (Nagy, 1987; Capellini et al., 2010; Savage et al., 2004). Under the MTE framework, b is invariant with activity level, so b_{FMR} should be 0.75 (or statistically indistinguishable from 0.75, West et al., 1997; Brown et al., 2004; Savage et al., 2004). Under MLBH, the relationship between b and metabolic level for FMR is

less certain, as FMR lies between SMR and MMR. If base costs (i.e. SMR) make up a large proportion of FMR, b_{FMR} should follow the pattern of b_{SMR}, having a negative relationship with metabolic level (Glazier, 2010). However, it could also be argued that b_{FMR} should be greater than b_{SMR} as volume constraints such as muscle power become limiting and b_{FMR} moves closer to 1 (isometric scaling, Glazier, 2009, 2010).

Considering temperature, there is particular uncertainty around whether UTD applies to FMR. In the field, organisms may be able to compensate for the temperature effects on their SMRs by reducing other components of FMR (Richards, 2010). For example, fish experiencing higher temperatures may reduce their food intake to reduce specific dynamic action (Norin and Clark, 2017; Jutfelt et al., 2021). As FMR is a more ecologically relevant measure of metabolic rate (Treberg et al., 2016), ascertaining b_{FMR} and E_{FMR} for fish is crucial to understanding how fish might respond to unfavourable temperature increases under climate change.

4.2.4 The importance of field metabolic rate scaling in fish

Along with enabling a better understanding of metabolic scaling in ectotherms, focusing on FMR scaling in fish has particular practical importance for humans. Globally 7 % of all protein consumed by humans is from fish, and an estimated 59.51 million people are employed in fisheries or aquaculture (FAO, 2020), therefore there is a clear and urgent need to predict the impacts of climate change on marine ecosystems.

Predicting the impacts of climate change, and other anthropogenic stressors, on marine ecosystems is primarily achieved through global and regional scale models (Tittensor et al., 2018), most of which rely on inputs directly related to, or derived from, metabolic scaling (Chapter 1, Table 1.2, Cheung et al., 2008, 2013; Blanchard et al., 2012; Harfoot et al., 2014; Jennings and Collingridge, 2015; Carozza et al., 2016; Audzijonyte et al., 2019). The macroecological model is the most explicitly based on MTE, incorporating the full MTE equation (equation 4.3) to predict fish biomass, production and distribution (Jennings and Collingridge, 2015). The majority of global and regional ecosystem models use a single body mass scaling exponent, usually between 0.67 and 0.75, and a single E between 0.60 and 0.70. However, information theoretical approaches suggest that single scaling relationships are unlikely to be sufficient to describe the relationships between metabolic rate, body mass and temperature at macroecological scales (White et al., 2012b). Furthermore, few marine ecosystem models consider FMR, instead using MTE or values of b derived from laboratory measures (Cheung et al., 2008; Blanchard et al., 2012; Jennings and Collingridge, 2015; Carozza et al., 2016; Audzijonyte et al., 2019).

One ecosystem model which does consider FMR is the general ecosystem model (also called the Madingley model, Harfoot et al., 2014). The general ecosystem model is not explicitly marine - instead it can be applied aquatic and terrestrial ecosystems (Tittensor et al., 2018). The general ecosystem model uses values for b_{FMR} derived from doubly-labelled water studies of terrestrial endo- and ectotherms (b_{FMR} = 0.70 and 0.88, respectively, Nagy et al., 1999; Harfoot et al., 2014). While the general ecosystem model considers both FMR and variations in b more than the majority of other ecosystem models, a b_{FMR} value from marine ectotherms could make it more applicable to marine systems. Ultimately, if we are to understand how climate change will impact marine ecosystems, we must have a good understanding of how fish FMR varies with body mass and temperature.

4.2.5 Beyond body mass and temperature variation

Although body mass and temperature are primary drivers of metabolic rates (West et al., 1997; Gillooly et al., 2001; Brown et al., 2004), studies show variation in metabolic rates *after* body mass and temperature are accounted for. Within the teleost fishes, metabolic rates have been shown to vary with taxonomic group (Clarke and Johnston, 1999; Uyeda et al., 2017), activity level (Gordon, 1972; Glazier, 2009; Killen et al., 2010, 2016), depth (Drazen and Seibel, 2007; Seibel and Drazen, 2007; Drazen et al., 2015; Ikeda, 2016), thermal realm (Scholander et al., 1953; Wohlschlag, 1960; White et al., 2012a) and habitat (Gordon, 1972; Koslow, 1996; Drazen and Seibel, 2007; Seibel and Drazen, 2007; Killen et al., 2010, 2016). Given the many components that make up FMR (Chapter 1 section 1.1, Treberg et al., 2016), combined with the ability for wild fishes to mitigate potential temperature effects (and potentially other stressors) on their SMR (Norin and Clark, 2017; Jutfelt et al., 2021), there is likely a large amount of unexplained variance in FMR after accounting for body mass and temperature effects.

Estimates of phylogenetic signal (Harvey and Pagel, 1991) allow us to ascertain the the level of phylogenetic influence on model residuals, or how similar the trait of interest is among closely related species after accounting for fixed effects (Kamilar and Cooper, 2013). MMR in particular has been found to show phylogenetic signal after accounting for body mass and temperature (λ = 0.62, Killen et al., 2016), indicating that allometric and thermodynamic effects alone cannot fully explain variation in MMR across the fishes, and that these variations are somewhat conserved. I would expect to see similar phylogenetic signal for FMR if traits other than body mass and temperature are relatively phylogenetically conserved (i.e. more similar in close relatives). By examining how FMR varies across the phylogenetic tree, after accounting for body mass and temperature, we can begin to ascertain which ecological traits may also significantly influence FMR.

Alongside providing information about potential influences of FMR, phylogenetically informed models ensure robustness by avoiding pseudo-replication among closely related species, due to their shared evolutionary history (Harvey and Pagel, 1991).

4.2.6 Aims

In this study, I used phylogenetically-informed mixed models to investigate the body mass and temperature scaling of otolith-derived estimates of the proportion of metabolic carbon in a fish's blood - C_{resp} values (Trueman et al., 2016; Chung et al., 2019a,b) - which I converted into oxygen consumption rates. I compared my absolute oxygen consumption values, along with b_{FMR} and E_{FMR} to values previously determined for SMR and MMR in fishes (from Killen et al., 2016). Finally, I investigated the phylogenetic signal of residual variation in FMR, and compared mass- and temperature- normalised FMR across different taxonomic groups, with the goal of informing future studies.

4.3 Methods

4.3.1 Statistical analyses

To investigate the relationships of C_{resp} values with body mass and temperature, I ran a model incorporating logged body mass ($ln(bm)$) and $\delta^{18}O_{oto}$-derived experienced temperature ($temp_{exp}$, Chapter 2 section 2.5):

$$C_{resp} \sim ln(bm) + temp_{exp} \tag{4.4}$$

To investigate the values of the scaling exponents for body mass (b) and temperature (E) with FMR, I first estimated field oxygen consumption from C_{resp} values, using the equation:

$$C_{resp} = C(1 - e^{-kO}) \tag{4.5}$$

where O is oxygen consumption (mg kg^{-1} h^{-1}), C is the upper bound of C_{resp} values, and k is the decay constant of the relationship between C_{resp} values and oxygen consumption. I set k to 0.004 according to Martino et al. (2020). As there is no information on the value of C for a dataset spanning such a large range of C_{resp} values as this one, I arbitrarily set C to 0.64, which was the maximum C_{resp} value in my dataset plus 0.01. The aim of setting C to 0.64 was to keep the conversion between C_{resp} values and oxygen consumption within the linear portion of the relationship, as it is unlikely that fish would reach the upper bound (C) under natural conditions (Chung et al., 2019b; Martino et al., 2020).

To estimate whole-organism oxygen consumption (mg h^{-1}), I multiplied the mass-specific oxygen consumption for each individual by its body mass. I modelled mass-specific and whole-organism field oxygen consumption according to the MTE equation (Brown et al., 2004):

$$ln(O) \sim ln(bm) + temp_{inv} \tag{4.6}$$

where $ln(O)$ is the natural log of oxygen consumption (mass-specific or whole-organism), and $temp_{inv}$ is the inverse temperature according to an Arrhenius relationship:

$$temp_{inv} = \frac{1}{kT} \tag{4.7}$$

where k is Boltzmann's constant (8.62×10^{-5}) and T is the temperature in kelvin (K). I did not include interaction terms in the models as these are not present in MTE equations (Brown et al., 2004).

To enable comparisons with other studies, I converted E to Q_{10} values, which describe the rate change (in this case of FMR) over 10 °C, using the following equation:

$$ln(Q_{10}) = \frac{E}{k} \times \frac{10}{T_2 \times T_1} \tag{4.8}$$

where T_1 and T_2 are the minimum and maximum temperatures over which metabolic rates were measured (Aisami et al., 2017).

All models were generalised linear mixed-models, therefore I z-scored (standardised) all continuous predictors, so they were inputted as standard deviations from the mean. Using z-scored predictors means the constant a represents the FMR at mean values of the predictors, and b represents the change in FMR per standard deviation of the predictor. To convert back to a natural scale, I divided b by the standard deviation of the predictor in question.

I ran all models in R version 4.1.2 (R Core Team, 2021a), using the `MCMCglmm` package (Hadfield, 2010) to run Bayesian phylogenetic mixed models. All models included random effects of species-relatedness, intraspecific effects and the random effect of data source (Chapter 2). Following Hadfield (2010), I used regularising inverse-Wishart priors for all random factors, with variance (V) set to 1 and the belief parameter (ν) set to 0.02. I incorporated uncertainties (as standard errors of mean estimates) of both C_{resp} values and experienced temperatures by setting these as random factors with constant variances and fixed priors.

I ran all models for 5,000,000 iterations, with a burn-in of 15,000 and a thinning parameter of 500. I checked all models for convergence and mixing via visual inspection of traceplots, Geweke's diagnostic and the Heidelberger-Welch diagnostic (Plummer et al., 2006). All parameters for all models had an effective sample size $>$ 2000 (Hadfield, 2010). I ran the standard sensitivity tests (section 2.8), the results of which are summarised in Appendix H.

I used values derived from equation 4.4 to scale C_{resp} values to a common body mass and temperature of 200 g and 10 °C, as these values were close to the mean values across the dataset.

4.3.2 Comparison to fish resting and maximum metabolic rate

To ascertain where FMR sits between SMR and MMR, I compared average C_{resp}-derived oxygen consumption values to 13 species resting metbolic rate (RMR) and MMR values from Killen et al. (2016).

For comparison to data from Killen et al. (2016) I normalised oxygen consumption rates to a common body mass and temperature of 1000 g and 15 °C. While I used the b derived from my models, as with other normalisation procedures, I used an E of 0.65 to normalise to common temperatures, as normalisation aims to remove the enzyme-kinetic effects, rather than context-dependent responses to temperature. I was unable to do this for C_{resp} values, as there is no context-independent equivalent of the universal 0.65 E for C_{resp} values.

4.4 Results

The mean C_{resp} value across species was 0.193 ($\pm$ 0.109) and ranged from 0.006 for *Trachyrincus scabrus* (roughsnout grenadier) to 0.623 for *Thunnus orientalis* (Pacific bluefin tuna). The estimates for mass-specific field oxygen consumption from equation 4.5) ranged from 2 mg O_2 kg^{-1} h^{-1} to 1037 mg O_2 kg^{-1} h^{-1}, with a mean mass-specific oxygen consumption rate of 103 mg O_2 kg^{-1} h^{-1} ($\pm$ 90).

4.4.1 C_{resp} value scaling with body mass and temperature

C_{resp} values had a negative scaling relationship with logged body mass (Figure 4.1A), and a positive scaling relationship with temperature (Figure 4.1B). When corrected to a natural scale, the scaling exponents (b) for logged body mass and temperature were -0.01 ($\pm < 0.01$) and 0.01 ($\pm < 0.01$), respectively.

4.4.2 Field oxygen consumption scaling with body mass

Estimated mass-specific field oxygen consumption had a negative scaling relationship with logged body mass (Figure 4.2), while whole-organism field oxygen consumption had a positive relationship with body mass. When converted to a natural scale, the body mass scaling exponents were -0.09 ($\pm < 0.01$) for mass-specific oxygen consumption, and 0.90 ($\pm$ 0.01) for whole-organism oxygen consumption. These exponents were significantly different from 0.75 as predicted by MTE (equivalent to -0.250 for scaling of mass-specific metabolic rate, Brown et al., 2004), and 0.80 (equivalent to -0.20 for mass-specific, Winberg, 1956) proposed for fish (Figure 4.2).

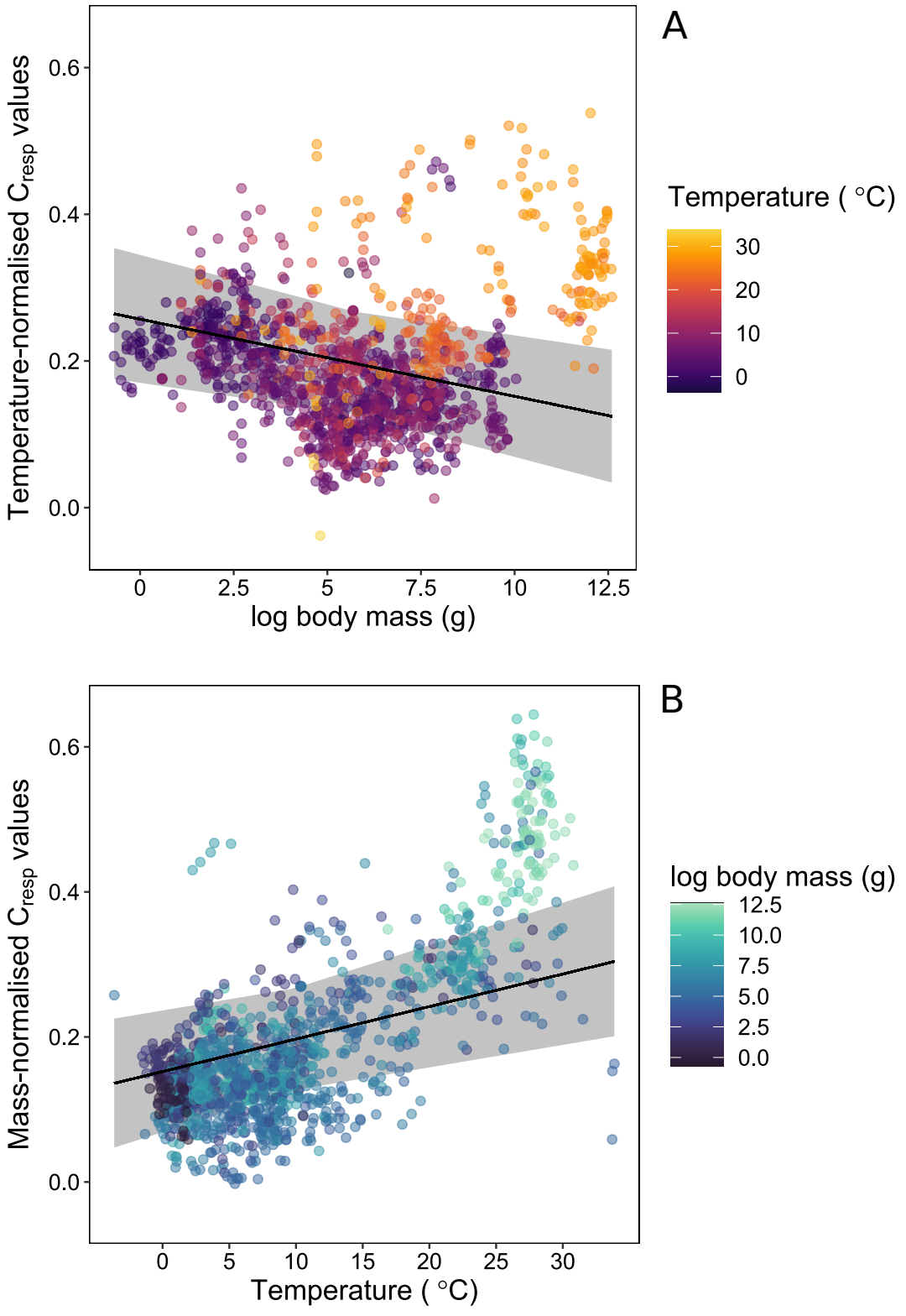

FIGURE 4.1: Individual C_{resp} values plotted by: (A) log body mass (g), normalised to 10 °C, and (B) experienced temperature (°C) normalised to 300 g body mass using the partial correlation coefficients from equation 4.4. On both plots the black line shows the significant relationship from the model described by equation 4.4, with 95% confidence intervals shaded in grey. The partial correlation coefficients are -0.01 for body mass, and 0.01 for temperature.

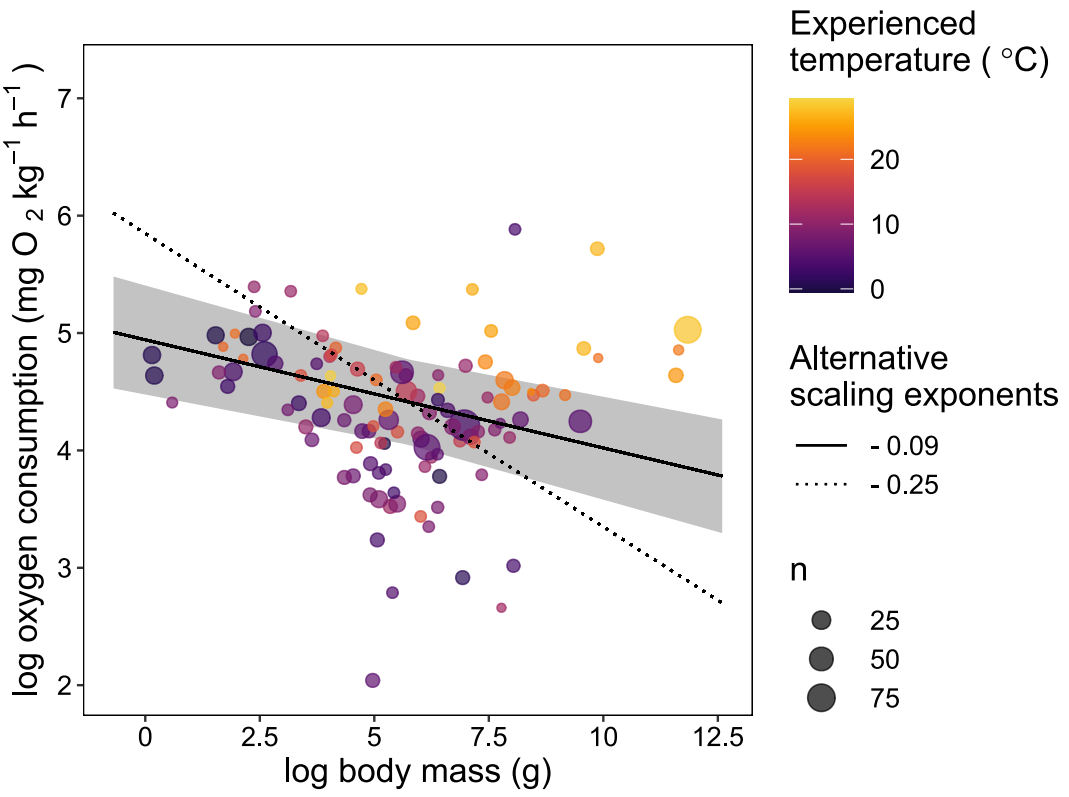

FIGURE 4.2: Temperature-corrected mass-specific field oxygen consumption (mg O^2 kg^{-1} h^{-1}) plotted against body mass (g) on a log-log scale. Field oxygen consumption was corrected to a common temperature of 10 °C, using the best-fit activation energy of 0.26 eV from equation 4.7. Each data point is a species' average, point size denoting the number of data points per species (n). The black line shows the significant relationship between field oxygen consumption and log body mass, as determined by equation 4.7, with a scaling exponent (*b*) of -0.09. 95% confidence intervals are shaded in grey. The dotted line shows the proposed universal value of *b* of -0.25, (West et al., 1997; Brown et al., 2004)

.

4.4.3 Field oxygen consumption scaling with temperature

Both estimated mass-specific and whole-organism oxygen consumption rates had positive relationships with temperature (Figure 4.3). When converted to a natural scale, these relationships resulted in Arrhenius activation energies (E) of 0.26 eV ($\pm$ 0.03) for both measures. This is significantly different from the E of 0.65 eV proposed by UTD (Figure 4.3). Using equation 4.8, an E of 0.26 eV equates to a Q_{10} value of 1.4.

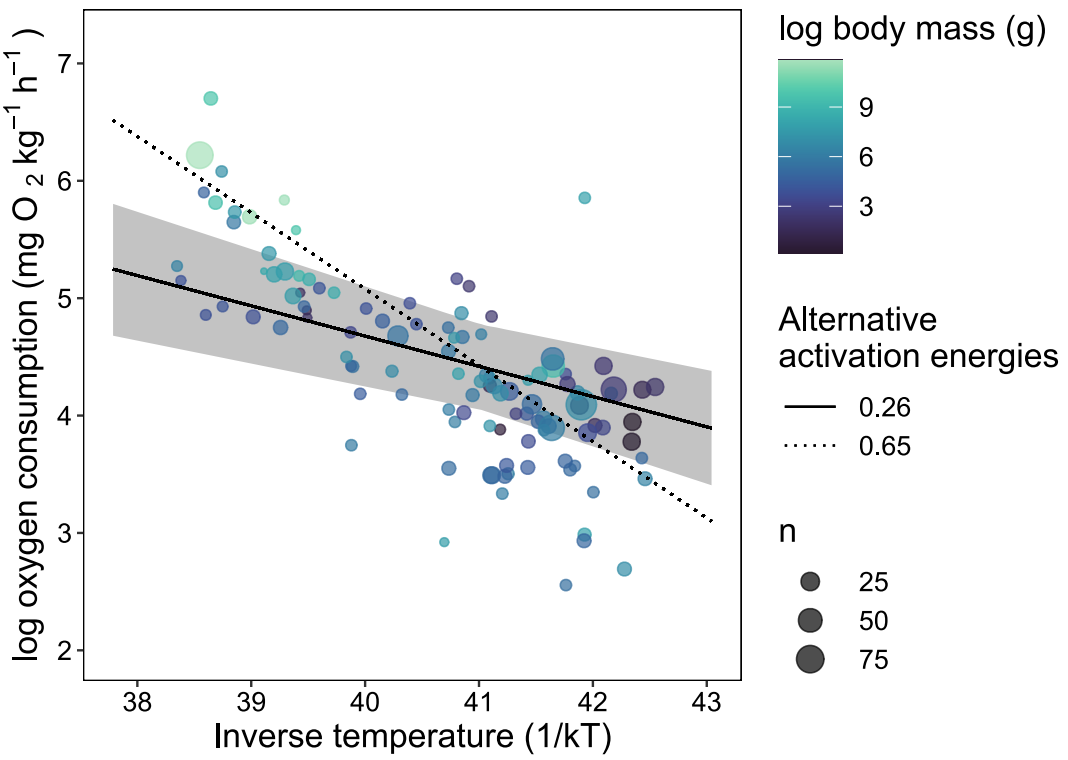

FIGURE 4.3: Logged mass-specific field oxygen consumption (mg O^2 kg^{-1} h^{-1}) plotted against inverse temperature ($1/kT$). Field oxygen consumption was corrected to a common body mass of 300 g, using the best-fit scaling exponent of -0.09 from 4.7. Each data point is a species' average, point size denoting the number of data points per species (n). The black line shows the significant relationship between field oxygen consumption and temperature, as determined by equation 4.7, with an activation energy of 0.26 eV. 95% confidence intervals are shaded in grey. The dotted line shows the proposed universal activation energy of 0.65 eV, (Gillooly et al., 2001, 2006))

.

4.4.4 Comparison to resting and maximum metabolic rates

Of the thirteen species common to my study and Killen et al. (2016), eleven had FMRs greater than *resting* metabolic rates (RMR). The two exceptions were *Merlangius merlangus* (whiting) and *Thunnus orientalis* (Pacific bluefin tuna, Figure 4.4).

Of the ten species with MMR data, nine had greater MMRs than FMRs (Figure 4.4). The sole exception was the *Cyclopterus lumpus* (lumpfish), which my study estimated to have an unusually high FMR (section 4.4.5). Aside from the above exceptions, species had estimated FMRs closer to their RMR than MMR (Figure 4.4).

Of the species which followed the expected pattern (RMR $<$ FMR, and FMR $<$ MMR where data were available), FMR was 1.2 to 5.9x RMR, with a mean of 1.8. *Artediellus atlanticus* (Atlantic hookear sculpin) had a much higher ratio of FMR to RMR than other species, having an FMR almost 6x RMR, while other species ranged from 1.2 to 1.8x.

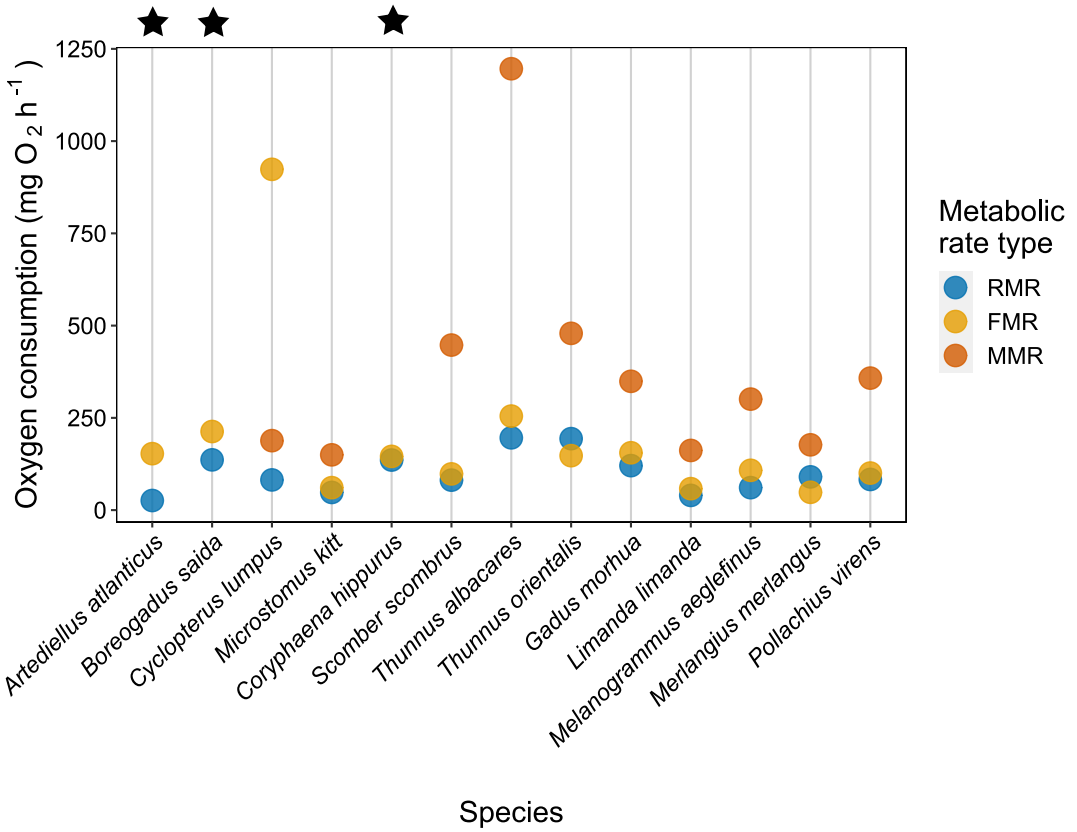

FIGURE 4.4: Resting (blue), field (yellow) and maximum (orange) metabolic rates (mg O^2 kg^{-1} h^{-1} for thirteen species of teleost fishes. Field metabolic rates are estimated from C_{resp} values from this study. Resting and maximum metabolic rates are from Killen et al. (2016). Metabolic rates are normalised to a common body mass and temperature of 1000 g and 15 °C respectively. Black stars indicate species where maximum metabolic rates were unavailable.

4.4.5 Effect of species' relatedness on otolith-derived field metabolic rates

Phylogenetic signal of the residuals for the C_{resp} model (described by equation 4.4) was relatively high (λ = 0.921), compared to the phylogenetic signal for oxygen consumption models (e.g. mass-specific oxygen consumption, equation 4.7, λ = 0.575).

Across the phylogenetic tree, there were clear trends within some orders (Figure 4.5). The Pleuronectiformes (flatfish) had consistently low C_{resp} values (C_{resp} value = 0.12 $\pm$ 0.04) and oxygen consumption rates (mass-specific O_2 consumption = 52 $\pm$ 15), as did the Beryciformes (mass-specific O_2 consumption = 43 $\pm$ 13) and the Gadiformes (cods and their relatives, C_{resp} value = 0.13 $\pm$ 0.04, mass-specific O_2 consumption = 59 $\pm$ 15). The Myctophiformes (lanternfish) also had relatively consistent, low C_{resp} values (C_{resp} value = 0.16 $\pm$ 0.04, mass-specific O_2 consumption = 73 $\pm$ 23). The Scombriformes had relatively high C_{resp} values (C_{resp} value = 0.32 $\pm$ 0.11), and oxygen consumption rates (mass-specific O_2 consumption = 194 $\pm$ 121), however, there was considerable variation among species within this order.

Within the dataset, a handful of species stood out by having relatively high C_{resp} values compared to their closest relatives. The most extreme example of an anomalous species was *Cyclopterus lumpus* (lumpfish, Figure 4.5), which had a C_{resp} value of 0.48 $\pm$ 0.01 (mass-specific O_2 consumption = 447 $\pm$ 13), much greater than other species within its order (Perciformes, C_{resp} = 0.23 $\pm$ 0.09).

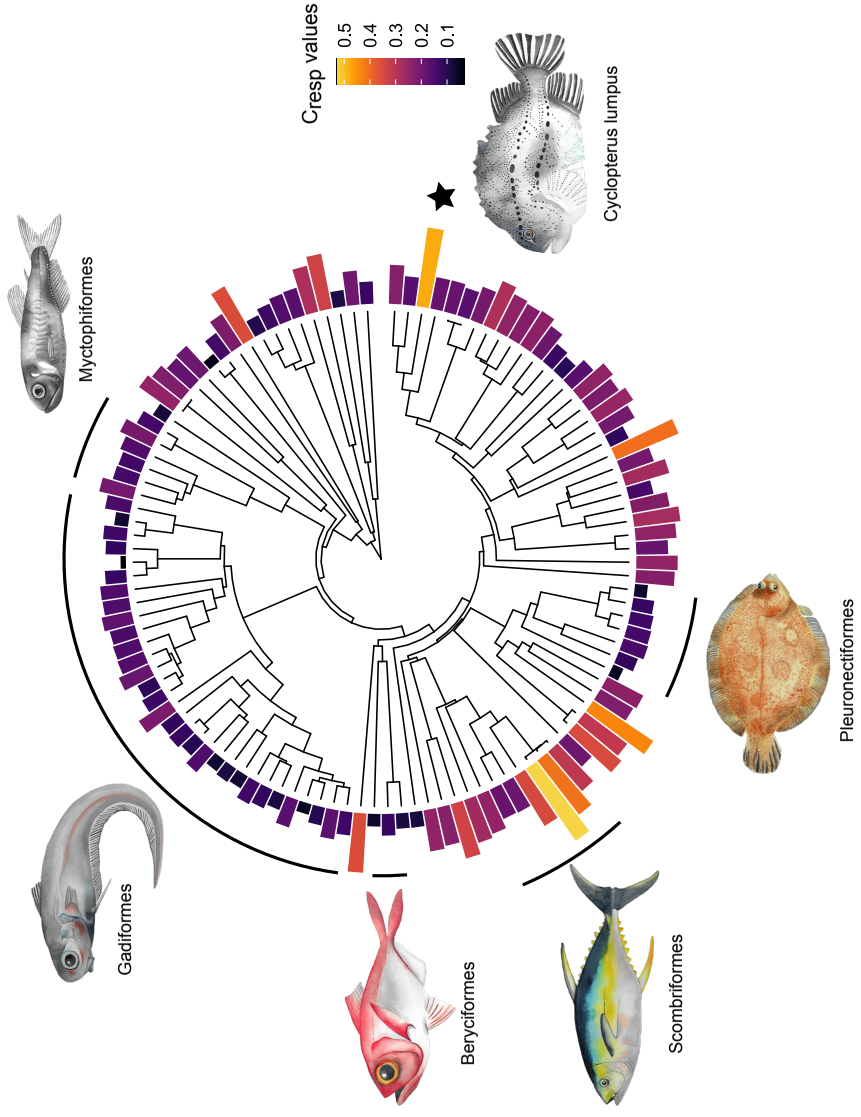

FIGURE 4.5: Phylogenetic patterns of field metabolic rates in fish, as estimated using C_{resp} values. C_{resp} values are normalised to a body mass of 300 g and a temperature of 10 °C. Illustrated are the Pleuronectiformes (*Microstomus kitt*, lemon sole), Scombriformes (*Thunnus albacares*, yellowfin tuna), Beryciformes (*Beryx splendens*, splendid alfonsino), Gadiformes (*Coryphaenoides rupestris*, roundnose grenadier) and the Myctophiformes (*Electrona antarctica*, Antarctic lanternfish). Also highlighted by the black star is *Cyclopterus lumpus* (lumpfish).

4.5 Discussion

4.5.1 Relationships between resting, field and maximum metabolic rates

In comparing resting, field and maximum metabolic rates within 13 species, most followed the expected pattern: RMR being the lowest, followed by FMR and then MMR. The finding that FMR was usually 1.2 - 1.8x greater than RMR slightly contrasts previous studies, which have found that fish need oxygen supplies 2 - 5x greater than predicted by SMR (Deutsch et al., 2015; Duncan et al., 2020). However, one species, *Artediellus atlanticus* (Atlantic hookear sculpin), had an FMR that was 5.9x its RMR. Additionally, the data from Killen et al. (2016) was *resting* rather than *standard* metabolic rates, which may account for our lower ratio compared to previous studies. The use of RMR may also account for the lower RMR than FMR for two species: *Thunnus albacares* and *Merlangius merlangus*. In general it is logical that within species, FMR values are closer to RMR than to MMR. MMRs are usually measured over short time periods and under extreme stress (Clark et al., 2013), producing metabolic rates which would be unsustainable in the wild, especially in the long-term (Norin and Clark, 2016).

Cyclopterus lumpus was the only species to have a greater FMR than MMR, a result which should be impossible, as MMR should represent the maximum aerobic capacity of an organism (Norin and Clark, 2016). The field oxygen consumption rates (and C_{resp} values from which they were derived) in *C. lumpus* are much higher than expected (section 4.5.4).

Equation 4.5 is particularly useful for estimating oxygen consumption rates at lower C_{resp} values, where the relationship between C_{resp} values and oxygen consumption rates is linear (Chung et al., 2019b; Martino et al., 2020). Converting to oxygen consumption from C_{resp} values becomes more difficult at higher C_{resp} values, due to the sensitivity of of high C_{resp} value conversions to the poorly known upper bound (C). C is also less well defined and more variable that the decay constant (k, Chung et al., 2019b; Martino et al., 2020). Further research is needed to calibrate C_{resp} values with oxygen consumption rates across a range of species, particularly those with high C_{resp} values.

4.5.2 Body mass scaling

In finding a value of 0.90 for b_{FMR}, this study joins a growing number which find that the value of b for fishes is greater than the 0.75 value proposed by MTE (West et al., 1997; Brown et al., 2004), instead lying within the range of 0.78 and 0.95 (Winberg, 1956; Clarke and Johnston, 1999; White et al., 2006; Killen et al., 2016). According to the metabolic-level boundaries hypothesis (MLBH, Glazier, 2005, 2009, 2010), groups with a low metabolic level (i.e. ectotherms, including fish) will have greater values of b_{SMR} than groups with higher metabolic levels (i.e. endotherms). Furthermore, MLBH asserts that b_{FMR} will also be greater in groups with lower metabolic levels, if a large proportion of FMR is comprised of basal costs (SMR, Glazier, 2010), which our study supports. The b_{FMR} of 0.90 found here for fishes is greater than b_{FMR} found previously for birds and mammals (b_{FMR} = 0.68 and 0.73 respectively, Nagy et al., 1999), which supports the MLBH prediction of higher b_{FMR} in lower metabolic level groups (Glazier, 2010).

A further prediction of MLBH is that metabolic rate should move closer to isometric scaling with body mass (b = 1) with increasing activity level, as volume restrictions become the dominant constraint (Glazier, 2005, 2009, 2010). It is difficult to compare our value of b_{FMR} to values of b_{SMR} and b_{MMR}, as there are few interspecific studies of b in fishes, and each study uses a dataset comprised of different species, which may alter the best-fitting value of b. Nevertheless, our value of b_{FMR} of 0.90 is greater than the value of b_{SMR} for most studies, which range from 0.78 to 0.88 (Winberg, 1956; Clarke and Johnston, 1999; White et al., 2006; Uyeda et al., 2017), which appears to support the MLBH prediction that b increases with activity level. The exceptions to this were Killen et al. (2016) and Bigman et al. (2021), which found relatively high b_{SMR} values of 0.95 and 0.92 respectively. More research is needed on how b varies with activity level, and ideally this research should be carried out within the same study, and using the same species to reduce confounding factors. However, it is clear that the value of b for fishes, including FMR, is significantly greater (in both biological and statistical terms) than the 0.75 value proposed by MTE.

The majority of marine ecosystem models use values of b based on, or close to, the 0.75 value proposed by MTE (Chapter 1 Table 1.2, Cheung et al., 2008, 2013; Blanchard et al., 2012; Harfoot et al., 2014; Jennings and Collingridge, 2015; Carozza et al., 2016; Audzijonyte et al., 2019), which as discussed is likely lower than the value for b for fishes, which is found to range between 0.78 and 0.95 for SMR (Winberg, 1956; Clarke and Johnston, 1999; White et al., 2006; Killen et al., 2016; Uyeda et al., 2017), and is found by this study to be 0.90 for FMR. Using a lower value of b within marine ecosystem models is likely to over-estimate the effects of body mass on mass-specific metabolic rates. For example, Cheung et al. (2013) used a value for b of 0.70 to predict widespread reductions in fish body size with climate change. As has been pointed out

in other papers (Lefevre et al., 2017, 2018; Norin and Gamperl, 2018), the use of such a low scaling exponent likely overestimated the magnitude of the relationship between body size and the effects of climate warming.

Although most of the ecosystem models considered here employ relatively low values of b, the general ecosystem model (Harfoot et al., 2014) uses a value of b_{FMR} for ectotherms of 0.88, which is relatively close to the 0.90 found by my study for fishes. The value of 0.88 in the general ecosystem model was obtained from a doubly-labelled water study of reptiles (Nagy et al., 1999), suggesting that when choosing scaling exponents for modelling, thermoregulatory strategy is an important consideration. Ultimately, where marine ecosystem models are concerned with the energetic costs of life in the field, effects of or on body mass would be best determined using the b_{FMR} determined here.

4.5.3 Temperature scaling

The temperature sensitivity of otolith-derived field oxygen consumption rates, as quantified by Arrhenius activation energy (E) was 0.26, which is outside the range of 0.6 to 0.7 proposed by the universal temperature dependence hypothesis (UTD, Gillooly et al., 2001, 2006). E of FMR was also lower than the range typically seen for SMR within teleost fish (0.34 to 0.59, Clarke and Johnston, 1999; Killen et al., 2016; White et al., 2012b), instead being closer to the E found for MMR (0.25, Killen et al., 2016). The E for FMR from our study lay between that of SMR (0.34) and MMR (0.25) from Killen et al. (2016). Given that SMR is itself a component of FMR (Treberg et al., 2016), it may seem counter-intuitive that FMR E is closer to that of MMR than FMR. However, two key differences between laboratory-based and field-based measures of metabolic rates may explain the lower temperature sensitivity of FMR than SMR.

The first difference between E_{FMR} and E_{SMR} is that fish living in the wild are likely to be living at or below their thermal optimum so as to avoid the sharp drop in performance which results above the thermal optimum (Chapter 1, section 1.2.2, Martin and Huey, 2008; Schulte, 2015; Chung et al., 2021b). Secondly, free-living fish can likely modify their behaviour to compensate for the kinetic effects of temperature on their basal metabolism (Richards, 2010). For example, fish experiencing higher temperatures in laboratory settings have been found to reduce their food intake to reduce specific dynamic action, which is the cost of digesting and assimilating meals (Norin and Clark, 2017; Jutfelt et al., 2021). The ability for wild-living fish to compensate for, or move away from, unfavourable temperature adds complexity when using FMR to predict the effects of climate warming on fish.

Marine ecosystem models, which among other things, aim to predict the effects of increased temperatures on marine ecosystems, typically employ the UTD framework

to estimate the effects of temperature on biological rates (Chapter 1, Table 1.2, Cheung et al., 2008, 2013; Blanchard et al., 2012; Harfoot et al., 2014; Jennings and Collingridge, 2015; Carozza et al., 2016; Audzijonyte et al., 2019), setting E between 0.6 and 0.7 eV (Gillooly et al., 2001, 2006). Using UTD captures the thermal kinetic effects of increasing temperature on metabolic rate reactions, but does not capture the behavioural compensations of wild fishes to increasing temperatures, nor the trade-offs that these behaviours incur. For example, the previously mentioned ability for fish to reduce their specific dynamic action by eating smaller meals comes at the cost of reduced growth efficiency, particularly if the food quality is reduced (Norin and Clark, 2017; Jutfelt et al., 2021). Trade-offs are also likely when reducing other aspects of FMR: reducing movement is likely to have implications for the ability to feed and reproduce (Richards, 2010). Ultimately, more research is needed to better understand the costs and benefits for fish modifying their behaviour to cope with unfavourable temperatures.

4.5.4 Species' relatedness: drivers beyond body mass and temperature

The phylogenetic signal of field oxygen consumption (λ = 0.58) was closer to that previously found for MMR (λ = 0.62) than that for SMR (λ = 0.49, Killen et al., 2016), which mirrors previous results in this study suggesting that FMR scales more similarly to MMR than SMR, in terms of body mass and temperature. The λ of field oxygen consumption (0.58) indicates that there there is a reasonable amount of phylogenetic signal in the residuals, which supports previous studies finding considerable variation in metabolic rate after accounting for body mass and temperature (Clarke and Johnston, 1999; Drazen and Seibel, 2007; White et al., 2012a; Drazen et al., 2015; Ikeda, 2016; Killen et al., 2016). By examining patterns in FMRs across the phylogenetic tree, in combination with knowledge about the traits of various lineages, we can begin to unpick which factors, other than body mass and temperature, may drive variation in FMR.

The consistently low C_{resp} values and field oxygen consumption estimates for the Pleuronectiformes (flatfish) reflects the low SMR and MMR measures previously found for this order (Killen et al., 2016). The subfamily Pleuronectinae, within the order Pleuronectiformes had been found to have a lower body mass scaling intercept than other fishes (Uyeda et al., 2017), which is consistent with my findings of low C_{resp} values and field oxygen consumption rates. Pleuronectiformes are a commercially important group and thus often of interest when developing models for ecosystem based fishery management (Pauly, 1994; Girardin et al., 2018). My results support that flatfishes may have FMRs different to those of other fishes, perhaps due to their benthic lifestyle, therefore established estimates and theories may not be suitable if focusing on this group.

Similarly to the flatfishes, the Gadiformes (cods and relatives) also have relatively consistently low FMRs. This may be due to the high proportion of deep-sea species within this order, particularly due to the prevalence of Macrouridae (grenadiers) in my dataset, which are a family exclusively found in the deep-sea. A depth-dependent decline in metabolic rates, which cannot be accounted for by body mass and temperature effects alone, is a prominent trend within the metabolic ecology for fishes (Drazen and Seibel, 2007; Seibel and Drazen, 2007; Drazen et al., 2015; Ikeda, 2016). Further support for potential effect of depth can be seen within the Beryciformes, which also have relatively low FMRs. All of the beryciform species within this study have a minimum depth of occurrence greater than 100 m (Appendix A). The low FMRs of deep-living groups in this study, such as the Gadiformes and the Beryciformes, indicate that depth could be a potential driver for variation in FMR (Chapter 6).

Despite C_{resp} values and field oxygen consumption estimates being fairly similar within most taxonomic groups, *Cyclopterus lumpus* were a clear anomaly in terms of having high FMRs compared to their closest related species in the dataset. Despite long being thought of as benthic, adult *C. lumpus* adopt a "semi-pelagic" lifestyle, particularly during spawning (Blacker, 1983; Kennedy et al., 2016). Given that adult *C. lumpus* spend a large part of their time within the water column despite having a morphology unsuited to a pelagic lifestyle, adult *C. lumpus* may be expending a large amount of energy on locomotion, which may account for their high FMRs. Other possibilities include their need to feed near continuously, which may elevate their FMR through specific dynamic action, or their large investment in gonadal tissues (J. Kennedy, per. comms. 2021). Whatever the underlying mechanism, anomalous species such as the *C. lumpus* highlight the need to investigate the FMRs of a broad range of species, particularly if those species are of commercial interest.

4.5.5 Conclusion

This study has shown the C_{resp} method to be effective in estimating field oxygen consumption rates in a wide range teleost fish species, enabling for the first time an investigation of the scaling of fish FMR with body mass and temperature.

C_{resp}-derived FMR scaled with body mass with an exponent of 0.90 (Figure 4.2), which is significantly different to the 0.75 exponent proposed by MTE. The widespread use of MTE-based body mass scaling exponents in marine ecosystem models is likely overestimating the effects of body mass on mass-specific metabolic rates, with significant consequences for model outputs. Instead, MLBH may offer a more congruent framework with which to describe patterns in metabolic rate scaling across different taxa. C_{resp}-derived FMR scaled with temperature according to an Arrhenius activation energy of 0.26 (Figure 4.3), equivalent to a Q_{10} of 1.4, reflecting the ability for wild fishes to compensate for the biochemical effects of temperature on their metabolic reactions.

Despite the clear scaling relationships of FMR with body mass and temperature, a large amount of variation remains unexplained. Analyses of patterns across the phylogenetic tree suggests that ecological factors such as depth and habitat may be important drivers of variation in FMR, and are worthy of future exploration. The C_{resp} method offers a practical and robust method for investigating fish FMRs, especially at a macroecological scale.

Chapter 5

Do cold fish run hot? The effect of thermal realm on C_{resp} values

5.1 Abstract

Temperature is a key driver of variation in metabolic rates among organisms, especially for ectotherms whose body temperatures are determined by the ambient environment. Although the effect of temperature on metabolic rate is often described by Arrhenius reaction kinetics, the actual relationship between temperature and metabolic rate within whole organisms is likely to be more complex, especially for organisms living in the field. The relationship between temperature and metabolic rate in ectotherms is thought to depend upon the thermal characteristics of the environment to which an organism is adapted. Two key theories describe how metabolic rates might vary according to an organisms thermal realm: metabolic cold adaptation and thermal sensitivity trade-offs.

Metabolic cold adaptation deals with the elevation of metabolic rate, proposing that polar species have higher metabolic rates than would be expected for organisms living at such cold temperatures, assuming a constant scaling of metabolic rate with temperature. The thermal sensitivity trade-off hypothesis challenges the idea that the scaling between metabolic rate and temperature is constant, instead proposing that stenothermic species have a steeper scaling relationship between metabolic rate and temperature compared to eurythermal species. Despite extensive study, metabolic cold adaptation in particular remains controversial, and large-scale marine ecosystem models assume a constant relationship between temperature and metabolic rate.

This study uses C_{resp} values, a proxy for field metabolic rates, to test metabolic cold adaptation and the thermal sensitivity trade-off hypothesis in marine teleost fishes. I find that there is clear systematic variation in the relationship between experienced

temperature and metabolic rate across different thermal realms. This study shows partial support for metabolic cold adaptation, with polar species having higher C_{resp} values than temperate species, after accounting for body mass and experienced temperature. However, there is no support for metabolic cold adaptation when comparing the C_{resp} values of polar and tropical or subtropical species. Furthermore, this study shows support for the thermal sensitivity trade-off hypothesis, with stenotherms having a steeper scaling relationship between C_{resp} values and experienced temperatures than eurytherms. Overall, this study shows that using a single exponent to describe the relationship between whole organism metabolic rates and temperature may underestimate the vulnerability of different groups to climate change. Furthermore, I highlight the importance of considering both field- and laboratory-derived measures of metabolic rate, to better ascertain the costs associated with mitigating temperature increases in wild organisms.

5.2 Introduction

Alongside body mass, temperature is one of the primary drivers of variation in metabolic rates among organisms, both in the short term and over evolutionary timescales. At the level of enzyme-catalysed metabolic reactions, the relationship between temperature and metabolic rate can be described by the Arrhenius equation:

$$Y \propto e^{\frac{-E}{kT}} \tag{5.1}$$

where k is the Boltzmann constant, T is the temperature in kelvin, E is the activation energy, and Y is a physiological rate (metabolic rate in our case, Gillooly et al., 2001; Brown et al., 2004; Gillooly et al., 2006). According to the universal temperature dependence hypothesis, the relationship between metabolic rate and temperature can be described with an average value for E of 0.65 eV, which is the average temperature dependence of enzyme-catalysed metabolic reactions (Gillooly et al., 2001, 2006). However, while universal temperature dependence may describe enzyme thermodynamics, relationships between metabolic rates and temperature in whole organisms are likely more complex, particularly when considering evolutionary adaptation to different thermal realms.

Across the globe, organisms are adapted to a wide range of temperature conditions: from the extreme but relatively stable temperatures in the poles and tropics, to the relatively mild but fluctuating temperatures in the temperate regions. Temperature conditions are particularly important for metabolic rates in ectotherms, whose body temperature is set by the external environment. Two key hypotheses seek to describe and explain variation in temperature sensitivity of metabolic rate across thermal realms: the metabolic cold adaptation hypothesis and the thermal sensitivity trade-off hypothesis.

5.2.1 Metabolic cold adaptation

According to reaction kinetics described by the Arrhenius equation (equation 5.1), metabolic rates increase with increasing temperatures and decrease with decreasing temperatures. This pattern is seen across ectotherms, where tropical species have higher mass-normalised metabolic rates than polar species (Scholander et al., 1953; Wohlschlag, 1960; Clarke and Johnston, 1999). However, ectotherms living in cold polar environments are still able to function despite the depressive effects of temperature on the enzyme-catalysed reactions which comprise metabolic rate (Ege and Krogh, 1914; Scholander et al., 1953; Wohlschlag, 1960). Metabolic cold adaptation proposes that the reason polar ectotherms are able to function in cold temperatures is

that their metabolic rates are elevated at cold temperatures compared to non-polar ectotherms (Ege and Krogh, 1914; Scholander et al., 1953; Wohlschlag, 1960). While evidence for metabolic cold adaptation has been found across diverse taxa such as insects (Addo-Bediako et al., 2002) and reptiles (Dupoué et al., 2017), the early studies of metabolic cold adaptation hypothesis focused on on aquatic ectotherms (Ege and Krogh, 1914; Scholander et al., 1953; Wohlschlag, 1960).

Early studies typically tested for metabolic cold adaptation by normalising metabolic rates to a common temperature, comparing these among species from different thermal realms (Scholander et al., 1953; Wohlschlag, 1960). For example, Scholander et al. (1953) compared metabolic rates between Arctic and tropical ectotherms. When normalised to 0 °C, the Arctic ectotherms had metabolic rates which were 30 - 40 times greater than the tropical ectotherms (Scholander et al., 1953). However, these early comparative studies were criticised on two main counts. Firstly, normalising metabolic rates to a common (usually extreme) temperature is, by definition, extrapolating the metabolic rate outside of the species normal temperature range. Outside of a species normal temperature range, established relationships between metabolic rate and temperature are unlikely to be appropriate (Knies and Kingsolver, 2010). Secondly, alongside being more prone to handling stress, polar ectotherms require relatively longer acclimation and starvation times before respirometry, therefore using the same experimental procedures for both polar and tropical ectotherms is likely to have elevate metabolic rates in polar ectotherms (Holeton, 1974; Steffensen, 2002).

To overcome issues associated with handling stress, researchers approximated species metabolic rates without the need for live organisms through the use of electron-transport system activity (ETS, Torres and Somero, 1988; Crockett and Sidell, 1990) or tissue respiration rates (Gordon, 1972). ETS has a further advantage over respirometry in that assays can be carried out at a set temperature, which removes the need for statistical normalisation to a common temperature (Crockett and Sidell, 1990).

Studies using ETS to test for metabolic cold adaptation found higher FMRs in polar organisms when compared to temperate ectotherms (Torres and Somero, 1988; Crockett and Sidell, 1990). For example, when comparing assays carried out at 1 °C, white muscle citrate synthase activity (a measure of aerobic metabolism) was 1.5 to 5x higher in polar fish compared to temperate fish (Crockett and Sidell, 1990). More recently, studies have taken a macroecological focus, rather than comparing one or two species. A macroecological study found evidence supporting the metabolic cold adaptation hypothesis in the form of elevated temperature-normalised SMR and citrate synthase activity at high absolute latitudes (i.e. polar regions, White et al., 2012a). This macroecological study also accounted for species relatedness (White et al., 2012a), which is particularly important when considering metabolic cold adaptation as most Antarctic fish are from a single family, the Nototheniidae (Clarke and Johnston, 1999).

The study of White et al. (2012a) made clear improvements in investigating metabolic cold adaptation in fishes, however, it has two key limitations. Firstly, ETS measures metabolic rate at the level of the enzyme, which, as discussed previously, may not scale up to whole organism metabolic rate. Considering whole organism metabolic rate is particularly in the case of FMR, where animals may be able to use behavioural adaptations to mitigate temperature effects on enzyme-catalysed reaction rates (Norin and Clark, 2017; Richards, 2010; Jutfelt et al., 2021). Secondly, White et al. (2012a) did not include data points for citrate synthase activity from tropical regions (< 30 degrees latitude). While a high *standard* or *routine* metabolic rate is typically seen as representing a cost to the organism (Holeton, 1974; Clarke and Johnston, 1999), a high *field* metabolic rate may indicate greater capacity for movement, digestion, reproduction and growth (Chapter 1, section 1.1, Crockett and Sidell, 1990; Treberg et al., 2016). Thus while great improvements have been made in studying metabolic cold adaptation, the hypothesis remains controversial (Steffensen, 2002), and further study is warranted.

5.2.2 Thermal sensitivity trade-off hypothesis

Across the natural world, organisms face a trade-off between being specialists - adapted to a narrow range of relatively extreme conditions - and generalists - adapted to a wider range of relatively intermediate conditions. In terms of thermal adaptation, organisms are typically classified as eurytherms - adapted to a wide range of temperatures - or stenotherms - adapted to a relatively small temperature range. According to the trade-off hypothesis, the metabolic rates of eurythermal species will be less sensitive to temperature, as eurythermal species have metabolic enzymes which are able to operate across a wide temperature range (Clarke and Fraser, 2004). In contrast, stenothermal species will have metabolic rates which are more sensitive to temperature, as they are specialised towards narrower, more extreme temperature ranges (Scholander et al., 1953; Wohlschlag, 1960; Clarke and Fraser, 2004; Pörtner et al., 2005; Schulte, 2015).

Comparative studies have shown support for the thermal sensitivity trade-off hypothesis. For example, stenothermal Antarctic eelpout (*Pachycara brachycephalum*) have greater thermal sensitivities of SMR compared to eurythermal European eelpout (*Zoarces viviparous*) as quantified by Q_{10} values (5.2 vs. 3.0, respectively, Van Dijk et al., 1999). More recently, a macroecological study found a negative relationship between the thermal sensitivity of standard metabolic rates (as determined by Arrhenius E, Equation 5.1) and species temperature range in fishes (Dahlke et al., 2020), supporting the trade-off hypothesis.

While several studies have used laboratory-based measurements (usually SMR) to compare the thermal sensitivities of metabolic rates among eurythermal and

stenothermal species, there has been little consideration for how thermal sensitivity of metabolic rates might vary between eurytherms and stenotherms in the field. Across species of marine teleosts, field metabolic rates (FMR) are less sensitive to temperature than would be predicted by Arrhenius reaction kinetics (Chapter 4), as wild-living fish can mitigate the thermodynamic increases in their SMR by adopting behaviours which reduce other components of their FMR (Richards, 2010; Treberg et al., 2016; Norin and Clark, 2017; Jutfelt et al., 2021).

A growing number of ecosystem models are used to predict the potential impacts of climate change on the marine environment (Cheung et al., 2008, 2013; Blanchard et al., 2012; Harfoot et al., 2014; Jennings and Collingridge, 2015; Carozza et al., 2016; Tittensor et al., 2018; Audzijonyte et al., 2019), with particular interest paid teleost fish, given their global importance to food and economic security (FAO, 2020). Most of the ecosystem models which predict the impacts of temperature change on marine ecosystems do so either by using Arrhenius E or Q_{10} values, with these parameters typically set at a single value (E = 0.60 - 0.69, Blanchard et al., 2012; Harfoot et al., 2014; Jennings and Collingridge, 2015; Audzijonyte et al., 2019; Q_{10} = 2.4, Cheung et al., 2013). If the thermal sensitivity of FMR is greater for stenotherms than eurytherms, this could indicate that stenotherms are less able to mitigate the thermodynamic effects of increased temperature on their SMRs, and consequently are more at risk from climate change.

5.2.3 Aims

In this study I investigated both metabolic cold adaptation and the thermal sensitivity trade-off hypothesis by examining otolith-derived field metabolic rates (C_{resp} values) across fish species from a range of thermal realms. C_{resp} values of wild fishes are not subject to handling stress (Trueman et al., 2016; Chung et al., 2019a,b; Martino et al., 2020). By analysing my data using phylogenetically-informed models (Hadfield, 2010; Harvey and Pagel, 1991), I accounted for effects of species-relatedness on C_{resp} values.

To investigate metabolic cold adaptation I examined whether polar species had elevated metabolic rates compared to non-polar species, after accounting for body mass and temperature, by using mixed-effects models. Similarly, to investigate the thermal sensitivity trade-off hypothesis, I tested whether thermal realm had an effect on the relationship between C_{resp} values and temperature, after accounting for body mass. Finally, to further test the thermal sensitivity trade-off hypothesis, I tested whether species thermal tolerance range had an effect on the relationship between C_{resp} values and temperature, after accounting for body mass.

5.3 Methods

5.3.1 Thermal adaptation variables

To investigate both metabolic cold adaptation and thermal sensitivity trade-offs, I categorised species according to their thermal realm. Full details on the thermal realm classification procedure can be found in Chapter 2, section 2.7.4, but briefly: I classified species' thermal realm as either tropical, subtropical, temperate or polar, based on the mean latitude of individual occurrence records for each species from the Ocean Biodiversity Information System (OBIS, IOC-UNESCO, 2021).

Along with thermal realm classifications, I used individual occurrence records from OBIS to set species temperature range ($temp_{range}$). As these analyses consider sea surface temperatures, I excluded deep-sea species from the dataset (species with a minimum depth of occurrence $>$ 200 m).

5.3.2 Metabolic cold adaptation

To test whether polar species had elevated C_{resp} values given body mass and temperature, I ran two models incorporating log body mass ($log_{10}(bm)$) and $\delta^{18}O_{oto}$ derived experienced temperature ($temp_{exp}$) as continuous variables, and species' thermal realm ($realm$) as a categorical variable:

$$C_{resp} \sim log_{10}(bm) + temp_{exp} + realm \tag{5.2}$$

I did not include interaction effects in this model, because metabolic cold adaptation considers whether polar species have elevated metabolic rates given a constant temperature effect across thermal realms (Scholander et al., 1953). If the polar group has a higher model mean C_{resp} value compared to non-polar thermal realms, this would indicate support for the metabolic cold adaptation hypothesis.

To further test whether polar species have elevated metabolic rates, given body mass and temperature, I compared mean C_{resp} values among the different thermal realms, after normalising the C_{resp} values to a common body mass and temperature of 200 g and 10 °C, which are approximately the mean values for these variables within my dataset. As metabolic cold adaptation assumes a constant temperature effect across thermal realms (Scholander et al., 1953), I used the scaling relationship between C_{resp} values, log body mass and experienced temperature from Chapter 4 to normalise C_{resp} values.

5.3.3 Thermal sensitivity trade-offs

To test the thermal sensitivity hypothesis, I ran a model investigating the effects of experienced temperature ($temp_{exp}$) and temperature range ($temp_{range}$) on C_{resp} values. I also included the effects of log body mass ($log_{10}(bm)$) on C_{resp} values, as body mass is a primary driver of metabolic rates (Rubner, 1883; Kleiber, 1947; Brown et al., 2004). The model also included interaction terms between effects:

$$C_{resp} \sim log_{10}(bm) + temp_{exp} + temp_{range} + log_{10}(bm) \times temp_{range} + temp_{exp} \times temp_{range} \tag{5.3}$$

To test whether stenothermal groups had greater thermal sensitivities of their FMR, I was principally interested in the interaction between the effects of experienced temperature and temperature range on C_{resp} values. Assuming that experienced temperature had a positive relationship with C_{resp} values, a negative interaction effect would support the thermal sensitivity trade-off hypothesis. A negative interaction effect would indicate that the effect of experienced temperature on C_{resp} values, and therefore FMR was less for eurythermal groups than for stenothermal groups, thereby supporting the thermal sensitivity trade-off hypothesis.

To further test the thermal sensitivity trade-off hypothesis, I ran a model investigating the effects of thermal realm ($realm$) classification on C_{resp} values, along with $log_{10}(bm)$ and $temp_{exp}$:

$$C_{resp} \sim log_{10}(bm) + temp_{exp} + realm + log_{10}(bm) \times realm + temp_{exp} \times realm \tag{5.4}$$

This model is similar to the one used to test for metabolic cold adaptation (equation 5.2), however, equation 5.4 includes interaction effects to test for variation in the relationship between C_{resp} values and experienced temperature among different thermal realms. If C_{resp} values were more sensitive to temperature in stenothermal groups (polar and tropical) than eurythermal groups (temperate and subtropical), this would support the thermal sensitivity trade-off hypothesis.

5.3.4 Stability of body mass scaling

A secondary effect of using interaction models (equations 5.3 and 5.4) is that I was able to test the stability of C_{resp} value scaling with body mass across different groups. If no significant interactions between body mass and any of the thermal adaptation variables are found, this would indicate that C_{resp} values scale with body mass consistently across groups of teleosts adapted to different temperaturers.

5.3.5 Statistical analyses

All models were general linear mixed-models, therefore I z-scored (standardised) all continuous predictors, so they were inputted as standard deviations from the mean. This means the constant a represents the C_{resp} value at mean values of the predictors, and b represents the change in C_{resp} values per standard deviation of the predictor.

I ran all models in R version 4.1.2 (R Core Team, 2021a), using the `MCMCglmm` package (Hadfield, 2010) to run Bayesian phylogenetic mixed models. All models included random effects of species-relatedness, intraspecific effects and the random effect of data source (Chapter 2). Following Hadfield (2010), I used regularising inverse-Wishart priors for all random factors, with variance (V) set to 1 and the belief parameter (ν) set to 0.02. I incorporated uncertainties (as standard errors of mean estimates) of both C_{resp} values and experienced temperatures by setting these as random factors with constant variances and fixed priors. I removed five mesothermic species from the dataset prior to analyses, as mesotherms have elevated metabolic rates compared to ectotherms, and the otolith-derived temperature from mesothermic species represents their internal, rather than experienced temperature (Radtke et al., 1987).

I ran all models for 5,000,000 iterations, with a burn-in of 15,000 and a thinning parameter of 500. I checked all models for convergence and mixing via visual inspection of traceplots, Geweke's diagnostic and the Heidelberger-Welch diagnostic (Plummer et al., 2006). All parameters for all models had an effective sample size $>$ 2000.

In addition to the standard sensitivity models, I ran an interaction model on thermal realm (equation 5.4) without polar species, to explore the effect this group had on overall model outcomes.

5.4 Results

5.4.1 Metabolic cold adaptation

Compared to the temperate group, the polar group had an elevated mean C_{resp} value, both before (raw mean = 0.19) and after (model mean = 0.21) accounting for log body mass and temperature (Figure 5.1). The temperate group had the lowest mean C_{resp} value of all the thermal realm groups (raw mean = 0.16, model mean = 0.20). The tropical group had raw and model mean C_{resp} values of 0.28 and 0.26 respectively. The subtropical group had the highest mean C_{resp} values, both before and after accounting for log body mass and temperature (raw mean = 0.32, model mean = 0.29).

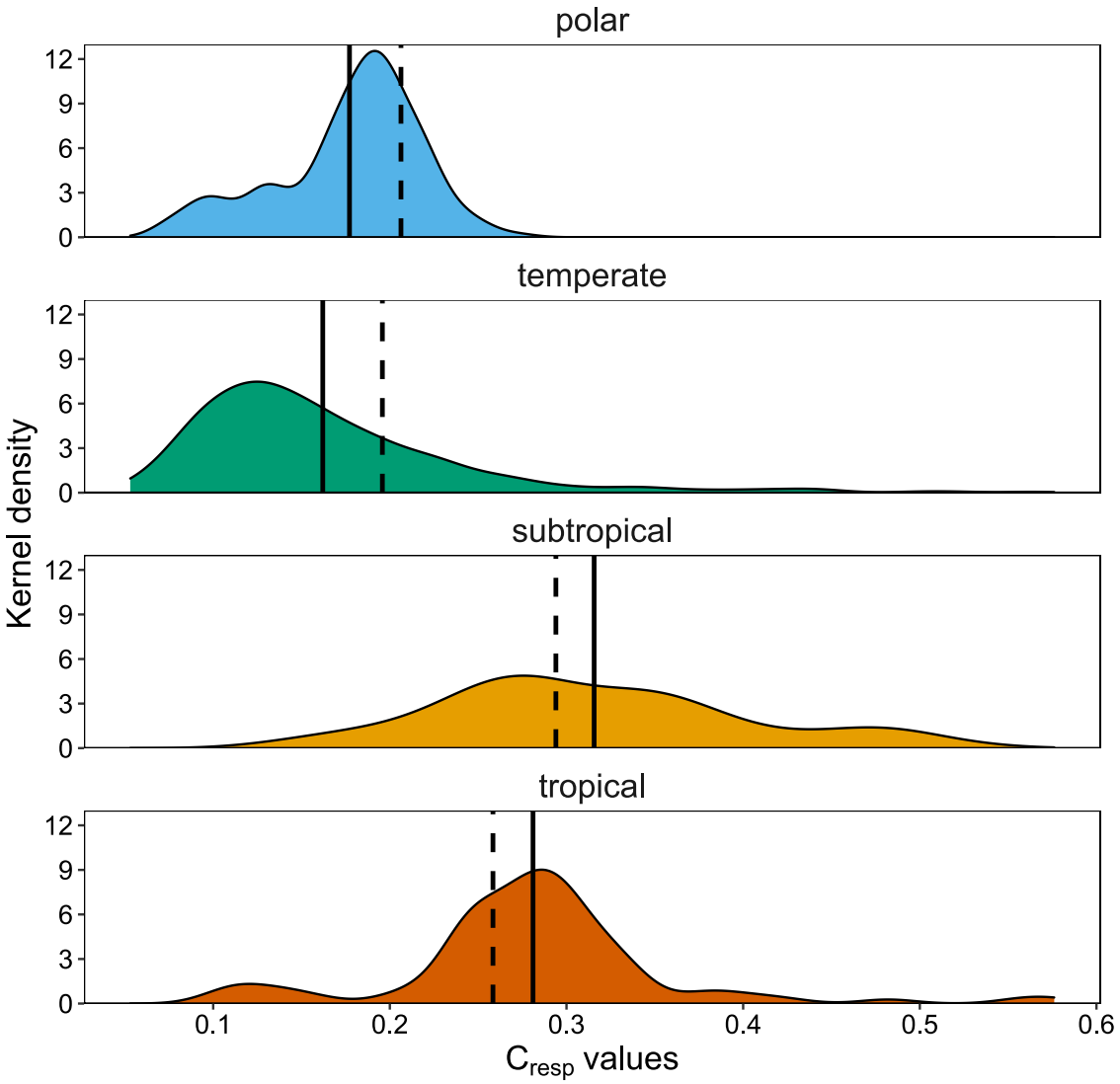

FIGURE 5.1: Kernel density of individual C_{resp} values grouped by thermal realm (blue = polar, green = temperate, yellow = subtropical, orange = tropical). Solid lines show the mean C_{resp} value for each thermal realm. Dotted lines show the expected mean C_{resp} values according to the model described by equation 5.2.

When normalised to common body mass and temperature of 200 g and 10 °C (Figure 5.2), polar species again had a mean C_{resp} value higher than that of the temperate group (polar = 0.22, temperate = 0.20), but lower than the tropical and subtropical groups (tropical = 0.31, subtropical = 0.36).

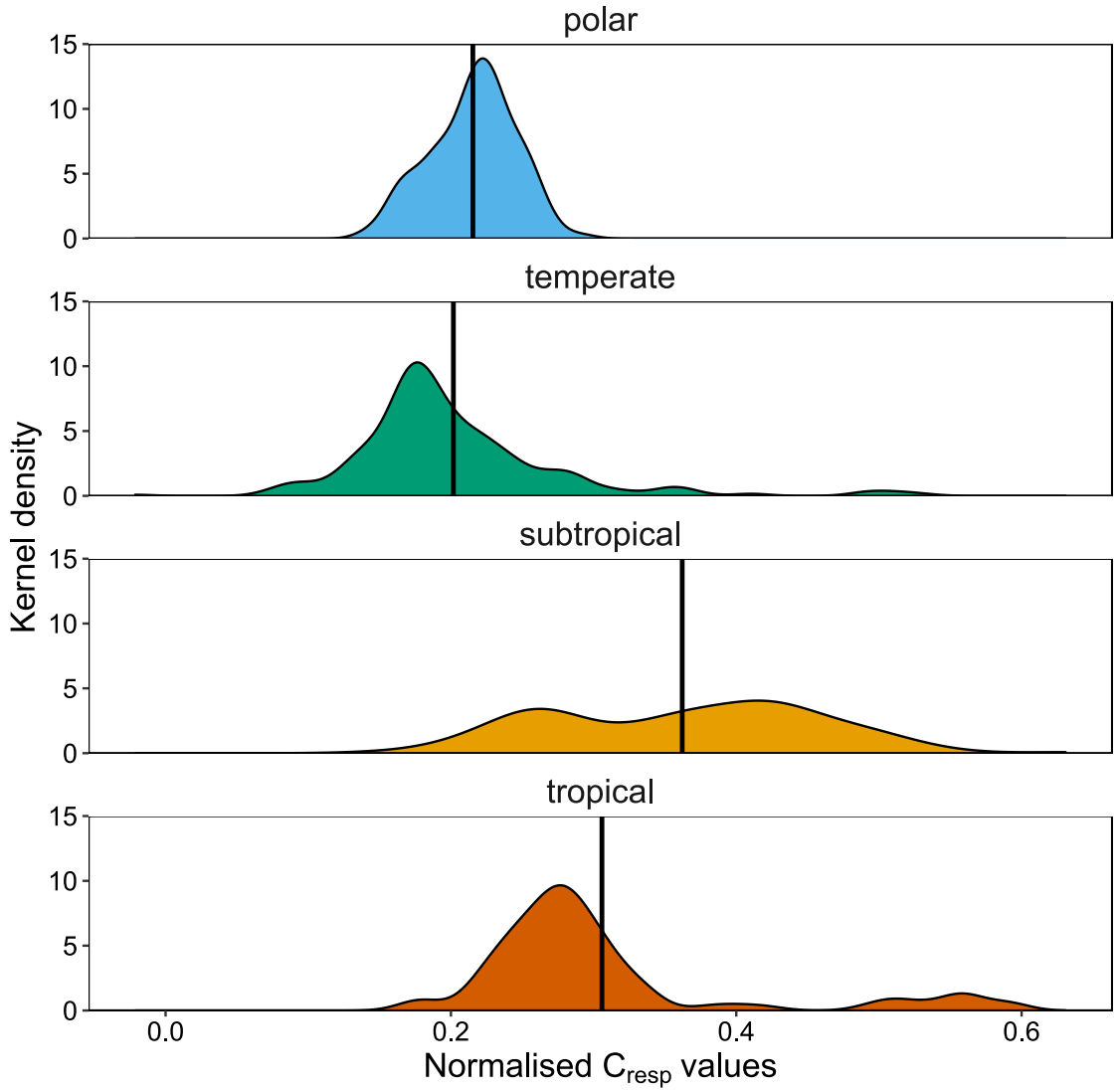

FIGURE 5.2: Kernel density of individual C_{resp}, normalised to a common body mass and temperature of 200 g and 10 °C, grouped by thermal realm (blue = polar, green = temperate, yellow = subtropical, orange = tropical). Solid lines show the mean normalised C_{resp} value for each thermal realm.

5.4.2 Thermal sensitivity trade-off

After accounting for body mass and experienced temperature, species' temperature range had a negative relationship with C_{resp} values (b_{temp_range} = -0.08 $\pm$ 0.01) meaning eurythermal species tended towards lower C_{resp} values (Figure 5.3A). Overall, C_{resp} values increased with experienced temperature (b_{temp_exp} = 0.02 $\pm$ 0.01, Figure 5.3A), however, this increase was reduced for species with a large temperature range ($b_{temp\_exp \times temp\_range}$ = -0.01 $\pm$ 0.01, Figure 5.3B).

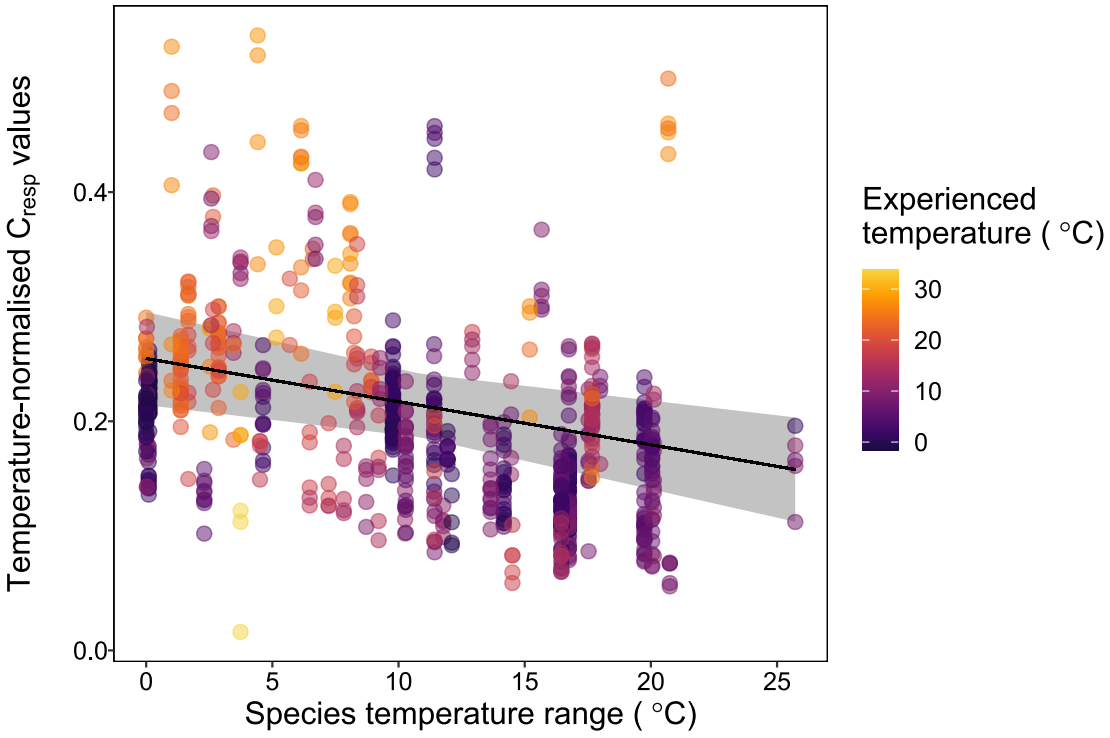

FIGURE 5.3: C_{resp} values plotted against species temperature range (°C), coloured by individual experienced temperature (°C). C_{resp} values are normalised to a common temperature of 10 °C, using the partial correlation coefficient from equation 5.3. The black line shows the significant negative relationship between species temperature range and temperature-normalised C_{resp} values (equation 5.3), with 50% confidence intervals shaded in grey.

After accounting for body mass, there were significant differences in the relationship between C_{resp} values and experienced temperature among the different thermal realms (Figure 5.4), indicating that temperature scaling differed among the thermal realm groups. The tropical group had the greatest positive scaling between C_{resp} and experienced temperature ($temp_{tropical}$ = 0.10 $\pm$ 0.03, Figure 5.4D). The polar group also showed strong scaling of C_{resp} values with temperature, however, the scaling was negative ($temp_{polar}$ = -0.08 $\pm$ 0.02), with C_{resp} values in the polar group decreasing with increasing temperature (Figure 5.4A). However, the negative temperature scaling of the polar group was only present when including literature data. When literature

data was omitted, the temperature scaling of the polar group became positive (Appendix H.3).

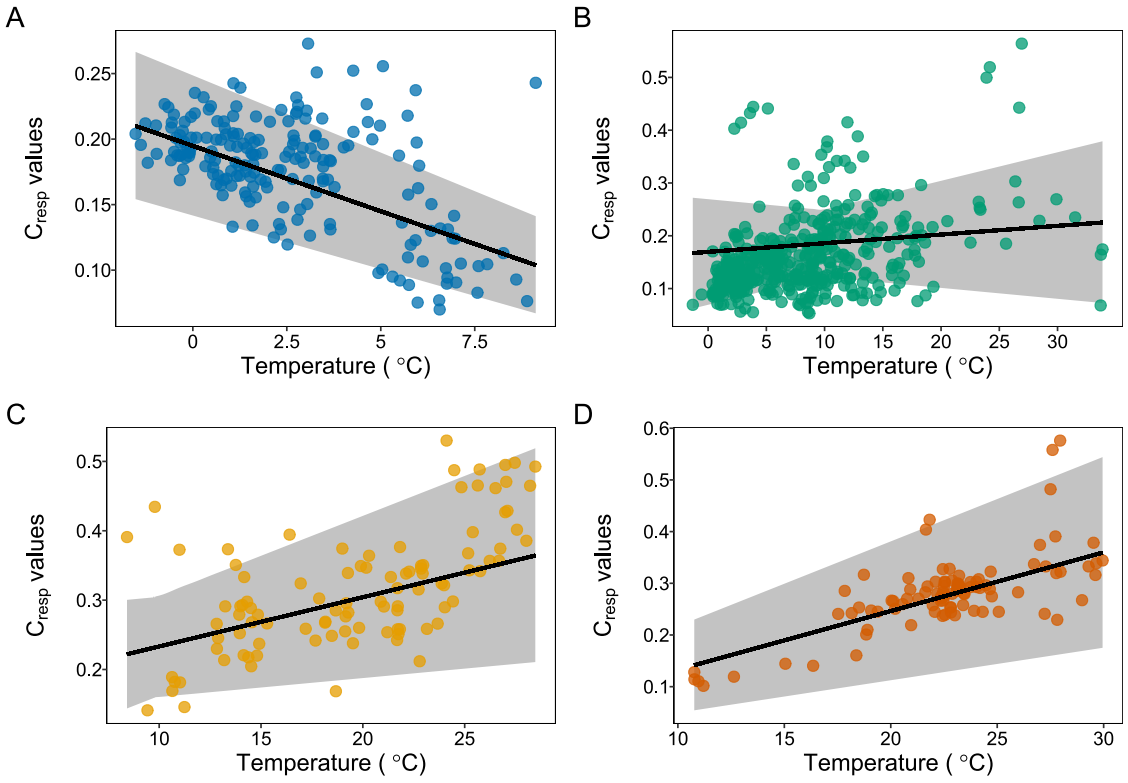

FIGURE 5.4: Temperature (°C) plotted against C_{resp} values for the four thermal realm groupings: A = polar, B = temperate, C = subtropical, D = tropical. Black lines show the C_{resp} scaling with temperature according to equation 5.2, with 50% confidence intervals shaded in grey.

The temperate group had very shallow scaling of C_{resp} values with temperature ($temp_{temperate}$ = 0.01 $\pm$ < 0.01, Figure 5.4B), indicating that this group has a relatively low sensitivity of FMR to experienced temperature. Finally, the subtropical group showed a positive relationship between C_{resp} values and temperature, although the scaling was not as steep as the tropical and polar groups ($temp_{subtropical}$ = 0.06 $\pm$ 0.02).

5.4.3 Stability of body mass scaling

Across all models there were no significant interaction effects with any variable and log body mass, indicating that body mass scaling is stable across different thermal realms and temperature ranges.

5.5 Discussion

5.5.1 Metabolic cold adaptation

In this study, the polar group of fishes showed an elevated mean metabolic rate compared to the temperate group across raw means, model means and temperature normalised means. Elevated metabolic rates in polar fishes compared to temperate fishes supports the findings of previous smaller-scale studies (Torres and Somero, 1988; Crockett and Sidell, 1990). The elevation of metabolic rate in polar fishes compared to temperate fishes indicates that polar fishes are able to maintain a higher FMR, despite the negative effects of low temperatures on enzyme thermodynamics (Scholander et al., 1953; Wohlschlag, 1960; Clarke and Johnston, 1999; White et al., 2012a). Therefore, this study suggests that polar fishes have some level of metabolic cold adaptation which occurs at the level of the organism. An elevated FMR is likely beneficial for these polar fishes, as FMR includes fitness components of metabolic rates, such as growth and reproductive costs (Crockett and Sidell, 1990; Treberg et al., 2016).

In contrast to previous macroecological investigations of metabolic cold adaptation (Addo-Bediako et al., 2002; White et al., 2012a), this study found that polar ectotherms did not have elevated metabolic rates compared to tropical and subtropical ectotherms. However, some metabolic cold adaptation is likely a component in the variation of mass- and temperature-independent metabolic rates.

5.5.2 Thermal sensitivity trade-off hypothesis

A key finding of this study is that stenothermic groups have greater thermal sensitivity of their FMRs compared to the eurythermic group. Furthermore, the tropical group, which is typically characterised as stenothermic, showed the strongest relationships between C_{resp} values and temperature. In contrast, within the eurythermic temperate group there was very little correlation between experienced temperature and C_{resp} values. The finding of variable thermal sensitivity of C_{resp} values along the stenotherm-eurytherm spectrum reflects that of previous studies, which found a difference in temperature sensitivity of metabolic rates across a latitudinal gradient (DeLong et al., 2018; Dahlke et al., 2020).

5.5.3 Implications for modelling marine ecosystems under climate change

While some marine ecosystem models recognise variation in the relationship between body mass and metabolic rate across taxa (Blanchard et al., 2012; Harfoot et al., 2014),

none so far systematically incorporate variation in the relationship between temperature and metabolic rates.

In the marine realm, tropical fishes are thought to be the most at risk from climate change, as they are typically stenothermal and experience temperatures closer to their thermal maxima than their non-tropical counterparts (Comte and Olden, 2017; Pinsky et al., 2019; Lam et al., 2020). My study has shown that FMR increases with experienced temperature at a faster rate for tropical fishes compared to non-tropical fishes, which suggests that tropical fishes are less able to mitigate thermodynamic effects on their SMR. Tropical fish may be less able to compensate for the effect of temperature on their SMR because they are less able to undertake behaviours which reduce metabolic expenditure, or (or additionally) because their adaptation to more extreme warm temperatures has increased their thermodynamic sensitivity of SMR to the point where behavioural mitigations cannot compensate (Richards, 2010; DeLong et al., 2018; Jutfelt et al., 2021). In contrast, the shallow relationship between C_{resp} values and experienced temperature in the temperate group suggests that this group either has adapted to have an SMR less sensitive to temperature changes (i.e. one that can operate over a broad range of temperatures), or that temperate species are better able to mitigate the effects of thermodynamics on their SMR (Richards, 2010; DeLong et al., 2018; Jutfelt et al., 2021). The use of a single value to quantify the relationship between metabolic rates and temperature across a broad range of fish species ignores asymmetric differences in thermal sensitivity among groups of fishes, potentially missing the groups that are most at risk from climate warming.

In addition to overlooking differences in thermal sensitivity of metabolic rates among different thermal realms, the use of a single relationship to quantify the effects of temperature on metabolic rate would not capture the elevated metabolic rates in polar ectotherms (Scholander et al., 1953; Wohlschlag, 1960; White et al., 2012a; DeLong et al., 2018). My study has found evidence that polar fishes have elevated metabolic rates compared to temperate fishes, after accounting for body mass and experienced temperature. If this partial metabolic cold adaptation is not accounted for in marine ecosystem models, this could lead to an underestimation of the relatively high FMRs of polar species.

While a higher FMR is typically considered advantageous - as FMR includes fitness costs such as growth and reproduction (Treberg et al., 2016) - having a high FMR may become detrimental if food and oxygen supplies are unable to meet high metabolic demands. Lack of oxygen may be a particular issue for tropical and subtropical species, as tropical waters typically contain less dissolved oxygen than temperate or polar waters (Garcia et al., 2019). Similarly, alongside relatively low dissolved oxygen, subtropical waters are often oligotrophic, having limited net primary productivity (Woodward, 2007). Combined with resource limitation, the high temperature

sensitivity of FMR in the subtropical group may also put these species at particular risk of climate change.

The idea of aerobic scope - the difference between aerobic supply (MMR) and demand (SMR) - being limiting is the basis for many macroecological models of metabolic rate in fish (Pörtner et al., 2017; Deutsch et al., 2020) For example, metabolic index, which quantifies the difference between oxygen demand and the dissolved oxygen concentration in seawater, has shown that species living in tropical regions typically have a lower metabolic index, and therefore less difference between oxygen demand and availability, compared to polar regions (Deutsch et al., 2015). However, the aforementioned ability for free-living fish to compensate for thermodynamic effects on their SMR (Richards, 2010; Norin and Clark, 2017; Jutfelt et al., 2021) means that FMR is less sensitive to temperature changes than laboratory-based measurements of SMR (Chapter 4).

While the lower thermal sensitivity of FMR may indicate that metabolic effects of climate warming on free-living fish have been overinflated, behaviours which mitigate SMR increase due to temperature come with trade-offs. For example, fish which reduce movement to compensate for increased temperature may have less success in foraging and reproduction (Richards, 2010). Less obviously, fish exposed to high temperatures may eat few large meals, instead opting for smaller, more frequent meals to reduce the costs of specific dynamic action (Norin and Clark, 2017; Jutfelt et al., 2021). While this may protect aerobic capacity, eating smaller meals comes at the cost of reduced growth capacity, particularly if those smaller meals are of lower nutritional quality (Norin and Clark, 2017). Furthermore, this study considered estimates of C_{resp} values at adult and juvenile life stages. However, embryonic, larval and spawning fishes may be more vulnerable to temperature fluctuations than adults and juveniles, due to having a limited aerobic scope (Killen et al., 2007; Dahlke et al., 2020, though the latter has recently been criticised by Pottier et al., 2022). Examining the temperature scaling of SMR and FMR together, and across life stages, would give a clearer picture of the benefits, costs, and capacities to protecting aerobic capacity, and a better understanding of how fish might cope with, or adapt to, climate warming.

5.5.4 Temperature sensitivity of field metabolic rates in polar fishes

The negative relationship between C_{resp} values and experienced temperature in polar species is surprising, as metabolic rates increase with temperature across a physiologically relevant temperature range (Holeton, 1974; Gillooly et al., 2001; Brown et al., 2004; Knies and Kingsolver, 2010), and it is unlikely that wild, free-ranging fishes would stay long-term outside their optimal range (Martin and Huey, 2008; Farrell, 2016). Therefore, the reason for the negative relationship with temperature in the polar group is unclear, and may be an artefact of the inclusion of literature data (see section 5.4 and Appendix H.3). Specifically, *Dissostichus eleginoides* (Patagonian toothfish) was the only polar species in the dataset for whom C_{resp} values were derived from literature data. *D. eleginoides* could arguably be classified as either polar or temperate, as while it tends to inhabit waters with cold sea surface temperatures (mean = 0.7 °C $\pm$ 2.92), the species is also found in warmer waters (max = 18.0 °C, Appendix A, IOC-UNESCO, 2021). Given that *D. eleginoides* had relatively low C_{resp} values (mean = 0.14 $\pm$ 0.01) compared to other polar species, while also experiencing relatively high temperatures (mean experienced temperatures = 5.4 °C), this is what contributed to the negative relationship between temperature and C_{resp} values in the polar group.

In the other direction, *Cyclopterus lumpus* (lumpfish), which I classified as temperate in this study, could arguably be classified as temperate or polar. While *C. lumpus* is typically found in areas with warm sea surface temperatures (mean = 7.4 °C $\pm$ 2.6), it is also regularly found around more polar regions of Iceland and the Barents Sea (IOC-UNESCO, 2021). The examples of *D. eleginoides* and *C. lumpus* highlight that, while thermal realms themselves may not be entirely arbitrary, the boundaries between them are not clear cut.

5.5.5 Conclusion

This study, which examined C_{resp} values across a global dataset of marine teleost fishes, found evidence for both metabolic cold adaptation and the thermal sensitivity trade-off hypothesis. Within marine fishes, there is evidence that polar species are partially cold-adapted, having an elevated FMR compared to temperate species, after body mass and temperature are accounted for. However, unlike previous studies, there was no evidence for polar species having FMRs elevated above subtropical or tropical species. Furthermore, the relationship between C_{resp} values and temperature was dependent upon thermal tolerance range, with the tropical group having a stronger positive relationship between temperature and C_{resp} values than the temperate group.

Overall, this study found systematic differences in the relationship between C_{resp} values and temperature across thermal realms and tolerance ranges. Systematic heterogeneity in the relationship between metabolic rate and temperature is not currently incorporated into the majority of marine ecosystem models. Assuming consistent relationships between metabolic rate and temperature across broad scales is likely obscuring different metabolic costs and temperature sensitivities across thermal realms, and the abilities and costs of individuals using behavioural changes to mitigate temperature fluctuations.

More work is needed to quantify systematic differences in the scaling of metabolic rate with temperature, and to investigate the costs of behaviours which mitigate the impacts of temperature on metabolic rates. However, assigning categorical traits to species should be undertaken with caution, and a more specific approach would be ideal where a species of interest sits on the boundary of trait categories.

Chapter 6

Effect of depth of occurrence on C_{resp} values

6.1 Abstract

Mass- and temperature-corrected metabolic rates of marine animals commonly decrease with increasing depth of occurrence. However, due to their inaccessibility, it is notoriously difficult to measure metabolic rates in deep-sea species, which has thus far precluded the study of metabolic rates in deep-sea species at a large scale. The geographical bias of studies investigating metabolic rate with depth means that the global applicability of depth-dependent declines in metabolic rate is uncertain. Furthermore, few previous studies have considered the impacts of species relatedness on the metabolic-depth effect, and the drivers of the depth-limited metabolism are still debated. Fresh insights into the universality of the metabolic-depth effect and potential drivers could be drawn by compiling estimates of metabolic rate across a wide range of taxa, derived using a common measure.

Here, I used C_{resp} values, a proxy of fish field metabolic rates (FMR), to study whether species' depth of occurrence correlates with metabolic rate, while accounting for the effects of body mass, temperature, habitat and species' relatedness. Using a dataset with global coverage across a broad ($\sim$ 4800 m) depth range, I found that C_{resp} values decrease with increasing depth of occurrence. In contrast to previous studies, C_{resp} values continued to decrease with depth past 1000 m. The continued decline of metabolic rates past 1000 m suggests that reduced light levels (i.e. the visual interaction hypothesis) is not the sole driver of reduced metabolic rates with depth, and instead acts in conjunction with food limitation to limit metabolic rates at depth.

The limitation of metabolic rates at depth has implications for the proposal that deeper waters may act as refugia for marine species in the face of sea surface

warming. While deeper waters may provide refuge for shallower species belonging to lineages which have already colonised the deep-sea, such as the Gadiformes, food and light limitation are likely to prevent groups with higher metabolic rates, such as the Scombriformes, from using deeper waters as a climate refuge.

6.2 Introduction

Multiple studies have shown metabolic rates of marine animals decreasing with depth at oceanic scales, and that this decrease cannot be explained by body mass and temperature effects alone (Torres et al., 1979; Drazen and Seibel, 2007; Seibel and Drazen, 2007; Drazen et al., 2015; Ikeda, 2016). Depth-dependent declines in metabolic rates (hereafter referred to as "the metabolic-depth effect") have been found across marine taxa, including teleosts, cephalopods, crustaceans and holothurians (Drazen and Seibel, 2007; Seibel and Drazen, 2007; Drazen et al., 2015; Ikeda, 2016; Gerringer et al., 2017; Brown et al., 2018). Previous studies of the metabolic-depth effect have found that the decrease in metabolic rate is most prominent in the epipelagic depth (0 - 200 m), with the rate of decline plateauing at bathypelagic depths (800 - 1000 m) in most taxa (Childress, 1995; Drazen and Seibel, 2007; Seibel and Drazen, 2007). Due to the relative inaccessibility of the deep-sea, most previous studies of the metabolic-depth effect used electron transport system activity assays (ETS) as a proxy for metabolic rate (Chapter 1 section 1.4.2, Drazen and Seibel, 2007; Drazen et al., 2015), though some smaller-scale studies have used in-situ (Bailey et al., 2002; Brown et al., 2018) or capture respirometry (Torres et al., 1979).

Within teleost fishes, the metabolic-depth effect occurs in conjunction with changes in body composition (Drazen, 2007) and body shape (Neat and Campbell, 2013; Martinez et al., 2021). Deep-sea fishes tend to have tissues with higher water and lower protein contents than their shallow water counterparts, reflected in relatively high proportions of watery muscle and gelatinous tissue (Koslow, 1996; Drazen, 2007). Furthermore, deep-sea fishes tend towards elongate body shapes, which enable highly efficient yet relatively slow swimming (Neat and Campbell, 2013; Martinez et al., 2021). Alongside the reduction in locomotory costs, basal costs (standard metabolic rate, SMR) may also be reduced due to the lack of metabolically expensive tissues required for high locomotory power (Glazier, 2005, 2010).

6.2.1 Proposed drivers of the metabolic-depth effect

Broadly, there are four proposed primary universal drivers of the metabolic-depth effect. These are:

1. Oxygen limitations in midwater oxygen minimum zones.
2. Food limitation with increasing depth.
3. Visual interaction hypothesis.
4. Reduced habitat complexity with increasing depth.

Below, I describe each hypothesis in more detail, and outline how the C_{resp} method could support or refute each hypothesis. Each hypothesis is summarised in Table 6.1.

6.2.1.1 Oxygen limitation

Many studies of metabolic rate with depth thus far have come from organisms sampled in Monterey Bay in the North Pacific (Torres et al., 1979; Childress, 1995; Drazen and Seibel, 2007; Seibel and Drazen, 2007; Drazen et al., 2015). At Monterey Bay there is a prominent oxygen minimum zone (OMZ) in the mesopelagic zone (200 - 1000 m), where dissolved oxygen concentrations are < 0.5 ml l^{-1} (Levin, 2003). It has been proposed that the OMZ at Monterey Bay may have resulted in reductions in metabolic rates for the organisms living there as they adapt to hypoxic conditions, thus driving the observed decline in metabolic rate with depth. However, metabolic rates of organisms from below 1000 m in Monterey Bay, outside the OMZ, have also shown reduced metabolic rates compared to shallow waters, indicating that the OMZ is not the only driver of the metabolic-depth effect (Childress, 1995; Drazen and Seibel, 2007; Seibel and Drazen, 2007; Drazen et al., 2015). Despite the OMZ being a confounding factor, relatively few studies have investigated the metabolic-depth effect outside of the eastern Pacific.

6.2.1.2 Food limitation

Aside from relatively rare features such as hydrothermal vents, all primary production occurs at the ocean's surface, in the epipelagic zone (Smith et al., 2008). To reach the deep-sea, primary production must either be actively transported by migrating biota, or sink to the deep-ocean. Both sinking and transportation reduces the quantity of available food and its quality, due to inefficiencies in microbial and trophic processing (Lampitt and Antia, 1997; Smith et al., 2008). Resource limitation may necessitate deep-sea taxa having low metabolic rates, so as to maintain life in a food limited environment (Childress, 1971; Poulson, 2001).

Given that food quality and quantity continue to decrease past 1000 m (Poulson, 2001), whereas many studies have found that metabolic rate reductions taper off at 1000 m (Childress, 1995; Drazen and Seibel, 2007; Seibel and Drazen, 2007), food limitation is often refuted as a driver of the metabolic-depth effect. However, metabolic rates have been found to continue declining with depth past 1000 m in some taxa (Brown et al., 2018), and may in fact increase with depth at sites of relative food abundance, such as hadal trenches (Gerringer et al., 2017), therefore food-limitation remains a possible universal driver for the metabolic-depth effect.

6.2.1.3 Visual interaction hypothesis

The visual interaction hypothesis proposes that the reduction in light levels reduces the importance of vision-based predation with increasing depth, thereby reducing the distances over which predator-prey interactions occur (Childress, 1995; Drazen and Seibel, 2007; Seibel and Drazen, 2007; Drazen et al., 2015). The reduction in interaction distances is proposed to relax the selection for locomotory capacity, meaning deep-sea organisms attain relatively low field metabolic rates (FMRs). The reduction in locomotory capacity in turn leads to a reduction in basal costs (SMR), as organisms have no need to maintain expensive metabolic machinery (Seibel and Drazen, 2007). Instead, deep-sea organisms tend to have large amounts of metabolically inexpensive gelatinous tissue (Seibel and Drazen, 2007; Drazen and Seibel, 2007; Drazen, 2007) and an elongate body shape, which enables highly efficient but slow swimming (Neat and Campbell, 2013; Martinez et al., 2021).

As all visible light is attenuated at 1000 m, the visual interaction hypothesis has been proposed to explain why the decline in metabolic rate with depth levels off around this depth (Childress, 1995; Drazen and Seibel, 2007; Seibel and Drazen, 2007; Drazen et al., 2015). The visual interaction hypothesis may further explain why the metabolic-depth effect is most strongly seen among pelagic organisms with vision-forming eyes, as these are the most likely to experience longer-distance visual predator-prey interactions where light allows (Drazen and Seibel, 2007; Seibel and Drazen, 2007). In contrast, benthic, benthopelagic and non-visual organisms show less decline in metabolic rate with depth (Drazen and Seibel, 2007; Drazen et al., 2015), however, a reduction in metabolic rates has been found in non-visual organisms and below 1000 m depth (Brown et al., 2018), raising questions as to the universal applicability the visual interaction hypothesis. Furthermore, the visual interaction hypothesis assumes that metabolic rates represent a cost to the organism (Seibel and Drazen, 2007). While SMRs may represent a cost, FMRs is also represent fitness capabilities such as growth and reproduction (Treberg et al., 2016), therefore it is unclear why FMRs would not remain high and organisms would instead redirect savings in SMR and locomotory costs to growth and reproduction.

6.2.1.4 Reduced habitat complexity

The deep-sea is typically a less complex and less turbulent environment compared to the epipelagic zone (Brown et al., 2018; Martinez et al., 2021). It has been proposed that the relative simplicity of habitat in the deep-sea reduces the selection for locomotory capacity in a similar way to the visual interaction hypothesis (Brown et al., 2018; Martinez et al., 2021), enabling the adoption of metabolically efficient body shapes and tissues (Seibel and Drazen, 2007; Drazen and Seibel, 2007; Drazen, 2007; Neat and

Campbell, 2013; Martinez et al., 2021). However, not all deep-sea habitats are lacking in complexity. While abyssal plains are relatively simple, a variety of complex habitats exist within the deep-sea, such as continental slopes, seamounts, hydrothermal vents and oceanic trenches. Living in complex and/or turbid habitats may necessitate greater locomotory capabilities than are proposed by this hypothesis: for example seamount-associated orange roughy (*Hoplosteuthis atlanticus*), which contend with strong currents, have higher metabolic rates than their non-seamount associated counterparts (Koslow, 1996). As with the visual interaction hypothesis, the hypothesis of reducted habitat complexity considers metabolic rates to be a cost to an organism, rather than something which includes fitness capabilities (Treberg et al., 2016).

6.3 Aims

In this study, I used the C_{resp} method (Chapter 2 section 2.4, Chung et al., 2019a,b) to investigate whether a reduction in FMR with depth was present, after accounting for effects of body mass, and $\delta_{18}O_{oto}$-derived experienced temperatures (Chapter 2, section 2.5). I investigated the metabolic-depth effect using a large dataset ($\sim$ 100 species), and used phylogenetic mixed-models to account for phylogenetic non-independence (Harvey and Pagel, 1991) to test the large-scale validity of the metabolic-depth effect in marine teleost fish.

I examined the patterns in C_{resp} values with depth to investigate the four proposed drivers of the metabolic-depth effect. I addressed oxygen limitation as a proposed driver by using a dataset where C_{resp} values were derived from individuals collected primarily from the North Atlantic (Chapter 2, section 2.7.2), where there are no extensive regions of sub-oxic waters, (Childress, 1995; Levin, 2003; Seibel and Drazen, 2007). If a reduction in C_{resp} values is found within this dataset, this would rule out oxygen limitation as a primary, universal driver of the metabolic-depth effect.

Considering the visual interaction hypothesis, if the decline in C_{resp} values with depth levels off around 1000 m, this would provide support for the visual interaction hypothesis. Similarly, if the rate of decline in C_{resp} values with depth is greatest in the upper 200 m, this would also be consistent with the visual interaction hypothesis, as this is where light is attenuated most rapidly (Childress, 1995; Drazen and Seibel, 2007). Conversely, if the decline in C_{resp} values with depth continues past 1000 m, this would support food limitation as a proposed driver of the metabolic-depth effect, as food quality and quantity continue to decline past 1000 m (Poulson, 2001).

The hypothesis that reduced habitat complexity in the deep-sea is a driver of the metabolic-depth effect is difficult to test at a macroecological scale, due to a lack of fine-scale information concerning the complexity of the habitats occupied by individuals in the dataset. However, were habitat complexity to be a universal

primary driver of the metabolic-depth effect, I would expect to see a reduction in C_{resp} values at the transition to the abyssal zone ($\sim$ 3000 m), with relatively little reduction occurring along the continental shelf and slope depths (0 - 1000 m).

TABLE 6.1: Summary of proposed universal drivers of the decrease in metabolic rates with depth after accounting for body mass and temperature. OMZs = oxygen minimum zones.

Hypothesis		**Outline**	**Expectation with C_{resp} values**
Type	Hypothesis		
Resource limitation	**Oxygen limitation**	Deep-sea organisms have lower metabolic rates to cope with lower food availability at deeper depths	C_{resp} values decrease with depth throughout the water column as food availability and quality decrease
	Food limitation	Organisms living within OMZs have reduced metabolic rates as an adaptation to hypoxia	C_{resp} values decrease with depth despite a relative lack of OMZ in the North Atlantic
Relaxation of selection pressures	**Visual interaction hypothesis**	Low light levels in the deep-sea reduce visual predation, thereby reducing selection for locomotory capacities and selection for high metabolic rates	The rate of decrease in C_{resp}values is greatest from 0 - 200 m, and plateaus around 1000 m
	Reduced habitat complexity	Low habitat complexity and turbidity in the deep-sea reduces the selection pressure for locomotory capacity, thereby reducing metabolic rates	The rate of decrease in C_{resp}values is greatest at the transition to the abyssal zone (3000 m), while decreases in C_{resp}values are relatively minimal across continental shelves and slopes (0 - 1000 m)

6.4 Methods

6.4.1 Statistical analyses

To test whether depth of occurrence had an effect on C_{resp} values, I ran two models incorporating logged body mass ($log_{10}(bm)$) and temperature ($temp$) as continuous variables, and either minimum or maximum depth of occurrence ($depth_{min}$ and $depth_{max}$ respectively):

$$C_{resp} \sim log_{10}(bm) + temp + depth \tag{6.1}$$

As these are mixed-effects models, I z-scored (standardised) all continuous predictors, so they were inputted to the model as standard deviations from the mean. This means the constant a represents the expected C_{resp} value at mean values of the predictors, rather than the C_{resp} value when the predictors are set to zero. Similarly, the effect sizes (b) represent the change in C_{resp} values per standard deviation of the predictor. Given that changes in environmental and ecological variables with depth occur fastest in the epipelagic zone, and rate of change decreases with increasing depth (Childress, 1995; Drazen and Seibel, 2007; Seibel and Drazen, 2007), I modelled these effects using a negative exponential link function:

$$e^{-\mu} \tag{6.2}$$

This gives a final equation of:

$$y = e^{-(a+bx)} \tag{6.3}$$

where y is the C_{resp} value, x is the predictor ($log_{10}(bm)$, $temp$ or $depth$), a is the constant and b are the effect sizes.

I ran all models in R version 4.1.2 (R Core Team, 2021a), using the `MCMCglmm` package (Hadfield, 2010) to run Bayesian phylogenetic mixed models. All models included random effects of species-relatedness, intraspecific effects and the random effect of data source (Chapter 2). Following Hadfield (2010), I used regularising inverse-Wishart priors for all random effects, with variance (V) set to 1 and the belief parameter (ν) set to 0.02. I incorporated uncertainties as standard errors of mean estimates of both C_{resp} values and experienced temperatures by setting these as random effects with constant variances and fixed priors. As mesotherms have elevated metabolic rates compared to ectotherms, I removed five mesothermic species from the dataset prior to analyses.

Habitat is thought to be a key, potentially confounding factor when examining depth-trends in metabolic rates, as pelagic species tend to have higher metabolic rates than benthic or benthopelagic fishes (Drazen and Seibel, 2007; Killen et al., 2010, 2016; Gordon, 1972; Glazier, 2009). Unfortunately, when I included habitat as a main effect with all habitat categories present (pelagic, benthopelagic and benthic), the models did not converge. This was largely due to high uncertainty as to the effect of a benthopelagic habitat, likely as this category is broad and overlaps significantly with benthic and pelagic habitats. For this reason, I simplified the habitat categories to pelagic and non-pelagic species, which enabled model convergence:

$$C_{resp} \sim log_{10}(bm) + temp + pelagic + depth \tag{6.4}$$

where *pelagic* is the effect of a species living in a pelagic habitat.

To further address the issue of habitat effects, I ran the main models (equation 6.1) within the order Gadiformes (cods and their relatives), as all but one of the gadiform species were assigned as benthopelagic (Appendix A). I removed the single pelagic gadiform species from this dataset: *Micromessistius poutassou* (blue whiting) to avoid this confounding the analyses.

I ran all models for 7,500,000 iterations, with a burn-in of 15,000 and a thinning parameter of 750, aside from the Gadiformes models, which I ran for 5,000,000 iterations, with a burn-in of 10,000 and a thinning parameter of 500. I checked all models for convergence and mixing via visual inspection of traceplots, Geweke's diagnostic and the Heidelberger-Welch diagnostic (Plummer et al., 2006). All parameters for all models had an effective sample size > 2000.

6.4.2 Model sensitivity

In addition to the standard sensitivity tests (Chapter 2, section 2.8), I ran a model without the two deepest-living species, *Coryphanoides profundicolus* and *C. armatus* (deepwater and abyssal grenadiers) to ensure that these species were not overly influencing the results.

6.5 Results

Depth of occurrence ranged from 0 to 4865 m (Figure 6.1). The deepest-living species in the dataset, *Coryphaenodies profundicolus* (deepwater grenadier) has been observed between 3639 - 4865 m, and a had a mean C_{resp} value of 0.04 ($\pm$ 0.03). Similarly, the species with the lowest mean C_{resp} value in the dataset, *Trachyrincus scabrus* (roughsnout grenadier, C_{resp} value = 0.02 $\pm$ 0.02), has a relatively deep depth range of 300 - 1700 m. While epipelagic species showed a full range of C_{resp} values, of those species classified as "deep-sea" (with a minimum depth of occurrence $\geq$ 200 m), C_{resp} values greater than 0.20 were rare, with the greatest C_{resp} species mean value being 0.24 ($\pm$ 0.09), from *Aphanopus carbo* (black scabbard). Below a minimum depth of occurrence of 0 m, all but one of the species examined had a species mean C_{resp} value of $<$ 0.30 (Figure 6.2B). In contrast, the shallowest living species by maximum depth of occurrence, *Gobius bucchichi* (Bucchich's goby), with a depth range of 0 - 3 m, had a mean C_{resp} value of 0.34 ($\pm$ 0.01). The species with the highest mean C_{resp} value (0.50 $\pm$ 0.09), *Chaetodon ulietensis* (Pacific double-saddle butterflyfish) has a depth range of 2 - 30 m.

Both minimum and maximum depths of occurrence were negatively correlated with C_{resp} values, after accounting for log_{10} body mass and experienced temperature (Figure 6.2). Considering minimum depth of occurrence, there was a sharp decrease in number of species showing high C_{resp} values once no longer in contact with the surface (minimum depth $>$ 0 m, Figure 6.2B). Among species and individuals living below 200 m depth, C_{resp} values were rarely higher than 0.20 (Figure 6.2). Minimum depth of occurrence had a larger effect size than maximum depth of occurrence (b_{max_depth} = 0.10 $\pm$ 0.05, vs. b_{min_depth} 0.14 $\pm$ 0.04), however, both depth metrics had smaller standardised effect sizes on C_{resp} values than either log_{10} body mass or experienced temperature (Table 6.2).

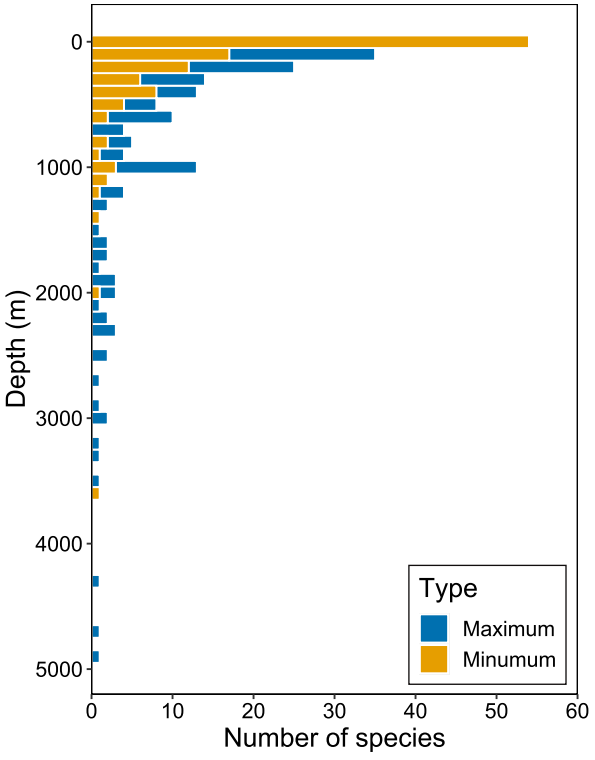

FIGURE 6.1: Number of species coloured by minimum (yellow) and maximum (blue) depth of occurrence. This plot is a repeat of Figure 2.13 in Chapter 2.

Removing the two deepest-living species (*Coryphaenoides profundicolus* and *C. armatus*) decreased the effect size of

maximum depth of occurrence (b_{max_depth} = 0.10 ± 0.05, vs. b_{max_depth} = 0.08 ± 0.05), but there was no decrease in effect size for minimum depth of occurrence. Overall, the significant correlation between C_{resp} values and minimum depth of occurrence was more robust to sensitivity tests than C_{resp} values and maximum depth of occurrence.

Although there was considerable overlap, pelagic species tended to have higher C_{resp} values than non-pelagic species (Figure 6.2). Habitat slightly reduced the effect size of both minimum and maximum depth of occurrence on C_{resp} values, however, the effect remains clear (Table 6.2).

Within the order Gadiformes, maximum depth of occurrence had no effect on C_{resp} values (Figure 6.3). There was an effect of minimum depth of occurrence on C_{resp} values within the Gadiformes (Figure 6.3), with the effect size being very similar to that for the models run on the full dataset (b_{min_depth} = 0.11 ± 0.09, vs. b_{min_depth} = 0.11 ± 0.04, Table 6.2). However, there was increased uncertainty for the posterior prediction for b_{min_depth} in the Gadiformes model (SD a = 0.24 vs. SD a = 0.14).

TABLE 6.2: Partial correlation coefficients for the main models investigating the relationships between C_{resp} values and species' depth of occurrence ($depth$), while accounting for the effects of body mass ($log_{10}(bm)$) and otolith-derived experienced temperature ($temp$). λ is the maximum likelihood of Pagel's λ, which estimates the phylogenetic signal of the model residuals.

Parameter	**Partial correlation coefficients**					
	Maximum depth			**Minimum depth**		
	max_main	max_pelagic	max_gads	min_main	min_pelagic	min_gads
a	1.77 ± 0.13	1.80 ± 0.13	2.19 ± 0.24	1.77 ± 0.14	1.80 ± 0.14	2.17 ± 0.24
$log_{10}(bm)$	0.14 ±0.04	0.13 ± 0.04	0.15 ± 0.06	0.14 ± 0.04	0.14 ± 0.04	0.16 ± 0.06
$temp$	0.22 ± 0.05	0.23 ± 0.05	0.12 ± 0.07	0.23 ± 0.05	0.23 ± 0.05	0.01 ± 0.07
$depth$	0.10 ± 0.05	0.10± 0.05	0.06 ± 0.09	0.11 ± 0.04	0.11 ± 0.04	0.11 ± 0.08
λ	0.98	0.98	0.99	0.99	0.99	0.98

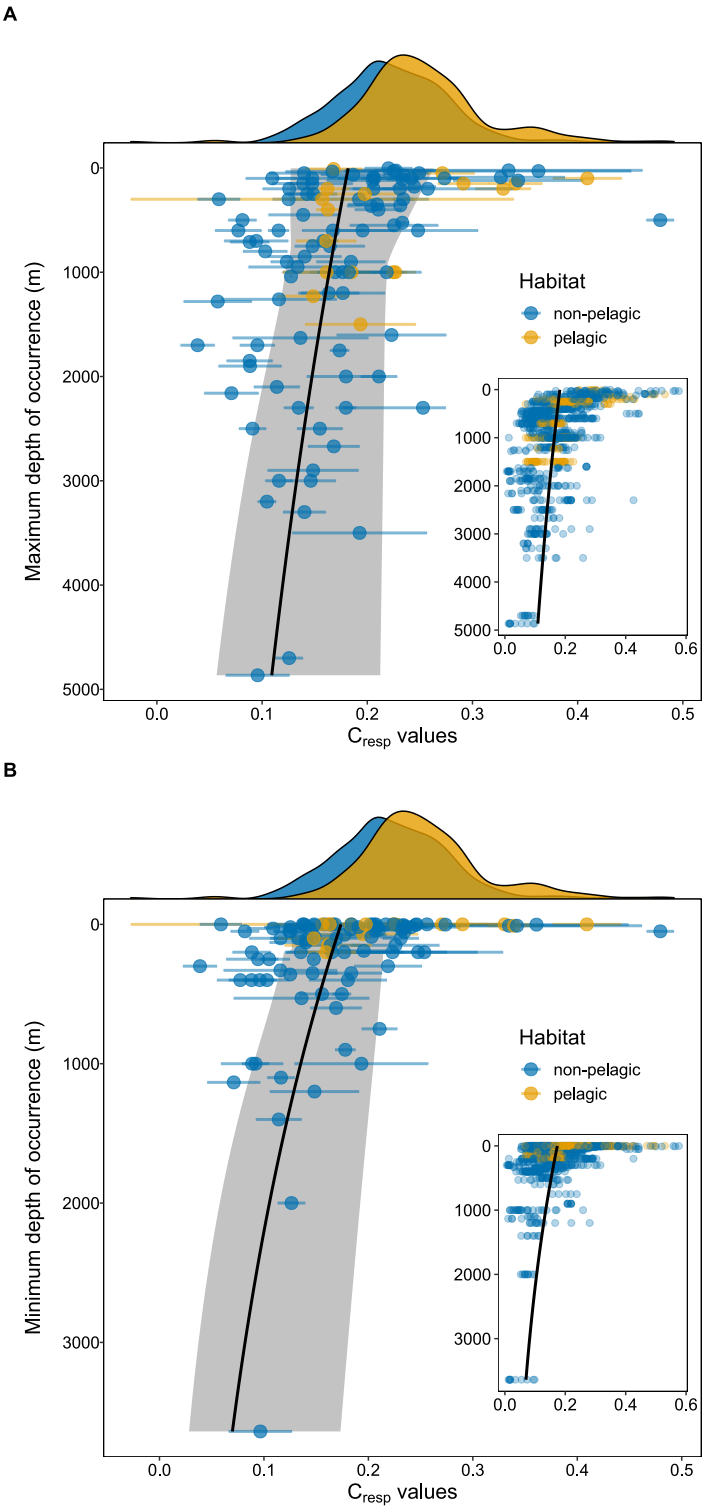

FIGURE 6.2: C_{resp} values plotted against species' maximum (A) and minimum (B) depth of occurrence, coloured by habitat (yellow = pelagic, blue = non-pelagic). C_{resp} values are plotted as species means and standard deviations (error bars), normalised to a common body mass of 200 g and temperature of 10°C (according to $C_{resp} = e^{-(1.803+0.131\times log_{10}(bm)+-0.231\times temp)}$). The inset plots show the non-normalised individual data points on which the models (max_pelagic and min_pelagic, black line) were fitted. 95% confidence intervals for the model fit are shown in the main plot, shaded in grey.

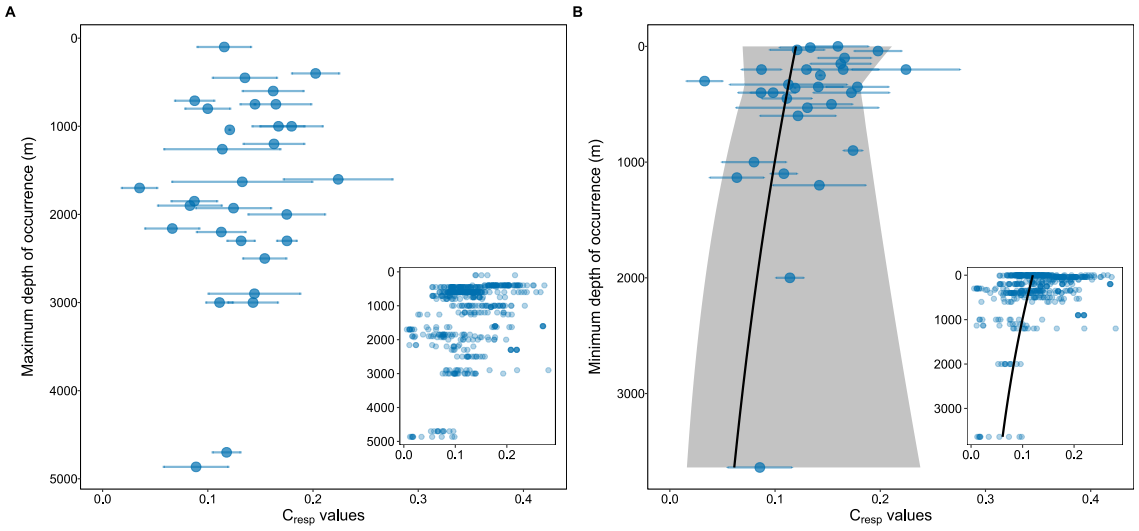

FIGURE 6.3: C_{resp} values plotted against species' maximum (A) and minimum (B) depth of occurrence, within the benthopelagic Gadiformes. C_{resp} values are plotted as species means and standard deviations (error bars), normalised to a common body mass of 200 g and temperature of 10°C (according to $C_{resp} = e^{-(2.185+0.153\times log_{10}(bm)+-0.120\times temp)}$). The inset plot shows the untransformed individual data points.

6.6 Discussion

C_{resp} values, a proxy for field metabolic rates (FMRs), decreased with both minimum and maximum depth of occurrence after accounting for the effects of body mass, experienced temperatures, and species' relatedness. Furthermore, the negative relationship between C_{resp} values and depth of occurrence persisted when including the effect of habitat. My study adds to the body of work which shows that depth has a negative relationship with FMR in marine fish, which cannot be explained by the effects of body mass and temperature alone (Torres et al., 1979; Drazen and Seibel, 2007; Seibel and Drazen, 2007; Drazen et al., 2015; Ikeda, 2016). Put simply, my study supports that the metabolic-depth effect is broadly applicable to marine teleost fish.

C_{resp} values decreased with both minimum and maximum depth of occurrence, according to a curvilinear relationship, although the trends seen with minimum depth were both greater in effect size (Table 6.2) and more robust to sensitivity testing (Appendix H.4), than trends with maximum depth. The fact that the metabolic-depth effect is both stronger and more robust with minimum depth has particular implications for groups which carry out diel vertical migrations, such as lanternfish (family Myctophidae, Gjøsæter and Kawaguchi, 1980; Davison et al., 2013), as these groups are likely to have metabolic rates which are more similar to species which remain in the epipelagic zone than their deep-sea counterparts (Seibel and Drazen,

2007). The difference in trends of C_{resp} values between minimum and maximum depth of occurrence can help to discern the potential drivers of the metabolic-depth effect.

6.6.1 Implications for proposed universal drivers of the metabolic-depth effect

6.6.1.1 Oxygen limitation

The dataset used in my study has a global coverage, however, the majority of deep-sea samples ($\geq$ 200 m) were from the North Atlantic, where the oxygen minimum zone (OMZ) is relatively minor compared to Monterey Bay, where most previous broad-scale studies of the metabolic-depth effect have been carried out (Childress, 1995; Levin, 2003; Seibel and Drazen, 2007). The persistence of the metabolic-depth effect at a large spatial scale supports previous assertions that the metabolic-depth effect is not universally driven by oxygen limitation within OMZs (Childress, 1995; Drazen and Seibel, 2007; Seibel and Drazen, 2007; Drazen et al., 2015).

6.6.1.2 Food limitation

As with previous studies which investigated the relationship between depth and metabolic rate (Drazen and Seibel, 2007; Seibel and Drazen, 2007; Drazen et al., 2015; Ikeda, 2016), my results show a decrease in metabolic rate with depth according to a curvilinear relationship. Particulate organic carbon (POC) flux, the principle source of primary production for deep-sea ecosystems (Smith et al., 2008), also decreases with depth throughout the water column according to a curvilinear relationship (Pace et al., 1987).

Food limitation had previously been ruled out as a driver of the metabolic-depth effect, as studies showed a levelling-off of the metabolic-depth effect at $\sim$ 1000 m (Childress, 1995; Drazen and Seibel, 2007; Seibel and Drazen, 2007), despite food quantity and quality continuing to decrease below 1000 m (Poulson, 2001). In contrast, my study shows that C_{resp} values continue to decrease with depth past 1000 m, thereby supporting food limitation as a possible primary universal driver of the metabolic-depth effect. However, caution must be taken, as few species had minimum depths of occurrence $\geq$ 1000 m (n = 8), which had a more robust correlation with C_{resp} values compared to maximum depth of occurrence. Furthermore, support for one hypothesis does not necessarily rule out others, as several drivers may be acting concurrently, or in different parts of the water column, or in different spatial locations.

6.6.1.3 Visual interaction hypothesis

Previous studies have proposed two key lines of evidence for the support of the visual interaction hypothesis. The first was that the reduction in metabolic rate with depth levelled off around 1000 m (Childress, 1995; Drazen and Seibel, 2007; Seibel and Drazen, 2007; Drazen et al., 2015). As stated above, this is not the case for my data, where C_{resp} values continue to decline below 1000 m. Secondly, some previous studies found reduced evidence for the depth-trend among non-pelagic groups (Drazen and Seibel, 2007; Seibel and Drazen, 2007). However, my data show a reduction in C_{resp} values with depth which persists when including habitat effects. Furthermore, C_{resp} values decreased with minimum depth of occurrence within the benthopelagic Gadiformes. The finding of a reduced metabolic rate with depth independent of habitat, reflects more recent studies showing a reduced (but still present) depth trend within benthic and/or benthopelagic groups (Seibel and Drazen, 2007; Drazen and Seibel, 2007; Drazen et al., 2015; Brown et al., 2018).

While my findings do not support the visual interaction hypothesis as a singular universal driver of the metabolic-depth effect, I cannot necessarily rule it out. The visual interaction hypothesis may be acting upon species living between 0 - 1000 m, likely in conjunction with other drivers. What remains unclear is why relaxed selection pressure for locomotory capacity would favour a reduction in FMR, rather than redirecting energy savings to fitness components such as growth or reproduction (Treberg et al., 2016). Therefore, it is likely that a form of resource limitation, such as food limitation, is also a universal driver of the decline in metabolic rates with depth.

6.6.1.4 Reduction in habitat complexity

Although it is difficult to test at a macroecological scale, several features of the relationship between depth and C_{resp} values enable me to rule out a reduction in habitat complexity with depth as the primary driver of the metabolic-depth effect. Firstly, the rate of reduction in C_{resp} values with depth is greatest in the epipelagic zone, where habitats remain complex and subject to turbulence (Smith et al., 2008; Brown et al., 2018; Martinez et al., 2021). Secondly, the habitat below 3000 m is expected to be relatively uniform and stable (Smith et al., 2008), which according to the theory of reduced habitat complexity as a universal driver of the metabolic-depth effect, should lead to a reduction in C_{resp} values at this point (Brown et al., 2018; Martinez et al., 2021). In contrast, my data show that at 3000 m the rate of reduction in C_{resp} values with depth, while still present, is reduced compared to the rate of reduction at epipelagic depths.

Finally, *Hoplosteuthis atlanticus*, cited in a previous study (Koslow, 1996) as having relatively high metabolic rates due to their association with seamounts, were found to

have relatively low C_{resp} values in this study (species mean C_{resp} value = 0.076 $\pm$ 0.016) and a previous study (Trueman et al., 2013). Taking these three points together, my data suggest it is unlikely that reduced selection for locomotory capacity, driven by reduced habitat complexity within the deep-sea, is a driver for the metabolic-depth effect.

6.6.2 Implications for fish under climate change

Alongside moving poleward, moving deeper has been proposed as a potential response by which fish (and other aquatic taxa) might avoid warming surface temperatures (Pinsky et al., 2013, 2019). However, my results suggest food and light limitation as two potential factors which may constrain fish FMRs with increasing depth. Although light limitation with increasing depth has been proposed as to relax selection pressures on fish through evolutionary time (Childress, 1995; Drazen and Seibel, 2007; Seibel and Drazen, 2007; Drazen et al., 2015), in the short term it is likely to act as a barrier to moving to deeper waters, particularly for species which rely heavily on visual predation and/or predator avoidance. Both food and light limitation, though particularly food limitation, are likely to preclude high FMR species and groups from moving to deeper climate refugia.

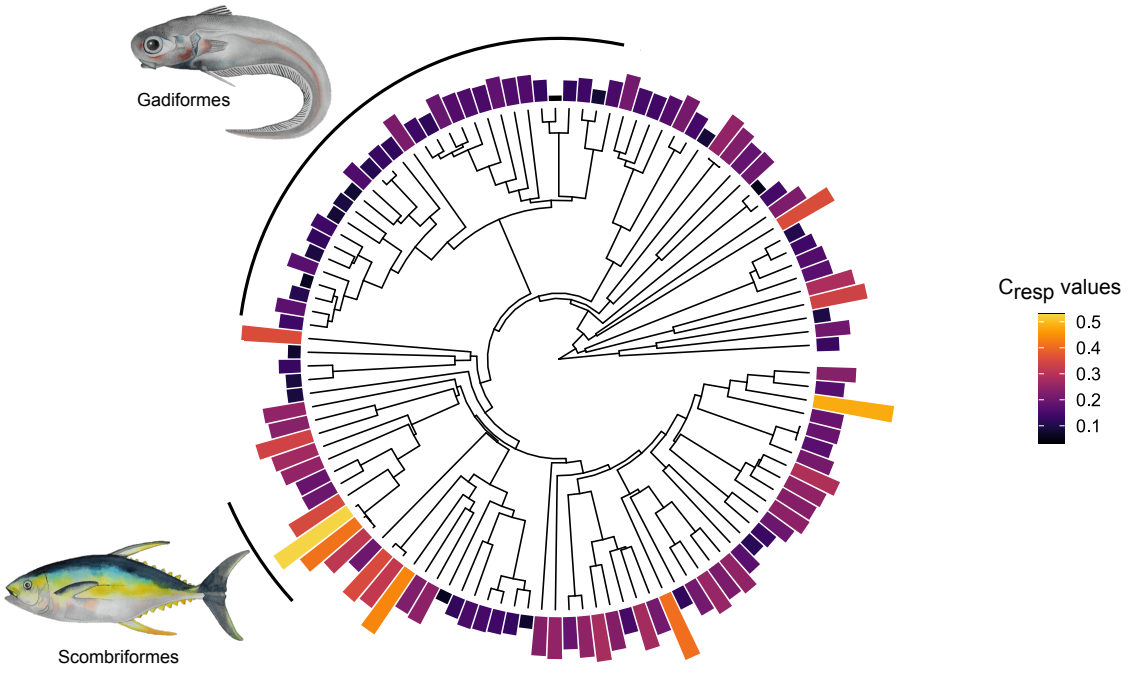

FIGURE 6.4: Phylogenetic patterns of mass- and temperature- normalised C_{resp} values in teleost fishes. Illustrated are the Gadiformes (*Coryphaenoides rupestris*) and the Scombriformes (*Thunnus albacares*). This plot is a repeat of Figure 4.5 in Chapter 4

.

If light and food limitation do act as a barrier to high FMR species moving deeper, this gives insight into which groups may or may not be able to use deeper waters as climate refugia. The Gadiformes are an example of a lineage which has managed to successfully colonise both the deep and shallow seas (Siebenaller et al., 1982; Cohen et al., 1990; Brown and Thatje, 2014), which may be due in part to their consistently low FMRs (Figure 6.4). In contrast, groups such as the Scombriformes may be precluded from moving deeper, as the lack of food in deeper waters may be unable to sustain their high FMRs (Figure 6.4). Food and light limitation may be a particular barrier for mesothermic species such as tunas (tribe Thunnini) and billfishes (order Istiophoriformes) from seeking cooler deeper waters. Although excluded from this study, mesothermic species have very high C_{resp} values and rely heavily on visual predation (Kawamura et al., 1981). Overall food and light limitation may act as barriers to teleosts using deeper waters as climate refugia, particularly for high FMR species.

6.6.3 Conclusions

In summary, my study showed a decrease in C_{resp} values with increasing depth after accounting for the effects of body mass, temperature, species' relatedness and habitat. Food and/or light limitation are the most likely drivers of this trend, though may be acting in different parts of the water column. It is possible that the physiological impact of reduced food and light may preclude high FMR species or groups from moving to deeper waters to avoid sea-surface warming.

Chapter 7

Conclusions

7.1 Thesis summary

The aim of this thesis was to investigate drivers of field metabolic rate (FMR) in marine teleost fishes at a macroecological scale. Specifically, I was interested in how fish FMR scaled interspecifically with body mass and temperature, and which ecological factors drive variation mass- and temperature-independent FMR.

To achieve the thesis aim, I first built a dataset of FMR across a broad range of taxonomic and ecological groups of fishes. Chapter 2 describes how I built the dataset of C_{resp} values (a proxy for fish FMR) and how I compiled body mass, experienced temperature and ecological variables. Using data from my own laboratory work, and data compiled from the literature, the dataset comprised 114 species from across the world's oceans, with representatives from a multitude of taxonomic groups and with different key ecological traits.

Next I investigated body mass and temperature scaling of C_{resp} values in lanternfish (family Myctophidae) from the Scotia Sea in the Southern Ocean (Chapter 3). I chose lanternfish as a case study due to their importance in biochemical cycling (Hidaka et al., 2001; Davison et al., 2013; Anderson et al., 2018) and the difficulty in obtaining live specimens for respirometry (Torres et al., 1979; Torres and Somero, 1988; Catul et al., 2011). Unlike other chapters, Chapter 3 was relatively small scale, both in terms of spatial and taxonomic coverage. Lanternfish from the Scotia Sea, had similar body masses and temperatures, and as such these were less important drivers of C_{resp} values than ecological correlates, such as differences in habitat.

Next, I used the full dataset to determine body mass and temperature scaling of fish FMR at a macroecological scale. I found a higher body mass scaling exponent (b = 0.90) compared to that predicted by the metabolic theory of ecology (b = 0.75, West et al., 1997; Brown et al., 2004), likely reflecting the greater importance of mass-volume

restrictions on fish FMR, as opposed to surface area-volume restrictions which likely drive metabolic rate scaling in endotherms (Brown et al., 2004; Glazier, 2005, 2010). Additionally, I found that FMR scaled with temperature with a lower activation energy (E) than is predicted by the metabolic theory of ecology (West et al., 1997; Brown et al., 2004) and the universal temperature dependence hypothesis (Gillooly et al., 2001, 2006). The lower E for FMR compared to standard metabolic rates (SMR) likely reflects the capacity for wild fish to mitigate the thermodynamic effects of increased temperatures on their enzyme-catalysed metabolic reactions (Richards, 2010; Norin and Clark, 2017; Jutfelt et al., 2021).

After establishing the body mass and temperature scaling relationships of fish FMR, I investigated ecological drivers of variation in fish FMR - specifically thermal realm adaptation and depth of occurrence. Both thermal realm and thermal range showed correlation with C_{resp} values after accounting for the effects of body mass and temperature. Polar fishes had an average C_{resp} value which was greater than that of temperate fishes, after accounting for body mass and temperature effects, indicating partial metabolic cold adaptation. Furthermore, adaptations to different thermal realms changed the scaling of C_{resp} values with temperature. The scaling relationship between C_{resp} values and temperature was steeper (i.e. E was greater) in stenothermic groups compared to eurythermic groups. In contrast, the scaling of FMR with body mass remain constant across different thermal realms. Depth of occurrence also had a significant effect on C_{resp} values after body mass and temperature. C_{resp} values decreased with depth of occurrence throughout the depth range investigated in my thesis (0 - 4800 m), likely due to increasing food- and light-limitations with increasing depth.

7.2 Implications of thesis findings

My thesis joins a plethora of other studies which have found that fish metabolic rates (standard, field and maximum) are best modelled using body mass scaling exponents (b) of approximately 0.80 to 0.90 (Winberg, 1956; Clarke and Johnston, 1999; White et al., 2006; Killen et al., 2016). The finding that fish FMR scales with body mass according to b = 0.90 has profound implications for marine ecosystem models. Most global and regional marine ecosystem models incorporate metabolic rate, either as a parameter in itself, or to derive other biological rates such as growth rate (Tittensor et al., 2018). Despite previous studies finding that fish metabolic rates scale with body mass according to b = 0.80 to 0.90 (Winberg, 1956; Clarke and Johnston, 1999; White et al., 2006; Killen et al., 2016), the majority of marine ecosystem models use a value of b ranging from 0.67 to 0.75 (Cheung et al., 2008; Blanchard et al., 2012; Jennings and Collingridge, 2015; Carozza et al., 2016; Audzijonyte et al., 2019), following the metabolic theory of ecology and traditional surface area-volume relationships (Kleiber, 1932, 1947; West et al., 1997; Brown et al., 2004). While the difference between the theoretical and empirical values of b may seem trivial, when dealing with exponential relationships, such as that between metabolic rate and body mass, a small change in the value of the scaling exponent can lead to very different estimations of metabolic rates (Cheung et al., 2013; Lefevre et al., 2017, 2018). As the value of b approaches 1, the scaling of metabolic rate with body mass moves closer to isometry, with the result for mass-specific metabolic rates being no relationship with body mass. In summary, the use of b values of 0.67 to 0.75 in marine ecosystem models is likely overestimating the effects of body mass effects on metabolic rates.

As with body mass, marine ecosystem models typically use a single value of E to describe the relationship between temperature and metabolic rates (Cheung et al., 2008, 2013; Blanchard et al., 2012; Harfoot et al., 2014; Jennings and Collingridge, 2015; Carozza et al., 2016; Audzijonyte et al., 2019). Following the metabolic theory of ecology and universal temperature dependence (West et al., 1997; Gillooly et al., 2001; Brown et al., 2004; Gillooly et al., 2006), the value of E in marine ecosystem models is usually set between 0.6 and 0.7. However, my thesis joins other studies showing that the relationship between metabolic rates and temperature are much more complex than is suggested by enzyme-catalysed reaction thermodynamics (Knies and Kingsolver, 2010; White et al., 2012b; Norin and Clark, 2017). Considering *field* metabolic rates adds an additional layer of complexity to the relationship between metabolic rates and temperature, as wild living fish likely have the ability to mitigate the effects of temperature on their standard metabolic rates by reducing other metabolic costs (Richards, 2010; Norin and Clark, 2017; Jutfelt et al., 2021).

Studying FMR alone is not enough to fully understand the implications of temperature on fish metabolic rates, as behaviours which mitigate temperature change

effects on overall FMRs have fitness and survival implications. For instance, while a fish may be able to mitigate a short term temperature increase on its metabolic costs by reducing movement, if the temperature increase is sustained the continued reduction in movement will impair the fish's ability to forage, evade predators and reproduce (Richards, 2010).

Despite the important roles they play in ocean biogeochemical cycles, deeper-dwelling fishes, such as those in the meso- and bathy-pelagic, are relatively understudied, particularly when concerning metabolic rates. Results from my thesis support previous findings that deeper-dwelling fishes tend towards lower metabolic rates, even after accounting for body mass and temperature (Drazen and Seibel, 2007; Seibel and Drazen, 2007; Drazen et al., 2015; Ikeda, 2016; Gerringer et al., 2017), likely due to living in a food- and light-limited environment. While some have controversially proposed that fish might move deeper to escape increasing sea-surface temperatures (Pinsky et al., 2013, 2019), the limitations on FMR by low light and food levels in the deep-sea are likely to act as a barrier, particularly to species with high FMRs.

Finally, while macroecological studies are useful for describing large-scale drivers of metabolic rates, care should be taken if attempting to apply global patterns to smaller regional scales (Belcher et al., 2020). Despite body mass and temperature being key interspecific drivers of FMR at a macroecological scale, neither were important drivers of C_{resp} values within lanternfish living in the Scotia Sea. When considering groups or species of interest, the study of drivers of metabolic rate within that particular species or group would be ideal. However, I recognise that logistical and funding considerations mean that small-scale studies are not always possible, and macroecological patterns offer useful first predictions in these cases.

7.3 C_{resp} values as a measure of field metabolic rate in fishes - opportunities, challenges and future directions

My thesis has added to recent studies showing the C_{resp} method to be a powerful tool in investigating FMRs in marine teleost fishes (Trueman et al., 2016; Chung et al., 2019b, 2021b; Smoliński et al., 2021). Furthermore, the C_{resp} fills an important methodological gap in the study of FMR across vertebrates - namely the ability to estimate FMR in aquatic organisms (Treberg et al., 2016).

In many ways, the C_{resp} method is an ideal tool for macroecological studies of FMR in fishes. Firstly, the C_{resp} method does not require the use of live fish, which removes the ethical considerations associated with experimentation on live fish (Sloman et al., 2019). Furthermore, the lack of a requirement for live, healthy fish enables application of the C_{resp} method to fragile and deep-sea species (Torres et al., 1979; Torres and Somero, 1988; Seibel and Drazen, 2007; Catul et al., 2011; Drazen et al., 2015).

Secondly, the C_{resp} method does not require fish to be harvested specifically for FMR estimation, in contrast to electron-transport system (ETS) studies (Cammen et al., 1990; Hernández-León et al., 2019). Instead, the C_{resp} method can be conducted on archived otoliths. Given the prominence of otoliths in ageing studies (Campana, 1999), many fisheries institutions and museums hold large otolith collections which can be sampled to extract a wealth of C_{resp} values. This is particularly useful for macroecological studies, as C_{resp} values can be obtained from a large number of diverse species, without the logistical difficulty and expense of many respirometry trials or ETS assays.

While the C_{resp} method is very useful for macroecological studies of FMR in fishes, it has a few limitations, as does any scientific technique. The first key limitation of the C_{resp} method is that it requires destructive sampling of the otolith to obtain a sample for stable isotope analysis (Chapter 2). The need for destructive sampling of otoliths for the C_{resp} method was a key barrier in obtaining otoliths for the dataset, particularly where those otoliths came from museum collections or institutional archives (Freedman et al., 2018).

A second key limitation in the C_{resp} method, particularly when using archived or museum otolith collections, was that it was often difficult to obtain the necessary metadata required, such as body size and catch data. Ideally, archive and museum collections would all be catalogued with easy access to metadata associated with the specimens. However, chronic underfunding and undervaluing of archives and museums collections (e.g. Viscardi, 2013), particularly where curatorial work is concerned, means comprehensive and detailed catalogues are not always available. This situation is not unique to C_{resp} studies; instead it highlights the importance of proper funding of collections management and curation.

Thirdly, it can be difficult to obtain the $\delta^{13}C_{diet}$ and $\delta^{13}C_{DIC}$ values necessary to estimate C_{resp} values. Specifically, $\delta^{13}C_{diet}$ values can be hard to find for poorly studied species, and $\delta^{13}C_{DIC}$ values are much more variable in freshwater and brackish environments than in fully marine environments. The high variability of $\delta^{13}C_{DIC}$ values in freshwater (Bade et al., 2004) meant that my thesis was restricted to marine fishes. It would be possible to apply the C_{resp} method to freshwater fishes, although this would likely require direct measurement of $\delta^{13}C_{DIC}$ values, rather than estimation for isoscapes. The additional logistical difficulty of having to measure $\delta^{13}C_{DIC}$ values in freshwater environments will likely restrict the macroecological application of the C_{resp} method in freshwater fishes.

Finally, the C_{resp} method is still in development, and more research is needed on the method itself. My study has shown that deriving oxygen consumption from C_{resp} values using a single calibration gives reasonable estimates across a range of species. However, the reverse exponential relationship between oxygen consumption rates and C_{resp} values (Chung et al., 2019a,b; Martino et al., 2020) means that estimates of oxygen consumption rates derived from C_{resp} values are sensitive to the upper bound (C, equation 4.5) in high C_{resp} value species. Within the curvilinear portion of the relationship, close to the upper bound, a small change in C_{resp} value represents a very large change in oxygen consumption rate. Estimates of oxygen consumption rate derived from C_{resp} values can be carried out with more certainty in the linear portion of the calibration curve, at lower C_{resp} values. Furthermore, the cause of the upper bound in the relationship between C_{resp} values and oxygen consumption rates is still unclear (C. Trueman, 2022, per. comms.). The uncertainty associated with the upper bound may limit our certainty in using C_{resp} values to estimate field oxygen consumption from species with high metabolic rates, such as those living at high temperatures (Chapters 4 & 5) or athletic fishes such as tunas (Chapter 5). At present, direct calibrations between C_{resp} values and oxygen consumption rates are only available for two relatively large, benthopelagic species (Chung et al., 2019b; Martino et al., 2020). More studies calibrating C_{resp} values to oxygen consumption, especially among a range of species, would be invaluable in further developing the C_{resp} method.

Appendix A

Ecological information

A.1 Ecological information table

TABLE A.1: Ecological information for species in the main dataset. * = *Incertae sedis* Abbreviations are as follows: for thermal realm, P = polar, Te = temperate, STr = subtropical, Tr = tropical and D = deep-sea; for habitat, B = benthic, BP = benthopelagic, P = pelagic, R = (coral) reef-associated.

Classification		Thermal realm	SST		Habitat	Depth	
Species	Order		Min.	Max.		Min.	Max.
Acanthurus triostegus	Acanthuriformes	Tr	21.97	29.46	R	0	90
Chaetodon ulietensis	Acanthuriformes	Tr	25.04	29.46	R	2	30
Alepocephalus agassizii	Alepocephaliformes	D	NA	NA	BP	600	2670
Alepocephalus bairdii	Alepocephaliformes	D	NA	NA	BP	500	1750
Rouleina attrita	Alepocephaliformes	D	NA	NA	BP	1400	2100
Xenodermichthys copei	Alepocephaliformes	Te	0.43	26.15	P	100	1230
Conger conger	Anguilliformes	Te	9.98	24.44	B	0	100
Synaphobranchus kaupii	Anguilliformes	D	NA	NA	BP	250	3200
Argentina silus	Argentiniformes	Te	0.19	18.18	BP	150	550

Ateleopus japonicus	Ateleopodiformes	Tr	19.06	25.54	BP	130	850
Ijimaia dofleini	Ateleopodiformes	D	NA	NA	BP	NA	1281
Bathysaurus ferox	Aulopiformes	D	NA	NA	B	1000	3500
Bathypterois dubius	Aulopiformes	D	NA	NA	B	750	2000
Saurida lessepsianus	Aulopiformes	STr	NA	NA	BP	20	100
Saurida undosquamis	Aulopiformes	STr	20.43	28.67	BP	20	350
Exocoetus volitans	Beloniformes	Tr	23.33	23.33	P	0	10
Beryx splendens	Beryciformes	D	NA	NA	BP	400	600
Hoplostethus atlanticus	Beryciformes	D	NA	NA	BP	400	1700
Hoplostethus mediterraneus	Beryciformes	Te	7.75	27.87	BP	100	950
Seriola dumerili	Carangiformes	STr	19.00	27.92	BP	18	72
Trachurus trachurus	Carangiformes	Te	10.13	19.40	BP	100	200
Coryphaena hippurus	Carangiformes	STr	7.79	28.48	P	0	100
Sprattus sprattus	Clupeiformes	Te	8.94	15.65	P	10	150
Engraulis encrasicolus	Clupeiformes	Te	9.13	24.80	P	0	150
Boreogadus saida	Gadiformes	P	-0.85	8.93	BP	40	400
Gadus morhua	Gadiformes	Te	-0.55	16.20	BP	0	600
Melanogrammus aeglefinus	Gadiformes	Te	2.32	18.77	BP	10	450
Merlangius merlangus	Gadiformes	Te	9.13	16.36	BP	30	100
Micromesistius poutassou	Gadiformes	Te	-0.03	20.02	P	150	1000

Pollachius virens	Gadiformes	Te	5.33	14.05	P	0	200
Molva dypterygia	Gadiformes	D	NA	NA	BP	350	1000
Bathygadus nipponicus	Gadiformes	D	NA	NA	BP	200	1602
Cetonurus globiceps	Gadiformes	D	NA	NA	BP	1000	1900
Coelorinchus caelorhincus	Gadiformes	D	NA	NA	BP	200	710
Coelorinchus fasciatus	Gadiformes	D	NA	NA	BP	400	800
Coelorinchus labiatus	Gadiformes	D	NA	NA	BP	450	2200
Coryphaenoides acrolepis	Gadiformes	D	NA	NA	BP	900	2300
Coryphaenoides armatus	Gadiformes	D	NA	NA	BP	2000	4700
Coryphaenoides guentheri	Gadiformes	D	NA	NA	BP	1100	3000
Coryphaenoides marginatus	Gadiformes	D	NA	NA	BP	250	750
Coryphaenoides mediterraneus	Gadiformes	D	NA	NA	BP	1200	2900
Coryphaenoides paramarshalli	Gadiformes	D	NA	NA	BP	1134	2160
Coryphaenoides profundicolus	Gadiformes	D	NA	NA	BP	3639	4865
Coryphaenoides rupestris	Gadiformes	D	NA	NA	BP	400	2000
Hymenocephalus lethonemus	Gadiformes	D	NA	NA	BP	360	1040
Malacocephalus laevis	Gadiformes	D	NA	NA	BP	200	750
Nezumia aequalis	Gadiformes	D	NA	NA	BP	200	2300
Nezumia duodecim	Gadiformes	D	NA	NA	BP	330	1260
Spicomacrurus kuronumai	Gadiformes	D	NA	NA	BP	350	650

Squalogadus modificatus	Gadiformes	D	NA	NA	NA	600	1929
Trachyrincus murrayi	Gadiformes	D	NA	NA	BP	530	1630
Trachyrincus scabrus	Gadiformes	D	NA	NA	BP	300	1700
Merluccius merluccius	Gadiformes	Te	9.72	20.01	BP	100	1000
Antimora rostrata	Gadiformes	D	NA	NA	BP	350	3000
Lepidion eques	Gadiformes	D	NA	NA	BP	400	1850
Mora moro	Gadiformes	D	NA	NA	BP	500	2500
Phycis blennoides	Gadiformes	Te	7.29	20.94	BP	150	1200
Gobius bucchichi	Gobiiformes	STr	NA	NA	B	0	3
Holocentrus adscensionis	Holocentriformes	STr	23.30	29.44	BP	NA	90
Plagiogeneion rubiginosum	Eupercaria*	Te	13.11	24.54	BP	50	900
Lutjanus fulviflamma	Eupercaria*	Tr	13.35	28.55	R	3	35
Lutjanus sebae	Eupercaria*	Tr	25.22	28.09	R	5	180
Pristipomoides filamentosus	Eupercaria*	Tr	NA	NA	BP	40	360
Pristipomoides multidens	Eupercaria*	Tr	26.34	27.71	BP	40	200
Kajikia albida	Istiophoriformes	Te	15.03	28.01	P	0	100
Makaira nigricans	Istiophoriformes	STr	14.45	27.20	P	0	200
Coris julis	Labriformes	STr	16.95	22.64	R	0	120
Electrona antarctica	Myctophiformes	P	-1.66	-1.54	P	0	1000
Electrona carlsbergi	Myctophiformes	Te	-0.44	11.50	P	0	400

Gymnoscopelus braueri	Myctophiformes	P	-1.66	-1.54	P	0	1000
Gymnoscopelus nicholsi	Myctophiformes	P	-1.64	-1.54	BP	0	700
Krefftichthys anderssoni	Myctophiformes	P	-1.58	-1.58	P	0	1000
Protomyctophum bolini	Myctophiformes	D	NA	NA	P	200	700
Neoscopelus microchir	Myctophiformes	D	NA	NA	BP	250	700
Halosauropsis macrochir	Notacanthiformes	Te	12.14	24.25	BP	110	3300
Cataetyx laticeps	Ophidiiformes	D	NA	NA	BP	1000	2500
Spectrunculus grandis	Ophidiiformes	D	NA	NA	BP	800	4255
Doederleinia berycoides	Pempheriformes	Tr	16.91	28.68	BP	100	600
Epigonus telescopus	Pempheriformes	Te	8.55	26.08	BP	75	1200
Champsocephalus gunnari	Perciformes	P	2.13	4.43	BP	30	250
Artediellus atlanticus	Perciformes	Te	-0.70	10.71	B	35	900
Triglops nybelini	Perciformes	D	NA	NA	B	200	600
Cyclopterus lumpus	Perciformes	Te	-0.16	11.27	BP	50	500
Dissostichus eleginoides	Perciformes	P	-1.71	18.03	P	70	1500
Helicolenus dactylopterus	Perciformes	D	NA	NA	BP	200	1000
Helicolenus mouchezi	Perciformes	STr	19.66	19.69	BP	190	600
Sebastes mentella	Perciformes	D	NA	NA	BP	300	1000
Epinephelus adscensionis	Perciformes	STr	26.57	28.24	BP	2	100
Epinephelus morio	Perciformes	STr	26.57	28.24	BP	5	25

Epinephelus multinotatus	Perciformes	Tr	26.04	27.40	BP	10	110
Hyporthodus nigritus	Perciformes	STr	NA	NA	BP	55	525
Lepidoperca coatsii	Perciformes	Te	14.38	15.20	BP	50	190
Lycodes gracilis	Perciformes	Te	5.73	10.36	B	90	365
Glyptocephalus cynoglossus	Pleuronectiformes	Te	0.10	20.85	B	50	500
Hippoglossoides platessoides	Pleuronectiformes	Te	-0.54	13.63	B	90	250
Limanda limanda	Pleuronectiformes	Te	9.13	13.64	B	0	150
Microstomus kitt	Pleuronectiformes	Te	7.27	15.10	B	20	200
Lepidorhombus whiffiagonis	Pleuronectiformes	Te	9.73	19.99	B	50	300
Scophthalmus maximus	Pleuronectiformes	Te	7.41	18.83	B	0	100
Solea solea	Pleuronectiformes	Te	9.83	24.34	BP	0	300
Salmo salar	Salmoniformes	Te	9.85	10.86	BP	10	23
Arripis georgianus	Scombriformes	STr	NA	NA	P	0	50
Acanthocybium solandri	Scombriformes	STr	21.20	29.29	P	0	200
Scomber colias	Scombriformes	Te	16.36	20.10	P	0	300
Scomber scombrus	Scombriformes	Te	4.89	22.56	P	0	250
Thunnus albacares	Scombriformes	Tr	21.55	29.44	P	0	100
Thunnus maccoyii	Scombriformes	STr	19.08	25.59	P	0	600
Thunnus orientalis	Scombriformes	STr	NA	NA	P	0	550
Aphanopus carbo	Scombriformes	D	NA	NA	BP	200	2300

Lethrinus harak	Spariformes	Tr	24.09	29.25	R	0	65
Lethrinus lentjan	Spariformes	Tr	24.26	26.79	R	0	50
Chrysophrys auratus	Spariformes	Te	13.56	22.77	R	10	150
Diplodus vulgaris	Spariformes	STr	16.49	23.09	BP	0	50
Oblada melanura	Spariformes	STr	17.24	25.60	BP	0	30
Pagellus erythrinus	Spariformes	STr	19.67	23.13	BP	20	300
Pagrus caeruleostictus	Spariformes	Tr	23.05	25.70	BP	0	200
Mullus barbatus	Syngnathiformes	Te	10.21	23.13	BP	5	300
Upeneus moluccensis	Syngnathiformes	STr	23.05	25.63	BP	10	120

A.1.1 Sources for ecological information table

A.1.1.1 General sources

- G. R. Allen. *Snappers of the world*, volume 6. Food and Agriculture Organization of the United Nations (FAO), Rome, 1985. ISBN 92-5-102321-2
- D. M. Bailey, M. A. Collins, J. D. M. Gordon, A. F. Zuur, and I. G. Priede. Long-term changes in deep-water fish populations in the northeast Atlantic: a deeper reaching effect of fisheries? *Proceedings of the Royal Society B: Biological Sciences*, 276:1965–1969, 2009
- K. Carpenter and G. R. Allen. *Emperor fishes and large-eye breams of the world*, volume 9. Food and Agriculture Organization of the United Nations (FAO), Rome, 1989. ISBN 92-5-102321-2
- K. E. Carpenter. *The living marine resources of the Western Central Atlantic*, volume 2. Food and Agriculture Organization of the United Nations (FAO), Rome, 2002
- K. E. Carpenter and N. De Angelis. *The living marine resources of the Eastern Central Atlantic*, volume 3–4. Food and Agriculture Organization of the United Nations (FAO), Rome, 2014. ISBN 978-92-5-109266-8

- B. W. Coad and J. D. Reist. *Annotated list of the Arctic marine fishes of Canada*. Fisheries and Oceans Canada Winnipeg, Canada, 2004
- D. M. Cohen, T. Inada, T. Iwamoto, and N. Scialabba. *Gadiform fishes of the world*, volume 10. Food and Agriculture Organization of the United Nations (FAO), Rome, 1990. ISBN 92-5-102890-7
- B. B. Collette and C. E. Nauen. *Scombrids of the world: an annotated and illustrated catalogue of tunas, mackerels, bonitos, and related species known to date.*, volume 2. Food and Agriculture Organization of the United Nations (FAO), Rome, 1983. ISBN 92-5-101381-0
- G. d'Onghia, C. Y. Politou, A. Bozzano, D. Lloris, G. Rotllant, L. Sión, and F. Mastrototaro. Deep-water fish assemblages in the Mediterranean Sea. *Scientia Marina*, 68(S3):87–99, 2004. ISSN 1886-8134
- R. Froese and D. Pauly. Fishbase, 2021. URL `www.fishbase.org`. Publisher: Fisheries Centre, University of British Columbia
- O. Gon and P. C. Heemstra. *Fishes of the Southern Ocean*, volume 1. J. L. B. Smith Institute of Ichthyology, Grahamstown, 1990. ISBN 8-86810-211-3
- T. Iwamoto, N. Nakayama, K. T. Shao, and H. C. Ho. Synopsis of the grenadier fishes (Gadiformes; Teleostei) of Taiwan. *Proceedings of the California Academy of Sciences*, 62:31–126, 2015
- N. R. Merrett, R. L. Haedrich, J. D. M. Gordon, and M. Stehmann. Deep demersal fish assemblage structure in the Porcupine Seabight (eastern North Atlantic): results of single warp trawling at lower slope to abyssal soundings. *Journal of the Marine Biological Association of the United Kingdom*, 71(2):359–373, 1991
- C. Mytilineou, C. Y. Politou, C. Papaconstantinou, S. Kavadas, G. d'Onghia, and L Sion. Deep-water fish fauna in the Eastern Ionian Sea. *Belgian Journal of Zoology*, 135(2):229, 2005
- I. Nakamura. *Billfishes of the world*, volume 5. Food and Agriculture Organization of the United Nations (FAO), Rome, 1985. ISBN 92-5-102232-1
- I. G. Priede, J. A. Godbold, N. J. King, M. A. Collins, D. M. Bailey, and J. D. M. Gordon. Deep-sea demersal fish species richness in the Porcupine Seabight, NE Atlantic Ocean: global and regional patterns. *Marine Ecology*, 31(1):247–260, 2010. ISSN 0173-9565
- R. A. Saunders, S. Fielding, S. E. Thorpe, and G. A. Tarling. School characteristics of mesopelagic fish at South Georgia. *Deep Sea Research Part I: Oceanographic Research Papers*, 81:62–77, 2013

- M. M. Smith and P. C. Heemstra. *Smiths' sea fishes*. Springer-Verlag, 2012. ISBN 3-540-16851-6
- P.J.P. Whitehead, M.L. Bauchot, J.C. Hureau, J. Nielsen, and E. Tortonese. *Fishes of the North-eastern Atlantic and Mediterranean*, volume 1–3. United Nations Educational, Scientific and Cultural Organisation (UNESCO), Paris, 1986. ISBN 92-3-002215-2

A.1.1.2 Species specific sources

- P. Abaunza, A. Murta, S. Mattiucci, R. Cimmaruta, G. Nascetti, A. Magoulas, A. Sanjuan, S. Comesaña, K. MacKenzie, and J. Molloy. Stock discrimination of horse mackerel (*trachurus* trachurus) in the Northeast Atlantic and Mediterranean Sea: integrating the results from different stock identification approaches. International Council for the Exploration of the Sea (ICES), 2004
- M. A. Abiom, G. M. Menezes, T. Schlitt, and A. D. Rogers. Genetic structure and history of populations of the deep-sea fish *Helicolenus dactylopterus* (Delaroche, 1809) inferred from mtDNA sequence analysis. *Molecular Ecology*, 14(5): 1343–1354, 2005.
- V. Allain, A. Biseau, and B. Kergoat. Preliminary estimates of French deepwater fishery discards in the Northeast Atlantic Ocean. *Fisheries Research*, 60(1): 185–192, 2003
- F Arreguín-Sánchez, M Contreras, V Moreno, R Burgos, and R Valdés. Population dynamics and stock assessment of red grouper (*Epinephelus morio*) fishery on Campeche Bank, Mexico. In *Biology, fisheries and culture of tropical groupers and snappers: ICLARM Conference Proceedings*, pages 202–217, 1996
- W. D. Anderson and P. C. Heemstra. Review of Atlantic and eastern Pacific anthiine fishes (Teleostei: Perciformes: Serranidae), with descriptions of two new genera. *Transactions of the American Philosophical Society*, 102(2):i–173, 2012
- T. Andrew. The Fishes of Tristan da Cunha and Gough Island (South Atlantic), and the effects of environmental seasonality on the biology of selected species. 1992. Publisher: Rhodes University
- A. H. Andrews, A. Pacicco, R. Allman, B. J. Falterman, E. T. Lang, and W. Golet. Age validation of yellowfin (*Thunnus albacares*) and bigeye (*Thunnus obesus*) tuna of the northwestern Atlantic Ocean. *Canadian Journal of Fisheries and Aquatic Sciences*, 77(4):637–643, 2020
- M. L. Artüz and R. Fricke. First and northernmost record of *Upeneus moluccensis* (Actinopterygii: Perciformes: Mullidae) from the Sea of Marmara. *Acta Ichthyologica et Piscatoria*, 49(1):53–58, 2019

- D. M. Bailey, B. Genard, M. A. Collins, J. F. Rees, S. K. Unsworth, E. J. V. Battle, P. M. Bagley, A. J. Jamieson, and I. G. Priede. High swimming and metabolic activity in the deep-sea eel *Synaphobranchus kaupii* revealed by integrated in situ and in vitro measurements. *Physiological and Biochemical Zoology*, 78(3):335–346, 2005

- R. Banón. New record of *Cataetyx laticeps* (Bythitidae) in northwestern Atlantic. 2001. Publisher: Société française d'ichtyologie

- R. W. Blacker. *Synopsis of Biological Data on Haddock: Melanogrammus aeglefinus (Linnaeus) 1758*. Food and Agriculture Organization of the United Nations (FAO), Rome, 1971

- B. A. Block, D. T. Booth, and F. G. Carey. Depth and temperature of the blue marlin, *Makaira nigricans*, observed by acoustic telemetry. *Marine Biology*, 114(2): 175–183, 1992

- O. A. Bergstad. Distribution, population structure, growth, and reproduction of the greater silver smelt, *Argentina silus* (Pisces, Argentinidae), of the Skagerrak and the north-eastern North Sea. *ICES Journal of Marine Science*, 50(2):129–143, 1993

- J. Burnett, M. R. Ross, and S. H. Clark. Several biological aspects of the witch flounder (*Glyptocephalus cynoglossus* (L.)) in the Gulf of Maine-Georges Bank region. *Journal of Northwest Atlantic Fishery Science*, 12:15–25, 1992

- M. L. Burton, J. C. Potts, and D. R. Carr. Age, growth, and natural mortality of rock hind, *Epinephelus adscensionis*, from the Gulf of Mexico. *Bulletin of Marine Science*, 88(4):903–917, 2012

- B. Busalacchi, T. Bottari, D. Giordano, A. Profeta, and P. Rinelli. Distribution and biological features of the common pandora, *Pagellus erythrinus* (Linnaeus, 1758), in the southern Tyrrhenian Sea (Central Mediterranean). *Helgoland Marine Research*, 68(4):491–501, 2014

- S. E. Campana, A. E. Valentin, S. E. MacLellan, and J. B. Groot. Image-enhanced burnt otoliths, bomb radiocarbon and the growth dynamics of redfish (*Sebastes mentella* and *S. fasciatus*) off the eastern coast of Canada. *Marine and Freshwater Research*, 67(7):925–936, 2016

- L. M. Cargnelli. Essential fish habitat source document. Witch flounder, *Glyptocephalus cynoglossus*, life history and habitat characteristics. Woods Hole, Massachusetts, 1999. National Oceanic and Atmospheric Administration (NOAA)

- P. Carpentieri, F. Colloca, M. Cardinale, A. Belluscio, and G. D. Ardizzone. Feeding habits of European hake (*Merluccius merluccius*) in the central Mediterranean Sea. *Fishery Bulletin*, 103(2):411–416, 2005
- J. M. Casas and C. Piñeiro. Growth and age estimation of greater fork-beard (*Phycis blennoides* Brünnich, 1768) in the north and northwest of the Iberian Peninsula (ICES Division VIIIc and IXa). *Fisheries Research*, 47(1):19–25, 2000
- J. E. Caselle, S. L. Hamilton, K. Davis, M. Bester, M. Wege, C. Thompson, A. Turchik, R. Jenkinson, D. Simpson, and J. Mayorga. Ecosystem assessment of the Tristan da Cunha Islands. St. Helena: Royal Society for Protection of Birds, Tristan da Cunha Government, 2017
- M. T. Chung. *Functional and life-history traits in deep-sea fishes*. PhD thesis, University of Southampton, Southampton, United Kingdom, 2015. URL https://eprints.soton.ac.uk/384568/
- R. A. Coggan, J. D. M. Gordon, and N. R. Merrett. Aspects of the biology of *Nezumia aequalis* from the continental slope west of the British Isles. *Journal of Fish Biology*, 54(1):152–170, 1999
- N. V. Collette, B. B.and Parin. Shallow-water fishes of Walters Shoals, Madagascar Ridge. *Bulletin of Marine Science*, 48(1):1–22, 1991
- I. B. Daban, A. Ismen, M. A. Ihsanoglu, and K. Cabbar. Age, growth and reproductive biology of the saddled seabream (*Oblada melanura*) in the North Aegean Sea, Eastern Mediterranean. *Oceanological and Hydrobiological Studies*, 49 (1):13–22, 2020
- T. T. Daley and R. T. Leaf. Age and growth of Atlantic chub mackerel (*Scomber colias*) in the Northwest Atlantic. *Journal of Northwest Atlantic Fishery Science*, 50, 2019
- J. Davenport. *Synopsis of biological data on the lumpsucker, Cyclopterus lumpus (Linnaeus, 1758)*. Food & Agriculture Organization of the United Nation (FAO), Rome, 1985. ISBN 92-5-102330-1
- J. Delgado, S. Reis, J. A. González, E. Isidro, M. Biscoito, M. Freitas, and V. M. Tuset. Reproduction and growth of *Aphanopus carbo* and *A. intermedius* (Teleostei: Trichiuridae) in the northeastern Atlantic. *Journal of Applied Ichthyology*, 29(5):1008–1014, 2013
- M. R. Dunn. Review and stock assessment of black cardinalfish (*Epigonus telescopus*) on the east coast North Island, New Zealand. *New Zealand Fisheries Assessment Report*, 39:55, 2009

- J. Dürr and J.A González. Feeding habits of *Beryx splendens* and *Beryx decadactylus* (Berycidae) off the Canary Islands. *Fisheries Research*, 54(3):363–374, 2002

- H. Endo, D. Tsutsui, and K. Amaoka. Range extensions of two deep-sea macrourids *Coryphaenoides filifer* and *Squalogadus modificatus* to the Sea of Okhotsk. *Japanese Journal of Ichthyology*, 41(3):330–333, 1994

- W. N. Eschmeyer and J. C. Hureau. *Sebastes mouchezi*, a senior synonym of *Helicolenus tristanensis*, with comments on *Sebastes capensis* and zoogeographical considerations. *Copeia*, 1971(3):576–579, 1971

- I. Farias, B. Morales-Nin, P. Lorance, and I. Figueiredo. Black scabbardfish, *Aphanopus carbo*, in the northeast Atlantic: distribution and hypothetical migratory cycle. *Aquatic Living Resources*, 26(4):333–342, 2013.

- I. Farias, E. Couto, N. Lagarto, J. Delgado, Adelino V.M. Canário, and I. Figueiredo. Sex steroids of black scabbardfish, *Aphanopus carbo*, in relation to reproductive and migratory dynamics. *Aquaculture and Fisheries*, 2020.

- G. E. Fenton, S. A. Short, and D. A. Ritz. Age determination of orange roughy, *Hoplostethus atlanticus* (Pisces: Trachichthyidae) using 210 Pb: 226 Ra disequilibria. *Marine Biology*, 109(2):197–202, 1991

- I. Fossen and O. A. Bergstad. Distribution and biology of blue hake, *Antimora rostrata* (Pisces: Moridae), along the mid-Atlantic Ridge and off Greenland. *Fisheries Research*, 82(1-3):19–29, 2006

- S. Furukawa, R. Kawabe, S. Ohshimo, K. Fujioka, G. N. Nishihara, Y. Tsuda, T. Aoshima, H. Kanehara, and H. Nakata. Vertical movement of dolphinfish *Coryphaena hippurus* as recorded by acceleration data-loggers in the northern East China Sea. *Environmental Biology of Fishes*, 92(1):89, 2011

- J. A. González, A. Matins, J. I. Santana Morales, R. Triay-Portella, C. Monteiro, V. García-Martín, Jiménez N. S., G. González Lorenzo, J. G. Pajuelo, and J. M. Lorenzo. New and rare records of teleost fishes from the Cape Verde Islands (eastern-central Atlantic Ocean). *Cybium*, 2014

- C. P. Goodyear, J. Luo, E. D. Prince, J. P. Hoolihan, D. Snodgrass, E. S. Orbesen, and J. E. Serafy. Vertical habitat use of Atlantic blue marlin *Makaira nigricans*: interaction with pelagic longline gear. *Marine Ecology Progress Series*, 365: 233–245, 2008

- J.D.M Gordon and J.A.R Duncan. The ecology of the deep-sea benthic and benthopelagic fish on the slopes of the Rockall Trough, Northeastern Atlantic. *Progress in Oceanography*, 15(1):37–69, 1985

- Baltic Marine Environment Protection Commission. Species information sheet: *Lycodes gracilis*. Technical report, 2013a. URL https://helcom.fi/media/red%20list%20species%20information%20sheet/HELCOM-Red-List-Lycodes-gracilis.pdf
- Baltic Marine Environment Protection Commission. Species information sheet: *Scomber scombrus*. Technical report, 2013b. URL https://helcom.fi/wp-content/uploads/2019/08/HELCOM-Red-List-Scomber-scombrus.pdf
- J. P. Hoolihan, J. Luo, D. Snodgrass, E. S. Orbesen, A. M. Barse, and E. D. Prince. Vertical and horizontal habitat use by white marlin *Kajikia albida* (Poey, 1860) in the western North Atlantic Ocean. *ICES Journal of Marine Science*, 72(8): 2364–2373, 2015
- K. H. Kock and I. Everson. Biology and ecology of mackerel icefish, *Champsocephalus gunnari*: an Antarctic fish lacking hemoglobin. *Comparative Biochemistry and Physiology Part A: Physiology*, 118(4):1067–1077, 1997
- A. Işmen. Age, growth and reproduction of the goldband goatfish, *Upeneus moluccensis* (Bleeker, 1855), in Iskenderun Bay, the Eastern Mediterranean. *Turkish Journal of Zoology*, 29(4):301–309, 2005
- T. Iwamoto. The macrourid fish *Cetonurus globiceps* in the Gulf of Mexico. *Copeia*, 1966:439–442, 1966
- S. Jennings, G. J. Hewlett, and S. Flatman. The distribution, migrations and stock integrity of lemon sole *Microstomus kitt* in the western English Channel. *Fisheries Research*, 18(3-4):377–388, 1993
- J. Kennedy, S. Jónsson, J. M. Kasper, and H. G. Olafsson. Movements of female lumpfish (*Cyclopterus lumpus*) around Iceland. *ICES Journal of Marine Science*, 72 (3):880–889, 2015
- J. Kennedy, S. Jónsson, H. G. Olafsson, and J. M. Kasper. Observations of vertical movements and depth distribution of migrating female lumpfish (*Cyclopterus lumpus*) in iceland from data storage tags and trawl surveys. *ICES Journal of Marine Science*, 73(4):1160–1169, 2016
- S. J. Lin, M. K. Musyl, S. P. Wang, N. J. Su, W. C. Chiang, C. P. Lu, K. Tone, C. Y. Wu, A. Sasaki, and I. Nakamura. Movement behaviour of released wild and farm-raised dolphinfish *Coryphaena hippurus* tracked by pop-up satellite archival tags. *Fisheries Science*, 85(5):779–790, 2019
- R. Lubbock and A. Edwards. The fishes of Saint Paul's rocks. *Journal of Fish Biology*, 18(2):135–157, 1981

- J. V. Magnússon. Distribution and some other biological parameters of two morid species *Lepidion eques* (Günther, 1887) and *Antimora rostrata* (Günther, 1878) in Icelandic waters. *Fisheries Research*, 51(2-3):267–281, 2001
- C. S. Manooch III and J. C. Potts. Age, growth, and mortality of greater amberjack, *Seriola dumerili*, from the US Gulf of Mexico headboat fishery. *Bulletin of Marine Science*, 61(3):671–683, 1997
- E. Massutí and B. Morales-Nin. Seasonality and reproduction of dolphin-fish (*Coryphaena hippurus*) in the western Mediterranean. *Scientia Marina*, 59(3-4): 357–364, 1995
- T. Matsui, S. Kato, and S. E. Smith. Biology and potential use of Pacific grenadier, *Coryphaenoides acrolepis*, off California. *Marine Fisheries Review*, 52(3):1–17, 1991
- M. R. S. Melo, A. C. Braga, G. W. A. Nunan, and P. A. S. Costa. On new collections of deep-sea Gadiformes (Actinopterygii: Teleostei) from the Brazilian continental slope, between 11 and 23 °S. *Zootaxa*, 2433(1):25–46, 2010
- N. R. Merrett. *Macrouridae of the eastern North Atlantic*. International Council for the Exploration of the Sea (ICES), 1986. ISBN 978-87-7482-954-6
- N .R. Merrett. Preliminary guide to the identification of the early life history stages of bathygadid & macrourid fishes of the western central North Atlantic. Florida, USA, 2003. National Oceanic and Atmospheric Administration (NOAA)
- W. Merten, R. Appeldoorn, R. Rivera, and D. Hammond. Diel vertical movements of adult male dolphinfish (*Coryphaena hippurus*) in the western central Atlantic as determined by use of pop-up satellite archival transmitters. *Marine Biology*, 161(8):1823–1834, 2014
- Marine Research Section. Acanthuridae. In *Fishes of the Maldives*. Ministry of Fisheries and Agriculture, Male, Republic of Maldives, 1997. ISBN 99915-62-12-5
- M. R. Navarro, B. Villamor, S. Myklevoll, J. Gil, P. Abaunza, and J. Canoura. Maximum size of Atlantic mackerel (*Scomber scombrus*) and Atlantic chub mackerel (*Scomber colias*) in the Northeast Atlantic. *Cybium*, 36(2):406–408, 2012
- E. T. Nolan, K. J. Downes, A. Richardson, A. Arkhipkin, P. Brickle, J. Brown, R. J. Mrowicki, Z. Shcherbich, N. Weber, and S. B. Weber. Life-history strategies of the rock hind grouper *Epinephelus adscensionis* at Ascension Island. *Journal of Fish Biology*, 91(6):1549–1568, 2017
- H. A. Oxenford. Biology of the dolphinfish (*Coryphaena hippurus*) in the western central Atlantic: a review. *Scientia Marina*, 63(3-4):277–301, 1999

- A. Pallaoro, P. Cetinić, J. Dulčić, I. Jardas, and M. Kraljević. Biological parameters of the saddled bream *Oblada melanura* in the eastern Adriatic. *Fisheries Research*, 38(2):199–205, 1998

- B. C. Russell, D. Golani, and Y. Tikochinski. *Saurida lessepsianus* a new species of lizardfish (Pisces: Synodontidae) from the Red Sea and Mediterranean Sea, with a key to *Saurida* species in the Red Sea. *Zootaxa*, 3956(4):559–568, 2015

- F. Sánchez, N. Pérez, and J. Landa. Distribution and abundance of megrim (*Lepidorhombus boscii* and *Lepidorhombus whiffiagonis*) on the northern Spanish shelf. *ICES Journal of Marine Science*, 55(3):494–514, 1998

- C. A. Sepulveda, S. A. Aalbers, S. Ortega-Garcia, N. C. Wegner, and D. Bernal. Depth distribution and temperature preferences of wahoo (*Acanthocybium solandri*) off Baja California Sur, Mexico. *Marine Biology*, 158(4):917–926, 2011

- R. A. Shinozaki-Mendes, F. H. V. Hazin, P. G. De Oliveira, and F. C. De Carvalho. Reproductive biology of the squirrelfish, *Holocentrus adscensionis* (Osbeck, 1765), caught off the coast of Pernambuco, Brazil. *Scientia Marina*, 71(4):715–722, 2007

- I. Solberg and S. Kaartvedt. The diel vertical migration patterns and individual swimming behavior of overwintering sprat *Sprattus sprattus*. *Progress in Oceanography*, 151:49–61, 2017

- G. W. Stunz and D. M. Coffey. A review of the ecological performance and habitat value of standing versus reefed oil and gas platform habitats in the Gulf of Mexico. Louisiana, USA, 2020. Gulf Offshore Research Institute (GORI)

- T. B. Sutton, T. T.and Letessier and B. Bardarson. Midwater fishes collected in the vicinity of the Sub-Polar Front, Mid-North Atlantic Ocean, during ECOMAR pelagic sampling. *Deep Sea Research Part II: Topical Studies in Oceanography*, 98: 292–300, 2013

- T. C. Theisen and J. D. Baldwin. Movements and depth/temperature distribution of the ectothermic Scombrid, *Acanthocybium solandri* (wahoo), in the western North Atlantic. *Marine Biology*, 159(10):2249–2258, 2012

- C. N. Trueman, R. E. M. Rickaby, and S. Shephard. Thermal, trophic and metabolic life histories of inaccessible fishes revealed from stable-isotope analyses: a case study using orange roughy *Hoplostethus atlanticus*. *Journal of Fish Biology*, 83(6):1613–1636, 2013

- G. Tserpes, F. Fiorentino, D. Levi, A. Cau, M. Murenu, A. Zamboni, and C. Papaconstantinou. Distribution of *Mullus barbatus* and *M. surmuletus* (Osteichthyes: Perciformes) in the Mediterranean continental shelf: implications for management. *Scientia Marina*, 66(S2):39–54, 2002

- K. Tsagarakis, M. Giannoulaki, S. Somarakis, and A. Machias. Variability in positional, energetic and morphometric descriptors of European anchovy *Engraulis encrasicolus* schools related to patterns of diurnal vertical migration. *Marine Ecology Progress Series*, 446:243–258, 2012
- J. J. Vaudo, M. E. Byrne, B. M. Wetherbee, G. M. Harvey, A. Mendillo Jr, and M. S. Shivji. Horizontal and vertical movements of white marlin, *Kajikia albida*, tagged off the Yucatán Peninsula. *ICES Journal of Marine Science*, 75(2):844–857, 2018
- B. L. Winner, K. E. Flaherty-Walia, T. S. Switzer, and J. L. Vecchio. Multidecadal evidence of recovery of nearshore red drum stocks off West-Central Florida and connectivity with inshore nurseries. *North American Journal of Fisheries Management*, 34(4):780–794, 2014.
- N. M. Whitney, M. Taquet, R. W. Brill, C. Girard, G. D. Schwieterman, L. Dagorn, and K. N. Holland. Swimming depth of dolphinfish (*Coryphaena hippurus*) associated and unassociated with fish aggregating devices. *Fishery Bulletin*, 114 (4), 2016
- Y. Yamanoue and K. Matsuura. *Doederleinia gracilispinis* (Fowler, 1943), a junior synonym of *Doederleinia berycoides* (Hilgendorf, 1879), with review of the genus. *Ichthyological Research*, 54(4):404–411, 2007

Appendix B

Length-weight parameters

B.1 Length-weight parameters

TABLE B.1: Parameters for the length-weight equation 2.8 ($W = aL^b$). For length types, TL = total length, SL = standard length, FL = fork length, HL = head length, GNPL = gnathoproctal length.

Species	Length type	a	b	Notes
Acanthocybium solandri	TL	0.0023	3.24	
Acanthurus triostegus	TL	0.0213	3.08	
Alepocephalus agassizii	SL	0.0035	3.29	
Alepocephalus bairdii	TL	0.0031	3.21	
Aphanopus carbo	TL	0.0005	3.21	
Antimora rostrata	TL	0.0008	3.58	
Argentina silus	TL	0.0030	3.26	
Arripus georgianus	FL	0.0065	2.85	From *Arripus trutta*
Ateleopus japonicus	TL	0.0001	3.51	From *Ijmaia antillarium*
Bathygadus nipponicus	TL	0.0389	2.95	Used average parameters for *Bathygadus*
Bathypterois dubius	TL	0.0016	3.29	
Bathysaurus ferox	SL	0.0011	3.47	
Beryx splendens	TL	0.0087	3.10	
Cataetyx laticeps	SL	0.0045	3.11	
Cetonurus globiceps	TL	0.0025	3.15	Used average parameters for Macrouridae
Chaetodon ulietensis	FL	0.0311	2.87	

Coelorinchus caelorhincus	TL	0.0046	3.04	
Coelorinchus fasciatus	TL	0.0046	3.04	From *Coelorinchus caelorhincus*
Coelorinchus labiatus	HL	0.1450	3.02	
Conger conger	TL	0.0003	3.43	
Coris julis	SL	0.0069	3.03	
Coryphaenoides acrolepis	FL	0.0006	3.45	
Coryphaenoides armatus	HL	0.2188	3.12	
Coryphaenoides guentheri	HL	0.8921	2.58	
Coryphaenoides marginatus	TL	0.0025	3.15	Used average parameters for Macrouridae
Coryphaenoides mediterraneus	HL	0.4966	3.04	
Coryphaenoides paramarshalli	HL	0.2610	3.35	From *Corypahenoides guentheri*
Coryphaenoides profundicolus	HL	0.2115	3.38	
Coryphaenoides rupestris	HL	0.2310	3.29	
Diplodus vulgaris	SL	0.0117	3.23	
Dissostichus eleginoides	SL	0.0059	3.24	
Electrona antarctica	SL	0.0074	3.27	
Engraulis japonicus	SL	0.0039	3.68	
Epigonus telescopus	SL	0.0111	3.16	
Epinephelus morio	TL	0.0123	3.04	
Epinephelus multinotatus	TL	0.0126	3.04	
Gadus morhua	TL	0.0066	3.10	
Gobius bucchichi	TL	0.0071	3.15	
Halosauropsis macrochir	GNPL	0.0084	3.18	
Hoplosteuthis atlanticus	SL	0.0074	2.78	
Hoplosteuthis mediterraneus	SL	0.0295	3.01	
Helicolenus dactylopterus	TL	0.0126	3.09	
Helicolenus mouchezi	TL	0.0126	3.09	From *Helicolenus dactylopterus*
Hymenocephalus lethonemus	TL	0.0077	2.45	
Hyporthodus nigritus	TL	0.0201	2.98	
Ijmaia dofleini	TL	0.0001	3.51	From *Ijmaia antillarium*
Kajikia albida	FL	0.0046	3.00	
Lepidoperca coatsii	TL	0.0046	3.15	Used average parameters for *Baldwinella*
Lepidorhombus whiffiagonis	TL	0.0036	3.17	
Lepidion eques	TL	0.0009	3.54	
Lethrinus harak	TL	0.0151	3.01	

Lethrinus lentjan	TL	0.0240	2.80	
Lutjanus sebae	FL	0.0148	3.09	
Makaira nigricans	FL	0.0054	3.07	
Malacocephalus laevis	TL	0.0324	2.94	
Melanogrammus aeglefinus	TL	0.0058	3.13	
Merluccius merluccius	TL	0.0047	3.21	
Molva dypterygia	TL	0.0019	3.15	
Mora moro	TL	0.0044	3.21	
Micromesistius poutassou	TL	0.0032	3.20	
Mullus barbatus	TL	0.0076	3.11	
Nezuma aequalis	HL	0.8878	3.78	
Nezuma duodecim	HL	0.8878	3.78	From *Nezuma aequalis*
Neoscopelus microchir	TL	0.0095	2.99	
Pagrus auratus	TL	0.0427	2.70	
Pagrus caeruleostictus	TL	0.0269	2.81	
Pagellus erythrinus	TL	0.0166	2.92	
Plagiogeneion rubiginosum	SL	0.0148	3.11	
Pollachius virens	TL	0.0072	3.05	
Phycis blennoides	TL	0.0042	3.19	
Pristipomoides multidens	FL	0.0224	2.95	
Rouleina attrita	SL	0.0137	2.87	
Saurida undosquamis	TL	0.0054	3.07	
Scomber colias	TL	0.0102	2.96	
Scomber scombrus	TL	0.0035	3.25	
Scophthalmus maximus	TL	0.0120	3.10	
Sebastes melanops	TL	0.0211	3.00	
Seriola dumerili	TL	0.0200	2.88	
Spectrunculus grandis	SL	0.0083	2.94	
Sebastes mentella	TL	0.0127	3.00	
Solea solea	TL	0.0066	3.10	
Squalogadus modificatus	TL	0.0025	3.15	Used average parameters for Macrouridae
Synaphobranchus kaupii	SL	0.0016	3.00	
Thunnus maccoyii	FL	0.0174	3.05	
Thunnus orientalis	FL	0.0166	3.00	
Trachyrincus murrayi	HL	0.1503	3.00	
Trachyrincus scabrus	HL	0.0444	3.53	
Upeneus moluccensis	TL	0.0060	3.25	
Xenodermichthys copei	TL	0.0058	3.00	

B.2 Sources

- R. Crec'Hriou, V. Zintzen, L. Moore, and C.D. Roberts. Length–weight relationships of 33 fish species from New Zealand. *Journal of Applied Ichthyology*, 31(3):558–561, 2015
  - *Halosauropsis macrochir*
- M. C. Deval, O. Güven, İ. Saygu, and T. Kabapçioğlu. Length-weight relationships of 10 fish species found off Antalya Bay, eastern Mediterranean. *Journal of Applied Ichthyology*, 30(3):567–568, 2014
  - *Hymenocephalus lethonemus*
- J. A. Godbold, D. M. Bailey, M. A. Collins, J. D. M. Gordon, W. A. Spallek, and I. G. Priede. Putative fishery-induced changes in biomass and population size structures of demersal deep-sea fishes in ICES Sub-area VII, Northeast Atlantic Ocean. *Biogeosciences*, 10(1):529–539, 2013
  - *Alepocephalus agassizii*
  - *Cataetyx laticeps*
  - *Coelorinchus labiatus*
  - *Coryphaenoides guentheri*
  - *Coryphaenoides mediterraneus*
  - *Coryphaenoides profundicolus*
  - *Coryphaenoides rupestris*
  - *Epigonus telescopus*
  - *Hoplosteuthis atlanticus*
  - *Nezuma aequalis*
  - *Rouleina attrita*
  - *Spectrunculus grandis*
  - *Trachyrincus murrayi*
  - *Trachyrincus scabrus*
- A. Soldo. Length-weight relationships for the fifty littoral and coastal marine fish species from the Eastern Adriatic Sea. *Acta Adriatica: International Journal of Marine Sciences*, 61(2):205–210, 2020
  - *Gobius bucchichi*
- R. Froese and D. Pauly. Fishbase, 2021. URL `www.fishbase.org`. Publisher: Fisheries Centre, University of British Columbia
  - All other species.

Appendix C

Morphometrics

C.1 Morphological information

TABLE C.1: Morphological information for species in the main dataset. * = *Incertae sedis* Abbreviations for body shape: Ee = eel like, El = elongate, FN = fusiform/normal, SD = short/deep.

Classification		Body shape	Body depth %	Caudal aspect ratio
Species	Order			
Acanthurus triostegus	Acanthuriformes	SD	41.70	1.92
Chaetodon ulietensis	Acanthuriformes	SD	51.40	2.26
Alepocephalus agassizii	Alepocephaliformes	El	19.20	2.29
Alepocephalus bairdii	Alepocephaliformes	El	15.60	1.38
Rouleina attrita	Alepocephaliformes	El	18.79	1.98
Xenodermichthys copei	Alepocephaliformes	El	17.46	1.91
Conger conger	Anguilliformes	Ee	7.70	NA
Synaphobranchus kaupii	Anguilliformes	Ee	7.30	NA
Argentina silus	Argentiniformes	El	16.88	1.48

Ateleopus japonicus	Ateleopodiformes	El	11.50	NA
Ijimaia dofleini	Ateleopodiformes	El	NA	NA
Bathysaurus ferox	Aulopiformes	Ee	9.54	1.12
Bathypterois dubius	Aulopiformes	El	12.03	2.49
Saurida lessepsianus	Aulopiformes	El	13.19	2.45
Saurida undosquamis	Aulopiformes	El	12.78	2.58
Exocoetus volitans	Beloniformes	El	12.80	1.66
Beryx splendens	Beryciformes	SD	29.11	3.26
Hoplostethus atlanticus	Beryciformes	SD	36.77	2.31
Hoplostethus mediterraneus	Beryciformes	SD	34.13	1.43
Seriola dumerili	Carangiformes	FN	26.46	2.83
Trachurus trachurus	Carangiformes	FN	19.67	2.90
Coryphaena hippurus	Carangiformes	El	18.18	1.82
Sprattus sprattus	Clupeiformes	FN	19.55	2.05
Engraulis encrasicolus	Clupeiformes	El	14.38	1.19
Boreogadus saida	Gadiformes	El	18.70	1.71
Gadus morhua	Gadiformes	FN	20.83	1.30
Melanogrammus aeglefinus	Gadiformes	FN	22.34	1.43
Merlangius merlangus	Gadiformes	FN	21.22	0.97
Micromesistius poutassou	Gadiformes	El	15.32	0.79

Pollachius virens	Gadiformes	FN	22.29	1.96
Molva dypterygia	Gadiformes	El	11.58	0.83
Bathygadus nipponicus	Gadiformes	El	14.25	NA
Cetonurus globiceps	Gadiformes	FN	21.88	NA
Coelorinchus caelorhincus	Gadiformes	El	15.51	NA
Coelorinchus fasciatus	Gadiformes	El	17.56	NA
Coelorinchus labiatus	Gadiformes	El	12.56	NA
Coryphaenoides acrolepis	Gadiformes	El	15.96	NA
Coryphaenoides armatus	Gadiformes	El	18.06	NA
Coryphaenoides guentheri	Gadiformes	El	13.93	NA
Coryphaenoides marginatus	Gadiformes	El	11.10	NA
Coryphaenoides mediterraneus	Gadiformes	El	17.81	NA
Coryphaenoides paramarshalli	Gadiformes	El	NA	NA
Coryphaenoides profundicolus	Gadiformes	El	NA	NA
Coryphaenoides rupestris	Gadiformes	El	14.61	0.21
Hymenocephalus lethonemus	Gadiformes	El	NA	NA
Malacocephalus laevis	Gadiformes	El	19.11	NA
Nezumia aequalis	Gadiformes	El	17.49	NA
Nezumia duodecim	Gadiformes	El	12.59	NA
Spicomacrurus kuronumai	Gadiformes	El	NA	NA

Squalogadus modificatus	Gadiformes	El	22.54	NA
Trachyrincus murrayi	Gadiformes	El	12.72	NA
Trachyrincus scabrus	Gadiformes	El	14.79	NA
Merluccius merluccius	Gadiformes	El	14.17	0.90
Antimora rostrata	Gadiformes	FN	26.27	1.90
Lepidion eques	Gadiformes	FN	19.93	0.74
Mora moro	Gadiformes	FN	22.97	0.93
Phycis blennoides	Gadiformes	FN	22.52	0.80
Gobius bucchichi	Gobiiformes	El	13.36	0.95
Holocentrus adscensionis	Holocentriformes	FN	26.49	2.11
Plagiogeneion rubiginosum	Eupercaria*	FN	24.73	3.37
Lutjanus fulviflamma	Eupercaria*	SD	29.27	2.14
Lutjanus sebae	Eupercaria*	SD	35.35	1.61
Pristipomoides filamentosus	Eupercaria*	FN	24.60	3.33
Pristipomoides multidens	Eupercaria*	FN	24.30	2.51
Kajikia albida	Istiophoriformes	El	10.40	7.82
Makaira nigricans	Istiophoriformes	El	15.30	7.77
Coris julis	Labriformes	FN	21.43	1.68
Electrona antarctica	Myctophiformes	FN	25.75	1.03
Electrona carlsbergi	Myctophiformes	FN	21.51	2.21

Gymnoscopelus braueri	Myctophiformes	El	14.36	NA
Gymnoscopelus nicholsi	Myctophiformes	El	15.33	2.61
Krefftichthys anderssoni	Myctophiformes	El	17.77	1.10
Protomyctophum bolini	Myctophiformes	El	12.59	NA
Neoscopelus microchir	Myctophiformes	FN	25.14	2.33
Halosauropsis macrochir	Notacanthiformes	Ee	7.70	NA
Cataetyx l aticeps	Ophidiiformes	El	16.22	NA
Spectrunculus grandis	Ophidiiformes	El	18.95	NA
Doederleinia berycoides	Pempheriformes	SD	29.08	1.12
Epigonus telescopus	Pempheriformes	FN	22.09	1.16
Champsocephalus gunnari	Perciformes	El	12.60	1.53
Artediellus atlanticus	Perciformes	El	18.20	0.55
Triglops nybelini	Perciformes	El	18.37	0.46
Cyclopterus lumpus	Perciformes	SD	34.83	0.73
Dissostichus eleginoides	Perciformes	El	17.70	1.23
Helicolenus dactylopterus	Perciformes	SD	28.79	2.12
Helicolenus mouchezi	Perciformes	FN	25.82	1.23
Sebastes mentella	Perciformes	SD	29.43	1.79
Epinephelus adscensionis	Perciformes	SD	29.37	0.97
Epinephelus morio	Perciformes	SD	29.60	1.02

Epinephelus multinotatus	Perciformes	FN	27.90	1.64
Hyporthodus nigritus	Perciformes	SD	33.70	1.08
Lepidoperca coatsii	Perciformes	SD	28.30	0.79
Lycodes gracilis	Perciformes	Ee	12.04	NA
Glyptocephalus cynoglossus	Pleuronectiformes	SD	32.52	1.11
Hippoglossoides platessoides	Pleuronectiformes	SD	36.30	1.26
Limanda limanda	Pleuronectiformes	SD	36.23	1.11
Microstomus kitt	Pleuronectiformes	SD	36.72	1.61
Lepidorhombus whiffiagonis	Pleuronectiformes	SD	29.33	1.10
Scophthalmus maximus	Pleuronectiformes	SD	54.87	1.77
Solea solea	Pleuronectiformes	SD	28.06	1.40
Salmo salar	Salmoniformes	El	16.15	3.18
Arripis georgianus	Scombriformes	FN	24.62	1.87
Acanthocybium solandri	Scombriformes	El	13.49	5.62
Scomber colias	Scombriformes	FN	20.33	2.21
Scomber scombrus	Scombriformes	El	17.30	3.05
Thunnus albacares	Scombriformes	FN	24.69	7.65
Thunnus maccoyii	Scombriformes	FN	27.17	5.80
Thunnus orientalis	Scombriformes	FN	23.94	4.86
Aphanopus carbo	Scombriformes	Ee	10.20	2.86

Lethrinus harak	Spariformes	SD	29.90	2.31
Lethrinus lentjan	Spariformes	SD	33.00	2.31
Chrysophrys auratus	Spariformes	SD	34.50	3.30
Diplodus vulgaris	Spariformes	SD	37.42	1.52
Oblada melanura	Spariformes	SD	29.47	2.49
Pagellus erythrinus	Spariformes	SD	29.85	2.60
Pagrus caeruleostictus	Spariformes	SD	33.55	1.44
Mullus barbatus	Syngnathiformes	FN	19.52	1.97
Upeneus moluccensis	Syngnathiformes	FN	21.93	1.98

C.2 Sources

- Anon. *Plagiogeneion rubiginosum*, 2019. URL https://www.fishbase.de/photos/UploadedBy.php?autoctr=36802&win=uploaded
- Banón Díaz R. Photo(s) contributed by Rafael Bañón Díaz, 2009. URL https://www.fishbase.se/photos/PhotosList.php?id=377&vCollaborator=Rafael+Ba%C3%B1%C3%B3n+D%C3%ADaz
- CSIRO Australian National Fish Collection. Softskin slickhead *Rouleina attrita*, No Date. URL https://fishesofaustralia.net.au/Images/Image/RouleinAttritCSIRO.jpg
- CSIRO Australian National Fish Collection. A giant cuskeel *Spectrunculus grandis*, 2017. URL https://fishesofaustralia.net.au/Images/Image/SpectruncGrandis2CSIRO.jpg
- Cousseau M. B. *Coelorinchus fasciatus*, 1999. URL https://www.fishbase.se/photos/PicturesSummary.php?ID=7131&what=species
- J. Nielsen, M. Nielsen, and P. Frandsen. Deep Sea Creatures of the North Atlantic (DESCNA), 2021. URL https://descna.com/en/
- A. Dolgov. *Trachyrincus murrayi*, 2003. URL https://www.fishbase.de/photos/PicturesSummary.php?ID=27730&what=species

- C. Dowling. *Arripis georgiana*, No Date. URL https://www.fishbase.de/photos/UploadedBy.php?autoctr=15337&win=uploaded
- L. Duchatelet, C. Hermans, G. Duhamel, Y. Cherel, C. Guinet, and J. Mallefet. Coelenterazine detection in five myctophid species from the Kerguelen Plateau. In *The Kerguelen Plateau: Marine Ecosystem + Fisheries: Proceedings of the Second Symposium*, 2019
- A. Garazo Fabregat. *Coryphaenoides rupestris*, 2002. URL https://www.fishbase.de/photos/PicturesSummary.php?ID=332&what=species
- J. A. González, A. Matins, J. I. Santana Morales, R. Triay-Portella, C. Monteiro, V. García-Martín, Jiménez N. S., G. González Lorenzo, J. G. Pajuelo, and J. M. Lorenzo. New and rare records of teleost fishes from the Cape Verde Islands (eastern-central Atlantic Ocean). *Cybium*, 2014
- H. Heessen. *Sprattus sprattus*, 2006. URL https://www.marinespecies.org/berms/aphia.php?p=image&tid=126425&pic=2318
- P. Koubbi and P. Pruvost. Specimen of *Krefftichthys anderssoni* (lanternfish), 2008. URL http://mersaustrales.mnhn.fr/blog-en/mersaustrales.mnhn.fr/blog_mission/images/Umitaka/01%2002%2008/UM16_02V.jpg
- V. Loeb. *Electrona antarctica*, 2018. URL https://en.wikipedia.org/wiki/File:Fish8712.jpg
- J. L. May and J. G. H. Maxwell. *Thunnus maccoyii*, 1986. URL https://www.fishbase.se/photos/PicturesSummary.php?StartRow=3&ID=145&what=species&TotRec=7
- R. M. McDowall. *Salmo salar*, 1990. URL https://www.fishbase.se/photos/PicturesSummary.php?StartRow=5&ID=236&what=species&TotRec=17
- M. McGrouther. A deepsea lizardfish, *Bathysaurus ferox*, No Date. URL https://fishesofaustralia.net.au/Images/Image/BathysaurusFeroxS047.jpg
- McPhee R. and M. McGrouther. Globehead whiptail, *Cetonurus globiceps*, No Date. URL https://fishesofaustralia.net.au/Images/Image/C-globiceps-S072_232_web.jpg
- T. Meyer. *Conger conger*, 2006. URL https://www.fishbase.se/photos/UploadedBy.php?autoctr=13419&win=uploaded
- Motomura H. Pacific bluefin tuna, 2022. URL https://fishider.org/en/guide/osteichthyes/scombridae/thunnus/thunnus-orientalis

- National Institute of Water and Atmospheric Research (NIWA). A selection of mesopelagic fish species caught in the deep scattering layers observed in the Antarctic Convergence Zone, 2018. URL https://niwa.co.nz/file/42902
- C. Nozères. *Triglops nybelini* - trio of bigeye sculpins, 2010. URL https://www.marinespecies.org/aphia.php?p=image&tid=127206&pic=30207
- C. Nozères. *Synaphobranchus kaupii* - northern cutthroat eel, 2011. URL https://www.marinespecies.org/photogallery.php?album=735&pic=37817
- A. Orlov. Photo(s) contributed by Alexei Orlov, 2009. URL https://www.fishbase.se/photos/PhotosList.php?id=1287&vCollaborator=Alexei+Orlov
- G. Paz. *Oblada melanura*, 2012. URL http://v3.boldsystems.org/pics/BIM/E137.1%2B978321600.JPG
- Pena L. *Trachyrincus scabrus*, 2002. URL http://www.ictioterm.es/nombre_cientifico.php?nc=322
- R. Pillon. *Gobius bucchichi*, 2016. URL https://www.fishbase.se/photos/PicturesSummary.php?StartRow=1&ID=46334&what=species&TotRec=3
- B. C. Russell, D. Golani, and Y. Tikochinski. *Saurida lessepsianus* a new species of lizardfish (Pisces: Synodontidae) from the Red Sea and Mediterranean Sea, with a key to *Saurida* species in the Red Sea. *Zootaxa*, 3956(4):559–568, 2015
- K. T. Shao. Photo(s) contributed by Kwang-Tsao Shao, 2009. URL https://www.fishbase.se/photos/PhotosList.php?id=41&vCollaborator=Kwang-Tsao+Shao
- Smithsonian National Museum of Natural History. *Lepidoperca coatsii*, USNM 394682, 2004. URL http://n2t.net/ark:/65665/338375a58-eae0-4225-b77d-e829767b914d
- K. Tse. Saithe (*Pollachius virens*), 2011. URL http://muskiebaitadventures.blogspot.com/p/saithe.html

Appendix D

$\delta^{13}C_{musc}$ values and sources

D.1 $\delta^{13}C_{musc}$ values

TABLE D.1: Estimated $\delta^{13}C$ values for muscle ($\delta^{13}C_{musc}$), used to estimate diet. $\delta^{13}C_{musc}$ values were assigned by species, year of capture, location (latitude and longitude in decimal degrees), and lipid correction status

Species	Year of collection		Location		$\delta^{13}C_{musc}$		Lipid corrected?
	Otolith	Muscle	Lat.	Long.	mean	s.d.	
Acanthocybium solandri	2019	2015	-8.68	-14.53	-17.05	0.64	Yes
Acanthocybium solandri	2015	2015	-8.68	-14.53	-17.05	0.64	Yes
Acanthocybium solandri	2018	2015	-8.68	-14.53	-17.05	0.64	Yes
Acanthurus triostegus	1994	2005	-15.74	-144.63	-14.05	2.35	No
Alepocephalus agassizii	2009	2009	57.70	-9.94	-18.53	0.30	No
Alepocephalus agassizii	2009	2009	57.65	-9.73	-18.53	0.30	No
Alepocephalus bairdii	2006	2006	54.08	-13.92	-18.64	0.54	No
Alepocephalus bairdii	2006	2006	54.08	-13.92	-18.64	0.54	No
Antimora rostrata	2006	2006	54.08	-13.92	-18.32	0.33	No
Antimora rostrata	2009	2009	57.38	-10.01	-18.32	0.33	No
Antimora rostrata	2006	2006	54.08	-13.92	-18.32	0.33	No
Aphanopus carbo	2006	2006	54.08	-13.92	-18.01	0.25	No
Aphanopus carbo	2009	2009	57.60	-12.91	-18.01	0.25	No
Aphanopus carbo	2011	2011	57.27	-9.52	-18.01	0.25	No
Argentina silus	2009	2009	58.74	-8.01	-18.89	0.60	No
Arripis georgianus	1998	2004	-29.24	114.90	-16.21	3.07	No
Arripis georgianus	1997	2004	-31.95	115.62	-16.21	3.07	No
Arripis georgianus	1997	2004	-33.32	115.61	-16.21	3.07	No
Arripis georgianus	1997	2004	-35.04	117.88	-16.21	3.07	No

Arripis georgianus	1997	2004	-33.86	121.91	-16.21	3.07	No
Arripis georgianus	1997	2004	-32.22	133.13	-16.21	3.07	No
Artediellus atlanticus	2019	2011	72.80	23.29	-18.22	0.73	Yes
Ateleopus japonicus	2013	2006	24.88	121.92	-15.37	1.76	No
Ateleopus japonicus	2010	2006	24.61	121.95	-15.37	1.76	No
Bathygadus nipponicus	2010	2009	22.43	120.10	-17.04	1.51	No
Bathypterois dubius	2006	2006	54.08	-13.92	-17.84	0.11	No
Bathypterois dubius	2009	2009	56.14	-9.66	-17.84	0.11	No
Bathypterois dubius	2009	2009	57.11	-12.07	-17.84	0.11	No
Bathysaurus ferox	1976	2008	31.74	-11.20	-17.59	0.08	Yes
Bathysaurus ferox	1982	2008	49.87	-12.95	-17.59	0.08	Yes
Bathysaurus ferox	1976	2008	21.15	-18.13	-17.59	0.08	Yes
Bathysaurus ferox	1992	2008	50.17	-12.82	-17.59	0.08	Yes
Beryx splendens	2018	2011	-37.20	-12.52	-19.23	0.45	No
Boreogadus saida	2019	2019	72.80	23.29	-22.59	0.18	No
Boreogadus saida	2017	2019	72.80	23.29	-22.59	0.18	No
Cataetyx laticeps	2006	2006	54.08	-13.92	-16.30	0.01	No
Cataetyx laticeps	2009	2009	57.66	-9.92	-16.30	0.01	No
Cetonurus globiceps	1950	2018	36.90	15.90	-18.90	0.01	No
Cetonurus globiceps	1987	2018	20.49	-18.45	-18.90	0.01	No
Cetonurus globiceps	1976	2018	29.12	-12.69	-18.90	0.01	No
Chaetodon ulietensis	1994	2009	-15.74	-114.63	-11.15	2.70	No
Champsocephalus gunnari	2006	2005	-52.38	-36.81	-25.76	0.21	No
Coelorinchus caelorhincus	2006	2010	54.08	-13.92	-17.46	0.36	No
Coelorinchus caelorhincus	2006	2010	54.08	-13.92	-17.46	0.36	No
Coelorinchus caelorhincus	2009	2010	57.63	-9.61	-17.46	0.36	No
Coelorinchus caelorhincus	2009	2010	57.65	-9.98	-17.46	0.36	No
Coelorinchus fasciatus	2018	2006	-37.25	-12.53	-15.00	0.42	No
Coelorinchus labiatus	2006	2006	54.08	-13.92	-17.80	0.01	No
Conger conger	2006	2006	41.18	-8.72	-16.49	1.48	Yes
Conger conger	2006	2006	39.66	-28.70	-16.49	1.48	Yes
Conger conger	2006	2006	32.63	-16.92	-16.49	1.48	Yes
Conger conger	2006	2005	39.85	3.32	-18.62	0.44	No
Coris julis	2014	2010	38.42	14.98	-18.62	0.55	No
Coris julis	2014	2010	38.47	14.98	-18.62	0.55	No
Coryphaena hippurus	2004	2007	40.11	2.46	-18.30	0.30	Yes
Coryphaenoides acrolepis	2010	2008	22.43	120.10	-18.68	0.73	Yes
Coryphaenoides armatus	1989	2001	48.79	-16.50	-17.12	0.90	No
Coryphaenoides guentheri	2006	2006	54.08	-13.92	-17.43	0.62	No
Coryphaenoides guentheri	2006	2006	57.11	-12.07	-17.43	0.62	No
Coryphaenoides guentheri	1979	2002	51.11	-13.28	-16.40	1.20	No

Coryphaenoides mediterraneus	2006	2006	54.08	-13.92	-17.64	0.61	Yes
Coryphaenoides mediterraneus	1979	2009	49.45	-13.47	-17.64	0.61	No
Coryphaenoides mediterraneus	1982	2009	51.44	-13.02	-17.64	0.61	No
Coryphaenoides mediterraneus	1982	2009	49.53	-12.48	-17.64	0.61	No
Coryphaenoides mediterraneus	1979	2009	49.56	-13.47	-17.64	0.61	No
Coryphaenoides mediterraneus	1980	2009	49.57	-12.70	-17.64	0.61	No
Coryphaenoides paramarshalli	1987	2005	21.48	-18.45	-16.16	0.91	No
Coryphaenoides paramarshalli	1983	2005	14.85	-17.84	-16.16	0.91	No
Coryphaenoides profundicolus	1990	1997	21.01	-20.97	-17.84	0.01	No
Coryphaenoides profundicolus	1993	1997	20.93	-31.19	-17.84	0.01	No
Coryphaenoides profundicolus	1990	1997	20.15	-24.82	-17.84	0.01	No
Coryphaenoides profundicolus	1993	1997	20.86	-31.25	-17.84	0.01	No
Coryphaenoides profundicolus	1994	1997	48.91	-16.79	-17.84	0.01	No
Coryphaenoides profundicolus	1981	1997	49.85	-13.96	-17.84	0.01	No
Coryphaenoides rupestris	2006	2006	54.08	-13.92	-18.80	0.48	No
Coryphaenoides rupestris	2006	2006	54.08	-13.92	-18.80	0.48	No
Cyclopterus lumpus	2020	2011	65.85	-20.83	-19.00	1.90	No
Diplodus vulgaris	2014	2010	38.42	14.98	-18.11	0.16	No
Diplodus vulgaris	2014	2010	38.47	14.98	-18.11	0.16	No
Dissostichus eleginoides	1999	2002	-47.10	-63.30	-21.82	0.70	Yes
Dissostichus eleginoides	1999	2013	-55.35	-35.24	-16.96	2.77	Yes
Doederleinia berycoides	2013	2002	23.18	121.51	-18.10	0.01	Yes
Engraulis encrasicolus	2017	2012	42.84	4.17	-19.11	0.22	No
Engraulis encrasicolus	2018	2012	42.84	4.17	-19.11	0.22	No
Engraulis encrasicolus	2016	2012	42.84	4.17	-19.11	0.22	No
Epigonus telescopus	2006	2006	54.08	-13.92	-18.37	0.35	No
Epigonus telescopus	2009	2009	59.10	-9.97	-18.37	0.35	No

Epigonus telescopus	2009	2009	57.21	-9.42	-18.37	0.35	No
Epigonus telescopus	2009	2009	59.37	-10.06	-18.37	0.35	No
Epinephelus adscensionis	2015	1973	-8.68	-14.53	-15.10	0.01	No
Epinephelus adscensionis	2017	1973	-8.68	-14.53	-15.10	0.01	No
Epinephelus adscensionis	2018	1973	-8.68	-14.53	-15.10	0.01	No
Epinephelus adscensionis	2019	1973	-8.68	-14.53	-15.10	0.01	No
Epinephelus morio	2016	2010	29.00	-84.00	-17.13	0.29	Yes
Epinephelus morio	2016	2010	26.00	-82.00	-17.13	0.29	Yes
Epinephelus morio	2017	2010	27.00	-80.00	-17.13	0.29	Yes
Epinephelus multinotatus	1990	2015	-24.90	113.40	-16.30	0.30	Yes
Epinephelus multinotatus	1988	2015	-21.90	113.90	-16.30	0.30	Yes
Epinephelus multinotatus	1987	2015	-20.30	115.40	-16.30	0.30	Yes
Epinephelus multinotatus	1988	2015	-20.70	115.60	-16.30	0.30	Yes
Epinephelus multinotatus	1993	2015	-20.20	115.70	-16.30	0.30	Yes
Epinephelus multinotatus	1994	2015	-20.20	115.70	-16.30	0.30	Yes
Epinephelus multinotatus	1993	2015	-20.50	116.70	-16.30	0.30	Yes
Epinephelus multinotatus	1994	2015	-20.50	116.70	-16.30	0.30	Yes
Epinephelus multinotatus	1996	2015	-20.50	116.70	-16.30	0.30	Yes
Epinephelus multinotatus	1993	2015	-19.70	117.80	-16.30	0.30	Yes
Epinephelus multinotatus	1994	2015	-19.70	117.80	-16.30	0.30	Yes
Epinephelus multinotatus	1996	2015	-19.70	117.80	-16.30	0.30	Yes
Epinephelus multinotatus	1988	2015	-19.90	119.80	-16.30	0.30	Yes
Epinephelus multinotatus	1990	2015	-16.30	121.30	-16.30	0.30	Yes
Exocoetus volitans	2018	2010	-8.68	-14.53	-17.34	0.57	Yes
Gadus morhua	2015	2005	64.32	-24.08	-16.82	0.28	Yes
Gadus morhua	2019	2019	72.80	23.29	-21.06	0.42	No
Gadus morhua	1994	1996	41.71	-56.00	-19.20	0.40	Yes
Gadus morhua	1950	1996	48.08	-49.34	-19.20	0.40	Yes
Gadus morhua	1971	1996	48.08	-49.34	-19.20	0.40	Yes
Gadus morhua	1979	1996	48.08	-49.34	-19.20	0.40	Yes
Gadus morhua	1983	1996	48.08	-49.34	-19.20	0.40	Yes
Gadus morhua	1987	1996	48.08	-49.34	-19.20	0.40	Yes
Gadus morhua	1993	1996	48.08	-49.34	-19.20	0.40	Yes
Gadus morhua	1994	1996	48.08	-49.34	-19.20	0.40	Yes
Gadus morhua	1996	1996	48.08	-49.34	-19.20	0.40	Yes
Gadus morhua	1996	1996	48.40	-52.08	-19.20	0.40	Yes
Gadus morhua	1951	1996	50.77	-53.05	-19.20	0.40	Yes
Gadus morhua	1987	1996	50.77	-53.05	-19.20	0.40	Yes
Gadus morhua	1971	1996	50.77	-53.05	-19.20	0.40	Yes
Gadus morhua	1991	1996	50.77	-53.05	-19.20	0.40	Yes
Gadus morhua	1996	1996	45.47	-52.16	-19.20	0.40	Yes

Gadus morhua	1973	2006	72.00	34.00	-18.33	0.71	No
Gadus morhua	1973	2006	70.50	39.00	-18.33	0.71	No
Gadus morhua	1991	2006	71.30	26.25	-18.60	1.10	No
Gadus morhua	1975	2006	61.65	-8.50	-18.60	1.10	No
Gadus morhua	1988	2006	57.60	0.58	-18.60	1.10	No
Gadus morhua	1988	2006	60.43	1.37	-18.60	1.10	No
Gadus morhua	1988	2006	54.07	2.43	-18.60	1.10	No
Gadus morhua	1988	2006	54.58	3.35	-18.60	1.10	No
Gadus morhua	1993	2015	51.43	-5.27	-17.14	0.63	No
Glyptocephalus cyanoglossus	2010	2011	57.16	1.53	-18.27	0.29	Yes
Glyptocephalus cyanoglossus	2010	2011	57.53	0.49	-18.27	0.29	Yes
Glyptocephalus cyanoglossus	2010	2011	55.82	1.20	-18.27	0.29	Yes
Glyptocephalus cyanoglossus	2010	2011	60.28	2.11	-18.27	0.29	Yes
Gobius bucchichi	2014	2007	38.42	14.98	-18.12	0.04	No
Gobius bucchichi	2014	2007	38.47	14.98	-18.12	0.04	No
Halosauropsis macrochir	1976	2007	20.84	-18.92	-17.63	0.81	Yes
Halosauropsis macrochir	1996	2007	-24.18	168.35	-17.63	0.81	Yes
Halosauropsis macrochir	1982	2007	50.77	-12.97	-17.63	0.81	Yes
Halosauropsis macrochir	1976	2007	21.15	-18.15	-17.63	0.81	Yes
Helicolenus dactylopterus	2006	2006	54.08	-13.92	-17.43	0.20	No
Helicolenus dactylopterus	2009	2009	56.93	-13.47	-17.43	0.20	No
Helicolenus mouchezi	2018	2009	-8.68	-14.53	-17.43	0.20	No
Hippoglossoides platessoides	2019	2007	72.80	23.29	-18.95	0.60	Yes
Holocentrus adscensionis	2016	2011	-8.68	-14.53	-11.67	0.28	No
Holocentrus adscensionis	2015	2011	-8.68	-14.53	-11.67	0.28	No
Hoplostethus atlanticus	2006	2006	54.08	-13.92	-18.37	0.50	No
Hoplostethus atlanticus	2009	2009	54.95	-10.56	-17.13	0.16	No
Hoplostethus mediterraneus	1950	2006	-12.38	89.88	-17.79	0.83	No
Hoplostethus mediterraneus	1978	2006	49.49	-11.64	-17.79	0.83	No
Hoplostethus mediterraneus	1976	2006	31.35	-10.69	-17.79	0.83	No
Hymenocephalus lethonemus	2010	2002	22.43	120.10	-17.82	0.35	No
Hyporthodus nigritus	2013	2003	27.75	-95.16	-16.70	0.70	No
Hyporthodus nigritus	2013	2003	28.44	-90.41	-16.70	0.70	No
Hyporthodus nigritus	2013	2003	29.56	-86.89	-16.70	0.70	No
Hyporthodus nigritus	2013	2003	26.81	-83.20	-16.70	0.70	No
Ijimaia dofleini	2010	2006	22.40	120.43	-15.26	1.80	No
Kajikia albida	1994	2002	25.03	-90.11	-16.70	0.30	Yes
Kajikia albida	1994	2002	23.96	-82.39	-16.70	0.30	Yes
Kajikia albida	1994	2002	NA	NA	-16.70	0.30	Yes
Lepidion eques	2006	2006	54.08	-13.92	-17.90	0.47	No
Lepidion eques	2009	2009	57.65	-9.73	-17.90	0.47	No

Lepidion eques	2009	2009	58.63	-8.81	-17.90	0.47	No
Lepidion eques	2006	2006	54.08	-13.92	-17.90	0.47	No
Lepidion eques	1979	2009	50.68	-14.07	-17.90	0.47	No
Lepidoperca coatsii	2018	1973	-8.68	-14.53	-15.10	0.01	No
Lepidorhombus whiffiagonis	1999	2015	48.75	-7.50	-18.34	0.57	No
Lethrinus harak	2008	2009	-6.70	39.30	-13.40	2.47	No
Lethrinus harak	2009	2009	-6.70	39.30	-13.40	2.47	No
Lethrinus lentjan	2008	2009	-6.70	39.30	-13.89	0.07	No
Lethrinus lentjan	2010	2009	-6.70	39.30	-13.89	0.07	No
Lethrinus lentjan	2012	2009	-6.70	39.30	-13.89	0.07	No
Limanda limanda	2011	2009	50.64	1.48	-16.66	0.90	No
Limanda limanda	2011	2009	50.59	1.43	-16.66	0.90	No
Limanda limanda	2011	2009	50.69	1.41	-16.66	0.90	No
Lutjanus fulviflamma	2007	2009	-6.70	39.30	-13.88	1.51	No
Lutjanus fulviflamma	2011	2009	-6.70	39.30	-13.88	1.51	No
Lutjanus fulviflamma	2010	2009	-6.70	39.30	-13.88	1.51	No
Lutjanus sebae	1991	2009	-27.50	113.50	-15.37	1.12	No
Lutjanus sebae	1989	2009	-25.40	113.20	-15.37	1.12	No
Lutjanus sebae	1988	2009	-23.10	113.40	-15.37	1.12	No
Lutjanus sebae	1989	2009	-23.10	113.40	-15.37	1.12	No
Lutjanus sebae	1988	2009	-21.80	114.00	-15.37	1.12	No
Lutjanus sebae	1986	2009	-21.50	114.50	-15.37	1.12	No
Lutjanus sebae	1987	2009	-21.70	114.30	-15.37	1.12	No
Lutjanus sebae	1986	2009	-21.70	114.70	-15.37	1.12	No
Lutjanus sebae	1988	2009	-20.50	115.50	-15.37	1.12	No
Lutjanus sebae	1993	2009	-20.20	115.70	-15.37	1.12	No
Lutjanus sebae	1994	2009	-20.20	115.70	-15.37	1.12	No
Lutjanus sebae	1993	2009	-20.00	116.70	-15.37	1.12	No
Lutjanus sebae	1994	2009	-20.00	116.80	-15.37	1.12	No
Lutjanus sebae	1993	2009	-19.60	117.80	-15.37	1.12	No
Lutjanus sebae	1994	2009	-19.60	117.80	-15.37	1.12	No
Lutjanus sebae	1996	2009	-19.70	117.80	-15.37	1.12	No
Lutjanus sebae	1997	2009	-19.80	117.90	-15.37	1.12	No
Lutjanus sebae	1997	2009	-18.80	118.80	-15.37	1.12	No
Lutjanus sebae	1990	2009	-16.40	121.10	-15.37	1.12	No
Lycodes gracilis	2019	2008	72.80	23.29	-18.15	1.06	Yes
Makaira nigricans	1994	2015	25.03	-90.11	-16.00	0.60	Yes
Makaira nigricans	1994	2015	23.96	-82.39	-16.00	0.60	Yes
Makaira nigricans	1994	2015	14.65	-77.36	-16.00	0.60	Yes
Malacocephalus laevis	1982	2011	49.46	-11.29	-18.03	0.20	No
Malacocephalus laevis	1982	2011	49.39	-11.57	-18.03	0.20	No

Malacocephalus laevis	1939	2011	-19.86	10.16	-18.03	0.20	No
Malacocephalus laevis	1939	2011	3.65	-12.16	-18.03	0.20	No
Melanogrammus aeglefinus	2019	2010	72.80	23.29	-20.13	0.60	Yes
Melanogrammus aeglefinus	2018	2010	72.80	23.29	-20.13	0.60	Yes
Melanogrammus aeglefinus	1994	1996	42.00	-66.21	-19.60	0.01	Yes
Melanogrammus aeglefinus	1995	1996	42.00	-66.21	-19.60	0.01	Yes
Melanogrammus aeglefinus	1996	1996	42.00	-66.21	-19.60	0.01	Yes
Melanogrammus aeglefinus	1997	1996	42.00	-66.21	-19.60	0.01	Yes
Melanogrammus aeglefinus	1994	1996	41.20	-69.24	-19.60	0.01	Yes
Melanogrammus aeglefinus	1995	1996	41.20	-69.24	-19.60	0.01	Yes
Melanogrammus aeglefinus	1996	1996	41.20	-69.24	-19.60	0.01	Yes
Melanogrammus aeglefinus	1997	1996	41.20	-69.24	-19.60	0.01	Yes
Melanogrammus aeglefinus	1996	1996	42.81	-70.18	-19.60	0.01	Yes
Melanogrammus aeglefinus	1996	1996	43.87	-66.63	-19.60	0.01	Yes
Merlangius merlangus	2011	2016	50.55	1.54	-16.88	0.28	No
Merlangius merlangus	2011	2016	50.69	1.41	-16.88	0.28	No
Merluccius merluccius	2018	2018	39.25	2.49	-19.52	0.30	No
Merluccius merluccius	2003	2003	39.23	2.77	-17.91	0.51	No
Merluccius merluccius	2004	2003	39.23	2.77	-17.91	0.51	No
Micromesistius poutassou	2006	2006	54.08	-13.92	-18.77	0.47	No
Micromesistius poutassou	2009	2009	57.10	-12.07	-18.77	0.47	No
Micromesistius poutassou	2006	2006	57.10	-12.07	-18.77	0.47	No
Micromesistius poutassou	2009	2009	57.10	-12.07	-18.77	0.47	No
Micromesistius poutassou	2018	2015	72.80	23.29	-19.10	0.14	No
Microstomus kitt	2017	2001	54.75	-0.50	-16.70	0.60	Yes
Molva dypterygia	2009	2009	56.24	-9.34	-18.58	0.38	No
Molva dypterygia	2009	2009	59.43	-10.13	-18.58	0.38	No
Molva dypterygia	2008	2008	54.08	-13.92	-18.58	0.38	No
Molva dypterygia	2009	2009	54.08	-13.92	-18.58	0.38	No
Mora moro	2006	2006	54.08	-13.92	-18.17	0.36	No
Mora moro	2009	2009	57.10	-12.07	-18.17	0.36	No
Mora moro	2007	2007	54.08	-13.92	-18.17	0.36	No
Mora moro	2009	2009	59.10	-9.97	-18.17	0.36	No
Mora moro	1950	1997	37.42	5.25	-17.09	0.11	Yes
Mullus barbatus	2013	2012	31.88	34.37	-19.50	0.20	Yes
Neoscopelus microchir	1987	2010	20.69	-17.99	-18.97	0.12	No
Nezumia aequalis	2009	2009	56.77	-9.16	-17.59	0.29	No
Nezumia duodecim	1983	2009	14.83	-17.73	-17.59	0.29	No
Nezumia duodecim	1987	2009	20.69	-17.99	-17.59	0.29	No
Oblada melanura	2019	1995	43.09	15.42	-18.35	0.70	No
Pagellus erythrinus	2012	2010	31.88	34.37	-17.77	0.26	No

Pagellus erythrinus	2013	2010	31.88	34.37	-17.77	0.26	No
Pagellus erythrinus	2013	2010	31.88	34.37	-17.77	0.26	No
Pagrus auratus	1998	2008	-25.13	113.64	-17.20	0.28	No
Pagrus auratus	1997	2008	-25.74	113.21	-17.20	0.28	No
Pagrus auratus	1998	2008	-25.70	113.78	-17.20	0.28	No
Pagrus auratus	1998	2008	-25.73	113.17	-17.20	0.28	No
Pagrus auratus	1997	2008	-25.47	113.50	-17.20	0.28	No
Pagrus auratus	1997	2008	-26.62	113.30	-17.20	0.28	No
Pagrus auratus	1997	2008	-26.01	113.32	-17.20	0.28	No
Pagrus caeruleostictus	2012	2004	31.88	34.37	-17.40	1.50	No
Phycis blennoides	2006	2006	54.08	-13.92	-18.00	0.56	No
Phycis blennoides	2009	2009	57.60	-9.58	-18.00	0.56	No
Phycis blennoides	2006	2006	54.08	-13.92	-18.00	0.56	No
Phycis blennoides	2007	2007	54.08	-13.92	-18.00	0.56	No
Plagiogeneion rubiginosum	1999	2002	-39.43	177.46	-17.99	1.70	No
Plagiogeneion rubiginosum	2000	2002	-39.43	177.46	-17.99	1.70	No
Pollachius virens	2010	2015	50.25	-8.50	-18.94	0.10	No
Pristipomoides filamentosus	1981	2009	23.75	-166.15	-17.70	0.53	No
Pristipomoides multidens	1996	2013	-23.50	113.25	-17.80	0.30	No
Pristipomoides multidens	1997	2013	-23.50	113.25	-17.80	0.30	No
Pristipomoides multidens	1996	2013	-19.75	116.00	-17.80	0.30	No
Pristipomoides multidens	1997	2013	-19.75	116.00	-17.80	0.30	No
Pristipomoides multidens	1996	2013	-17.92	120.43	-17.80	0.30	No
Pristipomoides multidens	1998	2013	-17.92	120.43	-17.80	0.30	No
Pristipomoides multidens	1996	2013	-12.75	124.43	-17.80	0.30	No
Pristipomoides multidens	1998	2013	-12.75	124.43	-17.80	0.30	No
Pristipomoides multidens	1996	2013	-10.25	129.80	-17.80	0.30	No
Pristipomoides multidens	1997	2013	-10.25	129.80	-17.80	0.30	No
Pristipomoides multidens	1996	2013	-9.93	135.50	-17.80	0.30	No
Pristipomoides multidens	1997	2013	-9.93	135.50	-17.80	0.30	No
Pristipomoides multidens	1998	2013	-10.33	123.87	-17.80	0.30	No
Pristipomoides multidens	1999	2013	-10.33	123.87	-17.80	0.30	No
Pristipomoides multidens	1998	2013	-5.53	146.12	-17.80	0.30	No
Rouleina attrita	2006	2002	54.08	-13.92	-17.68	0.40	No
Salmo salar	2009	2006	58.10	-4.57	-19.80	0.50	No
Saurida lessepsianus	2012	2006	31.88	34.37	-16.34	1.60	No
Saurida lessepsianus	2013	2006	31.88	34.37	-16.34	1.60	No
Saurida undosquamis	2012	2006	22.39	120.41	-17.30	0.17	No
Scomber colias	2019	2012	43.09	15.42	-18.50	0.47	Yes
Scomber colias	2018	2011	32.86	-16.76	-18.55	1.11	Yes
Scomber colias	2018	2011	32.51	-16.92	-18.55	1.11	Yes

Scomber colias	2018	2011	28.41	-16.19	-18.55	1.11	Yes
Scomber colias	2018	2011	41.17	-8.72	-18.55	1.11	Yes
Scomber colias	2018	2011	38.43	-9.10	-18.55	1.11	Yes
Scomber colias	2018	2011	37.05	-8.55	-18.55	1.11	Yes
Scomber scombrus	2020	2016	50.43	-3.43	-20.36	1.20	No
Scomber scombrus	2020	2016	50.75	-0.25	-20.36	1.20	No
Scomber scombrus	2018	2015	41.17	-8.72	-19.02	0.49	No
Scomber scombrus	2018	2015	43.59	-5.64	-19.02	0.49	No
Scomber scombrus	2018	2015	57.85	-8.57	-19.02	0.49	No
Scomber scombrus	2018	2015	50.54	-1.28	-19.02	0.49	No
Scomber scombrus	2018	2007	49.53	-58.95	-20.00	0.80	No
Scomber scombrus	2018	2007	40.44	-73.35	-20.00	0.80	No
Scopthalmus maximus	2000	2010	50.79	0.78	-16.89	0.55	No
Scopthalmus maximus	2000	2010	50.13	-1.76	-16.89	0.55	No
Scopthalmus maximus	2000	2010	49.96	0.96	-16.89	0.55	No
Scopthalmus maximus	2000	2010	49.39	-0.29	-16.89	0.55	No
Sebastes melanops	2010	2011	58.00	-155.00	-17.66	0.29	No
Sebastes melanops	2010	2011	60.00	-148.00	-17.66	0.29	No
Sebastes melanops	2011	2011	58.00	-137.00	-17.66	0.29	No
Sebastes melanops	2011	2011	57.00	-135.00	-17.66	0.29	No
Sebastes melanops	2010	2011	49.00	-126.00	-16.39	0.28	No
Sebastes melanops	2010	2011	48.00	-124.00	-16.39	0.28	No
Sebastes melanops	2010	2010	36.00	-122.00	-16.47	0.07	No
Sebastes mentella	2007	2008	54.08	-13.92	-19.79	0.84	Yes
Sebastes mentella	2007	2008	59.42	-10.25	-19.79	0.84	Yes
Sebastes mentella	2019	2012	72.80	23.29	-20.68	0.07	Yes
Seriola dumerili	2015	2006	-8.68	-14.53	-17.56	0.93	No
Solea solea	2017	2007	51.56	2.12	-16.93	0.56	No
Spectrunculus grandis	2009	2009	56.12	-9.91	-17.53	0.25	No
Sprattus sprattus	2018	2010	50.75	0.50	-18.10	0.01	No
Sprattus sprattus	2018	2010	50.25	1.50	-18.10	0.01	No
Sprattus sprattus	2018	2010	50.75	1.50	-18.10	0.01	No
Sprattus sprattus	2016	2010	52.25	1.82	-18.10	0.01	No
Sprattus sprattus	2017	2010	50.45	0.57	-18.10	0.01	No
Squalogadus modificatus	1996	2008	-25.15	168.90	-17.15	1.03	Yes
Squalogadus modificatus	1996	2008	-24.77	168.26	-17.15	1.03	Yes
Squalogadus modificatus	1996	2008	-24.81	168.29	-17.15	1.03	Yes
Squalogadus modificatus	1996	2008	-24.88	168.70	-17.15	1.03	Yes
Squalogadus modificatus	1996	2008	-25.80	167.20	-17.15	1.03	Yes
Squalogadus modificatus	1996	2008	-23.86	168.44	-17.15	1.03	Yes
Squalogadus modificatus	1996	2008	-24.86	162.14	-17.15	1.03	Yes

Synaphobranchus kaupii	1992	2006	57.27	-9.52	-19.70	1.00	No
Synaphobranchus kaupii	1990	2006	56.72	-9.50	-19.70	1.00	No
Synaphobranchus kaupii	1990	2006	57.27	-9.52	-19.70	1.00	No
Synaphobranchus kaupii	1992	2006	57.27	-9.52	-19.70	1.00	No
Thunnus albacares	2018	2013	-8.68	-14.53	-17.05	0.42	Yes
Thunnus albacares	2019	2013	-8.68	-14.53	-17.05	0.42	Yes
Thunnus albacares	2017	2013	-8.68	-14.53	-17.05	0.42	Yes
Thunnus maccoyii	2003	2005	-31.00	89.00	-20.20	0.01	No
Thunnus maccoyii	2005	2005	-8.75	115.37	-20.20	0.01	No
Thunnus orientalis	2014	2012	35.90	133.58	-17.60	0.63	Yes
Thunnus orientalis	2014	2012	41.65	141.27	-17.60	0.63	Yes
Thunnus orientalis	2015	2012	41.65	141.27	-17.60	0.63	Yes
Thunnus orientalis	2016	2012	35.90	133.58	-17.60	0.63	Yes
Thunnus orientalis	2013	2012	24.61	121.95	-17.60	0.63	Yes
Thunnus orientalis	2013	2012	22.40	120.44	-17.60	0.63	Yes
Thunnus orientalis	2016	2012	22.40	120.44	-17.60	0.63	Yes
Thunnus orientalis	2018	2012	22.40	120.44	-17.60	0.63	Yes
Trachurus trachurus	1969	2008	51.80	1.83	-18.19	1.33	No
Trachyrincus murrayi	2009	2009	57.61	-9.87	-17.74	0.32	No
Trachyrincus murrayi	1980	2009	51.60	-13.07	-17.74	0.32	No
Trachyrincus scabrus	1987	2010	20.69	-17.99	-17.59	0.50	Yes
Trachyrincus scabrus	1982	2010	51.85	-13.33	-17.59	0.50	Yes
Triglops nybelini	2019	2003	72.80	23.29	-20.50	0.10	Yes
Upeneus moluccensis	2013	2012	31.88	34.37	-17.40	0.01	Yes
Upeneus moluccensis	2013	2012	31.88	34.37	-17.40	0.01	Yes
Xenodermichthys copei	2009	2009	57.27	-9.52	-19.30	0.58	No
Xenodermichthys copei	2009	2009	57.27	-9.52	-19.30	0.58	No

D.2 Sources for $\delta^{13}C_{musc}$ values

- D. Agnetta, F. Badalamenti, G. D'Anna, M. Sinopoli, F. Andaloro, S. Vizzini, and C. Pipitone. Sizing up the role of predators on *Mullus barbatus* populations in Mediterranean trawl and no-trawl areas. *Fisheries Research*, 213:196–203, 2019

- O. R. J. Anderson, R. A. Phillips, R. A. McDonald, R. F. Shore, R. A. R McGill, and S. Bearhop. Influence of trophic position and foraging range on mercury levels within a seabird community. *Marine Ecology Progress Series*, 375:277–288, 2009

- E. S. Antonio, A. Kasai, M. Ueno, N. Won, Y. Ishihi, H. Yokoyama, and Y. Yamashita. Spatial variation in organic matter utilization by benthic communities from Yura River–Estuary to offshore of Tango Sea, Japan. *Estuarine, Coastal and Shelf Science*, 86(1):107–117, 2010

- K. A. Asante, T. Agusa, H. Mochizuki, K. Ramu, S. Inoue, T. Kubodera, S. Takahashi, A. Subramanian, and S. Tanabe. Trace elements and stable isotopes (δ^{13}C and δ^{15}N) in shallow and deep-water organisms from the East China Sea. *Environmental Pollution*, 156(3):862–873, 2008

- K. A. Asante, R. Kubota, T. Agusa, A. Subramanian, S. Tanabe, S. Nishida, M. Yamaguchi, K. Suetsugu, S. Ohta, and H. Yeh. Trace element and stable isotope analyses of deep sea fish from the Sulu Sea, Philippines. *West African Journal of Applied Ecology*, 14(1), 2009

- C. Barría, J. Navarro, and M. Coll. Feeding habits of four sympatric sharks in two deep-water fishery areas of the western Mediterranean Sea. *Deep Sea Research Part I: Oceanographic Research Papers*, 142:34–43, 2018

- N. Bodin, D. Lesperance, R. Albert, S. Hollanda, M. Degroote, C. Churlaud, and P. Bustamante. A preliminary study of trace elements in oceanic pelagic communities in the western-central Indian Ocean. 2016

- L. Cardona, I. Álvarez de Quevedo, A. Borrell, and A. Aguilar. Massive consumption of gelatinous plankton by mediterranean apex predators. *PLOS ONE*, 7(3):e31329, 2012

- T. Chouvelon, J. Spitz, F. Caurant, P. Mèndez-Fernandez, A. Chappuis, F. Laugier, E. Le Goff, and P. Bustamante. Revisiting the use of δ^{15}N in meso-scale studies of marine food webs by considering spatio-temporal variations in stable isotopic signatures–the case of an open ecosystem: The Bay of Biscay (North-East Atlantic). *Progress in Oceanography*, 101(1):92–105, 2012

- M. T. Chung. *Functional and life-history traits in deep-sea fishes*. PhD thesis, University of Southampton, Southampton, United Kingdom, 2015. URL https://eprints.soton.ac.uk/384568/

- A. Colaço, E. Giacomello, F. Porteiro, and G. M. Menezes. Trophodynamic studies on the condor seamount (Azores, Portugal, North Atlantic). *Deep Sea Research Part II: Topical Studies in Oceanography*, 98:178–189, 2013
- R. M. Connolly, T. A. Schlacher, and T. F. Gaston. Stable isotope evidence for trophic subsidy of coastal benthic fisheries by river discharge plumes off small estuaries. *Marine Biology Research*, 5(2):164–171, 2009
- S. Corsolini and G. Sarà. The trophic transfer of persistent pollutants (HCB, DDTs, PCBs) within polar marine food webs. *Chemosphere*, 177:189–199, 2017
- P. Cresson, L. Le Direach, E. Rouanet, E. Goberville, P. Astruch, M. Ourgaud, and M. Harmelin-Vivien. Biomass and isotopic data for fish community on artificial reefs in the bay of Marseille. Sea Open Scientific Data Publication (SEANOE), 2019
- K. Das, G. Lepoint, Y. Leroy, and J. M. Bouquegneau. Marine mammals from the southern North Sea: feeding ecology data from δ^{13}C and δ^{15}N measurements. *Marine Ecology Progress Series*, 263:287–298, 2003
- A. M. De Lecea, A. J. Smit, and S. T. Fennessy. Riverine dominance of a nearshore marine demersal food web: evidence from stable isotope and C/N ratio analysis. *African Journal of Marine Science*, 38:S181–S192, 2016
- A. W. J. Demopoulos and P. C. Sikkel. Enhanced understanding of ectoparasite–host trophic linkages on coral reefs through stable isotope analysis. *International Journal for Parasitology: Parasites and Wildlife*, 4(1):125–134, 2015
- J. B. Dempson, V. A. Braithwaite, D. Doherty, and M. Power. Stable isotope analysis of marine feeding signatures of Atlantic salmon in the North Atlantic. *ICES Journal of Marine Science*, 67(1):52–61, 2010
- S. Deudero, J. K. Pinnegar, N. V. C. Polunin, G. Morey, and B. Morales-Nin. Spatial variation and ontogenic shifts in the isotopic composition of Mediterranean littoral fishes. *Marine Biology*, 145(5):971–981, 2004
- K. S. Dillon, C. R. Fleming, C. Slife, and R. T. Leaf. Stable isotopic niche variability and overlap across four fish guilds in the north-central Gulf of Mexico. *Marine and Coastal Fisheries*, 13(3):213–227, 2021
- E. Fanelli, E. Azzurro, M. Bariche, J. E. Cartes, and F. Maynou. Depicting the novel Eastern Mediterranean food web: a stable isotopes study following Lessepsian fish invasion. *Biological Invasions*, 17(7):2163–2178, 2015
- E. Fanelli and J. E. Cartes. Temporal variations in the feeding habits and trophic levels of three deep-sea demersal fishes from the western Mediterranean Sea,

based on stomach contents and stable isotope analyses. *Marine Ecology Progress Series*, 402:213–232, 2010

- E. Fanelli, V. Papiol, J. E. Cartes, P. Rumolo, and C. López-Pérez. Trophic webs of deep-sea megafauna on mainland and insular slopes of the NW Mediterranean: a comparison by stable isotope analysis. *Marine Ecology Progress Series*, 490: 199–221, 2013

- R. Fernández, S. García-Tiscar, M. Begoña Santos, A. López, J. A. Martínez-Cedeira, J. Newton, and G. J. Pierce. Stable isotope analysis in two sympatric populations of bottlenose dolphins *Tursiops truncatus*: evidence of resource partitioning? *Marine Biology*, 158(5):1043–1055, 2011

- F. Ferraton, M. Harmelin-Vivien, C. Mellon-Duval, and A. Souplet. Spatio-temporal variation in diet may affect condition and abundance of juvenile european hake in the Gulf of Lions (NW Mediterranean). *Marine Ecology Progress Series*, 337:197–208, 2007

- S. Fredriksen. Food web studies in a Norwegian kelp forest based on stable isotope (δ^{13}C and δ^{15}N) analysis. *Marine Ecology Progress Series*, 260:71–81, 2003

- J. Giménez, A. Marçalo, F. Ramírez, P. Verborgh, P. Gauffier, R. Esteban, L. Nicolau, E. González-Ortegón, F. Baldó, C. Vilas, et al. Diet of bottlenose dolphins (*Tursiops truncatus*) from the Gulf of Cadiz: insights from stomach content and stable isotope analyses. *PLOS ONE*, 12(9):e0184673, 2017

- A. Gopakumar, J. Giebichenstein, E. Raskhozheva, and K. Borgå. Mercury in Barents Sea fish in the Arctic polar night: Species and spatial comparison. *Marine Pollution Bulletin*, 169:112501, 2021

- J. R. Gormly. *Stable carbon isotope variations in marine organic matter*. PhD thesis, Texas A & M University, Texas, 1975. URL https://www.proquest.com/openview/0ec705e99fa8ae532e2bc3c637dbdb2c/1?pq-origsite=gscholar&cbl=18750&diss=y

- A. K. Hilting, C. A. Currin, and R. K. Kosaki. Evidence for benthic primary production support of an apex predator–dominated coral reef food web. *Marine Biology*, 160(7):1681–1695, 2013

- S. Hirch and B. Christiansen. The trophic blockage hypothesis is not supported by the diets of fishes on Seine Seamount. *Marine Ecology*, 31:107–120, 2010

- J. C. Hoffman and T. T. Sutton. Lipid correction for carbon stable isotope analysis of deep-sea fishes. *Deep Sea Research Part I: Oceanographic Research Papers*, 57(8):956–964, 2010

- M. M. Igulu, I. Nagelkerken, G. van der Velde, and Y. D. Mgaya. Mangrove fish production is largely fuelled by external food sources: a stable isotope analysis of fishes at the individual, species, and community levels from across the globe. *Ecosystems*, 16(7):1336–1352, 2013

- K. Iken, T. Brey, U. Wand, J. Voigt, and P. Junghans. Food web structure of the benthic community at the Porcupine Abyssal Plain (NE Atlantic): a stable isotope analysis. *Progress in Oceanography*, 50(1-4):383–405, 2001

- O. E. Jansen, G. M. Aarts, K. Das, G. Lepoint, L. Michel, and P. J. H. Reijnders. Feeding ecology of harbour porpoises: Stable isotope analysis of carbon and nitrogen in muscle and bone. *Marine Biology Research*, 8(9):829–841, 2012

- S. Jennings, O Reñones, B. Morales-Nin, N. V. C. Polunin, J. Moranta, and J. Coll. Spatial variation in the 15N and 13C stable isotope composition of plants, invertebrates and fishes on Mediterranean reefs: implications for the study of trophic pathways. *Marine Ecology Progress Series*, 146:109–116, 1997

- E. K. Källgren. Population dynamics, diet and trophic positioning of three small demersal fish species within Porsangerfjord, Norway. Master's thesis, Universitetet i Tromsø, 2012

- T. Kitagawa and K. Fujioka. Rapid ontogenetic shift in juvenile Pacific bluefin tuna diet. *Marine Ecology Progress Series*, 571:253–257, 2017

- D. Kopp, S. Lefebvre, M. Cachera, M. C. Villanueva, and B. Ernande. Reorganization of a marine trophic network along an inshore–offshore gradient due to stronger pelagic–benthic coupling in coastal areas. *Progress in Oceanography*, 130:157–171, 2015

- D. Kopp, M. Robert, and L. Pawlowski. Characterization of food web structure of the upper continental slope of the Celtic Sea highlighting the trophic ecology of five deep-sea fishes. *Journal of Applied Ichthyology*, 34(1):73–80, 2018

- V. Lesage, M. O. Hammill, and K. M. Kovacs. Marine mammals and the community structure of the estuary and Gulf of St. Lawrence, Canada: evidence from stable isotope analysis. *Marine Ecology Progress Series*, 210:203–221, 2001

- J. M. Logan and M. E. Lutcavage. Assessment of trophic dynamics of cephalopods and large pelagic fishes in the central North Atlantic Ocean using stable isotope analysis. *Deep Sea Research Part II: Topical Studies in Oceanography*, 95:63–73, 2013

- T. S. Løkken. Carbon source and trophic structure along a depth gradient in Isfjorden, Svalbard. Master's thesis, Universitetet i Tromsø, 2013

- S. M. Lusseau and S. R. Wing. Importance of local production versus pelagic subsidies in the diet of an isolated population of bottlenose dolphins *Tursiops* sp. *Marine Ecology Progress Series*, 321:283–293, 2006

- P. L. Mancini and L. Bugoni. Resources partitioning by seabirds and their relationship with other consumers at and around a small tropical archipelago. *ICES Journal of Marine Science*, 71(9):2599–2607, 2014

- R. Mariano-Jelicich, S. Copello, J. P. Seco Pon, and M. Favero. Long-term changes in black-browed albatrosses diet as a result of fisheries expansion: an isotopic approach. *Marine Biology*, 164(6):1–12, 2017

- P. Matich, J. J. Kiszka, K. R. Gastrich, and M. R. Heithaus. Trophic redundancy among fishes in an east african nearshore seagrass community inferred from stable-isotope analysis. *Journal of Fish Biology*, 91(2):490–509, 2017

- N. Mavraki, S. Degraer, and J. Vanaverbeke. Offshore wind farms and the attraction–production hypothesis: insights from a combination of stomach content and stable isotope analyses. *Hydrobiologia*, 848(7):1639–1657, 2021

- S. M McCluskey, K. R. Sprogis, J. M. London, L. Bejder, and N. R. Loneragan. Foraging preferences of an apex marine predator revealed through stomach content and stable isotope analyses. *Global Ecology and Conservation*, 25:e01396, 2021

- B. C. McMeans, J. Svavarsson, S. Dennard, and A. T. Fisk. Diet and resource use among Greenland sharks (*Somniosus microcephalus*) and teleosts sampled in Icelandic waters, using δ^{13}C, δ^{15}N, and mercury. *Canadian Journal of Fisheries and Aquatic Sciences*, 67(9):1428–1438, 2010

- A. Mittermayr, S. E. Fox, and U. Sommer. Temporal variation in stable isotope composition (δ^{13}C, δ^{15}N and δ^{34}S) of a temperate *Zostera marina* food web. *Marine Ecology Progress Series*, 505:95–105, 2014

- J. Nelson, R. Wilson, F. Coleman, C. Koenig, D. DeVries, C. Gardner, and J. Chanton. Flux by fin: fish-mediated carbon and nutrient flux in the northeastern Gulf of Mexico. *Marine Biology*, 159(2):365–372, 2012

- M. Nilsen, T. Pedersen, E. M. Nilssen, and S. Fredriksen. Trophic studies in a high-latitude fjord ecosystem—a comparison of stable isotope analyses (δ^{13}C and δ^{15}N) and trophic-level estimates from a mass-balance model. *Canadian Journal of Fisheries and Aquatic Sciences*, 65(12):2791–2806, 2008

- J. Nyunja, M. Ntiba, J. Onyari, K. Mavuti, K. Soetaert, and S. Bouillon. Carbon sources supporting a diverse fish community in a tropical coastal ecosystem (Gazi Bay, Kenya). *Estuarine, Coastal and Shelf Science*, 83(3):333–341, 2009

- K. Owen, K. Charlton-Robb, and R. Thompson. Resolving the trophic relations of cryptic species: An example using stable isotope analysis of dolphin teeth. *PLOS ONE*, 6(2):e16457, 2011
- V. Papiol, J. E. Cartes, E. Fanelli, and P. Rumolo. Food web structure and seasonality of slope megafauna in the NW Mediterranean elucidated by stable isotopes: relationship with available food sources. *Journal of Sea Research*, 77: 53–69, 2013
- C. Parzanini, C. C. Parrish, J. F. Hamel, and A. Mercier. Trophic ecology of a deep-sea fish assemblage in the Northwest Atlantic. *Marine Biology*, 164(10):1–19, 2017
- J. K. Pinnegar and N. V. C. Polunin. Contributions of stable-isotope data to elucidating food webs of Mediterranean rocky littoral fishes. *Oecologia*, 122(3): 399–409, 2000
- N. V. C. Polunin, B. Morales-Nin, W. E. Pawsey, J. E. Cartes, J. K. Pinnegar, and J. Moranta. Feeding relationships in Mediterranean bathyal assemblages elucidated by stable nitrogen and carbon isotope data. *Marine Ecology Progress Series*, 220:13–23, 2001
- I. Preciado, J. E. Cartes, A. Punzón, I. Frutos, L. López-López, and A. Serrano. Food web functioning of the benthopelagic community in a deep-sea seamount based on diet and stable isotope analyses. *Deep Sea Research Part II: Topical Studies in Oceanography*, 137:56–68, 2017
- S. G. A. C. Ramos. Diet and trophic position of deep-sea sharks in the southwest coast of Portugal: using stable isotopes analysis and nucleic acids ratios (RNA/DNA). Master's thesis, University of the Algarve, 2018
- S. Ramsvatn and T. Pedersen. Ontogenetic niche changes in haddock *Melanogrammus aeglefinus* reflected by stable isotope signatures, δ^{13}C and δ^{15}N. *Marine Ecology Progress Series*, 451:175–185, 2012
- W. D. K. Reid, B. D. Wigham, R. A. R. McGill, and N. V. C. Polunin. Elucidating trophic pathways in benthic deep-sea assemblages of the Mid-Atlantic Ridge north and south of the Charlie-Gibbs Fracture Zone. *Marine Ecology Progress Series*, 463:89–103, 2012
- A. T. Revill, J. W. Young, and M. Lansdell. Stable isotopic evidence for trophic groupings and bio-regionalization of predators and their prey in oceanic waters off eastern Australia. *Marine Biology*, 156(6):1241–1253, 2009
- D. K. Sackett, J. C. Drazen, B. N. Popp, C. A. Choy, J. D. Blum, and M. W. Johnson. Carbon, nitrogen, and mercury isotope evidence for the

biogeochemical history of mercury in Hawaiian marine bottomfish. *Environmental Science & Technology*, 51(23):13976–13984, 2017

- P. Sallaberry-Pincheira, P. Galvez, B. E. Molina-Burgos, F. Fernandoy, R. Melendez, and S. A. Klarian. Diet and food consumption of the Patagonian toothfish (*Dissostichus eleginoides*) in South Pacific Antarctic waters. *Polar Biology*, 41(11):2379–2385, 2018

- G. Sarà, M. De Pirro, M. Sprovieri, P. Rumolo, H. P. Halldórsson, and J. Svavarsson. Carbon and nitrogen stable isotopic inventory of the most abundant demersal fish captured by benthic gears in southwestern Iceland (North Atlantic). *Helgoland Marine Research*, 63(4):309–315, 2009

- F. Sardenne, N. G. C. Diaha, M. J. Amandé, I. Zudaire, L. I. E. Couturier, L. Metral, F. Le Grand, and N. Bodin. Seasonal habitat and length influence on the trophic niche of co-occurring tropical tunas in the eastern Atlantic Ocean. *Canadian Journal of Fisheries and Aquatic Sciences*, 76(1):69–80, 2019

- F. Sardenne, S. Hollanda, S. Lawrence, R. Albert-Arrisol, M. Degroote, and N. Bodin. Trophic structures in tropical marine ecosystems: a comparative investigation using three different ecological tracers. *Ecological Indicators*, 81: 315–324, 2017

- J Sellanes, E Quiroga, and C Neira. Megafauna community structure and trophic relationships at the recently discovered Concepción Methane Seep Area, Chile, ∼36°S. *ICES Journal of Marine Science*, 65(7):1102–1111, 2008

- O. N. Shipley, C. S. Lee, N. S. Fisher, G. Burruss, M. G. Frisk, E. J. Brooks, Z. C. Zuckerman, A. D. Herrmann, and D. J. Madigan. Trophodynamics and mercury bioaccumulation in reef and open-ocean fishes from the Bahamas with a focus on two teleost predators. *Marine Ecology Progress Series*, 608:221–232, 2019

- M. J. Silberberger, P. E. Renaud, I. Kröncke, and H. Reiss. Food-web structure in four locations along the european shelf indicates spatial differences in ecosystem functioning. *Frontiers in Marine Science*, 5:119, 2018

- G. Stowasser, D. W. Pond, and M. A. Collins. Using fatty acid analysis to elucidate the feeding habits of Southern Ocean mesopelagic fish. *Marine Biology*, 156(11):2289–2302, 2009

- C. J. Svensson, G. A. Hyndes, and P. S. Lavery. Food web analysis in two permanently open temperate estuaries: consequences of saltmarsh loss? *Marine Environmental Research*, 64(3):286–304, 2007

- E. Svensson, V. Freitas, S. Schouten, J. J. Middelburg, H. W. van der Veer, and J. S. S. Damsté. Comparison of the stable carbon and nitrogen isotopic values of

gill and white muscle tissue of fish. *Journal of Experimental Marine Biology and Ecology*, 457:173–179, 2014

- T. Tamelander, P. E. Renaud, J. Hop, M. L. Carroll, W. G. Ambrose Jr, and K. A. Hobson. Trophic relationships and pelagic–benthic coupling during summer in the Barents Sea Marginal Ice Zone, revealed by stable carbon and nitrogen isotope measurements. *Marine Ecology Progress Series*, 310:33–46, 2006

- C. A. Timmerman, P. Marchal, M. Denamiel, C. Couvreur, and P. Cresson. Seasonal and ontogenetic variation of whiting diet in the Eastern English Channel and the Southern North Sea. *PLOS ONE*, 15(9):e0239436, 2020

- C. Trystram, D. Roos, D. Guyomard, and S. Jaquemet. Mechanisms of trophic partitioning within two fish communities associated with a tropical oceanic island. *Western Indian Ocean Journal of Marine Science*, 14(1&2):93–111, 2015

- A. Walters, M. Robert, P. Cresson, H. Le Bris, and D. Kopp. Food web structure in relation to environmental drivers across a continental shelf ecosystem. *Limnology and Oceanography*, 66(6):2563–2582, 2021

- T. V. Willis, K. A. Wilson, and B. J. Johnson. Diets and stable isotope derived food web structure of fishes from the inshore Gulf of Maine. *Estuaries and Coasts*, 40(3):889–904, 2017

- A. S. J. Wyatt, A. M. Waite, and S. Humphries. Variability in isotope discrimination factors in coral reef fishes: implications for diet and food web reconstruction. *PLOS ONE*, 5(10):e13682, 2010

- G. Zapata-Hernández, J. Sellanes, A. R. Thurber, L. A. Levin, F. Chazalon, and P. Linke. New insights on the trophic ecology of bathyal communities from the methane seep area off Concepción, Chile ($\sim$ 36 °S). *Marine Ecology*, 35(1):1–21, 2014

- Y. Zhu, S. P. Newman, W. D. K. Reid, and N. V. C. Polunin. Fish stable isotope community structure of a Bahamian coral reef. *Marine Biology*, 166(12):1–14, 2019

Appendix E

Temporal range of otolith samples

E.1 Summary

To estimate the amount of time incorporated into my otolith stable isotope samples, I prepared sagittal thin sections otoliths from a selection of species. Most of these were myctophids, from the lanternfish chapter (Chapter 3), as I generally had both otoliths from each individual within this group, which meant I had unsampled otoliths which I could use for sectioning. For the non-myctophids I was somewhat restricted as these had already been sampled and for the most part I did not have spare otoliths from these species. Additionally, the Covid-19 pandemic meant I did not have much time for otolith sectioning and was restricted to otoliths I could section myself using cyanoacrylate glue (Campana, No Date).

I mounted otoliths in cyanoacrylate glue on either a glass slide, or using the resin backing plates used for sample mounting. For the glass mounted otoliths, I polished each face using 30 and 3 μm aluminium oxide lapping paper. For the resin mounted otoliths I was only able to polish a single otolith face, though in many cases this was sufficient for a thin section. I photographed the sections using a Wild Heerbrugg 3M microscope using transmitted light. I took annuli to be a pair of hyaline and opaque bands, with the edge of an annulus taken as the edge of the opaque band. I analysed and annotated all images in ImageJ 1.52a (Schneider et al., 2018).

I attempted to section otoliths of some species which did not show any clear annuli. Species where I could not find clear annuli were *Synaphobranchus kaupii* (Kaup's arrowtooth eel), *Holocentrus adscensionis* (squirrelfish), *Rouleina attrita* (softskin smooth-head), *Halosauropsis macrochir* (abyssal halosaur) and *Pagrus caeruleostictus* (bluespotted seabream).

The ages of individuals in my sample ranged from 1.5 years (*Protomyctophum bolini*, Bolin's lanternfish) to 27.0 years (*Bathysaurus ferox*, deepsea lizardfish). The temporal

ranges of my otolith stable isotope samples ranged from 0.5 years (*Limanda limanda*, common dab) to 6.0 years (*Nezumia duodecim*, twelve-rayed grenadier), with a mean of 2.3 years.

TABLE E.1: Summary of temporal range of otolith stable isotope samples. ND = not determined. * = depending on sample position. ** = difficult section to interpret.

Order	**Species**	**Estimated age (years)**	**Temporal range (years)**	
			Time	Age
Aulopiformes	*Bathysaurus ferox*	27.0	3.0	25.0 - 27.0
Aulopiformes	*Saurida lessepsianus*	7.0	3.0	4.0 - 7.0
Gadiformes	*Nezumia duodecim*	9.0 - 10.0	4.0 or 6.0*	3.0 - 9.0 or 4.0 - 8.0*
Myctophiformes	*Electrona antarctica*	3.5	2.0	1.5 - 3.5
Myctophiformes	*Electrona carlsbergi*	3.0	1.0	2.0 - 3.0
Myctophiformes	*Gymnoscopelus braueri*	6.0	3.5	2.5 - 6.0
Myctophiformes	*Gymnoscopelus nicholsi*	5.0	2.5	2.5 - 5.0
Myctophiformes	*Krefftichthys anderssoni*	1.5	1.5	0 - 1.5
Myctophiformes	*Neoscopelus microchir*	5.0	0.5 - 1.0	3.5 - 4.0
Myctophiformes	*Protomyctophum bolini*	2.5	2.0	0.5 - 2.5
Perciformes	*Lepidoperca coatsii***	14.0 - 18.0	4.0	10.0 - 14.0 or 14.0 - 18.0
Pleuronectiformes	*Limanda limanda*	3.0	0.5	2.5 - 3.0
Pleuronectiformes	*Microstomus kitt*	7.0	1.5 - 2.0	5.0 - 7.0
Scombriformes	*Aphanopus carbo***	13.0	1.0	ND

E.2 Individual otolith ages and sections

E.2.1 Aulopiformes

E.2.1.1 *Bathysaurus ferox*

From an individual of 533 mm SL. I estimated the age as 27 years, and the time incorporated as 3 years, between the ages of 25 and 27 years.

FIGURE E.1: Section of an otolith from *Bathysaurus ferox* (BFE_244/BFE_94, 533 mm SL). White dots indicate estimated annuli (A) and the white polygon indicates approximate sampling area (B).

E.2.1.2 *Saurida lessepsianus*

From an individual of 142 mm TL. I estimated the age as 7 years, and the time incorporated as 3 years, between the ages of 4 and 7 years.

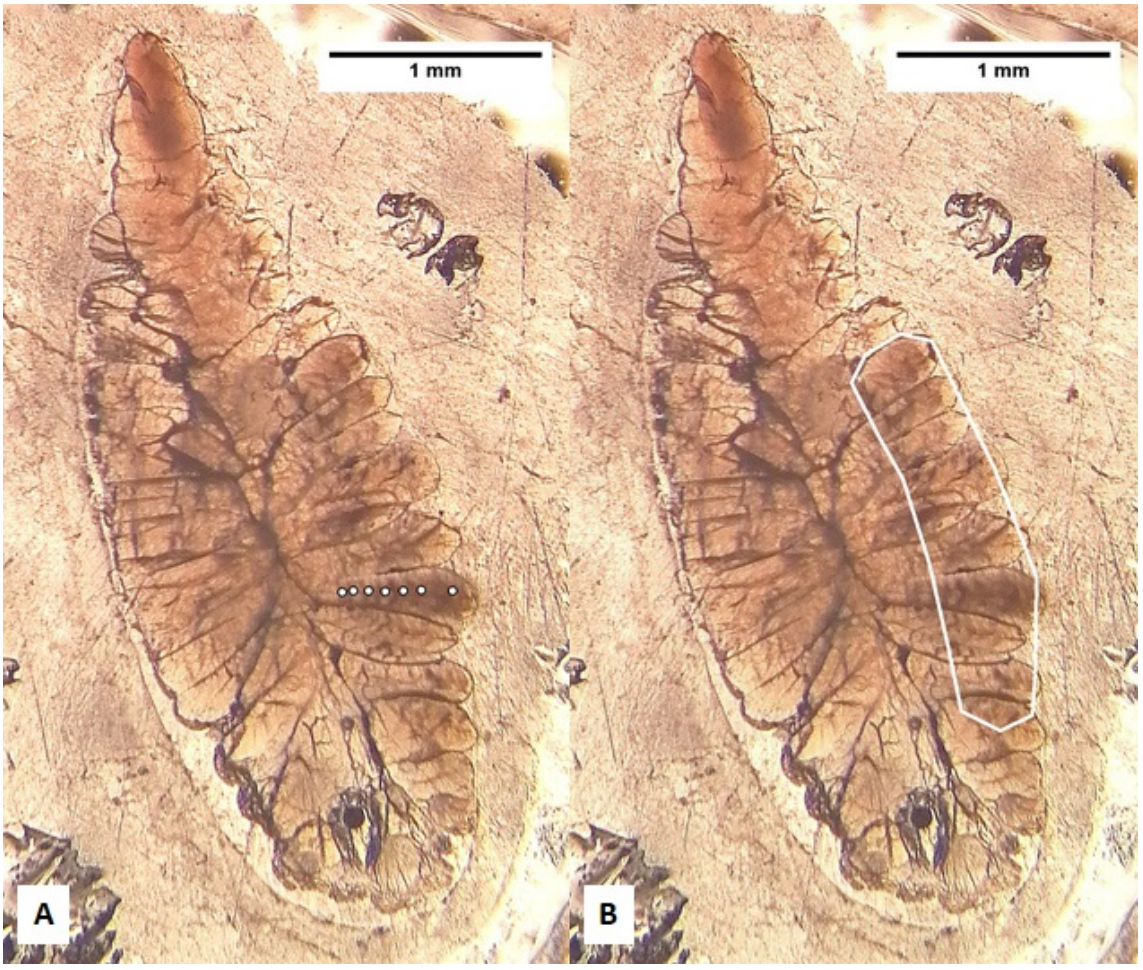

FIGURE E.2: Section of an otolith from *Saurida lessepsianus* (SLE_41/SLE_1121, 142 mm TL). White dots indicate estimated annuli (A) and the white polygon indicates approximate sampling area (B).

E.2.2 Gadiformes

E.2.2.1 *Nezumia duodecim*

From an individual of 26 mm HL. I estimated the age as 9-10 years, and the time incorporated as 4 or 6 years, between the ages of 3 and 9 years or 4 and 8 years (depending upon the sample location).

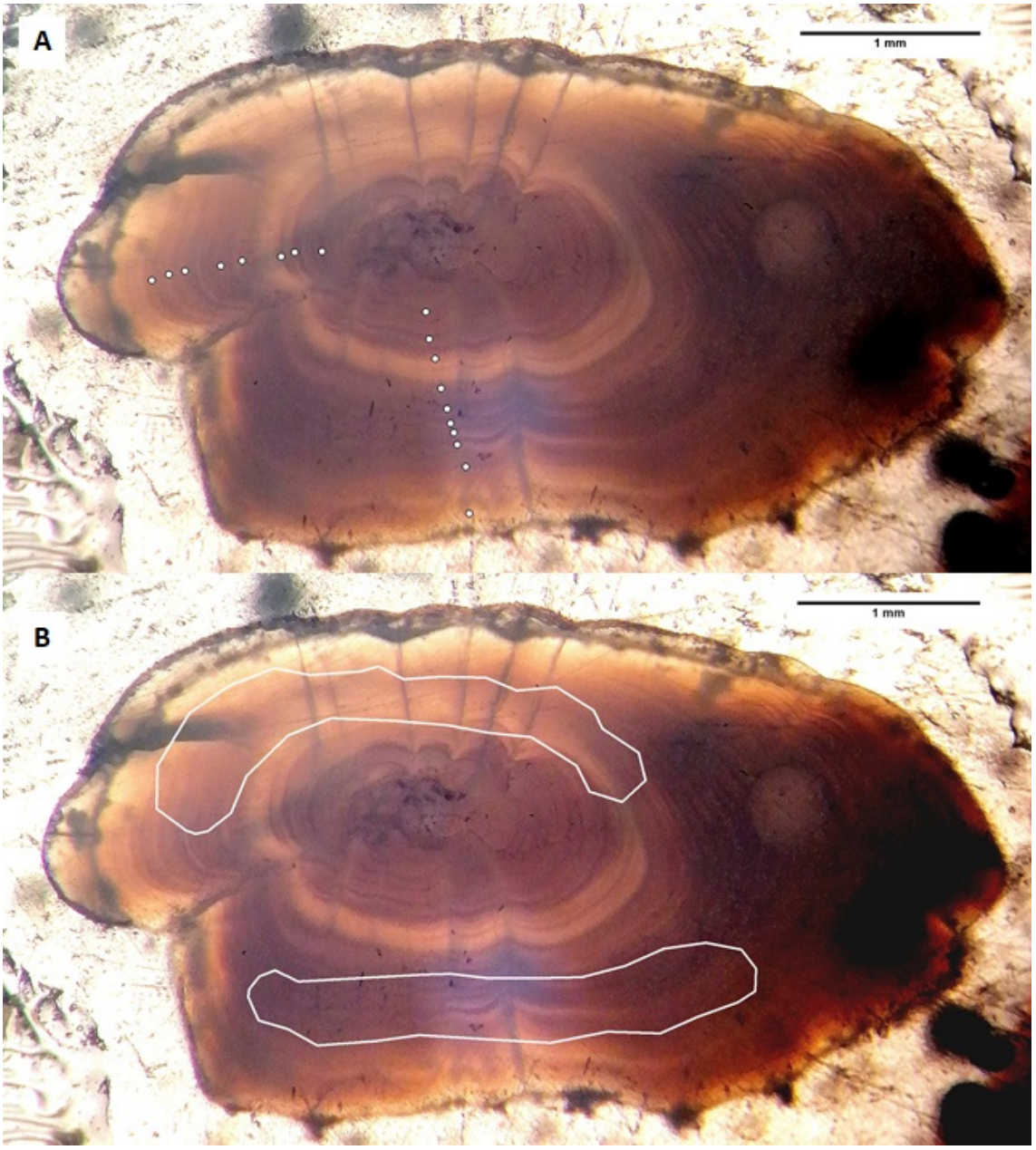

FIGURE E.3: Section of an otolith from *Nezumia duodecim* (NDU_975/NDU_981, 26 mm HL). White dots indicate estimated annuli (A) and the white polygon indicates approximate sampling area (B).

E.2.3 Myctophiformes

E.2.3.1 *Electrona antarctica*

From a female, of 71 mm SL (BAS_33). I estimated the age of the individual was 3.5 years, and the time incorporated as 2 years from ages 1.5 to 3.5 years.

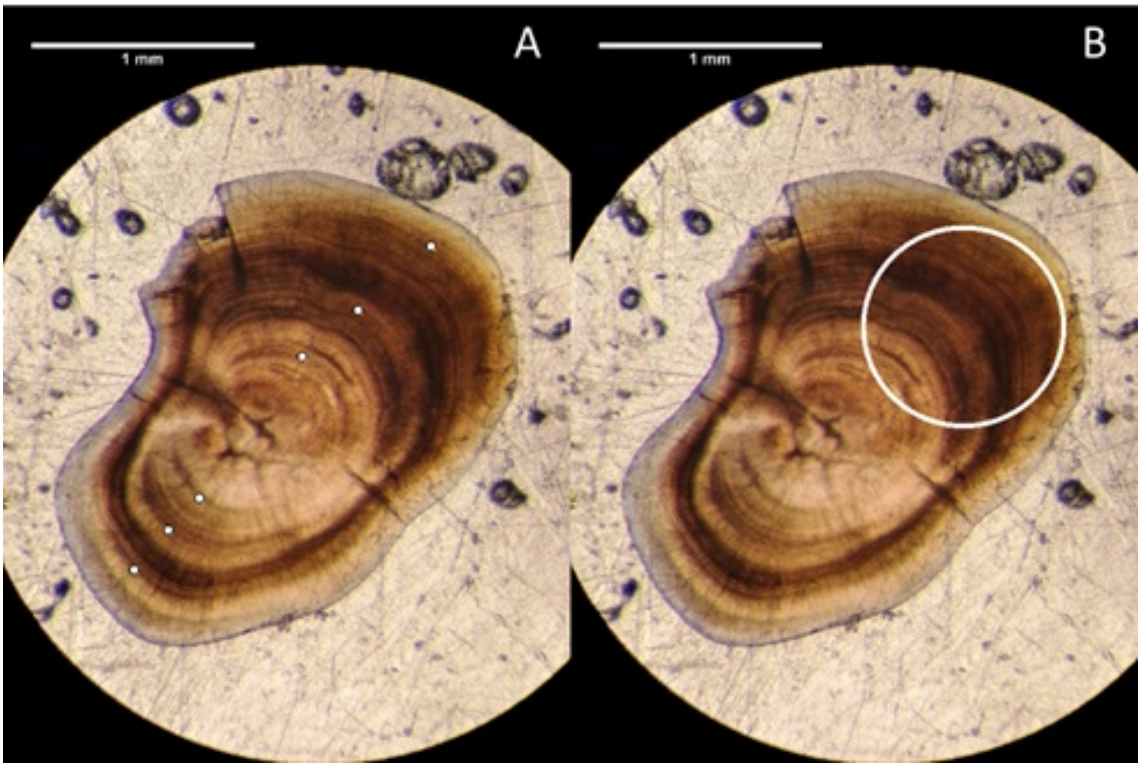

FIGURE E.4: Section of an otolith from *Electrona antarctica* (BAS_33, female, 71 mm SL). White dots indicate estimated annuli (A) and the white circle indicates a representative sampling point with a cut width of 895 μm (B).

E.2.3.2 *Electrona carlsbergi*

From an individual of undetermined length. I estimated the age of the individual was 3 years, and the time incorporated as 1 years from ages 2 to 3 years.

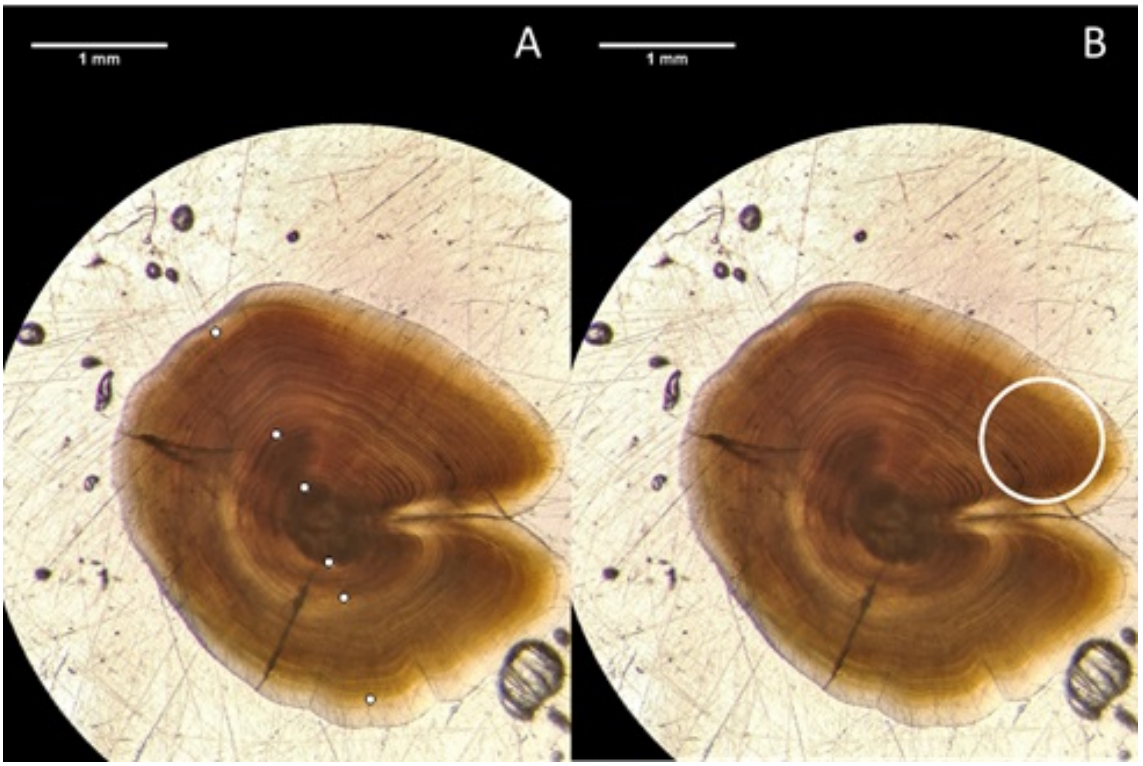

FIGURE E.5: Section of an otolith from *Electrona carlsbergi* (BAS_84). White dots indicate estimated annuli (A) and the white circle indicates a representative sampling point with a cut width of 895 μm (B).

E.2.3.3 *Gymnoscopelus braueri*

From an male, 124 mm SL. I estimated the age of the individual was 6 years, and the time incorporated as 3.5 years from ages 2.5 to 6 years.

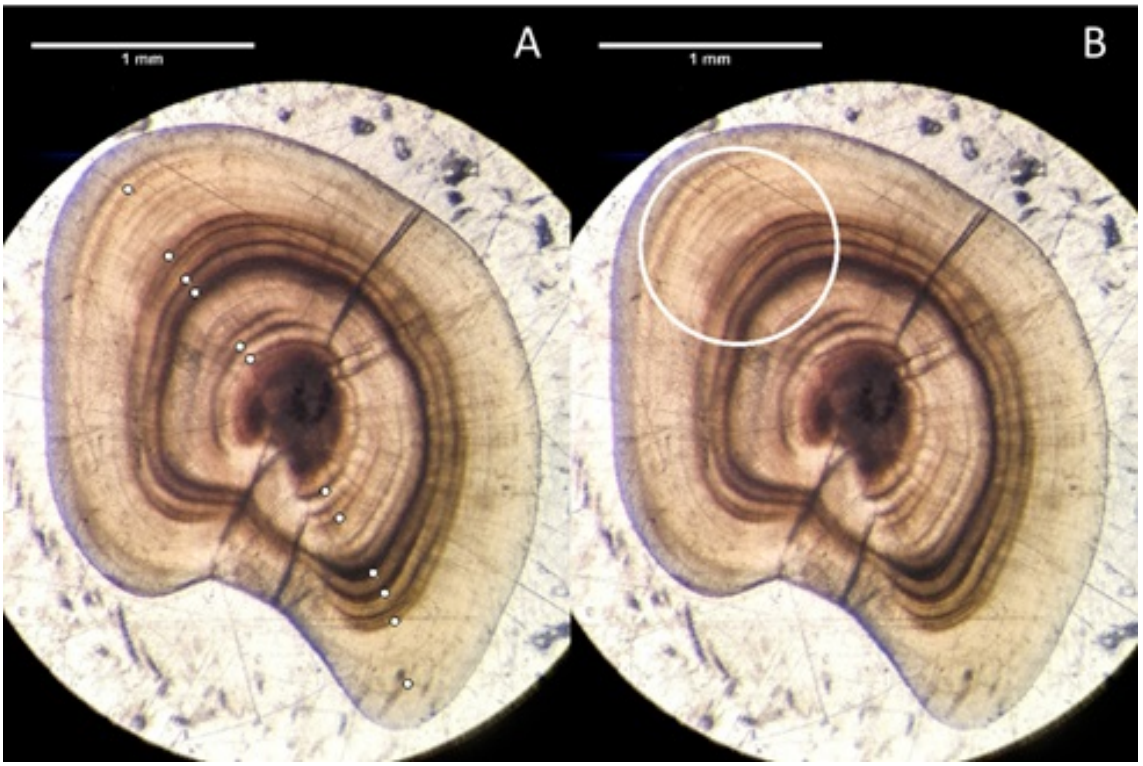

FIGURE E.6: Section of an otolith from *Gymnoscopelus braueri* (BAS_94, male, 124 mm SL). White dots indicate estimated annuli (A) and the white circle indicates a representative sampling point with a cut width of 895 μm (B).

E.2.3.4 *Gymnoscopelus nicholsi*

From an male, 151 mm SL. I estimated the age of the individual was 5 years, and the time incorporated as 2.5 years from ages 2.5 to 5 years.

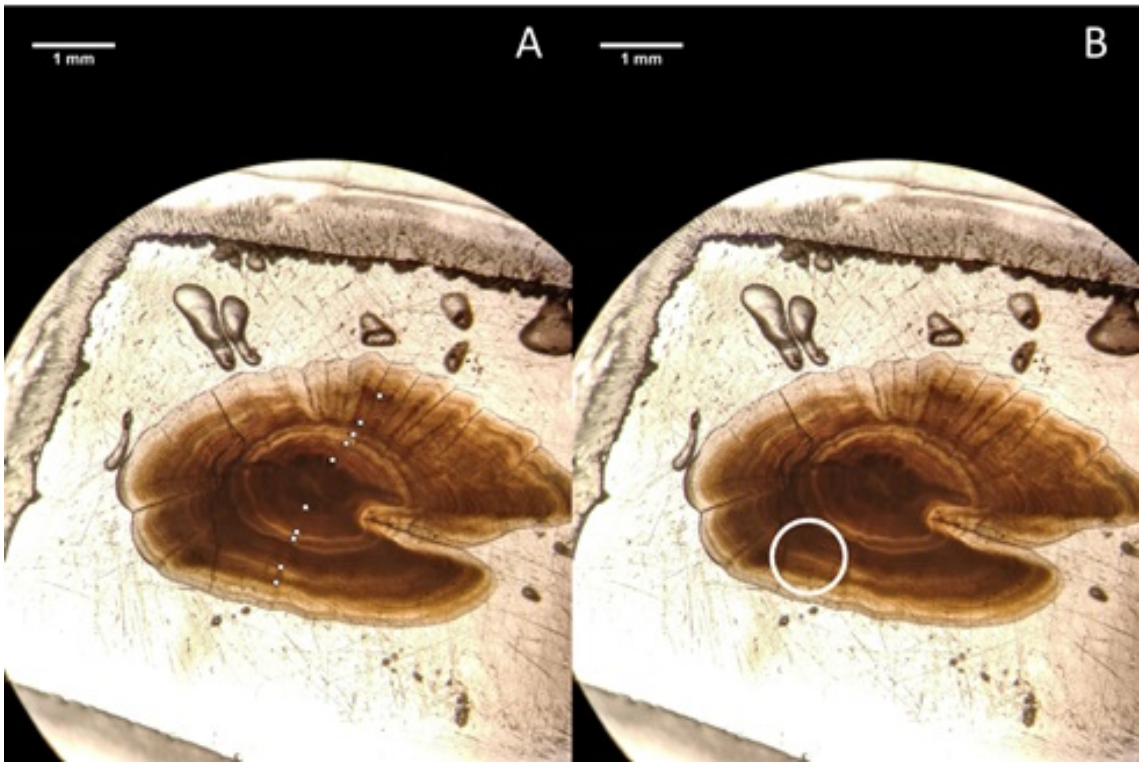

FIGURE E.7: Section of an otolith from *Gymnoscopelus nicholsi* (BAS_122, male, 151 mm SL). White dots indicate estimated annuli (A) and the white circle indicates a representative sampling point with a cut width of 895 μm (B).

E.2.3.5 *Krefftichthys anderssoni*

From an female, 43 mm SL. I estimated the age of the individual was 1.5 years. As *K. anderssoni* otoliths were all crushed, we estimated the amount of time incorporated in the otolith sample is also 1.5 years.

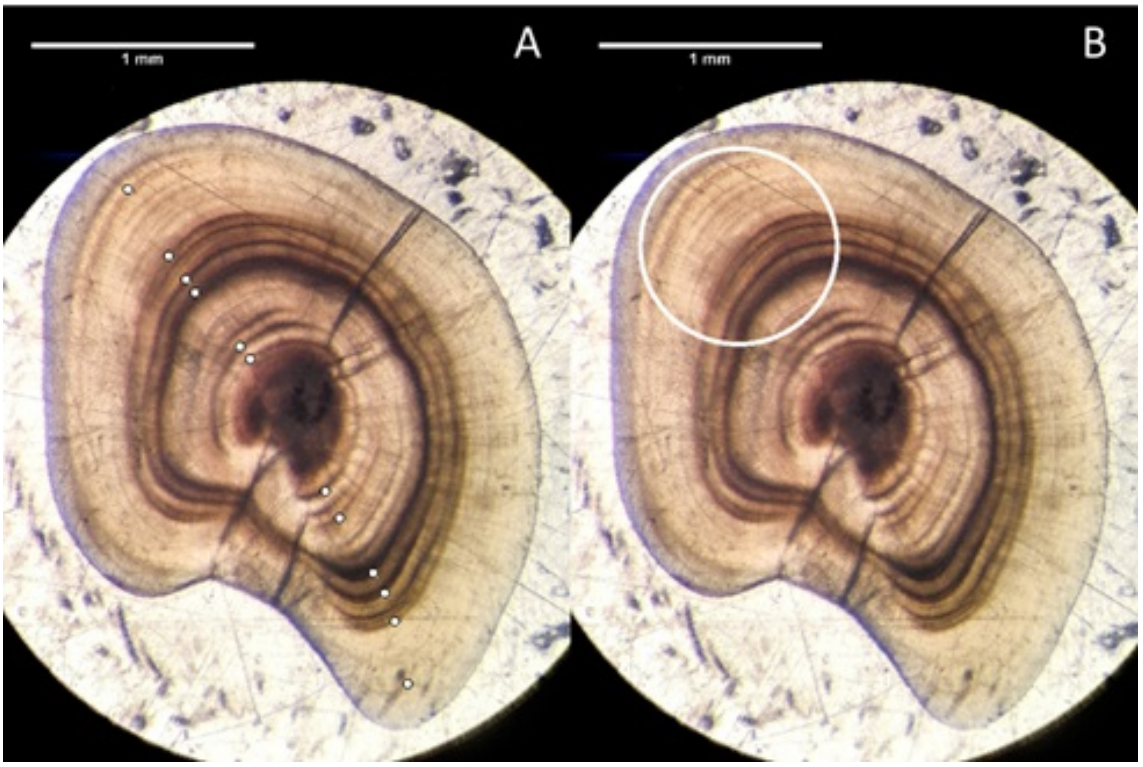

FIGURE E.8: Section of an otolith from *Gymnoscopelus nicholsi* (female, 43 mm SL). White dots indicate estimated annuli.

E.2.3.6 *Neoscopelus microchir*

From an individual of 39 mm HL. I estimated the age of the individual was 5 years, and the time incorporated as 0.5-1 years from ages 3.5 to 4 years.

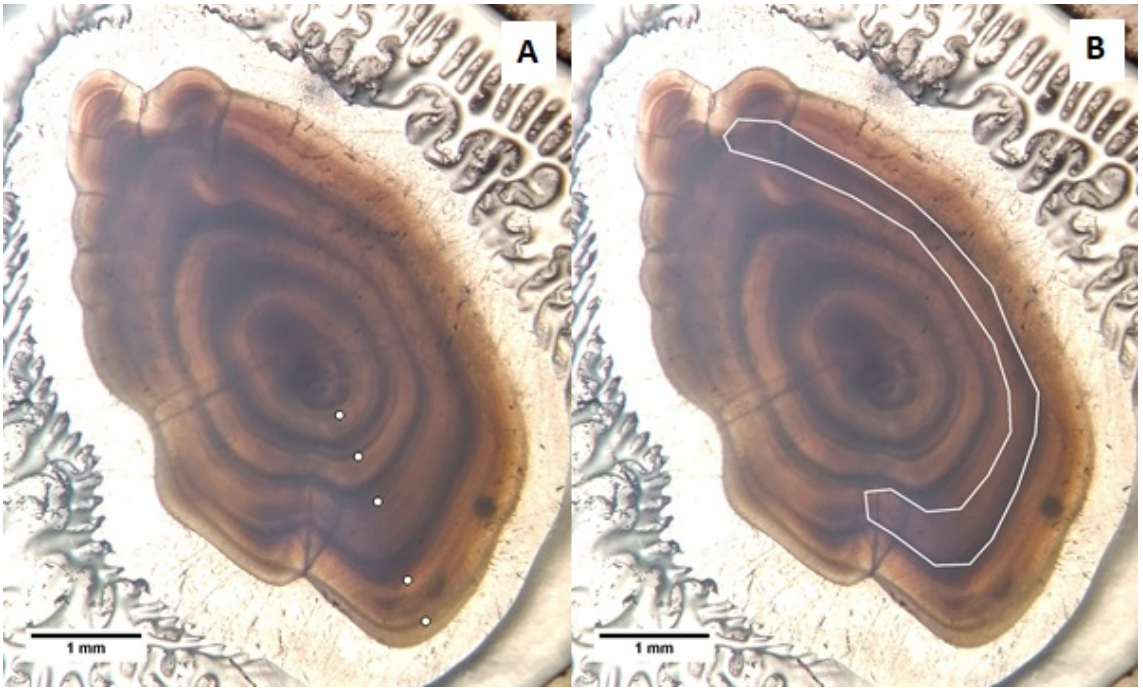

FIGURE E.9: Section of an otolith from *Neoscopelus microchir* (NMI_217/NMI_991, 39 mm HL). White dots indicate estimated annuli (A) and the white polygon indicates approximate sampling area (B).

E.2.3.7 *Protomyctophum bolini*

From an male, 44 mm SL. I estimated the age of the individual was 2.5 years, and the time incorporated as 2 years from ages 0.5 to 2.5 years.

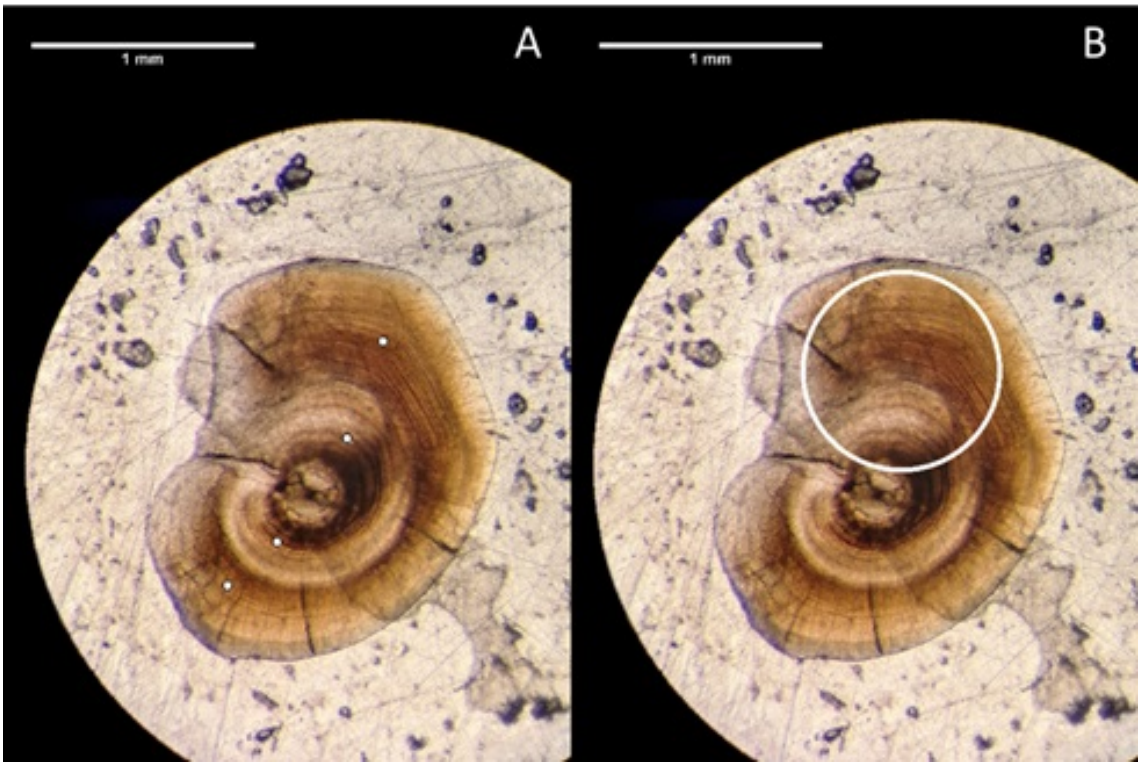

FIGURE E.10: Section of an otolith from *Protomyctophum bolini* (BAS_212, male, 44 mm SL). White dots indicate estimated annuli (A) and the white circle indicates a representative sampling point with a cut width of 895 μm (B).

E.2.4 Perciformes

E.2.4.1 *Lepidoperca coatsii*

From an individual of 210 mm TL. I estimated the age of the individual was between 14 and 18 years, and the time incorporated as 4 years from ages, either between 10 and 14 years, or 14 and 18 years.

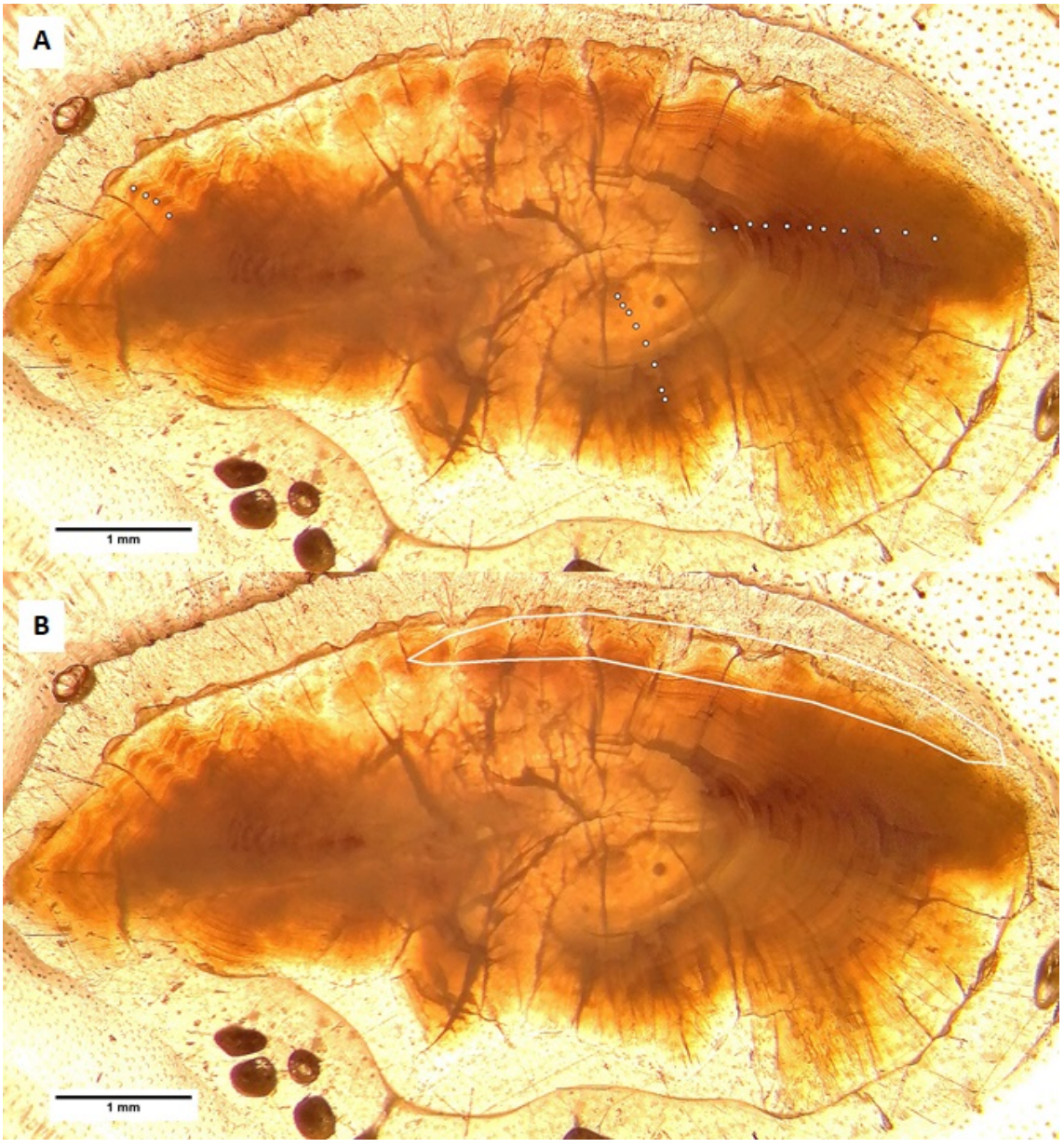

FIGURE E.11: Section of an otolith from *Lepidoperca coatsii* (LCO_2859/LCO_722, 39 mm HL). White dots indicate estimated annuli (A) and the white polygon indicates approximate sampling area (B).

E.2.5 Pleuronectiformes

E.2.5.1 *Limanda limanda*

From an individual of 230 mm SL. I estimated the age of the individual as 3 years, and the time incorporated as 0.5 years, between the ages of 2.5 and 3.0 years.

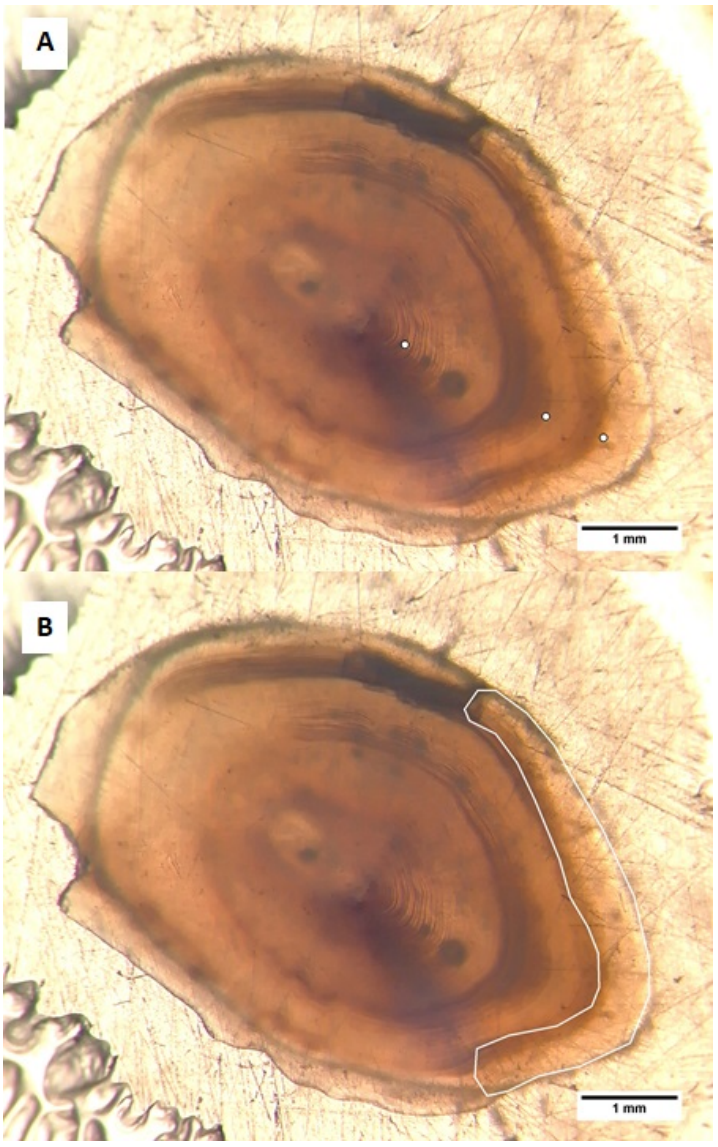

FIGURE E.12: Section of an otolith from *Limanda limanda* (LLI_09, 230 mm SL). White dots indicate estimated annuli (A) and the white polygon indicates approximate sampling area (B).

E.2.5.2 *Microstomus kitt*

From an individual of 250 mm SL. I estimated the age of the individual as 7 years, and the time incorporated as 1.5 to 2 years, between the ages of 5 and 7 years.

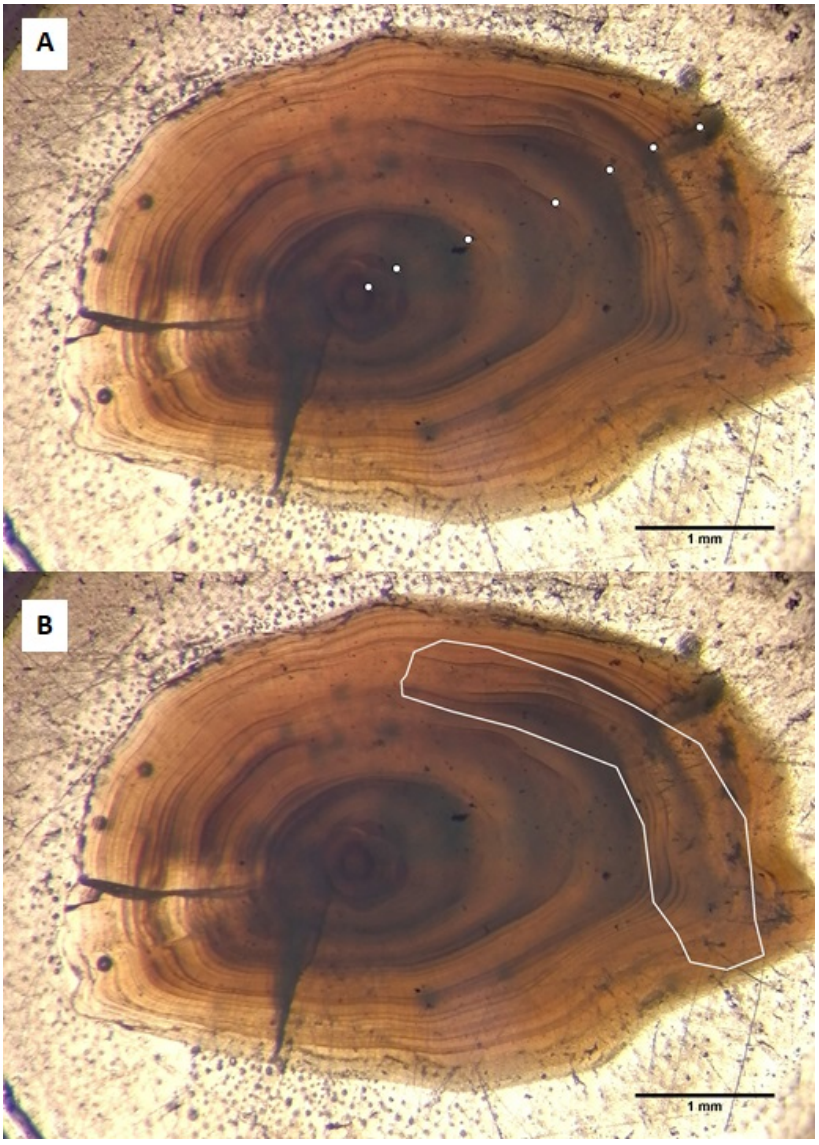

FIGURE E.13: Section of an otolith from *Microstomus kitt* (MKI_09, 250 mm SL). White dots indicate estimated annuli (A) and the white polygon indicates approximate sampling area (B).

E.2.6 Scombriformes

E.2.6.1 *Aphanopus carbo*

From an individual of 900 mm TL. I estimated the age of the individual as 13 years, and the time incorporated as 1 year.

FIGURE E.14: Section of an otolith from *Aphanopus carbo* (ACA_03/ACA_41, 250 mm SL). White dots indicate estimated annuli (A) and the white polygon indicates approximate sampling area (B).

Appendix F

References for phylogeny building

TABLE F.1: References for species additions to the Rabosky et al. (2018) phylogeny. Each species was added to its sister with an arbitrary branch length of 0.5.

Species	Family	Sister Species	Reference
Saurida lessepsianus	Synodontidae	*Saurida undosquamis*	Russell et al., 2015
Helicolenus mouchezi	Sebastidae	*Helicolenus dactylopterus*	Tikochinski et al., 2016
Lycodes gracilis	Zoarcidae	*Lycodes palearis*	Eschmeyer and Hureau, 1971
Spicomacrurus kuronami	Macrouridae	*Hymenocephalus italicus*	Schwarzhans, 2014
Cetonurus globiceps	Macroruidae	*Ventrifossa garmani*	Shi et al., 2016

Appendix G

Summaries of model diagnostics

G.1 Chapter 4: Body mass and temperature scaling

G.1.1 Main models

TABLE G.1: Diagnostics results for the sensitivity test models in the body mass and temperature scaling chapter (Chapter 4). Autocorrelation = 75% quartile for autocorrelation. ESS = minimum effective sample size. Geweke = Geweke's diagnostic. H-W = Heidelberger & Welch's diagnostic.

Model name	Traceplot	Autocorrelation	ESS	Geweke	H-W
c_resp_main	Good	0.010	9980	Acceptable	Passed
mass_specific_main	Good	0.007	9980	Good	Passed
whole_organism_main	Good	0.005	9980	Acceptable	Passed

G.1.2 Sensitivity tests

TABLE G.2: Diagnostics results for the sensitivity test models in the body mass and temperature scaling chapter (Chapter 4). Autocorrelation = 75% quartile for autocorrelation. ESS = minimum effective sample size. Geweke = Geweke's diagnostic. H-W = Heidelberger & Welch's diagnostic.

Model name	Traceplot	Autocorrelation	ESS	Geweke	H-W
c_resp_ours	Good	0.004	9980	Good	Passed
c_resp_outer	Divergent intercept	0.020	9980	Good	Passed
c_resp_priors	Good	0.050	9980	Acceptable	Passed
mass_specific_ours	Good	0.008	9980	Good	Passed
mass_specific_outer	Good	0.010	9980	Acceptable	Passed
mass_specific_priors	Good	0.010	9980	Good	Passed
whole_organism_ours	Divergent intercept	0.010	9980	Acceptable	Passed
whole_organism_outer	Good	0.010	9605	Acceptable	Passed
whole_organism_prior	Good	0.008	9980	Acceptable	Passed

G.2 Chapter 5: Thermal realm

G.2.1 Main models

TABLE G.3: Diagnostics results for the models models in the thermal realm chapter (Chapter 5). Autocorrelation = 75% quartile for autocorrelation. ESS = minimum effective sample size. Geweke = Geweke's diagnostic. H-W = Heidelberger & Welch's diagnostic.

Model name	Traceplot	Autocorrelation	ESS	Geweke	H-W
realm_main	Good	0.009	9604	Good	Passed
realm_interaction	Good	0.009	9657	Acceptable	Passed
range_interaction	Divergent intercept	0.011	9161	Acceptable	Failed log(bm):range

G.2.2 Sensitivity tests

TABLE G.4: Diagnostics results for the sensitivity test models in the body mass and temperature scaling chapter (Chapter 4). Autocorrelation = 75% quartile for autocorrelation. ESS = minimum effective sample size. Geweke = Geweke's diagnostic. H-W = Heidelberger & Welch's diagnostic.

Model name	Traceplot	Autocorrelation	ESS	Geweke	H-W
realm_main_ours	Divergent intercept	0.009	9980	Good	Failed several
realm_main_outer	Good	0.009	9980	Good	Failed tropical
realm_main_prior	Good	0.007	9228	Good	Failed temperate
realm_int_ours	Divergent intercept	0.009	9980	Concerning	Failed several
realm_int_outer	Good	0.009	9980	Acceptable	Failed log(bm):subtropical
realm_int_prior	Good	0.009	9401	Acceptable	Passed
realm_int_no_polar	Good	0.009	9129	Good	Passed
range_int_ours	Divergent intercept	0.011	9895	Good	Failed intercept
range_int_outer	Good	0.008	9823	Good	Passed
range_int_prior	Good	0.010	9643	Good	Failed log(bm):range

G.3 Chapter 6: Depth

G.3.1 Main models

TABLE G.5: Diagnostics results for the main models in the depth chapter (Chapter 6). Autocorrelation = 75% quartile for autocorrelation. ESS = minimum effective sample size. Geweke = Geweke's diagnostic. H-W = Heidelberger & Welch's diagnostic.

Model name	Traceplot	Autocorrelation	ESS	Geweke	H-W
max_main	Good	0.023	2552	Good	Passed
max_pelagic	Good	0.027	2639	Good	Passed
max_gads	Divergent intercept	0.034	2565	Good	Passed
min_main	Good	0.017	2557	Good	Passed
min_pelagic	Good	0.021	2283	Good	Passed
min_gads	Divergent intercept	0.043	2670	Good	Passed

G.3.2 Sensitivity tests

TABLE G.6: Diagnostics results for the sensitivity test models in the depth chapter (Chapter 6). Autocorrelation = 75% quartile for autocorrelation. ESS = minimum effective sample size. Geweke = Geweke's diagnostic. H-W = Heidelberger & Welch's diagnostic.

Model name	Traceplot	Autocorrelation	ESS	Geweke	H-W
max_depth_outer	Divergent intercept	0.032	2543	Good	Passed
max_depth_ours	Divergent intercept	0.024	2712	Acceptable	Passed
max_depth_prior	Good	0.007	9646	Good	Passed
max_depth_minus_two	Good	0.024	2442	Acceptable	Passed
min_depth_outer	Divergent intercept	0.040	2405	Concerning intercept	Passed
min_depth_ours	Divergent intercept	0.040	1731	Good	Passed
min_depth_prior	Good	0.006	9980	Good	Passed
min_depth_minus_two	Good	0.200	2402	Acceptable	Passed

Appendix H

Model sensitivity testing

H.1 Chapter 3: Myctophids

To test whether the method of otolith preparation (outer surface vs. whole-otolith sample) had a significant impact on resulting C_{resp} values, we modelled C_{resp} values as a function of otolith preparation method, with species as a random factor:

$$C_{resp} \sim a + b_{prep} \times prep + a\_Varspecies \tag{H.1}$$

Where $prep$ is the method of preparation assigned to a dummy variable (outer edge = 0, whole-otolith = 1) and b_{Prep} is the effect of crushing the otolith on C_{resp} values, and $a\_Var\_Species$ is the variable intercept for species. We did the same for temperature, modifying equation S1 to swap C_{resp} values for experienced temperature ($temp$):

$$temp \sim a + b_{prep} \times prep + a\_Varspecies \tag{H.2}$$

The use of whole-otolith samples significantly increased resulting C_{resp} values, as indicated by b_{Prep} 95% HDPIs not overlapping zero (Figure H.1), however, this significance was marginal; the value for b_{Prep} was 0.026 ± 0.019. Additionally this model's diagnostics did show some concerning behaviour (Gelman-Rubin diagnostic > 1.01 and low effective sample size), so should be treated with caution. There was no significant effect of preparation method on temperature (Figure H.1).

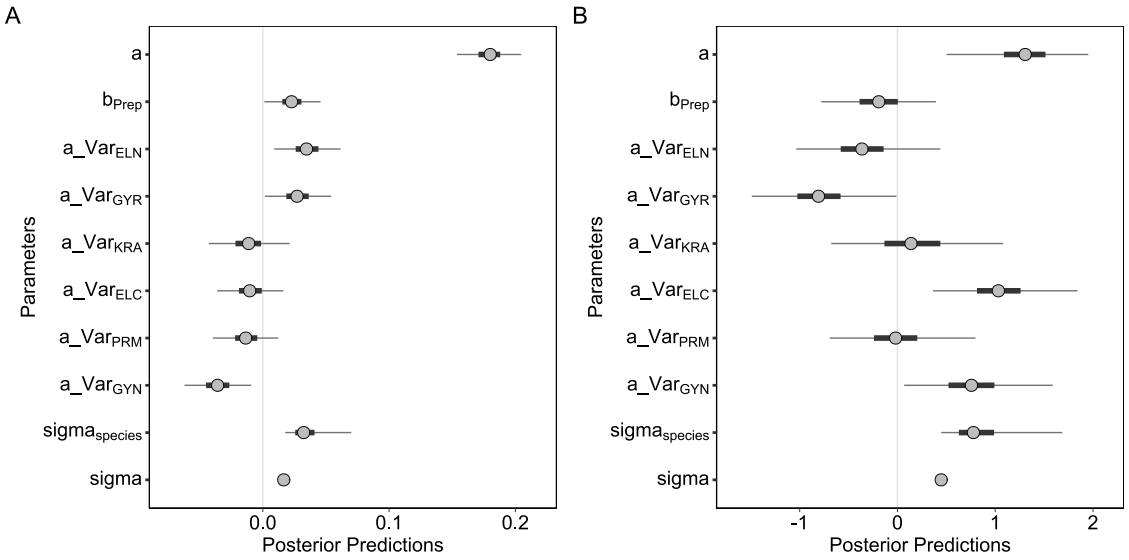

FIGURE H.1: Posterior predictions for (A) equation H.1 and (B) equation H.2. a is the intercept; b_{Prep} is the effect of using whole-otolith samples on C_{resp} and a_Var represents the variable intercept for each species; ELN = *Electrona antarctica*, GYR = *Gymnoscopelus braueri*, KRA = *Krefftichthys anderssoni*, ELC = *Electrona carlsbergi*, PRM = *Protomyctophum bolini* and GYN = *Gymnoscopelus nicholsi*. *sigma* indicates overall residual error, and $sigma_{Species}$ is residual error of the species variable intercept. Circles indicate the mean of the posterior predictions. Thick lines show the 50% posterior intervals, while thin lines show the 95% posterior intervals. Results are considered statistically significant if the 95% highest density posterior intervals do not overlap with zero.

Most otoliths from *Protomyctophum bolini* were milled, but two small otoliths were crushed. Therefore we ran the same model, without the variable intercept for species, to test for a difference in C_{resp} values or temperature between crushed and milled otoliths within *P. bolini*:

$$C_{resp} \sim a + b_{prep} \times prep \tag{H.3}$$

$$temp \sim a + b_{prep} \times prep \tag{H.4}$$

There was no significant effect of preparation method on Cresp values or temperature within this species (Figure H.2).

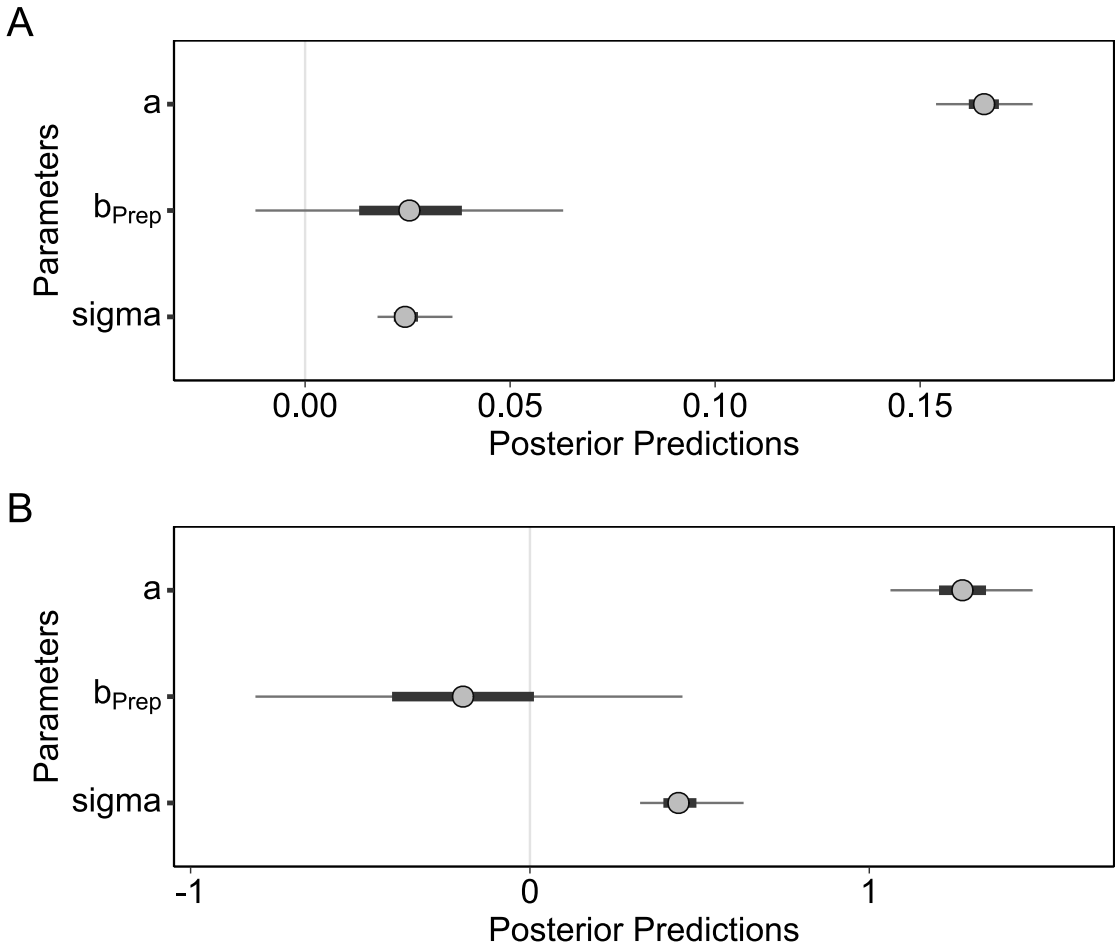

FIGURE H.2: Posterior predictions for (A) equation H.3 and (B) equation H.4 within *Protomyctophum bolini*. *a* is the intercept and b_{Prep} is the effect of using whole-otolith samples on C_{resp} and *sigma* is the residual error. Circles indicate the mean of the posterior predictions. Thick lines show the 50% posterior intervals and thin lines show the 95% posterior intervals. Sigma indicates error. Results are considered statistically significant if the 95% highest density posterior intervals do not overlap with zero.

Given the unbalanced design of these two models, it is unclear whether preparation method had a significant effect on Cresp values. Given that *Krefftichthys anderssoni* C_{resp} values were entirely estimated using crushed otolith samples, it is likely that *K. anderssoni* C_{resp} values are slightly higher due to this preparation method, and this should be born in mind when interpreting our results. As only two *P. bolini* otoliths were crushed, this is unlikely to have unduly influenced C_{resp} values for this species. It is unlikely that crushing had any significant effect on otolith-derived temperature.

H.2 Chapter 4: Body mass and temperature scaling

None of the sensitivity tests had any significant effect on the body mass or temperature scaling of C_{resp} values (Table H.1). Results were similar for the mass-specific (Table H.2) and whole organism (Table H.3) oxgyen consumption sensitvity tests. For oxygen consumption, removing literature data slightly decreased the standardised effect size of log body mass, and removing whole otolith samples slightly increased the standardized effect size of temperature (Table H.2). However, overall results remained consistent across the sensitivity tests.

TABLE H.1: Sensitivity tests for C_{resp} value models in the body mass and temperature scaling chapter (Chapter 4).

Model name	**intercept (*a*)**	**main effects (*b*)**		λ
		log(bm)	**temp**	
c_resp_main	0.20	-0.03	0.04	0.92
c_resp_ours	0.22	-0.02	0.04	0.93
c_resp_outer	0.20	-0.03	0.04	0.93
c_resp_prior	0.19	-0.03	0.04	0.93

TABLE H.2: Sensitivity tests for mass-specific oxygen consumption models in the body mass and temperature scaling chapter (Chapter 4).

Model name	**intercept (*a*)**	**main effects (*b*)**		λ
		log(bm)	**temp**	
mass_specific_main	4.41	-0.26	-0.31	0.58
mass_specific_ours	4.40	-0.20	-0.34	0.53
mass_specific_outer	4.24	-0.26	-0.36	0.62
mass_specific_prior	4.37	-0.26	-0.31	0.67

TABLE H.3: Sensitivity tests for whole organism oxygen consumption models in the body mass and temperature scaling chapter (Chapter 4).

Model name	**intercept (*a*)**	**main effects (*b*)**		λ
		log(bm)	**temp**	
whole_organism_main	3.24	2.53	-0.31	0.59
whole_organism_ours	2.50	2.05	-0.34	0.52
whole_organism_outer	3.06	2.50	-0.36	0.62
whole_organism_prior	3.20	2.52	-0.31	0.65

H.3 Chapter 5: Thermal realm

H.3.1 Thermal realm models

Removing literature data (therm_ours) changed the scaling of C_{resp} values with temperature in the polar group from negative to positive (Table H.4). Removing literature data also increased the scaling of C_{resp} values with temperature in the tropical group, while reducing the temperature scaling in the subtropical group (Table H.4). Neither removing whole-otolith samples (therm_outer) or changing priors (therm_prior) significantly altered the scaling effects for the interaction models (Table H.4).

TABLE H.4: Sensitivity tests for interaction effects models in the thermal realm chapter (Chapter 5).

Model name	**body mass (*b*)**	**polar**		**temperate**		**subtropical**		**tropical**		λ
		intercept (*a*)	temp (*b*)	intercept (*a*)	temp (*b*)	intercept (*a*)	temp (*b*)	intercept (a)	temp (b)	
therm_main	-0.03	0.10	-0.08	0.19	0.01	0.23	0.06	0.09	0.10	0.96
therm_ours	-0.02	0.32	0.04	0.29	0.03	0.38	0.02	0.27	0.14	0.99
therm_outer	-0.04	0.12	-0.08	0.18	0.03	0.23	0.05	0.12	0.11	0.97
therm_prior	-0.04	0.08	-0.07	0.18	0.02	0.25	0.04	0.06	0.10	0.94

Removing literature data (therm_ours) and removing whole-otolith samples (therm_outer) both reduced the model mean C_{resp} value for the tropical group (Table H.5). The sensitivity tests had no significant effects on body mass or temperature scaling, nor any significant effects on any other thermal realm groups.

TABLE H.5: Sensitivity tests for the main effects models in the thermal realm chapter (Chapter 5).

Model	**body mass (*b*)**	**temp (*b*)**	**intercept (*a*)**				λ
			polar	temperate	subtropical	tropical	
therm_main	-0.02	0.01	0.21	0.20	0.29	0.26	0.96
therm_ours	-0.02	0.03	0.23	0.21	0.27	0.21	0.99
therm_outer	-0.02	0.02	0.22	0.22	0.28	0.23	0.97
therm_prior	-0.02	0.02	0.20	0.19	0.29	0.26	0.95

H.3.2 Range sea-surface temperature models

Removing whole-otolith samples (range_outer) had the greatest effect on model outcomes, reducing the effect of range on C_{resp} values and altering interaction effects (Table H.6). Removing literature data (range_ours) increased the effect of temperature on C_{resp} values (Table H.6).

TABLE H.6: Results summary for sensitivity tests of interaction models concerning range in sea-surface temperature (Chapter 5). * = failed diagnostic tests (Appendix G)

Model	**Intercept (*a*)**	**Main effects (*b*)**			**Interaction effects (*b*)**		λ
		log(bm)	temp	range	log(bm):range	temp:range	
range_main	0.21	-0.02	0.02	-0.03	0.00	-0.01	0.96
range_ours	1.93*	-0.02	0.04	-0.02	0.00	-0.02	0.98
range_outer	0.20	-0.02	0.03	0.00	-0.02	0.01	0.97
range_prior	0.19	-0.02	0.03	-0.02	0.00*	-0.02	0.95

H.4 Chapter 6: Depth

Across all sensitivity tests, the effect of maximum depth on C_{resp} values decreased (Table H.7). However, sensitivity tests brought about no significant changes in any outcomes concerning minimum depth (Table H.8).

TABLE H.7: Results summary for sensitivity tests of maximum depth in the depth chapter (Chapter 6).

Model	**Intercept (*a*)**	**Main effects (*b*)**			λ
		log(bm)	temp	depth	
max_main	1.77	0.14	-0.22	0.10	0.98
max_ours	1.74	0.15	-0.25	0.08	0.98
max_outer	1.83	0.16	-0.23	0.07	0.98
max_prior	1.73	0.15	-0.23	0.08	0.78
max_minus_two	1.75	0.14	-0.23	0.08	0.97

TABLE H.8: Results summary for sensitivity tests of minimum depth in the depth chapter (Chapter 6).

Model	**Intercept (*a*)**	**Main effects (*b*)**			λ
		log(bm)	temp	depth	
max_main	1.77	0.14	-0.23	0.11	0.98
max_ours	1.75	0.16	-0.24	0.10	0.98
max_outer	1.83	0.16	-0.21	0.11	0.98
max_prior	1.74	0.15	-0.22	0.10	0.77
max_minus_two	1.76	0.14	-0.22	0.11	0.98

Appendix I

Extra analyses for Chapter 3: Myctophids

I.1 Effect of life stage on C_{resp} values

To test for possible effects of different life stages on C_{resp} values, we divided individual standard length (SL, mm) by maximum SL for that species and used this to model C_{resp} values:

$$C_{resp}sima + b\_R_{SL} \times R_{SL} + a\_Var_{Species} \tag{I.1}$$

Where R_{SL} is the ratio of SL to maximum SL and b_R_{SL} is the effect of that ratio on C_{resp} values. Only C_{resp} values from outer-edge samples were included in this model, as these samples best matched recorded SL for each individual. Although there appears to be a negative correlation between SL ratio and C_{resp} values (Figure I.1), which supports the use of C_{resp} as a metabolic proxy, we found that there was no effect of this ratio on C_{resp} when accounting for replication within species (Figure I.2).

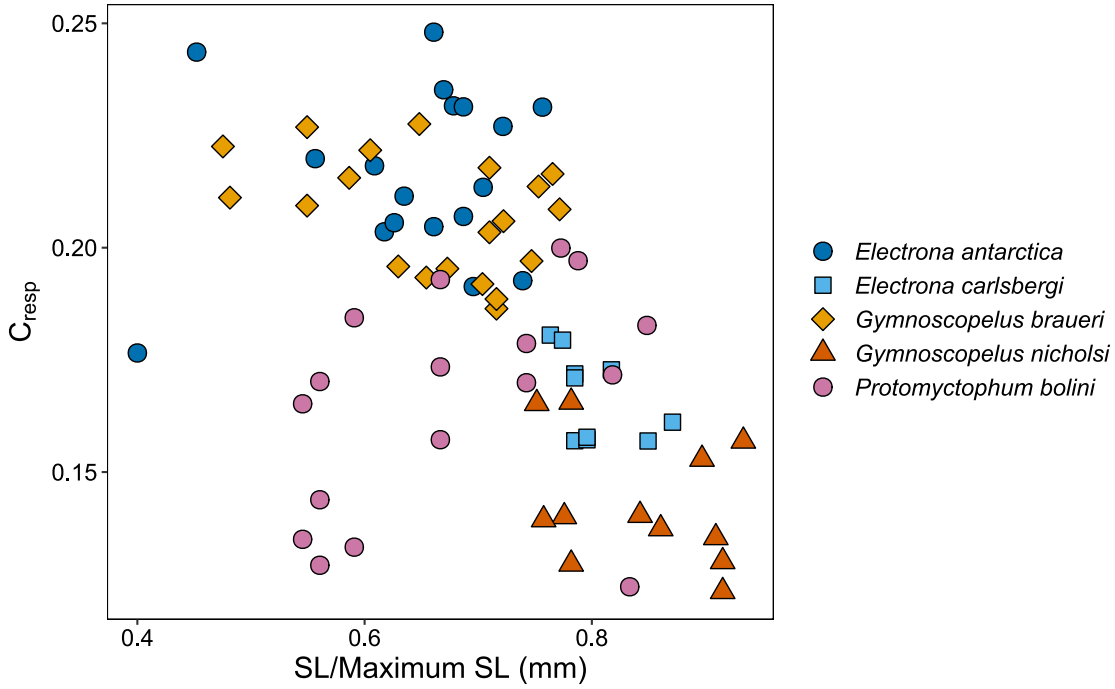

FIGURE I.1: C_{resp} values plotted against ratio of standard length (SL, mm) of the individual to maximum SL for that species, for individuals of five myctophid species.

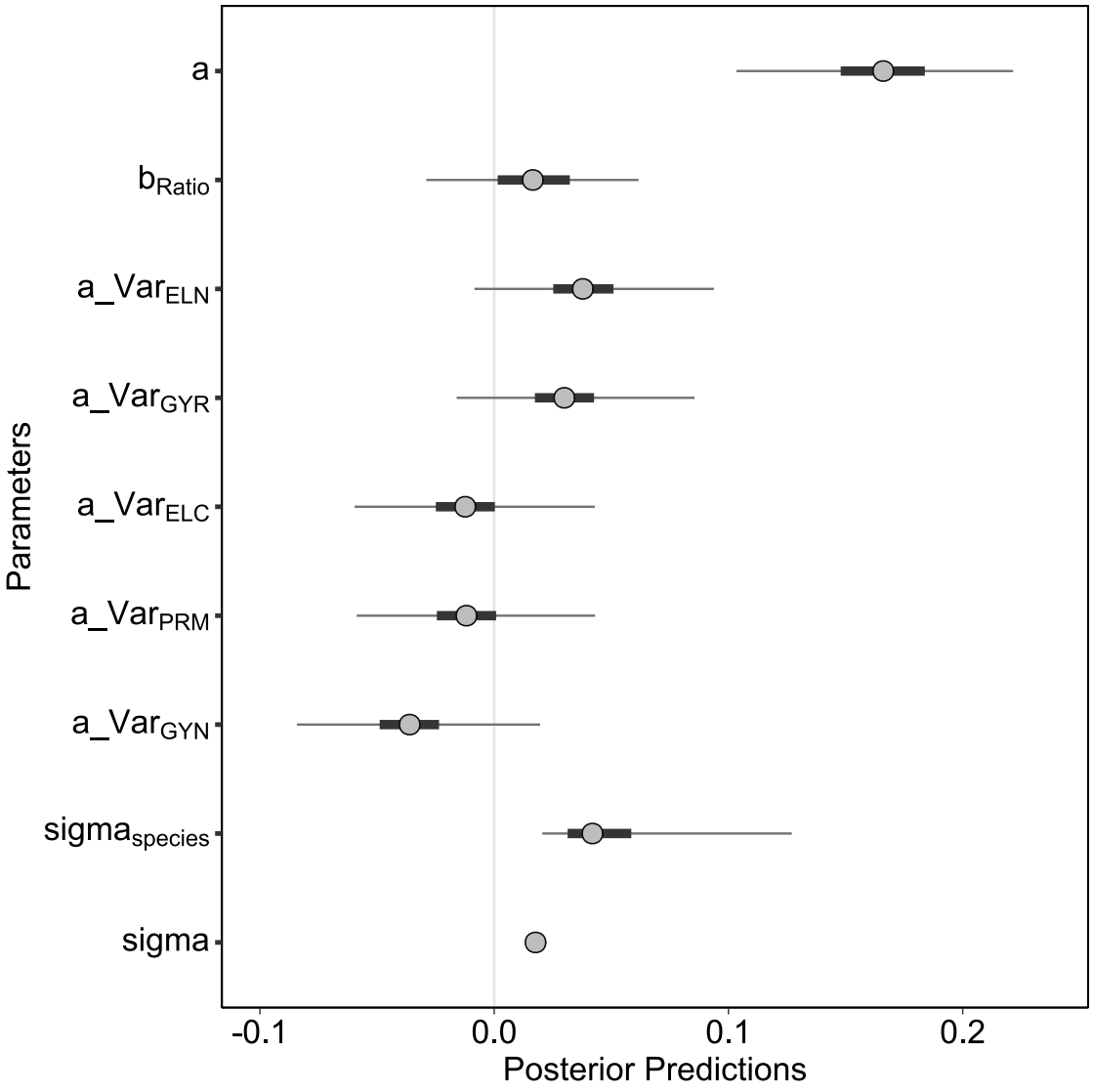

FIGURE I.2: Posterior predictions for equation I.1. *a* is the intercept; *bRatio* is the effect of the ratio of standard length (mm) to species maximum length on C_{resp} values, and *a_Var* represents the variable intercept for each species; ELN = *Electrona antarctica*, GYR = *Gymnoscopelus braueri*, KRA = *Krefftichthys anderssoni*, ELC = *Electrona carlsbergi*, PRM = *Protomyctophum bolini* and GYN = *Gymnoscopelus nicholsi*. *sigma* indicates overall residual error, and $sigma_{Species}$ is residual error of the species variable intercept. Circles indicate the mean of the posterior predictions. Thick lines show the 50% posterior intervals, while thin lines show the 95% posterior intervals. Results are considered statistically significant if the 95% highest density posterior intervals do not overlap with zero.

I.2 Effect of year of capture within species

We used the following model investigate whether year of capture had a significant effect on C_{resp} values within each species:

$$C_{resp} \sim a + b_{Year} + Year \tag{I.2}$$

Where b_{Year} is the effect of year of capture on C_{resp} values. Year of capture was assigned to a dummy variable (1998 = -1, 2008 = 0 and 2016 = 1). Within most species, year of capture had no significant effect on C_{resp} values. *Protomyctophum bolini* was the exception (Figure I.3), wherein individuals captured in 2016 had a higher mean C_{resp} value than those captured in 2008 (b_{Year} = 0.028 $\pm$ 0.01). This led to further investigations within *P. bolini* (see below).

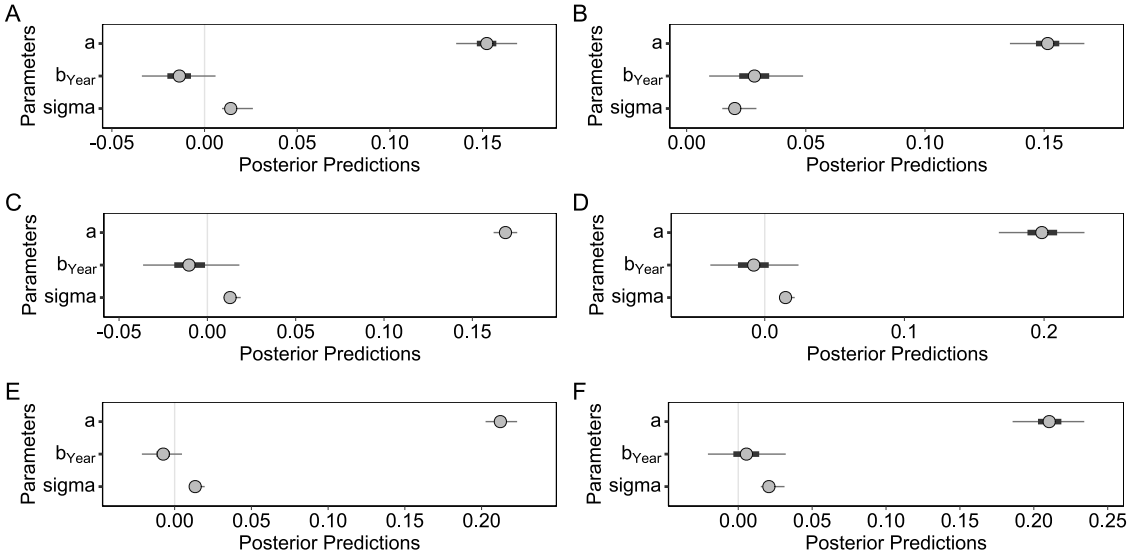

FIGURE I.3: Posterior predictions for equation I.2 within species. A = *Gymnoscopelus nicholsi*, B = *Protomyctophum bolini*, C = *Electrona carlsbergi*, D = *Krefftichthys anderssoni*, E = *Gymnoscopelus braueri*, F = *Electrona antarctica*). *a* is the intercept, b_{Year} is the effect of year of capture on C_{resp} values within that species, and *sigma* is residual error. Circles are the mean of the posterior predictions. Thin lines show the 95% highest density posterior intervals. Results are considered statistically significant if the 95% highest density posterior intervals do not overlap with zero.

I.3 Further investigations within species

I.3.1 *Protomyctophum bolini*

To test whether latitude had a significant effect on C_{resp} values within *P. bolini*, we modelled C_{resp} values as a function of latitude of capture:

$$C_{resp} \sim a + b_{Lat} \times Lat \tag{I.3}$$

where *Lat*itude is the latitude of capture in decimal degrees and b_{Lat} is the effect latitude of capture on C_{resp} values. *P. bolini* individuals captured further north had significantly lower C_{resp} values than those captured further south, as indicated by b_{Lat} 95% HDPIs not overlapping zero (Figure I.5).

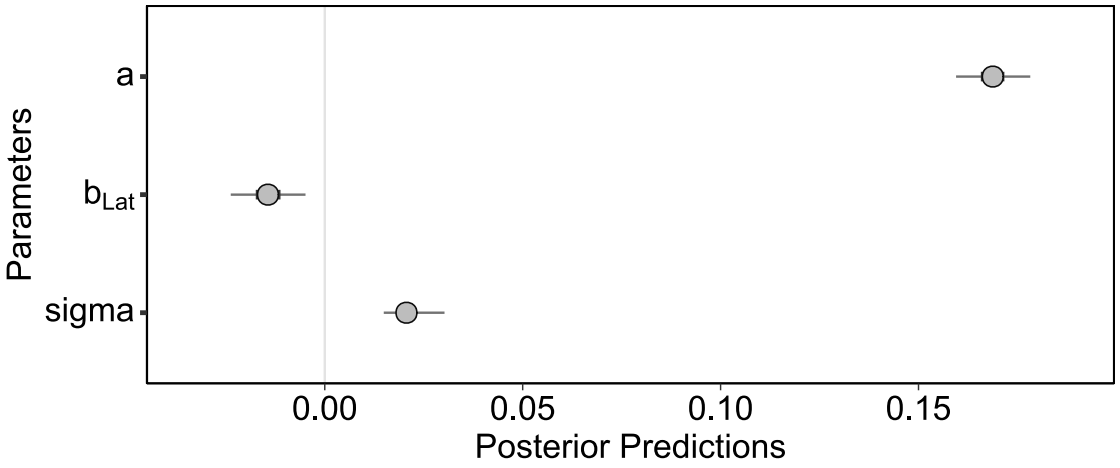

FIGURE I.4: Posterior predictions for equation I.3 within *Protomyctophum bolini*. *a* is the intercept and b_{Lat} is the effect of latitude of capture on C_{resp} values and *sigma* is the residual error. Circles indicate the mean of the posterior predictions. Thick lines show the 50% posterior intervals and thin lines show the 95% posterior intervals. Sigma indicates error. Results are considered statistically significant if the 95% highest density posterior intervals do not overlap with zero.

To investigate whether this phenomenon was specific to *P. bolini*, we ran the above model across all species, but also included a variable intercept of species ($a\_Var_{Species}$):

$$C_{resp} \sim a + b_{Lat} \times Lat + a\_Var_{Species} \tag{I.4}$$

When investigating all species together, there was no effect of latitude on C_{resp} values (Figure S14).

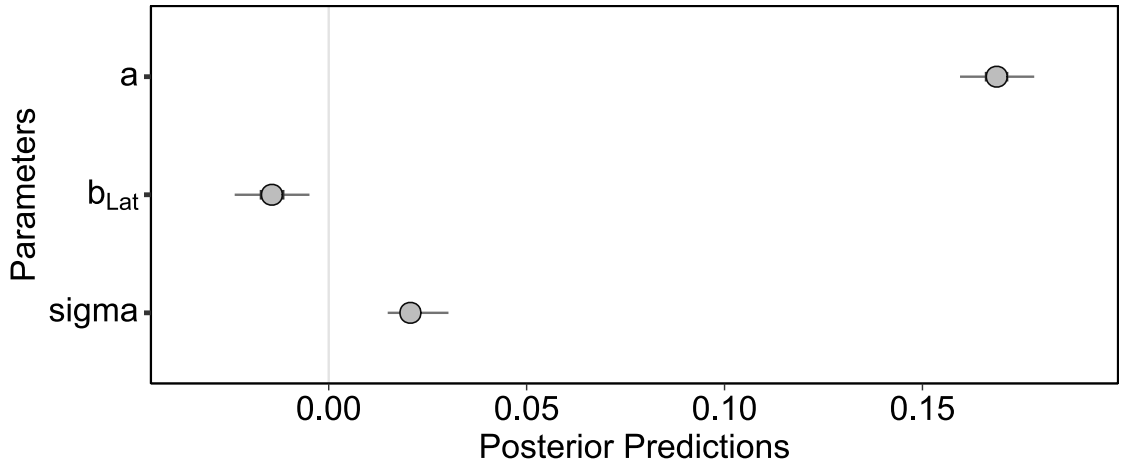

FIGURE I.5: Posterior predictions for equation I.4. a is the intercept; b_{Lat} is the effect of latitude on C_{resp} values, and a_Var represents the variable intercept for each species; ELN = *Electrona antarctica*, GYR = *Gymnoscopelus braueri*, KRA = *Krefftichthys anderssoni*, ELC = *Electrona carlsbergi*, PRM = *Protomyctophum bolini* and GYN = *Gymnoscopelus nicholsi*. $sigma$ indicates overall residual error, and $sigma_{Species}$ is residual error of the species variable intercept. Circles indicate the mean of the posterior predictions. Thick lines show the 50% posterior intervals, while thin lines show the 95% posterior intervals. Results are considered statistically significant if the 95% highest density posterior intervals do not overlap with zero.

To investigate whether diet could be the driver of this variation, we modified equation S8 to test for an effect of latitude on $\delta^{13}C$ of muscle ($\delta^{13}C_{musc}$), our proxy for $\delta^{13}C$ of diet.

$$\delta^{13}C \sim a + b_{Lat} \times Lat \tag{I.5}$$

We found no significant effect of latitude on $\delta^{13}C_{musc}$ (Figure I.6).

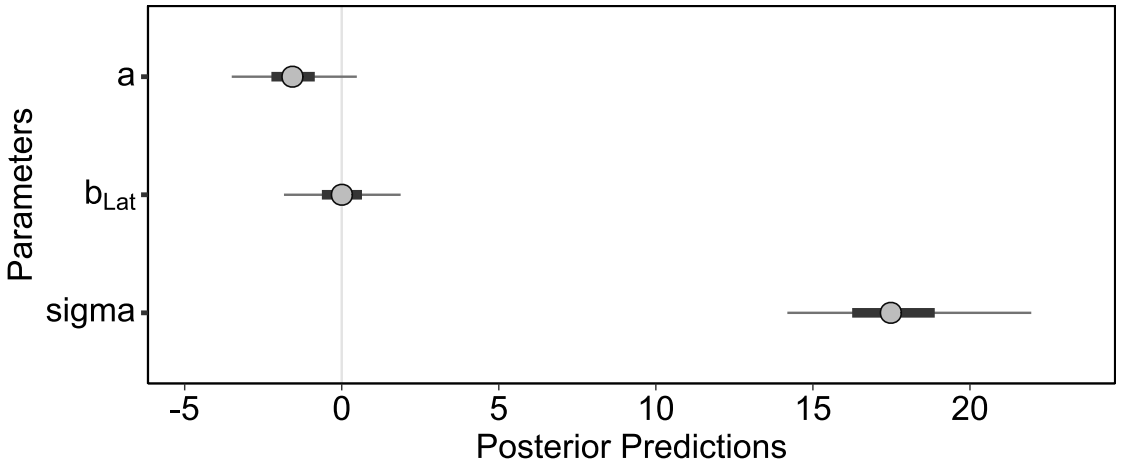

FIGURE I.6: Posterior predictions for equation I.5 within *Protomyctophum bolini*. *a* is the intercept and b_{Lat} is the effect of latitude of capture on C_{resp} values and *sigma* is the residual error. Circles indicate the mean of the posterior predictions. Thick lines show the 50% posterior intervals and thin lines show the 95% posterior intervals. Sigma indicates error. Results are considered statistically significant if the 95% highest density posterior intervals do not overlap with zero.

I.3.2 *Gymnoscopelus nicholsi*

We tested whether there was a significant difference between C_{resp} values of *G. nicholsi* individuals caught on the South Orkneys shelf breaks and those caught elsewhere. We did this by modelling C_{resp} values as a function of location:

$$C_{resp} \sim a + b_{Location} \times Location \tag{I.6}$$

Where *Location* is the location of capture assigned to a dummy variable (South Orkneys = 1, elsewhere = 0) and $b_{Location}$ is the effect of location being South Orkneys on C_{resp} values. There was no significant difference between C_{resp} values of *G. nicholsi* individuals captured at the South Orkneys compared to those captured elsewhere (Figure S16).

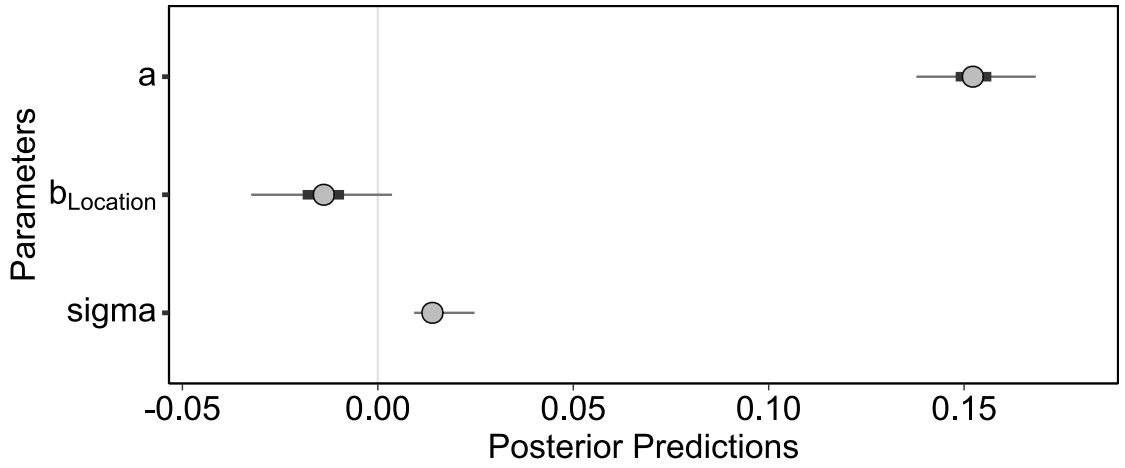

FIGURE I.7: Posterior predictions for equation I.6 within *Gymnoscopelus nicholsi*. *a* is the intercept and $b_{Location}$ is the effect of catch location being the South Orkneys on C_{resp} values and *sigma* is the residual error. Circles indicate the mean of the posterior predictions. Thick lines show the 50% posterior intervals and thin lines show the 95% posterior intervals. Sigma indicates error. Results are considered statistically significant if the 95% highest density posterior intervals do not overlap with zero.

I.4 Age estimations of study individuals from length

For Table 3.2, we estimated the age (t) of each individual using a rearranged von Bertalanffy growth function:

$$t = \frac{1}{K} ln \frac{L_\infty}{L_\infty - L_t} + t_0 \tag{I.7}$$

where K is the growth coefficient, L_t is standard length (mm) L_∞ is asymptotic standard length and t_0 is length at age 0. Table I.1 gives the parameters used and their sources. Unfortunately there are no reliable growth parameters for *Protomyctophum bolini*.

TABLE I.1: Growth function parameters for studied species. SL is standard length, L_∞ is asymptotic standard length, K is the growth coefficient and t_0 is length at age 0. ELN = *Electrona antarctica*, GYR = *Gymnoscopelus braueri*, KRA = *Krefftichthys anderssoni*, ELC = *Electrona carlsbergi* and GYN = *Gymnoscopelus nicholsi*.

Species	**SL Units**	L_∞	K	t_0	**Source**
ELN	cm	11.3	0.21	0.7	Linkowski (1987)
GYR	mm	133.22	0.29	-0.21	Saunders et al. (2020)
KRA	mm	68.6	0.71	-0.49	Saunders et al. (2020)
ELC	cm	9.7	0.55	-0.6	Linkowski (1987)
GYN	mm	163.8	0.41	0.081	Linkowski (1985)

References

P. Abaunza, A. Murta, S. Mattiucci, R. Cimmaruta, G. Nascetti, A. Magoulas, A. Sanjuan, S. Comesaña, K. MacKenzie, and J. Molloy. Stock discrimination of horse mackerel (*trachurus* trachurus) in the Northeast Atlantic and Mediterranean Sea: integrating the results from different stock identification approaches. International Council for the Exploration of the Sea (ICES), 2004.

M. A. Abiom, G. M. Menezes, T. Schlitt, and A. D. Rogers. Genetic structure and history of populations of the deep-sea fish *Helicolenus dactylopterus* (Delaroche, 1809) inferred from mtDNA sequence analysis. *Molecular Ecology*, 14(5):1343–1354, 2005. .

A. Addo-Bediako, S. L. Chown, and K. J. Gaston. Metabolic cold adaptation in insects: a large-scale perspective. *Functional Ecology*, 16(3):332–338, 2002.

D. Agnetta, F. Badalamenti, G. D'Anna, M. Sinopoli, F. Andaloro, S. Vizzini, and C. Pipitone. Sizing up the role of predators on *Mullus barbatus* populations in Mediterranean trawl and no-trawl areas. *Fisheries Research*, 213:196–203, 2019.

A. Aisami, N. A. Yasid, W. L. W. Johari, and M. Y. Shukor. Estimation of the q10 value; the temperature coefficient for the growth of *Pseudomonas* sp. aq5-04 on phenol. *Bioremediation Science and Technology Research*, 5(1):24–26, 2017.

S. R. Alewijnse, G. Stowasser, R. A. Saunders, A. Belcher, O. A. Crimmen, N. Cooper, and C. N. Trueman. Otolith-derived field metabolic rates of myctophids (Family Myctophidae) from the Scotia Sea (Southern Ocean). *Marine Ecology Progress Series*, 675:113–131, 2021.

V. Allain, A. Biseau, and B. Kergoat. Preliminary estimates of French deepwater fishery discards in the Northeast Atlantic Ocean. *Fisheries Research*, 60(1):185–192, 2003.

G. R. Allen. *Snappers of the world*, volume 6. Food and Agriculture Organization of the United Nations (FAO), Rome, 1985. ISBN 92-5-102321-2.

O. R. J. Anderson, R. A. Phillips, R. A. McDonald, R. F. Shore, R. A. R McGill, and S. Bearhop. Influence of trophic position and foraging range on mercury levels within a seabird community. *Marine Ecology Progress Series*, 375:277–288, 2009.

T. R. Anderson, A. P. Martin, R. S. Lampitt, C. N. Trueman, S. A. Henson, and D. J. Mayor. Quantifying carbon fluxes from primary production to mesopelagic fish using a simple food web model. *ICES Journal of Marine Science*, 76(3):690–701, 2018.

W. D. Anderson and P. C. Heemstra. Review of Atlantic and eastern Pacific anthiine fishes (Teleostei: Perciformes: Serranidae), with descriptions of two new genera. *Transactions of the American Philosophical Society*, 102(2):i–173, 2012.

T. Andrew. The Fishes of Tristan da Cunha and Gough Island (South Atlantic), and the effects of environmental seasonality on the biology of selected species. 1992. Publisher: Rhodes University.

A. H. Andrews, A. Pacicco, R. Allman, B. J. Falterman, E. T. Lang, and W. Golet. Age validation of yellowfin (*Thunnus albacares*) and bigeye (*Thunnus obesus*) tuna of the northwestern Atlantic Ocean. *Canadian Journal of Fisheries and Aquatic Sciences*, 77(4): 637–643, 2020.

A. P. Andriashev. A general review of the Antarctic fish fauna. *Biogeography and ecology in Antarctica*, pages 491–550, 1965.

Anon. *Plagiogeneion rubiginosum*, 2019. URL `https://www.fishbase.de/photos/UploadedBy.php?autoctr=36802&win=uploaded`.

E. S. Antonio, A. Kasai, M. Ueno, N. Won, Y. Ishihi, H. Yokoyama, and Y. Yamashita. Spatial variation in organic matter utilization by benthic communities from Yura River–Estuary to offshore of Tango Sea, Japan. *Estuarine, Coastal and Shelf Science*, 86 (1):107–117, 2010.

A. Ariza, J. C. Garijo, J. M. Landeira, F. Bordes, and S. Hernández-León. Migrant biomass and respiratory carbon flux by zooplankton and micronekton in the subtropical northeast Atlantic Ocean (Canary Islands). *Progress in Oceanography*, 134:330–342, 2015.

F Arreguín-Sánchez, M Contreras, V Moreno, R Burgos, and R Valdés. Population dynamics and stock assessment of red grouper (*Epinephelus morio*) fishery on Campeche Bank, Mexico. In *Biology, fisheries and culture of tropical groupers and snappers: ICLARM Conference Proceedings*, pages 202–217, 1996.

M. L. Artüz and R. Fricke. First and northernmost record of *Upeneus moluccensis* (Actinopterygii: Perciformes: Mullidae) from the Sea of Marmara. *Acta Ichthyologica et Piscatoria*, 49(1):53–58, 2019.

K. A. Asante, T. Agusa, H. Mochizuki, K. Ramu, S. Inoue, T. Kubodera, S. Takahashi, A. Subramanian, and S. Tanabe. Trace elements and stable isotopes (δ^{13}C and δ^{15}N) in shallow and deep-water organisms from the East China Sea. *Environmental Pollution*, 156(3):862–873, 2008.

K. A. Asante, R. Kubota, T. Agusa, A. Subramanian, S. Tanabe, S. Nishida, M. Yamaguchi, K. Suetsugu, S. Ohta, and H. Yeh. Trace element and stable isotope analyses of deep sea fish from the Sulu Sea, Philippines. *West African Journal of Applied Ecology*, 14(1), 2009.

J. Ashford and C. Jones. Oxygen and carbon stable isotopes in otoliths record spatial isolation of Patagonian toothfish (*Dissostichus eleginoides*). *Geochimica et Cosmochimica Acta*, 71(1):87–94, 2007.

A. Audzijonyte, H. Pethybridge, J. Porobic, R. Gorton, I. Kaplan, and E. A. Fulton. Atlantis: A spatially explicit end-to-end marine ecosystem model with dynamically integrated physics, ecology and socio-economic modules. *Methods in Ecology and Evolution*, 10(10):1814–1819, 2019.

CSIRO Australian National Fish Collection. A giant cuskeel *Spectrunculus grandis*, 2017. URL https://fishesofaustralia.net.au/Images/Image/SpectruncGrandis2CSIRO.jpg.

CSIRO Australian National Fish Collection. Softskin slickhead *Rouleina attrita*, No Date. URL https://fishesofaustralia.net.au/Images/Image/RouleinAttritCSIRO.jpg.

S. G. Ayvazian, T. P. Bastow, J. S. Edmonds, J. How, and G. B. Nowara. Stock structure of Australian herring (*Arripis georgiana*) in southwestern Australia. *Fisheries Research*, 67(1):39–53, 2004.

Cousseau M. B. *Coelorinchus fasciatus*, 1999. URL https://www.fishbase.se/photos/PicturesSummary.php?ID=7131&what=species.

D. L. Bade, S. R. Carpenter, J. J. Cole, P. C. Hanson, and R. H. Hesslein. Controls of δ^{13}C-DIC in lakes: Geochemistry, lake metabolism, and morphometry. *Limnology and Oceanography*, 49(4):1160–1172, 2004.

D. M. Bailey, A. J. Jamieson, P. M. Bagley, M. A. Collins, and I. G. Priede. Measurement of in situ oxygen consumption of deep-sea fish using an autonomous lander vehicle. *Deep Sea Research Part I: Oceanographic Research Papers*, 49(8):1519–1529, 2002.

D. M. Bailey, B. Genard, M. A. Collins, J. F. Rees, S. K. Unsworth, E. J. V. Battle, P. M. Bagley, A. J. Jamieson, and I. G. Priede. High swimming and metabolic activity in the deep-sea eel *Synaphobranchus kaupii* revealed by integrated in situ and in vitro measurements. *Physiological and Biochemical Zoology*, 78(3):335–346, 2005.

D. M. Bailey, M. A. Collins, J. D. M. Gordon, A. F. Zuur, and I. G. Priede. Long-term changes in deep-water fish populations in the northeast Atlantic: a deeper reaching effect of fisheries? *Proceedings of the Royal Society B: Biological Sciences*, 276: 1965–1969, 2009.

R. Banón. New record of *Cataetyx laticeps* (Bythitidae) in northwestern Atlantic. 2001. Publisher: Société française d'ichtyologie.

E. G. Barham. Deep scattering layer migration and composition: observations from a diving saucer. *Science*, 151(3716):1399–1403, 1966.

C. Barría, J. Navarro, and M. Coll. Feeding habits of four sympatric sharks in two deep-water fishery areas of the western Mediterranean Sea. *Deep Sea Research Part I: Oceanographic Research Papers*, 142:34–43, 2018.

T. P. Bastow, G. Jackson, and J. S. Edmonds. Elevated salinity and isotopic composition of fish otolith carbonate: stock delineation of pink snapper, *Pagrus auratus*, in Shark Bay, Western Australia. *Marine Biology*, 141(5):801–806, 2002.

A. Belcher, R. A. Saunders, and G. A. Tarling. Respiration rates and active carbon flux of mesopelagic fishes (Family Myctophidae) in the Scotia Sea, Southern Ocean. *Marine Ecology Progress Series*, 610:149–162, 2019.

A. Belcher, K. Cook, D. Bondyale-Juez, G. Stowasser, S. Fielding, R. A. Saunders, D. J. Mayor, and G. A. Tarling. Respiration of mesopelagic fish: a comparison of respiratory electron transport system (ETS) measurements and allometrically calculated rates in the Southern Ocean and Benguela Current. *ICES Journal of Marine Science*, (fsaa031), 2020. .

M. Belchier and J. Lawson. An analysis of temporal variability in abundance, diversity and growth rates within the coastal ichthyoplankton assemblage of South Georgia (sub-Antarctic). *Polar Biology*, 36(7):969–983, 2013.

M. V. Bell and D. R. Tocher. Biosynthesis of polyunsaturated fatty acids in aquatic ecosystems: general pathways and new directions. In *Lipids in aquatic ecosystems*, pages 211–236. Springer, 2009.

O. A. Bergstad. Distribution, population structure, growth, and reproduction of the greater silver smelt, *Argentina silus* (Pisces, Argentinidae), of the Skagerrak and the north-eastern North Sea. *ICES Journal of Marine Science*, 50(2):129–143, 1993.

D. Bianchi, D. A. Carozza, E. D. Galbraith, J. Guiet, and T. DeVries. Estimating global biomass and biogeochemical cycling of marine fish with and without fishing. *Science Advances*, 7(41):eabd7554, 2021.

J. S. Bigman, L. K. M'Gonigle, N. C. Wegner, and N. K. Dulvy. Respiratory capacity is twice as important as temperature in explaining patterns of metabolic rate across the vertebrate tree of life. *Science Advances*, 7(19):eabe5163, 2021.

R. W. Blacker. *Synopsis of Biological Data on Haddock: Melanogrammus aeglefinus (Linnaeus) 1758*. Food and Agriculture Organization of the United Nations (FAO), Rome, 1971.

R. W. Blacker. Pelagic records of the lumpsucker, *Cyclopterus lumpus* L. *Journal of Fish Biology*, 23(4):405–417, 1983.

J. L. Blanchard, S. Jennings, R. Holmes, J. Harle, G. Merino, J. I. Allen, J. Holt, N. K. Dulvy, and M. Barange. Potential consequences of climate change for primary production and fish production in large marine ecosystems. *Philosophical Transactions of the Royal Society B: Biological Sciences*, 367(1605):2979–2989, 2012.

B. A. Block, D. T. Booth, and F. G. Carey. Depth and temperature of the blue marlin, *Makaira nigricans*, observed by acoustic telemetry. *Marine Biology*, 114(2):175–183, 1992.

N. Bodin, D. Lesperance, R. Albert, S. Hollanda, M. Degroote, C. Churlaud, and P. Bustamante. A preliminary study of trace elements in oceanic pelagic communities in the western-central Indian Ocean. 2016.

F. Bokma. Evidence against universal metabolic allometry. *Functional Ecology*, pages 184–187, 2004.

J.R. Brett and N.R. Glass. Metabolic rates and critical swimming speeds of sockeye salmon (*Oncorhynchus nerka*) in relation to size and temperature. *Journal of the Fisheries Board of Canada*, 30(3):379–387, 1973.

C. J. Bridger and R. K. Booth. The effects of biotelemetry transmitter presence and attachment procedures on fish physiology and behavior. *Reviews in Fisheries Science*, 11(1):13–34, 2003.

S. Brodie, M. D. Taylor, J. A. Smith, I. M. Suthers, C. A. Gray, and N. L. Payne. Improving consumption rate estimates by incorporating wild activity into a bioenergetics model. *Ecology and Evolution*, 6(8):2262–2274, 2016.

A. Brown and S. Thatje. Explaining bathymetric diversity patterns in marine benthic invertebrates and demersal fishes: physiological contributions to adaptation of life at depth. *Biological Reviews*, 89(2):406–426, 2014.

A. Brown, C. Hauton, T. Stratmann, A. Sweetman, D. Van Oevelen, and D. O. B. Jones. Metabolic rates are significantly lower in abyssal Holothuroidea than in shallow-water Holothuroidea. *Royal Society Open Science*, 5(5):172162, 2018.

J. H. Brown. *Macroecology*. The University of Chicago Press, 1996. ISBN 9780226076157.

J. H. Brown, J. F. Gillooly, A. P. Allen, V. M. Savage, and G. B. West. Toward a metabolic theory of ecology. *Ecology*, 85(7):1771–1789, 2004.

J. Burnett, M. R. Ross, and S. H. Clark. Several biological aspects of the witch flounder (*Glyptocephalus cynoglossus* (L.)) in the Gulf of Maine-Georges Bank region. *Journal of Northwest Atlantic Fishery Science*, 12:15–25, 1992.

M. L. Burton, J. C. Potts, and D. R. Carr. Age, growth, and natural mortality of rock hind, *Epinephelus adscensionis*, from the Gulf of Mexico. *Bulletin of Marine Science*, 88 (4):903–917, 2012.

B. Busalacchi, T. Bottari, D. Giordano, A. Profeta, and P. Rinelli. Distribution and biological features of the common pandora, *Pagellus erythrinus* (Linnaeus, 1758), in the southern Tyrrhenian Sea (Central Mediterranean). *Helgoland Marine Research*, 68 (4):491–501, 2014.

P. J. Butler, J. A. Green, I. L. Boyd, and J. R. Speakman. Measuring metabolic rate in the field: the pros and cons of the doubly labelled water and heart rate methods. *Functional Ecology*, 18(2):168–183, 2004.

L. M. Cammen, S. Corwin, and J. P. Christensen. Electron transport system (ETS) activity as a measure of benthic macrofaunal metabolism. *Marine Ecology Progress Series*, 65(1):171–182, 1990.

S. E. Campana. Chemistry and composition of fish otoliths: pathways, mechanisms and applications. *Marine Ecology Progress Series*, 188:263–297, 1999.

S. E. Campana. Otolith microstructure preparation, No Date. URL `https://uni.hi.is/scampana/otoliths/methods/otolith-microstructure-preparation/`.

S. E. Campana, A. E. Valentin, S. E. MacLellan, and J. B. Groot. Image-enhanced burnt otoliths, bomb radiocarbon and the growth dynamics of redfish (*Sebastes mentella* and *S. fasciatus*) off the eastern coast of Canada. *Marine and Freshwater Research*, 67 (7):925–936, 2016.

I. Capellini, C. Venditti, and R. A. Barton. Phylogeny and metabolic scaling in mammals. *Ecology*, 91(9):2783–2793, 2010.

L. Cardona, I. Álvarez de Quevedo, A. Borrell, and A. Aguilar. Massive consumption of gelatinous plankton by mediterranean apex predators. *PLOS ONE*, 7(3):e31329, 2012.

L. M. Cargnelli. Essential fish habitat source document. Witch flounder, *Glyptocephalus cynoglossus*, life history and habitat characteristics. Woods Hole, Massachusetts, 1999. National Oceanic and Atmospheric Administration (NOAA).

D. A. Carozza, D. Bianchi, and E. D. Galbraith. The ecological module of BOATS-1.0: a bioenergetically constrained model of marine upper trophic levels suitable for studies of fisheries and ocean biogeochemistry. *Geoscientific Model Development*, 9(4): 1545–1565, 2016.

D. A. Carozza, D. Bianchi, and E. D. Galbraith. Metabolic impacts of climate change on marine ecosystems: Implications for fish communities and fisheries. *Global Ecology and Biogeography*, 28(2):158–169, 2019.

K. Carpenter and G. R. Allen. *Emperor fishes and large-eye breams of the world*, volume 9. Food and Agriculture Organization of the United Nations (FAO), Rome, 1989. ISBN 92-5-102321-2.

K. E. Carpenter. *The living marine resources of the Western Central Atlantic*, volume 2. Food and Agriculture Organization of the United Nations (FAO), Rome, 2002.

K. E. Carpenter and N. De Angelis. *The living marine resources of the Eastern Central Atlantic*, volume 3–4. Food and Agriculture Organization of the United Nations (FAO), Rome, 2014. ISBN 978-92-5-109266-8.

P. Carpentieri, F. Colloca, M. Cardinale, A. Belluscio, and G. D. Ardizzone. Feeding habits of European hake (*Merluccius merluccius*) in the central Mediterranean Sea. *Fishery Bulletin*, 103(2):411–416, 2005.

J. M. Casas and C. Piñeiro. Growth and age estimation of greater fork-beard (*Phycis blennoides* Brünnich, 1768) in the north and northwest of the Iberian Peninsula (ICES Division VIIIc and IXa). *Fisheries Research*, 47(1):19–25, 2000.

J. E. Caselle, S. L. Hamilton, K. Davis, M. Bester, M. Wege, C. Thompson, A. Turchik, R. Jenkinson, D. Simpson, and J. Mayorga. Ecosystem assessment of the Tristan da Cunha Islands. St. Helena: Royal Society for Protection of Birds, Tristan da Cunha Government, 2017.

I. Castejón-Silvo, J. Terrados, T. Nguyen, F. Jutfelt, and E. Infantes. Increased energy expenditure is an indirect effect of habitat structural complexity loss. *Functional Ecology*, 35(10):2316–2328, 2021.

V. Catul, M. Gauns, and P. K. Karuppasamy. A review on mesopelagic fishes belonging to family Myctophidae. *Reviews in Fish Biology and Fisheries*, 21(3):339–354, 2011.

D. Chabot, J. F. Steffensen, and A. P. Farrell. The determination of standard metabolic rate in fishes. *Journal of Fish Biology*, 88(1):81–121, 2016.

J. Chang, D. L. Rabosky, S. A. Smith, and M. E. Alfaro. An R package and online resource for macroevolutionary studies using the ray-finned fish tree of life. *Methods in Ecology and Evolution*, 10(7):1118–1124, 2019.

A. Chatelier, D. J. McKenzie, A. Prinet, R. Galois, J. Robin, J. Zambonino, and G. Claireaux. Associations between tissue fatty acid composition and physiological traits of performance and metabolism in the seabass (*Dicentrarchus labrax*). *Journal of Experimental Biology*, 209(17):3429–3439, 2006.

W. W. L. Cheung, C. Close, V. Lam, R. Watson, and D. Pauly. Application of macroecological theory to predict effects of climate change on global fisheries potential. *Marine Ecology Progress Series*, 365:187–197, 2008.

W. W. L. Cheung, J. L. Sarmiento, J. Dunne, T. L. Frölicher, V. W. Y. Lam, M. L. Deng Palomares, R. Watson, and D. Pauly. Shrinking of fishes exacerbates impacts of global ocean changes on marine ecosystems. *Nature Climate Change*, 3(3):254–258, 2013.

J. J. Childress. Respiratory rate and depth of occurrence of midwater animals. *Limnology and Oceanography*, 16(1):104–106, 1971.

J. J. Childress. Are there physiological and biochemical adaptations of metabolism in deep-sea animals? *Trends in Ecology & Evolution*, 10(1):30–36, 1995.

T. Chouvelon, J. Spitz, F. Caurant, P. Mèndez-Fernandez, A. Chappuis, F. Laugier, E. Le Goff, and P. Bustamante. Revisiting the use of δ^{15}N in meso-scale studies of marine food webs by considering spatio-temporal variations in stable isotopic signatures–the case of an open ecosystem: The Bay of Biscay (North-East Atlantic). *Progress in Oceanography*, 101(1):92–105, 2012.

V. Christensen and C. J. Walters. Ecopath with Ecosim: methods, capabilities and limitations. *Ecological Modelling*, 172(2-4):109–139, 2004.

V. Christensen, C. J. Walters, and D. Pauly. Ecopath with Ecosim: a user's guide. *Fisheries Centre, University of British Columbia, Vancouver*, 154, 2005.

M. T. Chung. *Functional and life-history traits in deep-sea fishes*. PhD thesis, University of Southampton, Southampton, United Kingdom, 2015. URL https://eprints.soton.ac.uk/384568/.

M. T. Chung, C. N. Trueman, J. A. Godiksen, and P. Grønkjær. Otolith δ^{13}C values as a metabolic proxy: approaches and mechanical underpinnings. *Marine and Freshwater Research*, 70(12):1747–1756, 2019a.

M. T. Chung, C. N. Trueman, J. A. Godiksen, M. E. Holmstrup, and P. Grønkjær. Field metabolic rates of teleost fishes are recorded in otolith carbonate. *Communications Biology*, 2(1):1–10, 2019b.

M. T. Chung, C. Y. Chen, J. C. Shiao, K. Shirai, and C. H. Wang. Metabolic proxy for cephalopods: Stable carbon isotope values recorded in different biogenic carbonates. *Methods in Ecology and Evolution*, 12(9):1648–1657, 2021a.

M. T. Chung, K. E. M. Jørgensen, C. N. Trueman, H. Knutsen, P. E. Jorde, and P. Grønkjær. First measurements of field metabolic rate in wild juvenile fishes show strong thermal sensitivity but variations between sympatric ecotypes. *Oikos*, 130(2): 287–299, 2021b.

T. D. Clark, E. Sandblom, and F. Jutfelt. Aerobic scope measurements of fishes in an era of climate change: respirometry, relevance and recommendations. *Journal of Experimental Biology*, 216(15):2771–2782, 2013.

A. Clarke. Is there a universal temperature dependence of metabolism? *Functional Ecology*, 18(2):252–256, 2004.

A. Clarke and K.P.P. Fraser. Why does metabolism scale with temperature? *Functional Ecology*, 18(2):243–251, 2004.

A. Clarke and N. M. Johnston. Scaling of metabolic rate with body mass and temperature in teleost fish. *Journal of Animal Ecology*, 68(5):893–905, 1999.

B. W. Coad and J. D. Reist. *Annotated list of the Arctic marine fishes of Canada*. Fisheries and Oceans Canada Winnipeg, Canada, 2004.

R. A. Coggan, J. D. M. Gordon, and N. R. Merrett. Aspects of the biology of *Nezumia aequalis* from the continental slope west of the British Isles. *Journal of Fish Biology*, 54 (1):152–170, 1999.

D. M. Cohen, T. Inada, T. Iwamoto, and N. Scialabba. *Gadiform fishes of the world*, volume 10. Food and Agriculture Organization of the United Nations (FAO), Rome, 1990. ISBN 92-5-102890-7.

A. Colaço, E. Giacomello, F. Porteiro, and G. M. Menezes. Trophodynamic studies on the condor seamount (Azores, Portugal, North Atlantic). *Deep Sea Research Part II: Topical Studies in Oceanography*, 98:178–189, 2013.

B. B. Collette and C. E. Nauen. *Scombrids of the world: an annotated and illustrated catalogue of tunas, mackerels, bonitos, and related species known to date.*, volume 2. Food and Agriculture Organization of the United Nations (FAO), Rome, 1983. ISBN 92-5-101381-0.

N. V. Collette, B. B.and Parin. Shallow-water fishes of Walters Shoals, Madagascar Ridge. *Bulletin of Marine Science*, 48(1):1–22, 1991.

M. A. Collins, J. C. Xavier, N. M. Johnston, A. W. North, P. Enderlein, G. A. Tarling, C. M. Waluda, E. J. Hawker, and N. J. Cunningham. Patterns in the distribution of myctophid fish in the northern Scotia Sea ecosystem. *Polar Biology*, 31(7):837–851, 2008.

M. A. Collins, G. Stowasser, S. Fielding, R. Shreeve, J. C. Xavier, H. J. Venables, P. Enderlein, Y. Cherel, and A. Van de Putte. Latitudinal and bathymetric patterns in the distribution and abundance of mesopelagic fish in the Scotia Sea. *Deep Sea Research Part II: Topical Studies in Oceanography*, 59:189–198, 2012.

Baltic Marine Environment Protection Commission. Species information sheet: *Lycodes gracilis*. Technical report, 2013a. URL `https://helcom.fi/media/red%20list%20species%20information%20sheet/HELCOM-Red-List-Lycodes-gracilis.pdf`.

Baltic Marine Environment Protection Commission. Species information sheet: *Scomber scombrus*. Technical report, 2013b. URL https://helcom.fi/wp-content/uploads/2019/08/HELCOM-Red-List-Scomber-scombrus.pdf.

L. Comte and J. D. Olden. Climatic vulnerability of the world's freshwater and marine fishes. *Nature Climate Change*, 7(10):718–722, 2017.

M. Connan, P. Mayzaud, G. Duhamel, B. T. Bonnevie, and Y. Cherel. Fatty acid signature analysis documents the diet of five myctophid fish from the Southern Ocean. *Marine Biology*, 157(10):2303–2316, 2010.

R. M. Connolly, T. A. Schlacher, and T. F. Gaston. Stable isotope evidence for trophic subsidy of coastal benthic fisheries by river discharge plumes off small estuaries. *Marine Biology Research*, 5(2):164–171, 2009.

S. J. Cooke, E. B. Thorstad, and S. G. Hinch. Activity and energetics of free-swimming fish: insights from electromyogram telemetry. *Fish and Fisheries*, 5(1):21–52, 2004.

A. T. Correia, F. Barros, and A. N. Sial. Stock discrimination of European conger eel (*Conger conger* L.) using otolith stable isotope ratios. *Fisheries Research*, 108(1):88–94, 2011.

A. T. Correia, A. Moura, R. Triay-Portella, P. T. Santos, E. Pinto, A. A. Almeida, A. N. Sial, and A. A. Muniz. Population structure of the chub mackerel (*Scomber colias*) in the NE Atlantic inferred from otolith elemental and isotopic signatures. *Fisheries Research*, 234:105785, 2021.

S. Corsolini and G. Sarà. The trophic transfer of persistent pollutants (HCB, DDTs, PCBs) within polar marine food webs. *Chemosphere*, 177:189–199, 2017.

D. P. Costa and B. Sinervo. Field physiology: physiological insights from animals in nature. *Annual Review of Physiology*, 66:209–238, 2004.

M. J. Costello, P. Tsai, P. S. Wong, A. K. L. Cheung, Z. Basher, and C. Chaudhary. Marine biogeographic realms and species endemicity. *Nature Communications*, 8(1): 1–10, 2017.

R. Crec'Hriou, V. Zintzen, L. Moore, and C.D. Roberts. Length–weight relationships of 33 fish species from New Zealand. *Journal of Applied Ichthyology*, 31(3):558–561, 2015.

P. Cresson, L. Le Direach, E. Rouanet, E. Goberville, P. Astruch, M. Ourgaud, and M. Harmelin-Vivien. Biomass and isotopic data for fish community on artificial reefs in the bay of Marseille. Sea Open Scientific Data Publication (SEANOE), 2019.

E. L. Crockett and B. D. Sidell. Some pathways of energy metabolism are cold adapted in Antarctic fishes. *Physiological Zoology*, 63(3):472–488, 1990.

I. B. Daban, A. Ismen, M. A. Ihsanoglu, and K. Cabbar. Age, growth and reproductive biology of the saddled seabream (*Oblada melanura*) in the North Aegean Sea, Eastern Mediterranean. *Oceanological and Hydrobiological Studies*, 49(1):13–22, 2020.

F. T. Dahlke, S. Wohlrab, M. Butzin, and H. O. Pörtner. Thermal bottlenecks in the life cycle define climate vulnerability of fish. *Science*, 369(6499):65–70, 2020.

T. T. Daley and R. T. Leaf. Age and growth of Atlantic chub mackerel (*Scomber colias*) in the Northwest Atlantic. *Journal of Northwest Atlantic Fishery Science*, 50, 2019.

K. Das, G. Lepoint, Y. Leroy, and J. M. Bouquegneau. Marine mammals from the southern North Sea: feeding ecology data from δ^{13}C and δ^{15}N measurements. *Marine Ecology Progress Series*, 263:287–298, 2003.

J. Davenport. *Synopsis of biological data on the lumpsucker, Cyclopterus lumpus (Linnaeus, 1758)*. Food & Agriculture Organization of the United Nation (FAO), Rome, 1985. ISBN 92-5-102330-1.

P. C. Davison, D. M. Checkley Jr., J. A. Koslow, and J. Barlow. Carbon export mediated by mesopelagic fishes in the northeast Pacific Ocean. *Progress in Oceanography*, 116: 14–30, 2013.

A. M. De Lecea, A. J. Smit, and S. T. Fennessy. Riverine dominance of a nearshore marine demersal food web: evidence from stable isotope and C/N ratio analysis. *African Journal of Marine Science*, 38:S181–S192, 2016.

C. M. del Rio. Metabolic theory or metabolic models? *Trends in Ecology & Evolution*, 23 (5):256–260, 2008.

J. Delgado, S. Reis, J. A. González, E. Isidro, M. Biscoito, M. Freitas, and V. M. Tuset. Reproduction and growth of *Aphanopus carbo* and *A. intermedius* (Teleostei: Trichiuridae) in the northeastern Atlantic. *Journal of Applied Ichthyology*, 29(5): 1008–1014, 2013.

J. P. DeLong, G. Bachman, J. P. Gibert, T. M. Luhring, K. L. Montooth, A. Neyer, and B. Reed. Habitat, latitude and body mass influence the temperature dependence of metabolic rate. *Biology Letters*, 14(8):20180442, 2018.

A. W. J. Demopoulos and P. C. Sikkel. Enhanced understanding of ectoparasite–host trophic linkages on coral reefs through stable isotope analysis. *International Journal for Parasitology: Parasites and Wildlife*, 4(1):125–134, 2015.

J. B. Dempson, V. A. Braithwaite, D. Doherty, and M. Power. Stable isotope analysis of marine feeding signatures of Atlantic salmon in the North Atlantic. *ICES Journal of Marine Science*, 67(1):52–61, 2010.

M. J. DeNiro and S. Epstein. Influence of diet on the distribution of carbon isotopes in animals. *Geochimica et Cosmochimica Acta*, 42(5):495–506, 1978.

S. Depaoli, S. D. Winter, and M. Visser. The importance of prior sensitivity analysis in Bayesian statistics: Demonstrations using an interactive Shiny app. *Frontiers in Psychology*, 11, 2020.

S. Deudero, J. K. Pinnegar, N. V. C. Polunin, G. Morey, and B. Morales-Nin. Spatial variation and ontogenic shifts in the isotopic composition of Mediterranean littoral fishes. *Marine Biology*, 145(5):971–981, 2004.

C. Deutsch, A. Ferrel, B. Seibel, H. O. Pörtner, and R. B. Huey. Climate change tightens a metabolic constraint on marine habitats. *Science*, 348(6239):1132–1135, 2015.

C. Deutsch, J. L. Penn, and B. Seibel. Metabolic trait diversity shapes marine biogeography. *Nature*, 585(7826):557–562, 2020.

M. C. Deval, O. Güven, İ. Saygu, and T. Kabapçioğlu. Length-weight relationships of 10 fish species found off Antalya Bay, eastern Mediterranean. *Journal of Applied Ichthyology*, 30(3):567–568, 2014.

K. S. Dillon, C. R. Fleming, C. Slife, and R. T. Leaf. Stable isotopic niche variability and overlap across four fish guilds in the north-central Gulf of Mexico. *Marine and Coastal Fisheries*, 13(3):213–227, 2021.

P. S. Dodds, D. H. Rothman, and J. S. Weitz. Re-examination of the "$\frac{3}{4}$-law" of metabolism. *Journal of Theoretical Biology*, 209(1):9–27, 2001.

A. Dolgov. *Trachyrincus murrayi*, 2003. URL `https://www.fishbase.de/photos/PicturesSummary.php?ID=27730&what=species`.

G. d'Onghia, C. Y. Politou, A. Bozzano, D. Lloris, G. Rotllant, L. Sión, and F. Mastrototaro. Deep-water fish assemblages in the Mediterranean Sea. *Scientia Marina*, 68(S3):87–99, 2004. ISSN 1886-8134.

J. Donnelly and J. J. Torres. Oxygen consumption of midwater fishes and crustaceans from the eastern Gulf of Mexico. *Marine Biology*, 97(4):483–494, 1988.

C. Dowling. *Arripis georgiana*, No Date. URL `https://www.fishbase.de/photos/UploadedBy.php?autoctr=15337&win=uploaded`.

J. Drazen. Energy budgets and feeding rates of *Coryphaenoides acrolepis* and *C. armatus*. *Marine Biology*, 140(4):677–686, 2002.

J. C. Drazen. Depth related trends in proximate composition of demersal fishes in the eastern North Pacific. *Deep Sea Research Part I: Oceanographic Research Papers*, 54(2): 203–219, 2007.

J. C. Drazen and B. A. Seibel. Depth-related trends in metabolism of benthic and benthopelagic deep-sea fishes. *Limnology and Oceanography*, 52(5):2306–2316, 2007.

J. C. Drazen, J. R. Friedman, Nicole E. Condon, E. J. Aus, M. E. Gerringer, A. A. Keller, and M. E. Clarke. Enzyme activities of demersal fishes from the shelf to the abyssal plain. *Deep Sea Research Part I: Oceanographic Research Papers*, 100:117–126, 2015.

L. Duchatelet, C. Hermans, G. Duhamel, Y. Cherel, C. Guinet, and J. Mallefet. Coelenterazine detection in five myctophid species from the Kerguelen Plateau. In *The Kerguelen Plateau: Marine Ecosystem + Fisheries: Proceedings of the Second Symposium*, 2019.

V. Dufour, C. Pierre, and J. Rancher. Stable isotopes in fish otoliths discriminate between lagoonal and oceanic residents of Taiaro Atoll (Tuamotu Archipelago, French Polynesia). *Coral Reefs*, 17(1):23–28, 1998.

G. Duhamel, P. Koubbi, and C. Ravier. Day and night mesopelagic fish assemblages off the Kerguelen Islands (Southern Ocean). *Polar Biology*, 23(2):106–112, 2000.

G. Duhamel, P. A. Hulley, R. Causse, P. Koubbi, M. Vacchi, P. Pruvost, S. Vigetta, J. O. Irisson, S. Mormède, M. Belchier, A. Dettai, H. W. Detrich, J. Gutt, C. D. Jones, K. H. Kock, L. J. Lopez Abellan, and A. P. Van de Putte. Biogeographic patterns of fish. In *Biogeographic atlas of the Southern Ocean*, pages 328–362. Scientific Committee on Antarctic Research, Cambridge, 2014. ISBN 0-948277-28-9. Edited by De Broyer, C. and Koubbi, P.

M. I. Duncan, N. C. James, W. M. Potts, and A. E. Bates. Different drivers, common mechanism; the distribution of a reef fish is restricted by local-scale oxygen and temperature constraints on aerobic metabolism. *Conservation Physiology*, 8(1): coaa090, 2020.

M. R. Dunn. Review and stock assessment of black cardinalfish (*Epigonus telescopus*) on the east coast North Island, New Zealand. *New Zealand Fisheries Assessment Report*, 39:55, 2009.

A. Dupoué, F. Brischoux, and O. Lourdais. Climate and foraging mode explain interspecific variation in snake metabolic rates. *Proceedings of the Royal Society B: Biological Sciences*, 284(1867):20172108, 2017.

J. Dürr and J.A González. Feeding habits of *Beryx splendens* and *Beryx decadactylus* (Berycidae) off the Canary Islands. *Fisheries Research*, 54(3):363–374, 2002.

R. Ege and A. Krogh. On the relation between the temperature and the respiratory exchange in fishes. *Internationale Revue der gesamten Hydrobiologie und Hydrographie*, 7(1):48–55, 1914.

M. Eide, A. Olsen, U. S. Ninnemann, and T. Eldevik. A global estimate of the full oceanic 13C Suess effect since the preindustrial. *Global Biogeochemical Cycles*, 31(3): 492–514, 2017.

H. Endo, D. Tsutsui, and K. Amaoka. Range extensions of two deep-sea macrourids *Coryphaenoides filifer* and *Squalogadus modificatus* to the Sea of Okhotsk. *Japanese Journal of Ichthyology*, 41(3):330–333, 1994.

W. N. Eschmeyer and J. C. Hureau. *Sebastes mouchezi*, a senior synonym of *Helicolenus tristanensis*, with comments on *Sebastes capensis* and zoogeographical considerations. *Copeia*, 1971(3):576–579, 1971.

E. Fanelli and J. E. Cartes. Temporal variations in the feeding habits and trophic levels of three deep-sea demersal fishes from the western Mediterranean Sea, based on stomach contents and stable isotope analyses. *Marine Ecology Progress Series*, 402: 213–232, 2010.

E. Fanelli, V. Papiol, J. E. Cartes, P. Rumolo, and C. López-Pérez. Trophic webs of deep-sea megafauna on mainland and insular slopes of the NW Mediterranean: a comparison by stable isotope analysis. *Marine Ecology Progress Series*, 490:199–221, 2013.

E. Fanelli, E. Azzurro, M. Bariche, J. E. Cartes, and F. Maynou. Depicting the novel Eastern Mediterranean food web: a stable isotopes study following Lessepsian fish invasion. *Biological Invasions*, 17(7):2163–2178, 2015.

FAO. The state of world fisheries and aquaculture. Technical report, Food and Agriculture Organization of the United Nations (FAO), Rome, 2018. URL https://www.fao.org/documents/card/en/c/I9540EN/.

FAO. The state of world fisheries and aquaculture. Technical report, Food and Agriculture Organization of the United Nations (FAO), Rome, 2020. URL https://doi.org/10.4060/ca9229en.

FAO. FAO Fisheries Glossary, 2021. URL http://www.fao.org/fishery/collection/glossary_fisheries/en.

I. Farias, B. Morales-Nin, P. Lorance, and I. Figueiredo. Black scabbardfish, *Aphanopus carbo*, in the northeast Atlantic: distribution and hypothetical migratory cycle. *Aquatic Living Resources*, 26(4):333–342, 2013. .

I. Farias, E. Couto, N. Lagarto, J. Delgado, Adelino V.M. Canário, and I. Figueiredo. Sex steroids of black scabbardfish, *Aphanopus carbo*, in relation to reproductive and migratory dynamics. *Aquaculture and Fisheries*, 2020. .

A.P. Farrell. Pragmatic perspective on aerobic scope: peaking, plummeting, pejus and apportioning. *Journal of Fish Biology*, 88(1):322–343, 2016.

G. E. Fenton, S. A. Short, and D. A. Ritz. Age determination of orange roughy, *Hoplostethus atlanticus* (Pisces: Trachichthyidae) using 210 Pb: 226 Ra disequilibria. *Marine Biology*, 109(2):197–202, 1991.

R. Fernández, S. García-Tiscar, M. Begoña Santos, A. López, J. A. Martínez-Cedeira, J. Newton, and G. J. Pierce. Stable isotope analysis in two sympatric populations of bottlenose dolphins *Tursiops truncatus*: evidence of resource partitioning? *Marine Biology*, 158(5):1043–1055, 2011.

F. Ferraton, M. Harmelin-Vivien, C. Mellon-Duval, and A. Souplet. Spatio-temporal variation in diet may affect condition and abundance of juvenile european hake in the Gulf of Lions (NW Mediterranean). *Marine Ecology Progress Series*, 337:197–208, 2007.

A. Fick. Ueber die Messung des Blutquantum in den Herzventrikeln. *Verhandlungen der Physikalisch-medizinische Gesellschaft zu Würzburg*, pages 16–17, 1870.

I. Fossen and O. A. Bergstad. Distribution and biology of blue hake, *Antimora rostrata* (Pisces: Moridae), along the mid-Atlantic Ridge and off Greenland. *Fisheries Research*, 82(1-3):19–29, 2006.

K. N. Frayn. Calculation of substrate oxidation rates in vivo from gaseous exchange. *Journal of Applied Physiology*, 55(2):628–634, 1983.

S. Fredriksen. Food web studies in a Norwegian kelp forest based on stable isotope (δ^{13}C and δ^{15}N) analysis. *Marine Ecology Progress Series*, 260:71–81, 2003.

J. Freedman, L. B. van Dorp, and S. Brace. Destructive sampling natural science collections: an overview for museum professionals and researchers. *Journal of Natural Science Collections*, 5:21–34, 2018.

R. Fricke, W. N. Eschmeyer, and van der Laan R. Eschmeyer's Catalog of Fishes: Genera, Species, References, 2022. URL `https://www.calacademy.org/scientists/projects/eschmeyers-catalog-of-fishes`.

R. Froese and D. Pauly. Fishbase, 2021. URL `www.fishbase.org`. Publisher: Fisheries Centre, University of British Columbia.

B. Fry. *Stable Isotope Ecology*, volume 521. Springer, New York, USA, 2006. ISBN 0-387-30513-0.

F. E. J. Fry and J. S. Hart. The relation of temperature to oxygen consumption in the goldfish. *The Biological Bulletin*, 94(1):66–77, 1948.

S. Furukawa, R. Kawabe, S. Ohshimo, K. Fujioka, G. N. Nishihara, Y. Tsuda, T. Aoshima, H. Kanehara, and H. Nakata. Vertical movement of dolphinfish *Coryphaena hippurus* as recorded by acceleration data-loggers in the northern East China Sea. *Environmental Biology of Fishes*, 92(1):89, 2011.

Y. Gao, H. P. Schwarcz, U. Brand, and E. Moksness. Seasonal stable isotope records of otoliths from ocean-pen reared and wild cod, *Gadus morhua*. *Environmental Biology of Fishes*, 61(4):445–453, 2001.

A. Garazo Fabregat. *Coryphaenoides rupestris*, 2002. URL https://www.fishbase.de/photos/PicturesSummary.php?ID=332&what=species.

H. E. Garcia, K. W. Weathers, C. R. Paver, I. Smolyar, T. P. Boyer, M. M. Locarnini, M. M. Zweng, A. V. Mishonov, O. K. Baranova, D. Seidov, et al. World Ocean Atlas 2018, Volume 3: Dissolved oxygen, apparent oxygen utilization, and dissolved oxygen saturation. 2019. URL https://www.ncei.noaa.gov/access/world-ocean-atlas-2018f/bin/woa18oxnuf.pl.

D. Gerdeaux and E. Dufour. Life history traits of the fish community in Lake Annecy: evidence from the stable isotope composition of otoliths. *Knowledge and Management of Aquatic Ecosystems*, (416):35, 2015.

M. E. Gerringer, J. C. Drazen, and P. H. Yancey. Metabolic enzyme activities of abyssal and hadal fishes: pressure effects and a re-evaluation of depth-related changes. *Deep Sea Research Part I: Oceanographic Research Papers*, 125:135–146, 2017.

L. A. Giguère, B. Côté, and J. F. St-Pierre. Metabolic rates scale isometrically in larval fishes. *Marine Ecology Progress Series*, 50:13–19, 1988.

J. F. Gillooly, J. H. Brown, G. B. West, V. M. Savage, and E. L. Charnov. Effects of size and temperature on metabolic rate. *Science*, 293(5538):2248–2251, 2001.

J. F. Gillooly, J. P. Gomez, and E. V. Mavrodiev. A broad-scale comparison of aerobic activity levels in vertebrates: endotherms versus ectotherms. *Proceedings of the Royal Society B: Biological Sciences*, 284(1849):20162328, 2017.

J.F. Gillooly, A.P. Allen, V.M. Savage, E.L. Charnov, G.B. West, and J.H. Brown. Response to Clarke and Fraser: effects of temperature on metabolic rate. *Functional Ecology*, 20(2):400–404, 2006.

J. Giménez, A. Marçalo, F. Ramírez, P. Verborgh, P. Gauffier, R. Esteban, L. Nicolau, E. González-Ortegón, F. Baldó, C. Vilas, et al. Diet of bottlenose dolphins (*Tursiops truncatus*) from the Gulf of Cadiz: insights from stomach content and stable isotope analyses. *PLOS ONE*, 12(9):e0184673, 2017.

R. Girardin, E. A. Fulton, S. Lehuta, M. Rolland, O. Thébaud, M. Travers-Trolet, Y. Vermard, and P. Marchal. Identification of the main processes underlying ecosystem functioning in the Eastern English Channel, with a focus on flatfish species, as revealed through the application of the Atlantis end-to-end model. *Estuarine, Coastal and Shelf Science*, 201:208–222, 2018.

J. Gjøsæter and K. Kawaguchi. *A review of the world resources of mesopelagic fish*. Food & Agriculture Organization of the United Nations (FAO), 1980. ISBN 92-5-100924-4. Issue: 193.

D. S. Glazier. Beyond the '3/4-power law': variation in the intra-and interspecific scaling of metabolic rate in animals. *Biological Reviews*, 80(4):611–662, 2005.

D. S. Glazier. Activity affects intraspecific body-size scaling of metabolic rate in ectothermic animals. *Journal of Comparative Physiology B*, 179(7):821–828, 2009.

D. S. Glazier. A unifying explanation for diverse metabolic scaling in animals and plants. *Biological Reviews*, 85(1):111–138, 2010.

D. S. Glazier. Is metabolic rate a universal 'pacemaker'for biological processes? *Biological Reviews*, 90(2):377–407, 2015.

D.S. Glazier. Biological scaling analyses are more than statistical line fitting. *Journal of Experimental Biology*, 224(11):jeb241059, 2021.

J. A. Godbold, D. M. Bailey, M. A. Collins, J. D. M. Gordon, W. A. Spallek, and I. G. Priede. Putative fishery-induced changes in biomass and population size structures of demersal deep-sea fishes in ICES Sub-area VII, Northeast Atlantic Ocean. *Biogeosciences*, 10(1):529–539, 2013.

M. Gómez, S. Torres, and S. Hernández-León. Modification of the electron transport system (ets) method for routine measurements of respiratory rates of zooplankton. *South African Journal of Marine Science*, 17(1):15–20, 1996.

O. Gon and P. C. Heemstra. *Fishes of the Southern Ocean*, volume 1. J. L. B. Smith Institute of Ichthyology, Grahamstown, 1990. ISBN 8-86810-211-3.

J. A. González, A. Matins, J. I. Santana Morales, R. Triay-Portella, C. Monteiro, V. García-Martín, Jiménez N. S., G. González Lorenzo, J. G. Pajuelo, and J. M. Lorenzo. New and rare records of teleost fishes from the Cape Verde Islands (eastern-central Atlantic Ocean). *Cybium*, 2014.

C. P. Goodyear, J. Luo, E. D. Prince, J. P. Hoolihan, D. Snodgrass, E. S. Orbesen, and J. E. Serafy. Vertical habitat use of Atlantic blue marlin *Makaira nigricans*: interaction with pelagic longline gear. *Marine Ecology Progress Series*, 365:233–245, 2008.

Google, 2021. URL `https://www.google.co.uk/maps/`.

A. Gopakumar, J. Giebichenstein, E. Raskhozheva, and K. Borgå. Mercury in Barents Sea fish in the Arctic polar night: Species and spatial comparison. *Marine Pollution Bulletin*, 169:112501, 2021.

J.D.M Gordon and J.A.R Duncan. The ecology of the deep-sea benthic and benthopelagic fish on the slopes of the Rockall Trough, Northeastern Atlantic. *Progress in Oceanography*, 15(1):37–69, 1985.

M. S. Gordon. Comparative studies on the metabolism of shallow-water and deep-sea marine fishes. I. White-muscle metabolism in shallow-water fishes. *Marine Biology*, 13(3):222–237, 1972.

J. R. Gormly. *Stable carbon isotope variations in marine organic matter*. PhD thesis, Texas A & M University, Texas, 1975. URL https://www.proquest.com/openview/0ec705e99fa8ae532e2bc3c637dbdb2c/1?pq-origsite=gscholar&cbl=18750&diss=y.

N. Gruber, C. D. Keeling, R. B. Bacastow, P. R. Guenther, T. J. Lueker, M. Wahlen, H. A. J. Meijer, W. G. Mook, and T. F. Stocker. Spatiotemporal patterns of carbon-13 in the global surface oceans and the oceanic Suess effect. *Global Biogeochemical Cycles*, 13(2):307–335, 1999.

N. Gruber, D. Clement, B. R. Carter, R. A. Feely, S. Van Heuven, M. Hoppema, M. Ishii, R. M. Key, A. Kozyr, S. K. Lauvset, C. Lo Monaco, J. T. Mathias, A. Murata, A. Olsen, F. F. Perez, C. L. Sabine, T. Tanhua, and R. Wanninkhof. The oceanic sink for anthropogenic CO_2 from 1994 to 2007. *Science*, 363(6432):1193–1199, 2019.

Motomura H. Pacific bluefin tuna, 2022. URL https://fishider.org/en/guide/osteichthyes/scombridae/thunnus/thunnus-orientalis.

J. D. Hadfield. MCMC methods for multi-response generalized linear mixed models: The MCMCglmm R package. *Journal of Statistical Software*, 33(2):1–22, 2010. URL https://www.jstatsoft.org/v33/i02/.

M. J. Hansen, D. Boisclair, S. B. Brandt, S. W. Hewett, J. F. Kitchell, M. C. Lucas, and J. J. Ney. Applications of bioenergetics models to fish ecology and management: where do we go from here? *Transactions of the American Fisheries Society*, 122(5): 1019–1030, 1993.

N. N. Hanson, C. M. Wurster, and C. D. Todd. Reconstructing marine life-history strategies of wild Atlantic salmon from the stable isotope composition of otoliths. *Marine Ecology Progress Series*, 475:249–266, 2013.

M. B. J. Harfoot, T. Newbold, D. P. Tittensor, S. Emmott, J. Hutton, V. Lyutsarev, M. J. Smith, J. P. W. Scharlemann, and D. W. Purves. Emergent global patterns of ecosystem structure and function from a mechanistic general ecosystem model. *PLOS Biology*, 12(4):e1001841, 2014.

P. H. Harvey and M. D. Pagel. *The comparative method in evolutionary biology*, volume 239. Oxford University Press, 1991.

H. Heessen. *Sprattus sprattus*, 2006. URL https://www.marinespecies.org/berms/aphia.php?p=image&tid=126425&pic=2318.

S. Hernández-León, S. Calles, and M. L. F. de Puelles. The estimation of metabolism in the mesopelagic zone: disentangling deep-sea zooplankton respiration. *Progress in Oceanography*, 178:102163, 2019.

K. Hidaka, K. Kawaguchi, M. Murakami, and M. Takahashi. Downward transport of organic carbon by diel migratory micronekton in the western equatorial Pacific: its quantitative and qualitative importance. *Deep Sea Research Part I: Oceanographic Research Papers*, 48(8):1923–1939, 2001.

M. Hidalgo, J. Tomás, H. Høie, B. Morales-Nin, and U. S. Ninnemann. Environmental influences on the recruitment process inferred from otolith stable isotopes in *Merluccius merluccius* off the Balearic Islands. *Aquatic Biology*, 3(3):195–207, 2008.

H. Hillebrand. On the generality of the latitudinal diversity gradient. *The American Naturalist*, 163(2):192–211, 2004.

A. K. Hilting, C. A. Currin, and R. K. Kosaki. Evidence for benthic primary production support of an apex predator–dominated coral reef food web. *Marine Biology*, 160(7): 1681–1695, 2013.

S. Hirch and B. Christiansen. The trophic blockage hypothesis is not supported by the diets of fishes on Seine Seamount. *Marine Ecology*, 31:107–120, 2010.

J. C. Hoffman and T. T. Sutton. Lipid correction for carbon stable isotope analysis of deep-sea fishes. *Deep Sea Research Part I: Oceanographic Research Papers*, 57(8): 956–964, 2010.

G. F. Holeton. Metabolic cold adaptation of polar fish: fact or artefact? *Physiological Zoology*, 47(3):137–152, 1974.

J. P. Hoolihan, J. Luo, D. Snodgrass, E. S. Orbesen, A. M. Barse, and E. D. Prince. Vertical and horizontal habitat use by white marlin *Kajikia albida* (Poey, 1860) in the western North Atlantic Ocean. *ICES Journal of Marine Science*, 72(8):2364–2373, 2015.

P. L. Horn, H. L. Neil, L. J. Paul, and P. J. McMillan. Age verification, growth and life history of rubyfish *Plagiogeneion rubiginosum*. *New Zealand Journal of Marine and Freshwater Research*, 46(3):353–368, 2012.

J. M. Hudson, D. K. Steinberg, T. T. Sutton, J. E. Graves, and R. J. Latour. Myctophid feeding ecology and carbon transport along the northern Mid-Atlantic Ridge. *Deep Sea Research Part I: Oceanographic Research Papers*, 93:104–116, 2014.

A. J. Hulbert and P. L. Else. Basal metabolic rate: history, composition, regulation, and usefulness. *Physiological and Biochemical Zoology*, 77(6):869–876, 2004.

P. A. Hulley. Results of the research cruises of FRV "Walther Herwig" to South America LVIII, Family Myctophidae (Osteichthyes, Myctophiformes). *Archiv fur Fishchereiwissenschaft*, 31:1–300, 1981.

H. Høie, E. Otterlei, and A. Folkvord. Temperature-dependent fractionation of stable oxygen isotopes in otoliths of juvenile cod (*Gadus morhua* L.). *ICES Journal of Marine Science*, 61(2):243–251, 2004.

A. Işmen. Age, growth and reproduction of the goldband goatfish, *Upeneus moluccensis* (Bleeker, 1855), in Iskenderun Bay, the Eastern Mediterranean. *Turkish Journal of Zoology*, 29(4):301–309, 2005.

M. M. Igulu, I. Nagelkerken, G. van der Velde, and Y. D. Mgaya. Mangrove fish production is largely fuelled by external food sources: a stable isotope analysis of fishes at the individual, species, and community levels from across the globe. *Ecosystems*, 16(7):1336–1352, 2013.

T. Ikeda. Estimated respiration rate of myctophid fish from the enzyme activity of the electron-transport-system. *Journal of the Oceanographical Society of Japan*, 45(3): 167–173, 1989.

T. Ikeda. Metabolism, body composition, and energy budget of the mesopelagic fish *Maurolicus muelleri* in the Sea of Japan. *Fishery Bulletin*, 94:49–58, 1996.

T. Ikeda. Routine metabolic rates of pelagic marine fishes and cephalopods as a function of body mass, habitat temperature and habitat depth. *Journal of Experimental Marine Biology and Ecology*, 480:74–86, 2016.

K. Iken, T. Brey, U. Wand, J. Voigt, and P. Junghans. Food web structure of the benthic community at the Porcupine Abyssal Plain (NE Atlantic): a stable isotope analysis. *Progress in Oceanography*, 50(1-4):383–405, 2001.

IOC-UNESCO. OBIS: Ocean Biodiversity Information System, 2021. URL www.obis.org. Intergovernmental Oceanographic Commission of UNESCO.

N. J. B. Isaac and C. Carbone. Why are metabolic scaling exponents so controversial? quantifying variance and testing hypotheses. *Ecology Letters*, 13(6):728–735, 2010.

T. Iwamoto. The macrourid fish *Cetonurus globiceps* in the Gulf of Mexico. *Copeia*, 1966: 439–442, 1966.

T. Iwamoto, N. Nakayama, K. T. Shao, and H. C. Ho. Synopsis of the grenadier fishes (Gadiformes; Teleostei) of Taiwan. *Proceedings of the California Academy of Sciences*, 62:31–126, 2015.

O. E. Jansen, G. M. Aarts, K. Das, G. Lepoint, L. Michel, and P. J. H. Reijnders. Feeding ecology of harbour porpoises: Stable isotope analysis of carbon and nitrogen in muscle and bone. *Marine Biology Research*, 8(9):829–841, 2012.

S. Jennings and K. Collingridge. Predicting consumer biomass, size-structure, production, catch potential, responses to fishing and associated uncertainties in the world's marine ecosystems. *PLOS ONE*, 10(7):e0133794, 2015.

S. Jennings, G. J. Hewlett, and S. Flatman. The distribution, migrations and stock integrity of lemon sole *Microstomus kitt* in the western English Channel. *Fisheries Research*, 18(3-4):377–388, 1993.

S. Jennings, O Reñones, B. Morales-Nin, N. V. C. Polunin, J. Moranta, and J. Coll. Spatial variation in the 15N and 13C stable isotope composition of plants, invertebrates and fishes on Mediterranean reefs: implications for the study of trophic pathways. *Marine Ecology Progress Series*, 146:109–116, 1997.

F. Jutfelt, T. Norin, E. R. Åsheim, L. E. Rowsey, A. H. Andreassen, R. Morgan, T. D. Clark, and B. Speers-Roesch. 'Aerobic scope protection'reduces ectotherm growth under warming. *Functional Ecology*, 35(7):1397–1407, 2021.

S. Kaartvedt, T. Torgersen, T. A. Klevjer, A. Røstad, and J. A. Devine. Behavior of individual mesopelagic fish in acoustic scattering layers of Norwegian fjords. *Marine Ecology Progress Series*, 360:201–209, 2008.

J. M. Kalish. δ^{13}C and δ^{18}O isotopic disequilibria in fish otoliths: metabolic and kinetic effects. *Marine Ecology Progress Series*, 75(2-3):191–203, 1991.

E. K. Källgren. Population dynamics, diet and trophic positioning of three small demersal fish species within Porsangerfjord, Norway. Master's thesis, Universitetet i Tromsø, 2012.

J. M. Kamilar and N. Cooper. Phylogenetic signal in primate behaviour, ecology and life history. *Philosophical Transactions of the Royal Society B: Biological Sciences*, 368 (1618):20120341, 2013.

G. Kawamura, W. Nishimura, S. Ueda, and T. Nishi. Vision in tunas and marlins. 南海研紀要, 2(1):3–47, 1981.

M. Kawazu, A. Tawa, T. Ishihara, Y. Uematsu, and S. Sakai. Discrimination of eastward trans-Pacific migration of the Pacific bluefin tuna *Thunnus orientalis* through otolith δ^{13}C and δ^{18}O analyses. *Marine Biology*, 167(8):1–7, 2020.

J. Kennedy, S. Jónsson, J. M. Kasper, and H. G. Olafsson. Movements of female lumpfish (*Cyclopterus lumpus*) around Iceland. *ICES Journal of Marine Science*, 72(3): 880–889, 2015.

J. Kennedy, S. Jónsson, H. G. Olafsson, and J. M. Kasper. Observations of vertical movements and depth distribution of migrating female lumpfish (*Cyclopterus lumpus*) in iceland from data storage tags and trawl surveys. *ICES Journal of Marine Science*, 73(4):1160–1169, 2016.

S. S. Killen, I. Costa, J. A. Brown, and A. K. Gamperl. Little left in the tank: metabolic scaling in marine teleosts and its implications for aerobic scope. *Proceedings of the Royal Society B: Biological Sciences*, 274(1608):431–438, 2007.

S. S. Killen, D. Atkinson, and D. S. Glazier. The intraspecific scaling of metabolic rate with body mass in fishes depends on lifestyle and temperature. *Ecology Letters*, 13 (2):184–193, 2010.

S. S. Killen, D. S. Glazier, E. L. Rezende, T. D. Clark, D. Atkinson, A. S. T. Willener, and L. G. Halsey. Ecological influences and morphological correlates of resting and maximal metabolic rates across teleost fish species. *The American Naturalist*, 187(5): 592–606, 2016.

I. A. Kimirei, I. Nagelkerken, Y. D. Mgaya, and C. M. Huijbers. The mangrove nursery paradigm revisited: otolith stable isotopes support nursery-to-reef movements by Indo-Pacific fishes. *PLOS ONE*, 8(6):e66320, 2013.

T. Kitagawa and K. Fujioka. Rapid ontogenetic shift in juvenile Pacific bluefin tuna diet. *Marine Ecology Progress Series*, 571:253–257, 2017.

M. Kleiber. Body size and metabolism. *Hilgardia*, 6(11):315–353, 1932.

M. Kleiber. Body size and metabolic rate. *Physiological Reviews*, 27(4):511–541, 1947.

J. L. Knies and J. G. Kingsolver. Erroneous Arrhenius: modified Arrhenius model best explains the temperature dependence of ectotherm fitness. *The American Naturalist*, 176(2):227–233, 2010.

K. H. Kock and I. Everson. Biology and ecology of mackerel icefish, *Champsocephalus gunnari*: an Antarctic fish lacking hemoglobin. *Comparative Biochemistry and Physiology Part A: Physiology*, 118(4):1067–1077, 1997.

D. Kopp, S. Lefebvre, M. Cachera, M. C. Villanueva, and B. Ernande. Reorganization of a marine trophic network along an inshore–offshore gradient due to stronger pelagic–benthic coupling in coastal areas. *Progress in Oceanography*, 130:157–171, 2015.

D. Kopp, M. Robert, and L. Pawlowski. Characterization of food web structure of the upper continental slope of the Celtic Sea highlighting the trophic ecology of five deep-sea fishes. *Journal of Applied Ichthyology*, 34(1):73–80, 2018.

J. A. Koslow. Energetic and life-history patterns of deep-sea benthic, benthopelagic and seamount-associated fish. *Journal of Fish Biology*, 49:54–74, 1996.

P. Koteja. On the relation between basal and field metabolic rates in birds and mammals. *Functional Ecology*, 5(1):56–64, 1991.

P. Koubbi and P. Pruvost. Specimen of *Krefftichthys anderssoni* (lanternfish), 2008. URL http://mersaustrales.mnhn.fr/blog-en/mersaustrales.mnhn.fr/blog_mission/images/Umitaka/01%2002%2008/UM16_02V.jpg.

A. N. Kozlov, K. V. Shust, and A. V. Zemsky. Seasonal and inter-annual variability in the distribution of *Electrona carlsbergi* in the Southern Polar Front area (the area to the north of South Georgia is used as an example). *CCAMLR Selected Scientific Papers*, 7:337–368, 1991.

J. Kozłowski and M. Konarzewski. Is West, Brown and Enquist's model of allometric scaling mathematically correct and biologically relevant? *Functional Ecology*, 18(2): 283–289, 2004.

Pena L. *Trachyrincus scabrus*, 2002. URL http://www.ictioterm.es/nombre_cientifico.php?nc=322.

V. W. Y. Lam, E. H. Allison, J. D. Bell, J. Blythe, W. W. L. Cheung, T. L. Frölicher, M. A. Gasalla, and U. R. Sumaila. Climate change, tropical fisheries and prospects for sustainable development. *Nature Reviews Earth & Environment*, 1(9):440–454, 2020.

R. S. Lampitt and A. N. Antia. Particle flux in deep seas: regional characteristics and temporal variability. *Deep Sea Research Part I: Oceanographic Research Papers*, 44(8): 1377–1403, 1997.

M. A. Lea, P. D. Nichols, and G. Wilson. Fatty acid composition of lipid-rich myctophids and mackerel icefish (*Champsocephalus gunnari*)–Southern Ocean food-web implications. *Polar Biology*, 25(11):843–854, 2002.

K. O. Lear, D. L. Morgan, J. M. Whitty, N. M. Whitney, E. E. Byrnes, S. J. Beatty, and A. C. Gleiss. Divergent field metabolic rates highlight the challenges of increasing temperatures and energy limitation in aquatic ectotherms. *Oecologia*, 193:311–323, 2020.

S. Lefevre, D. J. McKenzie, and G. E. Nilsson. Models projecting the fate of fish populations under climate change need to be based on valid physiological mechanisms. *Global Change Biology*, 23(9):3449–3459, 2017.

S. Lefevre, D. J. McKenzie, and G. E. Nilsson. In modelling effects of global warming, invalid assumptions lead to unrealistic projections. *Global Change Biology*, 24(2): 553–556, 2018.

A. N. LeGrande and G. A. Schmidt. Global gridded data set of the oxygen isotopic composition in seawater. *Geophysical Research Letters*, 33(12), 2006.

V. Lesage, M. O. Hammill, and K. M. Kovacs. Marine mammals and the community structure of the estuary and Gulf of St. Lawrence, Canada: evidence from stable isotope analysis. *Marine Ecology Progress Series*, 210:203–221, 2001.

L. A. Levin. Oxygen minimum zone benthos: adaptation and community response to hypoxia. In *Oceanography and Marine Biology, An Annual Review*, volume 41. CRC Press, 2003.

N. Lifson, G. B. Gordon, and R. McClintock. Measurement of total carbon dioxide production by means of D_2O^{18}. *Journal of Applied Physiology*, 7(6):704–710, 1955.

H. Y. Lin, J. C. Shiao, Y. G. Chen, and Y. Iizuka. Ontogenetic vertical migration of grenadiers revealed by otolith microstructures and stable isotopic composition. *Deep Sea Research Part I: Oceanographic Research Papers*, 61:123–130, 2012.

S. J. Lin, M. K. Musyl, S. P. Wang, N. J. Su, W. C. Chiang, C. P. Lu, K. Tone, C. Y. Wu, A. Sasaki, and I. Nakamura. Movement behaviour of released wild and farm-raised dolphinfish *Coryphaena hippurus* tracked by pop-up satellite archival tags. *Fisheries Science*, 85(5):779–790, 2019.

T. B. Linkowski. Population biology of the myctophid fish *Gymnoscopelus nicholsi* (Gillbert, 1911) from the western South Atlantic. *Journal of Fish Biology*, 27(6): 683–698, 1985.

T. B. Linkowski. Age and growth of four species of *Electrona* (Teleostei, Myctophidae). In *Proc. V Congr. Europ. Ichthyol.*, pages 435–442, Stockholm, 1987.

T. Linley. Grenadier basic external features, 2013. URL https://en.wikipedia.org/wiki/Fish_measurement#/media/File:Grenadier_basic_external_features.png.

V. Loeb. *Electrona antarctica*, 2018. URL https://en.wikipedia.org/wiki/File:Fish8712.jpg.

J. M. Logan and M. E. Lutcavage. Assessment of trophic dynamics of cephalopods and large pelagic fishes in the central North Atlantic Ocean using stable isotope analysis. *Deep Sea Research Part II: Topical Studies in Oceanography*, 95:63–73, 2013.

T. S. Løkken. Carbon source and trophic structure along a depth gradient in Isfjorden, Svalbard. Master's thesis, Universitetet i Tromsø, 2013.

S. Lourenço, R. A. Saunders, M. Collins, R. Shreeve, C. A. Assis, M. Belchier, J. L. Watkins, and J. C. Xavier. Life cycle, distribution and trophodynamics of the lanternfish *Krefftichthys anderssoni* (Lönnberg, 1905) in the Scotia Sea. *Polar Biology*, 40(6):1229–1245, 2017.

R. Lubbock and A. Edwards. The fishes of Saint Paul's rocks. *Journal of Fish Biology*, 18 (2):135–157, 1981.

T. G. Lubimova, K. V. Shust, and V. V. Popkov. Specific features in the ecology of Southern Ocean mesopelagic fish of the family Myctophidae. *Biological resources of the Arctic and Antarctic*, pages 320–337, 1987.

S. M. Lusseau and S. R. Wing. Importance of local production versus pelagic subsidies in the diet of an isolated population of bottlenose dolphins *Tursiops* sp. *Marine Ecology Progress Series*, 321:283–293, 2006.

J. V. Magnússon. Distribution and some other biological parameters of two morid species *Lepidion eques* (Günther, 1887) and *Antimora rostrata* (Günther, 1878) in Icelandic waters. *Fisheries Research*, 51(2-3):267–281, 2001.

P. L. Mancini and L. Bugoni. Resources partitioning by seabirds and their relationship with other consumers at and around a small tropical archipelago. *ICES Journal of Marine Science*, 71(9):2599–2607, 2014.

C. S. Manooch III and J. C. Potts. Age, growth, and mortality of greater amberjack, *Seriola dumerili*, from the US Gulf of Mexico headboat fishery. *Bulletin of Marine Science*, 61(3):671–683, 1997.

R. Mariano-Jelicich, S. Copello, J. P. Seco Pon, and M. Favero. Long-term changes in black-browed albatrosses diet as a result of fisheries expansion: an isotopic approach. *Marine Biology*, 164(6):1–12, 2017.

T. L. Martin and R. B. Huey. Why "suboptimal" is optimal: Jensen's inequality and ectotherm thermal preferences. *The American Naturalist*, 171(3):E102–E118, 2008.

C. M. Martinez, S. T. Friedman, K. A. Corn, O. Larouche, S. A. Price, and P. C. Wainwright. The deep sea is a hot spot of fish body shape evolution. *Ecology Letters*, 24(9):1788–1799, 2021.

J. C. Martino, Z. A. Doubleday, M. T. Chung, and B. M. Gillanders. Experimental support towards a metabolic proxy in fish using otolith carbon isotopes. *The Journal of Experimental Biology*, 223(6):jeb217091, 2020. .

E. Massutí and B. Morales-Nin. Seasonality and reproduction of dolphin-fish (*Coryphaena hippurus*) in the western Mediterranean. *Scientia Marina*, 59(3-4): 357–364, 1995.

P. Matich, J. J. Kiszka, K. R. Gastrich, and M. R. Heithaus. Trophic redundancy among fishes in an east african nearshore seagrass community inferred from stable-isotope analysis. *Journal of Fish Biology*, 91(2):490–509, 2017.

T. Matsui, S. Kato, and S. E. Smith. Biology and potential use of Pacific grenadier, *Coryphaenoides acrolepis*, off California. *Marine Fisheries Review*, 52(3):1–17, 1991.

N. Mavraki, S. Degraer, and J. Vanaverbeke. Offshore wind farms and the attraction–production hypothesis: insights from a combination of stomach content and stable isotope analyses. *Hydrobiologia*, 848(7):1639–1657, 2021.

J. L. May and J. G. H. Maxwell. *Thunnus maccoyii*, 1986. URL https://www.fishbase.se/photos/PicturesSummary.php?StartRow=3&ID=145&what=species&TotRec=7.

S. M McCluskey, K. R. Sprogis, J. M. London, L. Bejder, and N. R. Loneragan. Foraging preferences of an apex marine predator revealed through stomach content and stable isotope analyses. *Global Ecology and Conservation*, 25:e01396, 2021.

J. H. McCutchan Jr., W. M. Lewis Jr, C. Kendall, and C. C. McGrath. Variation in trophic shift for stable isotope ratios of carbon, nitrogen, and sulfur. *Oikos*, 102(2): 378–390, 2003.

R. M. McDowall. *Salmo salar*, 1990. URL https://www.fishbase.se/photos/PicturesSummary.php?StartRow=5&ID=236&what=species&TotRec=17.

R. McElreath. *rethinking: statistical rethinking book package*, 2020. URL https://www.rdocumentation.org/packages/rethinking/versions/2.01.

R. F. McGinnis. *Biogeography of lanternfishes (family Myctophidae) south of 30 °S*. University of Southern California, 1982.

M. McGrouther. A deepsea lizardfish, *Bathysaurus ferox*, No Date. URL https://fishesofaustralia.net.au/Images/Image/BathysaurusFeroxS047.jpg.

D. J. McKenzie. Effects of dietary fatty acids on the respiratory and cardiovascular physiology of fish. *Comparative Biochemistry and Physiology Part A: Molecular & Integrative Physiology*, 128(3):605–619, 2001.

B. C. McMeans, J. Svavarsson, S. Dennard, and A. T. Fisk. Diet and resource use among Greenland sharks (*Somniosus microcephalus*) and teleosts sampled in Icelandic waters, using δ^{13}C, δ^{15}N, and mercury. *Canadian Journal of Fisheries and Aquatic Sciences*, 67(9):1428–1438, 2010.

M. R. S. Melo, A. C. Braga, G. W. A. Nunan, and P. A. S. Costa. On new collections of deep-sea Gadiformes (Actinopterygii: Teleostei) from the Brazilian continental slope, between 11 and 23 °S. *Zootaxa*, 2433(1):25–46, 2010.

N. R. Merrett. *Macrouridae of the eastern North Atlantic*. International Council for the Exploration of the Sea (ICES), 1986. ISBN 978-87-7482-954-6.

N .R. Merrett. Preliminary guide to the identification of the early life history stages of bathygadid & macrourid fishes of the western central North Atlantic. Florida, USA, 2003. National Oceanic and Atmospheric Administration (NOAA).

N. R. Merrett, R. L. Haedrich, J. D. M. Gordon, and M. Stehmann. Deep demersal fish assemblage structure in the Porcupine Seabight (eastern North Atlantic): results of single warp trawling at lower slope to abyssal soundings. *Journal of the Marine Biological Association of the United Kingdom*, 71(2):359–373, 1991.

W. Merten, R. Appeldoorn, R. Rivera, and D. Hammond. Diel vertical movements of adult male dolphinfish (*Coryphaena hippurus*) in the western central Atlantic as determined by use of pop-up satellite archival transmitters. *Marine Biology*, 161(8): 1823–1834, 2014.

J. D. Metcalfe, S. Wright, C. Tudorache, and R. P. Wilson. Recent advances in telemetry for estimating the energy metabolism of wild fishes. *Journal of Fish Biology*, 88(1): 284–297, 2016.

T. Meyer. *Conger conger*, 2006. URL `https://www.fishbase.se/photos/UploadedBy.php?autoctr=13419&win=uploaded`.

A. Mirasole, B. M. Gillanders, P. Reis-Santos, F. Grassa, G. Capasso, G. Scopelliti, A. Mazzola, and S. Vizzini. The influence of high pCO_2 on otolith shape, chemical and carbon isotope composition of six coastal fish species in a Mediterranean shallow CO_2 vent. *Marine Biology*, 164(9):1–15, 2017.

A. Mittermayr, S. E. Fox, and U. Sommer. Temporal variation in stable isotope composition ($\delta^{13}C$, $\delta^{15}N$ and $\delta^{34}S$) of a temperate *Zostera marina* food web. *Marine Ecology Progress Series*, 505:95–105, 2014.

A. Moura, A. A. Muniz, E. Mullis, J. M. Wilson, R. P. Vieira, A. A. Almeida, E. Pinto, G. J. A. Brummer, P. V. Gaever, and J. M. S. Gonçalves. Population structure and dynamics of the Atlantic mackerel (*Scomber scombrus*) in the North Atlantic inferred from otolith chemical and shape signatures. *Fisheries Research*, 230:105621, 2020.

P. B. Moyle and J. J. Cech. *Fishes: an introduction to ichthyology*. 2004. ISBN 0-13-100847-1. Issue: 597.

C. Mytilineou, C. Y. Politou, C. Papaconstantinou, S. Kavadas, G. d'Onghia, and L Sion. Deep-water fish fauna in the Eastern Ionian Sea. *Belgian Journal of Zoology*, 135(2):229, 2005.

K. A. Nagy. Field metabolic rate and food requirement scaling in mammals and birds. *Ecological Monographs*, 57(2):111–128, 1987.

K. A. Nagy, I. A. Girard, and T. K. Brown. Energetics of free-ranging mammals, reptiles, and birds. *Annual Review of Nutrition*, 19(1):247–277, 1999.

I. Nakamura. *Billfishes of the world*, volume 5. Food and Agriculture Organization of the United Nations (FAO), Rome, 1985. ISBN 92-5-102232-1.

M. R. Navarro, B. Villamor, S. Myklevoll, J. Gil, P. Abaunza, and J. Canoura. Maximum size of Atlantic mackerel (*Scomber scombrus*) and Atlantic chub mackerel (*Scomber colias*) in the Northeast Atlantic. *Cybium*, 36(2):406–408, 2012.

F. C. Neat and N. Campbell. Proliferation of elongate fishes in the deep sea. *Journal of Fish Biology*, 83(6):1576–1591, 2013.

J. Nelson, R. Wilson, F. Coleman, C. Koenig, D. DeVries, C. Gardner, and J. Chanton. Flux by fin: fish-mediated carbon and nutrient flux in the northeastern Gulf of Mexico. *Marine Biology*, 159(2):365–372, 2012.

J. A. Nelson. Oxygen consumption rate v. rate of energy utilization of fishes: a comparison and brief history of the two measurements. *Journal of Fish Biology*, 88(1): 10–25, 2016. .

NERC. Coldfish, 2021. URL https://www.changing-arctic-ocean.ac.uk/project/coldfish/. Changing Arctic Ocean (CAO).

S. J. Newman, R. A. Steckis, J. S. Edmonds, and J. Lloyd. Stock structure of the goldband snapper *Pristipomoides multidens* (Pisces: Lutjanidae) from the waters of northern and western Australia by stable isotope ratio analysis of sagittal otolith carbonate. *Marine Ecology Progress Series*, 198:239–247, 2000. ISSN 0171-8630.

J. Nielsen, M. Nielsen, and P. Frandsen. Deep Sea Creatures of the North Atlantic (DESCNA), 2021. URL https://descna.com/en/.

M. Nilsen, T. Pedersen, E. M. Nilssen, and S. Fredriksen. Trophic studies in a high-latitude fjord ecosystem—a comparison of stable isotope analyses (δ^{13}C and δ^{15}N) and trophic-level estimates from a mass-balance model. *Canadian Journal of Fisheries and Aquatic Sciences*, 65(12):2791–2806, 2008.

E. T. Nolan, K. J. Downes, A. Richardson, A. Arkhipkin, P. Brickle, J. Brown, R. J. Mrowicki, Z. Shcherbich, N. Weber, and S. B. Weber. Life-history strategies of the rock hind grouper *Epinephelus adscensionis* at Ascension Island. *Journal of Fish Biology*, 91(6):1549–1568, 2017.

T. Norin and T. D. Clark. Fish face a trade-off between 'eating big' for growth efficiency and 'eating small' to retain aerobic capacity. *Biology Letters*, 13(9): 20170298, 2017.

T. Norin and T.D. Clark. Measurement and relevance of maximum metabolic rate in fishes. *Journal of Fish Biology*, 88(1):122–151, 2016.

T. Norin and A. K. Gamperl. Metabolic scaling of individuals vs. populations: evidence for variation in scaling exponents at different hierarchical levels. *Functional Ecology*, 32(2):379–388, 2018.

T. Norin and H. Malte. Intraspecific variation in aerobic metabolic rate of fish: relations with organ size and enzyme activity in brown trout. *Physiological and Biochemical Zoology*, 85(6):645–656, 2012.

C. Nozères. *Triglops nybelini* - trio of bigeye sculpins, 2010. URL https://www.marinespecies.org/aphia.php?p=image&tid=127206&pic=30207.

C. Nozères. *Synaphobranchus kaupii* - northern cutthroat eel, 2011. URL https://www.marinespecies.org/photogallery.php?album=735&pic=37817.

L. T. Nunes, D. R. Barneche, N. S. Lastrucci, A. A. Fraga, J. A. C. C. Nunes, C. E. L. Ferreira, and S. R. Floeter. Predicting the effects of body size, temperature and diet on animal feeding rates. *Functional Ecology*, 35(10):2229–2240, 2021.

J. Nyunja, M. Ntiba, J. Onyari, K. Mavuti, K. Soetaert, and S. Bouillon. Carbon sources supporting a diverse fish community in a tropical coastal ecosystem (Gazi Bay, Kenya). *Estuarine, Coastal and Shelf Science*, 83(3):333–341, 2009.

Smithsonian National Museum of Natural History. *Lepidoperca coatsii*, USNM 394682, 2004. URL http://n2t.net/ark:/65665/338375a58-eae0-4225-b77d-e829767b914d.

National Institute of Water and Atmospheric Research (NIWA). A selection of mesopelagic fish species caught in the deep scattering layers observed in the Antarctic Convergence Zone, 2018. URL https://niwa.co.nz/file/42902.

A. Olsen, R. M. Key, S. van Heuven, S. K. Lauvset, A. Velo, X. Lin, C. Schirnick, A. Kozyr, T. Tanhua, and M. Hoppema. The Global Ocean Data Analysis Project version 2 (GLODAPv2)–an internally consistent data product for the world ocean. *Earth System Science Data*, 8(2):297–323, 2016.

A. Orlov. Photo(s) contributed by Alexei Orlov, 2009. URL https://www.fishbase.se/photos/PhotosList.php?id=1287&vCollaborator=Alexei+Orlov.

L. S. Oven, M. P. Konstantinova, and N. F. Shevchenko. Aspects of reproduction and feeding of myctophids (Myctophidae) in the southwest Atlantic. *Journal of Ichthyology*, 30(2):115–127, 1990.

K. Owen, K. Charlton-Robb, and R. Thompson. Resolving the trophic relations of cryptic species: An example using stable isotope analysis of dolphin teeth. *PLOS ONE*, 6(2):e16457, 2011.

H. A. Oxenford. Biology of the dolphinfish (*Coryphaena hippurus*) in the western central Atlantic: a review. *Scientia Marina*, 63(3-4):277–301, 1999.

M. L. Pace, G. A. Knauer, D. M. Karl, and J. H. Martin. Primary production, new production and vertical flux in the eastern Pacific Ocean. *Nature*, 325(6107):803–804, 1987.

A. Pallaoro, P. Cetinić, J. Dulčić, I. Jardas, and M. Kraljević. Biological parameters of the saddled bream *Oblada melanura* in the eastern Adriatic. *Fisheries Research*, 38(2): 199–205, 1998.

M. L. Palomares and D. Pauly. A multiple regression model for prediction the food consumption of marine fish populations. *Marine and Freshwater Research*, 40(3): 259–273, 1989.

V. Papiol, J. E. Cartes, E. Fanelli, and P. Rumolo. Food web structure and seasonality of slope megafauna in the NW Mediterranean elucidated by stable isotopes: relationship with available food sources. *Journal of Sea Research*, 77:53–69, 2013.

C. Parzanini, C. C. Parrish, J. F. Hamel, and A. Mercier. Trophic ecology of a deep-sea fish assemblage in the Northwest Atlantic. *Marine Biology*, 164(10):1–19, 2017.

D. Pauly. A framework for latitudinal comparisons of flatfish recruitment. *Netherlands Journal of Sea Research*, 32(2):107–118, 1994.

G. Paz. *Oblada melanura*, 2012. URL http://v3.boldsystems.org/pics/BIM/E137.1%2B978321600.JPG.

C. C. Peterson, K. A. Nagy, and J. Diamond. Sustained metabolic scope. *Proceedings of the National Academy of Sciences*, 87(6):2324–2328, 1990.

C. F. Phleger, M. M. Nelson, B. D. Mooney, and P. D. Nichols. Wax esters versus triacylglycerols in myctophid fishes from the Southern Ocean. *Antarctic Science*, 11 (4):436–444, 1999.

U. Piatkowski, P. G. Rodhouse, M. G. White, D. G. Bone, and C. Symon. Nekton community of the Scotia Sea as sampled by the RMT 25 during austral summer. *Marine Ecology Progress Series*, 112:13–28, 1994.

R. Pillon. *Gobius bucchichi*, 2016. URL https://www.fishbase.se/photos/PicturesSummary.php?StartRow=1&ID=46334&what=species&TotRec=3.

J. K. Pinnegar and N. V. C. Polunin. Contributions of stable-isotope data to elucidating food webs of Mediterranean rocky littoral fishes. *Oecologia*, 122(3):399–409, 2000.

M. L. Pinsky, B. Worm, M. J. Fogarty, J. L. Sarmiento, and S. A. Levin. Marine taxa track local climate velocities. *Science*, 341(6151):1239–1242, 2013.

M. L. Pinsky, A. M. Eikeset, D. J. McCauley, J. L. Payne, and J. M. Sunday. Greater vulnerability to warming of marine versus terrestrial ectotherms. *Nature*, 569(7754): 108–111, 2019.

T. J. Pitcher and J. K. Parrish. Functions of shoaling behaviour in teleosts. In *The behaviour of teleost fishes*, pages 294–337. 1986.

M. Plummer. *rjags: Bayesian Graphical Models using MCMC*, 2019. URL https://CRAN.R-project.org/package=rjags. R package version 4-10.

N. Plummer, N. Best, K. Cowles, and K. Vines. Coda: Convergence diagnosis and output analysis for mcmc. *R News*, 6(1):7–11, 2006. URL https://journal.r-project.org/archive/.

T. Poisot, R. Sachse, J. Ashander, and T. Galili. The digitize package: extracting numerical data from scatterplots. *The R Journal*, 3(1):25–26, 2011.

N. V. C. Polunin, B. Morales-Nin, W. E. Pawsey, J. E. Cartes, J. K. Pinnegar, and J. Moranta. Feeding relationships in Mediterranean bathyal assemblages elucidated by stable nitrogen and carbon isotope data. *Marine Ecology Progress Series*, 220:13–23, 2001.

H. Pontzer, Y. Yamada, H. Sagayama, P. N. Ainslie, L. F. Andersen, L. J. Anderson, L. Arab, I. Baddou, K. Bedu-Addo, E. E. Blaak, et al. Daily energy expenditure through the human life course. *Science*, 373(6556):808–812, 2021.

H. O. Pörtner, D. Storch, and O. Heilmayer. Constraints and trade-offs in climate-dependent adaptation: energy budgets and growth in a latitudinal cline. *Scientia Marina*, 69(S2):271–285, 2005.

H. O. Pörtner, C. Bock, and F. C. Mark. Oxygen-and capacity-limited thermal tolerance: bridging ecology and physiology. *Journal of Experimental Biology*, 220(15): 2685–2696, 2017.

P. Pottier, S. Burke, S. M. Drobniak, and S. Nakagawa. Methodological inconsistencies define thermal bottlenecks in fish life cycle: a comment on dahlke et al. 2020. *Evolutionary Ecology*, pages 1–6, 2022.

T. L. Poulson. Adaptations of cave fishes with some comparisons to deep-sea fishes. *Environmental Biology of Fishes*, 62(1):345–364, 2001.

I. Preciado, J. E. Cartes, A. Punzón, I. Frutos, L. López-López, and A. Serrano. Food web functioning of the benthopelagic community in a deep-sea seamount based on diet and stable isotope analyses. *Deep Sea Research Part II: Topical Studies in Oceanography*, 137:56–68, 2017.

I. G. Priede, J. A. Godbold, N. J. King, M. A. Collins, D. M. Bailey, and J. D. M. Gordon. Deep-sea demersal fish species richness in the Porcupine Seabight, NE Atlantic Ocean: global and regional patterns. *Marine Ecology*, 31(1):247–260, 2010. ISSN 0173-9565.

T. S. Prinzing, Y. Zhang, N. C. Wegner, and N. K. Dulvy. Analytical methods matter too: Establishing a framework for estimating maximum metabolic rate for fishes. *Ecology and Evolution*, 11(15):9987–10003, 2021.

P. Provoost and S. Bosch. *robis: Ocean Biodiversity Information System (OBIS) Client*, 2020. URL `https://CRAN.R-project.org/package=robis`. R package version 2.3.9.

C. Pusch, P. A. Hulley, and K. H. Kock. Community structure and feeding ecology of mesopelagic fishes in the slope waters of King George Island (South Shetland Islands, Antarctica). *Deep Sea Research Part I: Oceanographic Research Papers*, 51(11): 1685–1708, 2004.

Banón Díaz R. Photo(s) contributed by Rafael Bañón Díaz, 2009. URL https://www.fishbase.se/photos/PhotosList.php?id=377&vCollaborator=Rafael+Ba%C3%B1%C3%B3n+D%C3%ADaz.

McPhee R. and M. McGrouther. Globehead whiptail, *Cetonurus globiceps*, No Date. URL https://fishesofaustralia.net.au/Images/Image/C-globiceps-S072_232_web.jpg.

R Core Team. *R: A Language and Environment for Statistical Computing*. R Foundation for Statistical Computing, Vienna, Austria, 2021a. URL https://www.R-project.org/.

R Core Team. *R: A Language and Environment for Statistical Computing*. R Foundation for Statistical Computing, Vienna, Austria, 2021b. URL https://www.R-project.org/.

D. L. Rabosky, J. Chang, P. O. Title, P. F. Cowman, L. Sallan, M. Friedman, K. Kaschner, C. Garilao, T. J. Near, and M. Coll. An inverse latitudinal gradient in speciation rate for marine fishes. *Nature*, 559(7714):392–395, 2018.

R. L. Radtke, D. F. Williams, and P. C. F. Hurley. The stable isotopic composition of bluefin tuna (*Thunnus thynnus*) otoliths: evidence for physiological regulation. *Comparative Biochemistry and Physiology Part A: Physiology*, 87(3):797–801, 1987.

B. C. Rall, U. Brose, M. Hartvig, G. Kalinkat, F. Schwarzmüller, O. Vucic-Pestic, and O. L. Petchey. Universal temperature and body-mass scaling of feeding rates. *Philosophical Transactions of the Royal Society B: Biological Sciences*, 367(1605): 2923–2934, 2012.

S. G. A. C. Ramos. Diet and trophic position of deep-sea sharks in the southwest coast of Portugal: using stable isotopes analysis and nucleic acids ratios (RNA/DNA). Master's thesis, University of the Algarve, 2018.

S. Ramsvatn and T. Pedersen. Ontogenetic niche changes in haddock *Melanogrammus aeglefinus* reflected by stable isotope signatures, δ^{13}C and δ^{15}N. *Marine Ecology Progress Series*, 451:175–185, 2012.

W. D. K. Reid, B. D. Wigham, R. A. R. McGill, and N. V. C. Polunin. Elucidating trophic pathways in benthic deep-sea assemblages of the Mid-Atlantic Ridge north and south of the Charlie-Gibbs Fracture Zone. *Marine Ecology Progress Series*, 463: 89–103, 2012.

S. B. Reinhardt and E. S. Van Vleet. Lipid composition of twenty-two species of Antarctic midwater zooplankton and fish. *Marine Biology*, 91(2):149–159, 1986.

A. T. Revill, J. W. Young, and M. Lansdell. Stable isotopic evidence for trophic groupings and bio-regionalization of predators and their prey in oceanic waters off eastern Australia. *Marine Biology*, 156(6):1241–1253, 2009.

J. G. Richards. Metabolic rate suppression as a mechanism for surviving environmental challenge in fish. In C. A. Navas and J. E. Carvalho, editors, *Aestivation*, volume 49 of *Progress in Molecular and Subcellular Biology*, pages 113–139. Springer, 2010.

D. Robinson. *fuzzyjoin: Join Tables Together on Inexact Matching*, 2020. URL `https://CRAN.R-project.org/package=fuzzyjoin`. R package version 0.1.6.

J. G. Rubalcaba, W. C. E. P. Verberk, A. J. Hendriks, B. Saris, and H. A. Woods. Oxygen limitation may affect the temperature and size dependence of metabolism in aquatic ectotherms. *Proceedings of the National Academy of Sciences*, 117(50):31963–31968, 2020.

M. Rubner. Ueber den einfluss der korpergrosse auf stoffund kaftwechsel. *Zeitschrift fur Biologie*, 19:535–562, 1883.

K. E. Ruck, D. K. Steinberg, and E. A. Canuel. Regional differences in quality of krill and fish as prey along the Western Antarctic Peninsula. *Marine Ecology Progress Series*, 509:39–55, 2014.

B. C. Russell, D. Golani, and Y. Tikochinski. *Saurida lessepsianus* a new species of lizardfish (Pisces: Synodontidae) from the Red Sea and Mediterranean Sea, with a key to *Saurida* species in the Red Sea. *Zootaxa*, 3956(4):559–568, 2015.

G. K. Saba, A. B. Burd, J. P. Dunne, S. Hernández-León, A. H. Martin, K. A. Rose, J. Salisbury, D. K. Steinberg, C. N. Trueman, R. W. Wilson, and S. E. Wilson. Toward a better understanding of fish-based contribution to ocean carbon flux. *Limnology and Oceanography*, 66(5):1639–1664, 2021.

D. K. Sackett, J. C. Drazen, B. N. Popp, C. A. Choy, J. D. Blum, and M. W. Johnson. Carbon, nitrogen, and mercury isotope evidence for the biogeochemical history of mercury in Hawaiian marine bottomfish. *Environmental Science & Technology*, 51(23): 13976–13984, 2017.

T. Sakamoto, K. Komatsu, M. Yoneda, T. Ishimura, T. Higuchi, K. Shirai, Y. Kamimura, C. Watanabe, and A. Kawabata. Temperature dependence of δ^{18}O in otolith of juvenile Japanese sardine: laboratory rearing experiment with micro-scale analysis. *Fisheries Research*, 194:55–59, 2017.

P. Sallaberry-Pincheira, P. Galvez, B. E. Molina-Burgos, F. Fernandoy, R. Melendez, and S. A. Klarian. Diet and food consumption of the Patagonian toothfish (*Dissostichus eleginoides*) in South Pacific Antarctic waters. *Polar Biology*, 41(11):2379–2385, 2018.

V. C. Sambilay Jr. Interrelationships between swimming speed, caudal fin aspect ratio and body length of fishes. *Fishbyte*, 8(3):16–20, 1990.

F. Sánchez, N. Pérez, and J. Landa. Distribution and abundance of megrim (*Lepidorhombus boscii* and *Lepidorhombus whiffiagonis*) on the northern Spanish shelf. *ICES Journal of Marine Science*, 55(3):494–514, 1998.

P. J. Sanchez, J. R. Rooker, M. Z. Sluis, J. Pinsky, M. A. Dance, B. Falterman, and R. J. Allman. Application of otolith chemistry at multiple life history stages to assess population structure of Warsaw grouper in the Gulf of Mexico. *Marine Ecology Progress Series*, 651:111–123, 2020.

G. Sarà, M. De Pirro, M. Sprovieri, P. Rumolo, H. P. Halldórsson, and J. Svavarsson. Carbon and nitrogen stable isotopic inventory of the most abundant demersal fish captured by benthic gears in southwestern Iceland (North Atlantic). *Helgoland Marine Research*, 63(4):309–315, 2009.

F. Sardenne, S. Hollanda, S. Lawrence, R. Albert-Arrisol, M. Degroote, and N. Bodin. Trophic structures in tropical marine ecosystems: a comparative investigation using three different ecological tracers. *Ecological Indicators*, 81:315–324, 2017.

F. Sardenne, N. G. C. Diaha, M. J. Amandé, I. Zudaire, L. I. E. Couturier, L. Metral, F. Le Grand, and N. Bodin. Seasonal habitat and length influence on the trophic niche of co-occurring tropical tunas in the eastern Atlantic Ocean. *Canadian Journal of Fisheries and Aquatic Sciences*, 76(1):69–80, 2019.

J. R. Sargent, R. R. Gatten, and R. McIntosh. Wax esters in the marine environment—their occurrence, formation, transformation and ultimate fates. *Marine Chemistry*, 5(4-6):573–584, 1977.

R. A. Saunders, S. Fielding, S. E. Thorpe, and G. A. Tarling. School characteristics of mesopelagic fish at South Georgia. *Deep Sea Research Part I: Oceanographic Research Papers*, 81:62–77, 2013.

R. A. Saunders, M. A. Collins, D. Foster, R. Shreeve, G. Stowasser, P. Ward, and G. A. Tarling. The trophodynamics of Southern Ocean Electrona (Myctophidae) in the Scotia Sea. *Polar Biology*, 37(6):789–807, 2014.

R. A. Saunders, M. A. Collins, P. Ward, G. Stowasser, S. L. Hill, R. Shreeve, and G. A. Tarling. Predatory impact of the myctophid fish community on zooplankton in the Scotia Sea (Southern Ocean). *Marine Ecology Progress Series*, 541:45–64, 2015a.

R. A. Saunders, M. A. Collins, P. Ward, G. Stowasser, R. Shreeve, and G. A. Tarling. Distribution, population structure and trophodynamics of Southern Ocean Gymnoscopelus (Myctophidae) in the Scotia Sea. *Polar Biology*, 38(3):287–308, 2015b.

R. A. Saunders, M. A. Collins, P. Ward, G. Stowasser, R. Shreeve, and G. A. Tarling. Trophodynamics of Protomyctophum (Myctophidae) in the Scotia Sea (Southern Ocean). *Journal of Fish Biology*, 87(4):1031–1058, 2015c.

R. A. Saunders, M. A. Collins, G. Stowasser, and G. A. Tarling. Southern ocean mesopelagic fish communities in the scotia sea are sustained by mass immigration. *Marine Ecology Progress Series*, 569:173–185, 2017.

R. A. Saunders, M. A. Collins, R. Shreeve, P. Ward, G. Stowasser, S. L. Hill, and G. A. Tarling. Seasonal variation in the predatory impact of myctophids on zooplankton in the Scotia Sea (Southern Ocean). *Progress in Oceanography*, 168:123–144, 2018.

R. A. Saunders, S. L. Hill, G. A. Tarling, and E. J. Murphy. Myctophid fish (Family Myctophidae) are central consumers in the food web of the Scotia Sea (Southern Ocean). *Frontiers in Marine Science*, page 530, 2019.

R. A. Saunders, S. Lourenço, R. P. Vieira, M. A. Collins, C. A. Assis, and J. C. Xavier. Age and growth of Brauer's lanternfish *Gymnoscopelus braueri* and rhombic lanternfish *Krefftichthys anderssoni* (Family Myctophidae) in the Scotia Sea, Southern Ocean. *Journal of Fish Biology*, 96(2):364–377, 2020.

R. A. Saunders, S. Lourenço, R. P. Vieira, M. A. Collins, and J. C. Xavier. Length–weight and otolith size to standard length relationships in 12 species of Southern Ocean Myctophidae: a tool for predator diet studies. *Journal of Applied Ichthyology*, 37(1):140–144, 2021.

V. M. Savage, J. F. Gillooly, J. H. Brown, G. B. West, and E. L. Charnov. Effects of body size and temperature on population growth. *The American Naturalist*, 163(3): 429–441, 2004.

G. A. Schmidt, G. R. Bigg, and E. J. Rohling. Global Seawater Oxygen-18 Database, 1999. URL https://data.giss.nasa.gov/o18data/.

C. A. Schneider, W. S. Rasband, and K. W. Eliceiri. ImageJ, 2018. URL http://imagej.nih.gov/ij.

P. F. Scholander, W. Flagg, V. Walters, and L. Irving. Climatic adaptation in arctic and tropical poikilotherms. *Physiological Zoology*, 26(1):67–92, 1953.

A. D. Schöne, B. R.and Wanamaker Jr, J. Fiebig, J. Thébault, and K. Kreutz. Annually resolved δ^{13}C shell chronologies of long-lived bivalve mollusks (*Arctica islandica*) reveal oceanic carbon dynamics in the temperate North Atlantic during recent centuries. *Palaeogeography, Palaeoclimatology, Palaeoecology*, 302(1-2):31–42, 2011.

P. M. Schulte. The effects of temperature on aerobic metabolism: towards a mechanistic understanding of the responses of ectotherms to a changing environment. *The Journal of Experimental Biology*, 218(12):1856–1866, 2015.

H. P. Schwarcz, Y. Gao, S. Campana, D. Browne, M. Knyf, and U. Brand. Stable carbon isotope variations in otoliths of Atlantic cod (*Gadus morhua*). *Canadian Journal of Fisheries and Aquatic Sciences*, 55(8):1798–1806, 1998.

W. Schwarzhans. Head and otolith morphology of the genera Hymenocephalus, Hymenogadus and Spicomacrurus (Macrouridae), with the description of three new species. *Zootaxa*, 3888(1):1–73, 2014.

Marine Research Section. Acanthuridae. In *Fishes of the Maldives*. Ministry of Fisheries and Agriculture, Male, Republic of Maldives, 1997. ISBN 99915-62-12-5.

B. A. Seibel and J. C. Drazen. The rate of metabolism in marine animals: environmental constraints, ecological demands and energetic opportunities. *Philosophical Transactions of the Royal Society B: Biological Sciences*, 362(1487): 2061–2078, 2007.

J Sellanes, E Quiroga, and C Neira. Megafauna community structure and trophic relationships at the recently discovered Concepción Methane Seep Area, Chile, ∼36°S. *ICES Journal of Marine Science*, 65(7):1102–1111, 2008.

C. A. Sepulveda, S. A. Aalbers, S. Ortega-Garcia, N. C. Wegner, and D. Bernal. Depth distribution and temperature preferences of wahoo (*Acanthocybium solandri*) off Baja California Sur, Mexico. *Marine Biology*, 158(4):917–926, 2011.

K. T. Shao. Photo(s) contributed by Kwang-Tsao Shao, 2009. URL `https://www.fishbase.se/photos/PhotosList.php?id=41&vCollaborator=Kwang-Tsao+Shao`.

E. Shaw. Schooling fishes. *American Scientist*, 66(2):166–175, 1978.

S. Shephard, C. Trueman, R. Rickaby, and E. Rogan. Juvenile life history of NE Atlantic orange roughy from otolith stable isotopes. *Deep Sea Research Part I: Oceanographic Research Papers*, 54(8):1221–1230, 2007.

G. D. Sherwood and G. A. Rose. Influence of swimming form on otolith δ^{13}C in marine fish. *Marine Ecology Progress Series*, 258:283–289, 2003. ISSN 0171-8630.

X. Shi, P. Tian, R. Lin, D. Huang, and J. Wang. Characterization of the complete mitochondrial genome sequence of the globose head whiptail *Cetonurus globiceps* (Gadiformes: Macrouridae) and its phylogenetic analysis. *PLOS ONE*, 11(4): e0153666, 2016.

J. C. Shiao, T. F. Yui, H. Høie, U. Ninnemann, and S. K. Chang. Otolith O and C stable isotope compositions of southern bluefin tuna *Thunnus maccoyii* (Pisces: Scombridae) as possible environmental and physiological indicators. *Zoological Studies*, 48(1):71–82, 2009.

J. C. Shiao, T. D. Sui, N. N. Chang, and C. W. Chang. Remarkable vertical shift in residence depth links pelagic larval and demersal adult jellynose fish. *Deep Sea Research Part I: Oceanographic Research Papers*, 121:160–168, 2017.

R. A. Shinozaki-Mendes, F. H. V. Hazin, P. G. De Oliveira, and F. C. De Carvalho. Reproductive biology of the squirrelfish, *Holocentrus adscensionis* (Osbeck, 1765), caught off the coast of Pernambuco, Brazil. *Scientia Marina*, 71(4):715–722, 2007.

O. N. Shipley, C. S. Lee, N. S. Fisher, G. Burruss, M. G. Frisk, E. J. Brooks, Z. C. Zuckerman, A. D. Herrmann, and D. J. Madigan. Trophodynamics and mercury bioaccumulation in reef and open-ocean fishes from the Bahamas with a focus on two teleost predators. *Marine Ecology Progress Series*, 608:221–232, 2019.

R. S. Shreeve, M. A. Collins, G. A. Tarling, C. E. Main, P. Ward, and N. M. Johnston. Feeding ecology of myctophid fishes in the northern Scotia Sea. *Marine Ecology Progress Series*, 386:221–236, 2009.

J. F. Siebenaller, G. N. Somero, and R. L. Haedrich. Biochemical characteristics of macrourid fishes differing in their depths of distribution. *The Biological Bulletin*, 163 (1):240–249, 1982.

M. J. Silberberger, P. E. Renaud, I. Kröncke, and H. Reiss. Food-web structure in four locations along the european shelf indicates spatial differences in ecosystem functioning. *Frontiers in Marine Science*, 5:119, 2018.

F. Silva-Brito, F. Timóteo, Â. Esteves, M. J. Peixoto, R. Ozorio, and L. Magnoni. Impact of the replacement of dietary fish oil by animal fats and environmental salinity on the metabolic response of european seabass (*Dicentrarchus labrax*). *Comparative Biochemistry and Physiology Part B: Biochemistry and Molecular Biology*, 233:46–59, 2019.

N. R. Sinnatamby, B. J. Dempson, J. D. Reist, and M. Power. Latitudinal variation in growth and otolith-inferred field metabolic rates of Canadian young-of-the-year Arctic charr. *Ecology of Freshwater Fish*, 24(3):478–488, 2015.

K. A. Sloman, I. A. Bouyoucos, E. J. Brooks, and L. U. Sneddon. Ethical considerations in fish research. *Journal of Fish Biology*, 94(4):556–577, 2019.

C. R. Smith, F. C. De Leo, A. F. Bernardino, A. K. Sweetman, and P. M. Arbizu. Abyssal food limitation, ecosystem structure and climate change. *Trends in Ecology & Evolution*, 23(9):518–528, 2008.

M. M. Smith and P. C. Heemstra. *Smiths' sea fishes*. Springer-Verlag, 2012. ISBN 3-540-16851-6.

S. Smoliński, C. Denechaud, G. von Leesen, A. J. Geffen, P. Grønkjær, J. A. Godiksen, and S. E. Campana. Differences in metabolic rate between two Atlantic cod (*Gadus morhua*) populations estimated with carbon isotopic composition in otoliths. *PLOS ONE*, 16(4), 2021.

I. Solberg and S. Kaartvedt. The diel vertical migration patterns and individual swimming behavior of overwintering sprat *Sprattus sprattus*. *Progress in Oceanography*, 151:49–61, 2017.

A. Soldo. Length-weight relationships for the fifty littoral and coastal marine fish species from the Eastern Adriatic Sea. *Acta Adriatica: International Journal of Marine Sciences*, 61(2):205–210, 2020.

C. T. Solomon, P. K. Weber, Jr Cech, J. J., B. L. Ingram, M. E. Conrad, M. V. Machavaram, A. R. Pogodina, and R. L. Franklin. Experimental determination of the sources of otolith carbon and associated isotopic fractionation. *Canadian Journal of Fisheries and Aquatic Sciences*, 63(1):79–89, 2006.

M. A. St John, A. Borja, G. Chust, M. Heath, I. Grigorov, P. Mariani, A. P. Martin, and R. S. Santos. A dark hole in our understanding of marine ecosystems and their services: perspectives from the mesopelagic community. *Frontiers in Marine Science*, 3:31, 2016.

J. F. Steffensen. Metabolic cold adaptation of polar fish based on measurements of aerobic oxygen consumption: fact or artefact? Artefact! *Comparative Biochemistry and Physiology Part A: Molecular & Integrative Physiology*, 132(4):789–795, 2002.

P. C. Stephenson, J. S. Edmonds, M. J. Moran, and N. Caputi. Analysis of stable isotope ratios to investigate stock structure of red emperor and Rankin cod in northern Western Australia. *Journal of Fish Biology*, 58(1):126–144, 2001.

B. C. Stock, A. L. Jackson, E. J. Ward, A. C. Parnell, D. L. Phillips, and B. X. Semmens. Analyzing mixing systems using a new generation of Bayesian tracer mixing models. *PeerJ*, 6:e5096, 2018.

G. Stowasser, D. W. Pond, and M. A. Collins. Using fatty acid analysis to elucidate the feeding habits of Southern Ocean mesopelagic fish. *Marine Biology*, 156(11): 2289–2302, 2009.

G. W. Stunz and D. M. Coffey. A review of the ecological performance and habitat value of standing versus reefed oil and gas platform habitats in the Gulf of Mexico. Louisiana, USA, 2020. Gulf Offshore Research Institute (GORI).

T. B. Sutton, T. T.and Letessier and B. Bardarson. Midwater fishes collected in the vicinity of the Sub-Polar Front, Mid-North Atlantic Ocean, during ECOMAR pelagic sampling. *Deep Sea Research Part II: Topical Studies in Oceanography*, 98:292–300, 2013.

C. J. Svensson, G. A. Hyndes, and P. S. Lavery. Food web analysis in two permanently open temperate estuaries: consequences of saltmarsh loss? *Marine Environmental Research*, 64(3):286–304, 2007.

E. Svensson, V. Freitas, S. Schouten, J. J. Middelburg, H. W. van der Veer, and J. S. S. Damsté. Comparison of the stable carbon and nitrogen isotopic values of gill and white muscle tissue of fish. *Journal of Experimental Marine Biology and Ecology*, 457: 173–179, 2014.

A. Tagliabue and L. Bopp. Towards understanding global variability in ocean carbon-13. *Global biogeochemical cycles*, 22(1), 2008. ISSN 0886-6236.

T. Tamelander, P. E. Renaud, J. Hop, M. L. Carroll, W. G. Ambrose Jr, and K. A. Hobson. Trophic relationships and pelagic–benthic coupling during summer in the Barents Sea Marginal Ice Zone, revealed by stable carbon and nitrogen isotope measurements. *Marine Ecology Progress Series*, 310:33–46, 2006.

Stan Development Team. *RStan: the R interface to Stan*, 2020. URL `https://mc-stan.org/`.

T. C. Theisen and J. D. Baldwin. Movements and depth/temperature distribution of the ectothermic Scombrid, *Acanthocybium solandri* (wahoo), in the western North Atlantic. *Marine Biology*, 159(10):2249–2258, 2012.

S. R. Thorrold, S. E. Campana, C. M. Jones, and P. K. Swart. Factors determining δ^{13}C and δ^{18}O fractionation in aragonitic otoliths of marine fish. *Geochimica et Cosmochimica Acta*, 61(14):2909–2919, 1997.

Y. Tikochinski, B. Russell, Y. Hyams, U. Motro, and D. Golani. Molecular analysis of the recently described lizardfish *Saurida lessepsianus* (Synodontidae) from the Red Sea and the Mediterranean, with remarks on its phylogeny and genetic bottleneck effect. *Marine Biology Research*, 12(4):419–425, 2016.

C. A. Timmerman, P. Marchal, M. Denamiel, C. Couvreur, and P. Cresson. Seasonal and ontogenetic variation of whiting diet in the Eastern English Channel and the Southern North Sea. *PLOS ONE*, 15(9):e0239436, 2020.

D. P. Tittensor, T. D. Eddy, H. K. Lotze, E. D. Galbraith, W. Cheung, M. Barange, J. L. Blanchard, L. Bopp, A. Bryndum-Buchholz, M. Büchner, et al. A protocol for the intercomparison of marine fishery and ecosystem models: Fish-MIP v1. 0. *Geoscientific Model Development*, 11(4):1421–1442, 2018.

H. Tohse and Y. Mugiya. Sources of otolith carbonate: experimental determination of carbon incorporation rates from water and metabolic CO_2, and their diel variations. *Aquatic Biology*, 1(3):259–268, 2008.

J. J. Torres and G. N. Somero. Metabolism, enzymic activities and cold adaptation in antarctic mesopelagic fishes. *Marine Biology*, 98(2):169–180, 1988.

J.J. Torres, B.W. Belman, and J.J. Childress. Oxygen consumption rates of midwater fishes as a function of depth of occurrence. *Deep Sea Research Part A. Oceanographic Research Papers*, 26(2):185–197, 1979.

J. R. Treberg, S. S. Killen, T. J. MacCormack, S. G. Lamarre, and E. C. Enders. Estimates of metabolic rate and major constituents of metabolic demand in fishes under field

conditions: methods, proxies, and new perspectives. *Comparative Biochemistry and Physiology Part A: Molecular & Integrative Physiology*, 202:10–22, 2016.

C. N. Trueman, R. E. M. Rickaby, and S. Shephard. Thermal, trophic and metabolic life histories of inaccessible fishes revealed from stable-isotope analyses: a case study using orange roughy *Hoplostethus atlanticus*. *Journal of Fish Biology*, 83(6):1613–1636, 2013.

C. N. Trueman, G. Johnston, B. O'hea, and K. M. MacKenzie. Trophic interactions of fish communities at midwater depths enhance long-term carbon storage and benthic production on continental slopes. *Proceedings of the Royal Society B: Biological Sciences*, 281(1787):20140669, 2014.

C. N. Trueman, M. T. Chung, and D. Shores. Ecogeochemistry potential in deep time biodiversity illustrated using a modern deep-water case study. *Philosophical Transactions of the Royal Society B: Biological Sciences*, 371(1691), 2016.

C. Trystram, D. Roos, D. Guyomard, and S. Jaquemet. Mechanisms of trophic partitioning within two fish communities associated with a tropical oceanic island. *Western Indian Ocean Journal of Marine Science*, 14(1&2):93–111, 2015.

K. Tsagarakis, M. Giannoulaki, S. Somarakis, and A. Machias. Variability in positional, energetic and morphometric descriptors of European anchovy *Engraulis encrasicolus* schools related to patterns of diurnal vertical migration. *Marine Ecology Progress Series*, 446:243–258, 2012.

K. Tse. Saithe (*Pollachius virens*), 2011. URL `http://muskiebaitadventures.blogspot.com/p/saithe.html`.

G. Tserpes, F. Fiorentino, D. Levi, A. Cau, M. Murenu, A. Zamboni, and C. Papaconstantinou. Distribution of *Mullus barbatus* and *M. surmuletus* (Osteichthyes: Perciformes) in the Mediterranean continental shelf: implications for management. *Scientia Marina*, 66(S2):39–54, 2002.

J. C. Uyeda, M. W. Pennell, E. T. Miller, R. Maia, and C. R. McClain. The evolution of energetic scaling across the vertebrate tree of life. *The American Naturalist*, 190(2): 185–199, 2017.

M. Vagner, J. L. Zambonino-Infante, D. Mazurais, N. Imbert-Auvray, N. Ouillon, E. Dubillot, H. Le Delliou, D. Akbar, and C. Lefrançois. Reduced n-3 highly unsaturated fatty acids dietary content expected with global change reduces the metabolic capacity of the golden grey mullet. *Marine Biology*, 161(11):2547–2562, 2014.

M. Vagner, T. Lacoue-Labarthe, J. L. Zambonino Infante, D. Mazurais, E. Dubillot, H. Le Delliou, P. Quazuguel, and C. Lefrançois. Depletion of essential fatty acids in

the food source affects aerobic capacities of the golden grey mullet *Liza aurata* in a warming seawater context. *PLOS ONE*, 10(6):e0126489, 2015.

M. Vagner, E. Pante, A. Viricel, T. Lacoue-Labarthe, J. L. Zambonino-Infante, P. Quazuguel, E. Dubillot, V. Huet, H. Le Delliou, C. Lefrançois, et al. Ocean warming combined with lower omega-3 nutritional availability impairs the cardio-respiratory function of a marine fish. *Journal of Experimental Biology*, 222(8): jeb187179, 2019.

P. L. Van Dijk, C. Tesch, I. Hardewig, and H. O. Portner. Physiological disturbances at critically high temperatures: a comparison between stenothermal antarctic and eurythermal temperate eelpouts (Zoarcidae). *Journal of Experimental Biology*, 202(24): 3611–3621, 1999.

V. van Ginneken and G. van den Thillart. Metabolic depression in fish measured by direct calorimetry: a review. *Thermochimica Acta*, 483(1-2):1–7, 2009.

J. J. Vaudo, M. E. Byrne, B. M. Wetherbee, G. M. Harvey, A. Mendillo Jr, and M. S. Shivji. Horizontal and vertical movements of white marlin, *Kajikia albida*, tagged off the Yucatán Peninsula. *ICES Journal of Marine Science*, 75(2):844–857, 2018.

H. Venables, M. P. Meredith, A. Atkinson, and P. Ward. Fronts and habitat zones in the Scotia Sea. *Deep Sea Research Part II: Topical Studies in Oceanography*, 59:14–24, 2012.

P. Viscardi. A survival strategy for natural science collections: the role of advocacy. *Journal of Natural Science Collections*, 1:4–7, 2013.

A. Walters, M. Robert, P. Cresson, H. Le Bris, and D. Kopp. Food web structure in relation to environmental drivers across a continental shelf ecosystem. *Limnology and Oceanography*, 66(6):2563–2582, 2021.

H. Watanabe, M. Moku, K. Kawaguchi, K. Ishimaru, and A. Ohno. Diel vertical migration of myctophid fishes (Family Myctophidae) in the transitional waters of the western North Pacific. *Fisheries Oceanography*, 8(2):115–127, 1999.

Y. Y. Watanabe and J. A. Goldbogen. Too big to study? The biologging approach to understanding the behavioural energetics of ocean giants. *Journal of Experimental Biology*, 224(13), 2021. .

A. J. Watson, U. Schuster, J. D. Shutler, T. Holding, I. G. C. Ashton, P. Landschützer, D. K. Woolf, and L. Goddijn-Murphy. Revised estimates of ocean-atmosphere co_2 flux are consistent with ocean carbon inventory. *Nature Communications*, 11(1):1–6, 2020.

C. R. Weidman and R. Millner. High-resolution stable isotope records from North Atlantic cod. *Fisheries Research*, 46(1-3):327–342, 2000.

R. J. D. Wells, J. R. Rooker, and E. D. Prince. Regional variation in the otolith chemistry of blue marlin (*Makaira nigricans*) and white marlin (*Tetrapturus albidus*) from the western North Atlantic Ocean. *Fisheries Research*, 106(3):430–435, 2010.

G. B. West, J. H. Brown, and B. J. Enquist. A general model for the origin of allometric scaling laws in biology. *Science*, 276(5309):122–126, 1997.

C. R. White, N. F. Phillips, and R. S. Seymour. The scaling and temperature dependence of vertebrate metabolism. *Biology Letters*, 2(1):125–127, 2006.

C. R. White, P. Cassey, and T. M. Blackburn. Allometric exponents do not support a universal metabolic allometry. *Ecology*, 88(2):315–323, 2007.

C. R. White, L. A. Alton, and P. B. Frappell. Metabolic cold adaptation in fishes occurs at the level of whole animal, mitochondria and enzyme. *Proceedings of the Royal Society B: Biological Sciences*, 279(1734):1740–1747, 2012a.

C. R. White, P. B. Frappell, and S. L. Chown. An information-theoretic approach to evaluating the size and temperature dependence of metabolic rate. *Proceedings of the Royal Society B: Biological Sciences*, 279(1742):3616–3621, 2012b.

P.J.P. Whitehead, M.L. Bauchot, J.C. Hureau, J. Nielsen, and E. Tortonese. *Fishes of the North-eastern Atlantic and Mediterranean*, volume 1–3. United Nations Educational, Scientific and Cultural Organisation (UNESCO), Paris, 1986. ISBN 92-3-002215-2.

N. M. Whitney, M. Taquet, R. W. Brill, C. Girard, G. D. Schwieterman, L. Dagorn, and K. N. Holland. Swimming depth of dolphinfish (*Coryphaena hippurus*) associated and unassociated with fish aggregating devices. *Fishery Bulletin*, 114(4), 2016.

T. V. Willis, K. A. Wilson, and B. J. Johnson. Diets and stable isotope derived food web structure of fishes from the inshore Gulf of Maine. *Estuaries and Coasts*, 40(3): 889–904, 2017.

G.G. Winberg. Rate of metabolism and food requirements of fishes. *Fisheries Research Board of Canada, Translation Series*, 194:202, 1956.

B. L. Winner, K. E. Flaherty-Walia, T. S. Switzer, and J. L. Vecchio. Multidecadal evidence of recovery of nearshore red drum stocks off West-Central Florida and connectivity with inshore nurseries. *North American Journal of Fisheries Management*, 34(4):780–794, 2014. .

D. E. Wohlschlag. Metabolism of an Antarctic fish and the phenomenon of cold adaptation. *Ecology*, 41(2):287–292, 1960.

F. I. Woodward. Global primary production. *Current Biology*, 17(8):R269–R273, 2007.

C. M. Wurster and W. P. Patterson. Metabolic rate of late Holocene freshwater fish: evidence from δ^{13}C values of otoliths. *Paleobiology*, 29(4):492–505, 2003.

C. M. Wurster, W. P. Patterson, D. J. Stewart, J. N. Bowlby, and T. J. Stewart. Thermal histories, stress, and metabolic rates of chinook salmon (*Oncorhynchus tshawytscha*) in Lake Ontario: evidence from intra-otolith stable isotope analyses. *Canadian Journal of Fisheries and Aquatic Sciences*, 62(3):700–713, 2005.

A. S. J. Wyatt, A. M. Waite, and S. Humphries. Variability in isotope discrimination factors in coral reef fishes: implications for diet and food web reconstruction. *PLOS ONE*, 5(10):e13682, 2010.

Y. Yamanoue and K. Matsuura. *Doederleinia gracilispinis* (Fowler, 1943), a junior synonym of *Doederleinia berycoides* (Hilgendorf, 1879), with review of the genus. *Ichthyological Research*, 54(4):404–411, 2007.

G. Zapata-Hernández, J. Sellanes, A. R. Thurber, L. A. Levin, F. Chazalon, and P. Linke. New insights on the trophic ecology of bathyal communities from the methane seep area off Concepción, Chile ($\sim$ 36 °S). *Marine Ecology*, 35(1):1–21, 2014.

Y. Zhu, S. P. Newman, W. D. K. Reid, and N. V. C. Polunin. Fish stable isotope community structure of a Bahamian coral reef. *Marine Biology*, 166(12):1–14, 2019.